

https://dspace.org/

Long term performance of thin spray-on liners for permanent support in underground mines

Kanda, Mpoyi Jacques

2020
https://hdl.handle.net/10539/31780

Downloaded from a DSpace repository. https://dspace.org/



UNIVERSITY OF THE
WITWATERSRAND,
JOHANNESBURG

LONG TERM PERFORMANCE OF THIN SPRAY-ON LINERS FOR PERMANENT SUPPORT IN UNDERGROUND MINES

Mpoyi Jacques Kanda

School of Mining Engineering

University of the Witwatersrand

Johannesburg, South Africa.

Supervisor: Professor T.R. Stacey

A thesis submitted to the Faculty of Engineering and the Built Environment, University of the Witwatersrand, Johannesburg, in fulfilment of the requirements for the degree of Doctor of Philosophy in Engineering.

Johannesburg, 2020

DECLARATION

I, Mpoyi Jacques Kanda, declare that this thesis is my own, unaided work. I have read the University Policy on Plagiarism and hereby confirm that no plagiarism exists in this thesis. I also confirm that there is no copying nor is there any copyright infringement. I willingly submit to any investigation in this regard by the School of Mining Engineering and I undertake to abide by the decision of any such investigation.



Mpoyi Jacques Kanda

The 26th of September 2020

ABSTRACT

Thin spray-on liners (TSLs) have been implemented for over 25 years. The feedback from their strength assessments has demonstrated high tensile strength and elongation capability. However, these supporting advantages are not always evidenced in the underground mining environment where it is often applied. This lack of practical constancy in TSL performance has given way to scepticism over its utilization, despite good results propagated by some laboratory tests. Thus this thesis's research study aims to assess the practical underground performances of TSL, taking into consideration its long-term performance aspect, so that its reliability might be clearly defined and placed at the reach of the users. Included in this thesis's research, is a critical review of existing literature provided by suppliers and other researchers, which assesses TSL performance capabilities. The TSL assessment techniques opted for in this research, are the field assessments, laboratory trials and numerical modelling analyses.

In summary, existing suppliers and research literature were found to present the following: TSL's high areal-support capabilities are its high tensile and adhesive strengths, as well as its high elongation capacity. The available reviewed laboratory testing was undertaken in "traditional" laboratory conditions, and only a few recent research-initiatives started examining the long-term performance of TSL. The latest long-term results show preliminary signs of TSL limitations when such are selected for permanent support. Thus due to the importance of the long-term aspect of TSL assessment, time-dependency information was reviewed in detail in this thesis. Yet throughout the whole review, no information was encountered on assessments of TSL that combined underground mine-like conditions such as humidity and temperature with relatively longer timing of exposure.

During the fieldwork activities, two South African underground platinum mines were visited: a deep mine and a shallow mine. The mine operators were still not sure where these liners were performant, but the suppliers highly advocated their utilization in most of the mines' openings. The following laboratory tests were

conducted on three TSLs in this thesis: uniaxial tensile strength (UTS), Brazilian indirect tensile (BIT) strength test and membrane displacement test (MBT), which is a punch-through test. In these tests, the focus was directed on the influence of the parameters that are characteristic of some deep underground mines, as well as on the performance behaviours of TSLs, particularly after long periods of exposure or long-term testing. To achieve this, three different environmental conditions were considered for testing, namely: the traditional laboratory condition (called room condition), the humid (saturated) condition, and a combined humid and high temperature (50°C) condition. The long-term performance of TSL under loading was assessed through creep testing.

The thesis's BIT tests were performed on TSL discs and on coated and uncoated shotcrete discs. Through these assessments, the impact of TSLs on coated shotcrete discs was assessed through short-term and long-term testing after prior longer exposures to various environmental conditions. The MBT testing method followed the testing conditions established for the UTS and BIT tests. Two assessing parameters were suggested for standard assessment of MBT performance. Numerical modelling analyses were also carried out. A coated BIT model was set using a Rocscience program, namely RS3.

From the short-term testing results, it was found that TSL generally shows a tensile strengthening trend in room conditions, and a weakening trend in humid conditions and in combined humid and high temperature conditions. An exception was however observed for water-based TSLs, which could still display a strengthening trend in humid condition, but which was overcome when the temperature parameter was added. Concerning the long-term performance of TSL, it was found that TSL could accommodate larger deformations for static and lighter loads. BIT shotcrete specimens coated with TSL could permanently succeed in resisting disturbing forces. Among the recommendations, TSL1-like materials should preferably not be used as permanent support in humid underground mines, unless combined with other mining supports. Also, it is inappropriate to design TSL underground support systems based on liner strength and deformation in room conditions.

ACKNOWLEDGEMENTS

This thesis was developed while I was a full-time PhD student at the School of Mining Engineering, University of the Witwatersrand, and is a product of support from many people, including family members, friends, colleagues and professionals from the mining sector.

First and foremost, I would like to thank my Creator, the Reason of my existence, namely my God, for giving me life, good health and strength to complete this thesis. I would never take these for granted. Thank you, my Lord.

I am greatly indebted to my Supervisor, Prof. Thomas Stacey for his invaluable and unlimited support, encouragement, and patience and time, without which this thesis would have not been completed. I am also grateful to Prof. Halil Yilmaz for assisting me with information and laboratory techniques during my earlier stage while accommodating with the topic. Prof. Frank Kienhofer, from the Wits School of Mechanical, Industrial & Aeronautical Engineering, Prof. Bryan Watson and Prof. Rudrajit Mitra are also thanked for their assistance.

May Prof. C. Musingwini, Head of School of Mining Engineering, find the expression of my grateful heart for his willingness and readiness to assist whenever I was going through hard times regarding the logistic availability for laboratory testing, funding, etc. Anzolette Saville, Sonja Douman, Lindy Dabrowski, Thobile Sedumedi and Siyabonga Mbatha are also acknowledged for their advice and assistance.

My gratitude is addressed to the “Instituto Superior Politecnico de Tete”, particularly to Dr. Bernardo Bene and Mr. Maenda Enda for allowing me to pursue my dream and reaching this doctorate milestone through funding and giving me the needed leave. The CINOP Global through the NICHE program, and especially René Lenssen, are also thanked for the program funding.

There is no word, adequate enough to address how grateful I am to Mr. A. Morgan, Senior Laboratory Technician in the Wits School of Mining Engineering. I call him the “Raven”, who in similarity with Elijah’s raven, came to my rescue while I was hopeless, at crossroad, and took to heart the urgent task to complete the creep logistic, working even after hours without bonuses, but also provided words of faith, encouragement and wisdom so that I stayed strong. Through him, I can say that miracles still exist.

I thank Nick Holland, CEO/Executive Director at Gold fields South Africa, for personally taking to heart to assist me with as much information as possible related to thin spray-on liner performance. In this regard, Sven Lunsche and Peter Andrews from Gold Fields are also thanked for their advice and encouragement.

I am grateful to Jeane Matsobane and Fanta Sibanda (Sibanye Platinum), Ephraim Mkhize and Francois Vanrooyen (Anglo American), Josef Ekkerd (De Beers Consolidated Mines), Les Gardner (Impala Platinum) for their assistance during the fieldworks.

Bryce Nhlapho and Ivan Shikwambana (Minova global), Gavin Borejszo (SA Mining), Henry Beckley (Concrete lining products) are thanked for being helpful while I needed some materials.

My gratitude goes also to Michal Dabrowski for editing this thesis, but also for reviving my faith.

To my mentor, Avelino Sousa Pousa, I address my gratitude. You have been there, making me believe in myself to embrace this road of greatness.

Finally, I would also give thanks to my family, particularly to my wife Nadia Mpoyi and my beloved daughter Naior-Blessing Tshiama Mpoyi for always encouraging me even when I felt the hardship was too much to bear. To my mother Madeleine Tshiama, I also express my gratitude for strengthening me and praying for me.

DEDICATION

To my God, the Most High, whose eyes saw my substance, being yet unformed.

CONTENTS

DECLARATION ..... **I**
ABSTRACT ..... **II**
ACKNOWLEDGEMENTS ..... **IV**
DEDICATION ..... **VI**
CONTENTS ..... **VII**
LIST OF FIGURES ..... **XIV**
LIST OF TABLES ..... **XXVII**
LIST OF SYMBOLS AND ACRONYMS ..... **XXXII**
CHAPTER 1 INTRODUCTION **1**
1.1 Background 1
1.2 Statement of the Problem 2
1.3 Aim and Objectives 3
1.4 Research Methodology 4
1.5 Envisaged Contribution to Knowledge 6
1.6 Layout of the Thesis 6
CHAPTER 2 CHARACTERISTICS OF THIN SPRAY-ON LINERS AND OTHER AREAL SUPPORTS **8**
2.1 General Statement on Ground Support Tools 8
2.2 Active and Passive Supports 10
2.3 Comparison between Wire Mesh and TSLs 11
2.4 Comparison between Shotcrete and TSLs 12
2.5 Replacing and Combining Mining Support Tools 14
2.5.1 Replacing some mining support tools 14
2.5.2 Combining TSLs with other mining support tools 15
2.6 Types of Thin Spray-on Liners 16
2.7 TSL Properties 18
2.7.1 Generic thin spray-on liners 18
2.7.2 TSL1 20
2.7.3 TSL2 20
2.7.4 TSL3 21

2.8 Mechanical Behaviour of TSLs 22
2.9 Design Principles 26
2.10 Application and Assessment of TSLs in the Mining Sector 27
2.10.1 Functions of a TSL in the mining sector 27
2.10.2 Field testing of TSL 28
TSL support performance from field testing 29
Advantages of TSL application 30
Disadvantages of TSL usage 32
2.11 Laboratory Testing of TSL Materials 33
2.11.1 Uniaxial tensile strength 37
2.11.2 Tensile bond strength 40
2.11.3 Membrane displacement test 42
2.12 Numerical Modelling of TSLs 46
2.13 Sample of Available Guidelines for Application of TSLs to Promote Stability 48
2.13.1 General guidelines for TSL utilization 48
2.13.2 Guidelines for laboratory testing of TSLs 49
2.13.3 Guidelines for *in situ* application of TSLs 51
2.14 Chapter Summary 52
CHAPTER 3 TIME-DEPENDENCY CONCEPTS IN THE MINING ENVIRONMENT 54
3.1 Introduction 54
3.2 Creep and Relaxation Behaviour in the Rock Mass Environment 54
3.3 Time-dependent Deformation in Jointed Rock Masses 59
3.3.1 Time-dependency of ductile and brittle rocks 59
3.3.2 Comparison of the results of post-failure relaxation behaviour of different types of rock materials 60
3.3.3 Long-term performance of rocks 60
3.4 Time-Dependent Deformation of Polymer-Based Materials 63
3.5 Creep Tests on TSLs 66
3.6 Rheological model concepts 67
3.6.1 H-K creep model 70
3.6.2 Burgers model 70

3.7 Accessories for Stress and Strain Measurement 71
3.7.1 Load cells and linear variable differential transformers 71
3.7.2 Wheatstone Bridge configuration 72
Introduction 72
Strain gauges 72
Wheatstone bridge structures 73
Balanced and unbalanced bridges *73*
One-gauge system *75*
Two-gauge system *76*
Input voltage *77*
Adopted Wheatstone bridge circuit *78*
3.8 Chapter Summary 80
CHAPTER 4 FIELD ASSESSMENT OF TSL PERFORMANCE 81
4.1 Introduction 81
4.2 Methodology of Field Assessment 81
4.2.1 Collection of data through a questionnaire and opinion 81
4.2.2 *In situ* inspection of TSL performance 83
4.2.3 Analysis of field data on TSL performance 85
4.3 Feedback from the Inquiry 85
4.3.1 Responses to the questionnaire on TSL performance 85
4.3.2 Briefing on a discussion between two technicians concerning a TSL performance 89
4.3.3 Analysis of the responses to the questionnaire and the opinions on a TSL performance 91
4.4 Inspection Report: Union Richard Shaft (relatively deep mine) 92
4.4.1 Introduction 92
4.4.2 14^{th} Level (690m below surface) 94
4.4.3 15^{th} Level (750 m below surface) 99
4.4.4 17^{th} Level (842 m below surface) 102
17^{th} Level “Old TSL” (11 years old at the time of field assessment) 103
17^{th} Level “Young TSL” (9 months old at the time of field assessment) 106
4.4.5 Interpretation of deep mine findings regarding TSL performance 108
4.5 Inspection Report: Bathopele Mine (shallow mine) 108

4.5.1 Introduction 108
4.5.2 Central Shaft, section 3W, bord 11 – Ventilation crossing 109
4.5.3 Central shaft strike, section 3 W, bord 10 – Belt drive 110
4.5.4 Central shaft, section 13E, bord 7 – Belt drive and section 14E, bord 5 – Belt take-up 112
4.5.5 Central shaft, section 15W, bord 6 – Belt drive 113
4.5.6 East shaft, section 12W, bord 8 – Bord 114
4.5.7 Interpretation of shallow mine findings regarding TSL performance 114
4.6 Chapter Summary 115
CHAPTER 5 LABORATORY TRIALS OF TSL PERFORMANCES.....118
5.1 Introduction 118
5.2 Setup of the Weighing System for Long-Term Tests 120
5.3 Uniaxial Tensile Strength Tests 124
5.3.1 Introduction 124
5.3.2 Specimen preparation 124
5.3.3 Materials and methods 126
Short-term tests 127
Long-term tests 129
Design 129
Calibration of the weighing of the tensile creep testing machine "M3" 131
Calibration of the displacement transducer of the tensile creep testing machine "M3" 132
Mode of operation of the UTS creep machine 135
5.3.4 Results from short-term tests 135
TSL1 sensitivity to environmental conditions 136
TSL2 sensitivity to environmental conditions 137
TSL3 sensitivity to environmental conditions 138
Environmental impact on TSL elongation and modulus 139
Analyses of the influence of environmental conditions on TSL performance depending on the exposure time 150
5.3.5 Results from long-term tests 151
Room condition 152

Humidity condition 153
Analysis of the influence of the environmental conditions on TSL for UTS long-term testing 155
5.4 Brazilian Indirect Tensile tests 156
5.4.1 Introduction 156
5.4.2 Specimen preparation 157
5.4.3 Materials and methods 161
Short-term tests 162
Long-term tests 163
Design 164
Calibration of Brazilian creep testing machines 166
Set up of displacement transducer 171
Determination of onset creep weights 176
5.4.4 Results of short-term BIT tests 177
Influence of the environmental conditions on uncoated shotcrete discs 178
Influence of the environmental conditions on TSL disc specimens 179
Influence of the environmental conditions on coated BIT specimens 180
Summary of BIT short-term test results 189
5.4.5 Results of long-term tests 190
Determination of 100% creep strengths for coated shotcrete tested in room and humid conditions 191
Influence of the environmental conditions on coated BIT specimens 193
Analysis of the influence of environmental conditions on TSL for BIT long-term testing 196
5.5 Membrane Displacement Tests 197
5.5.1 Introduction 197
5.5.2 Specimen preparation 197
5.5.3 Materials and Methods 199
Short-term tests 200
Long-term tests 206
Design 206
Calibration of the MBT creep testing machine 208
Calibration of displacement transducers for M2 creep testing machine 210

Mode of operation *211*
5.5.4 Results of short-term tests 211
Influence of environmental conditions on MBT strengths 212
Influence of environmental conditions on MBT strength and TSL elongation 215
Choice of efficient TSL on the basis of MBT indicators 221
5.5.5 Results of long-term tests 224
Room condition 224
Humidity condition 226
Analysis of the influence of environmental conditions on TSL for MBT long-term testing 228
5.6 Uniaxial Compressive Strength test 229
5.6.1 Introduction 229
5.6.2 Specimen preparation 229
5.6.3 Materials and Methods 230
5.6.4 Results of short-term tests 232
Results of shotcrete's UCS 232
Room condition *232*
Humid and high temperature condition *232*
Results of TSLs' UCS 233
Room condition *233*
Humidity and high temperature condition *233*
5.7 Triaxial Compressive Strength test 235
5.7.1 Introduction 235
5.7.2 Specimen preparation 236
5.7.3 Materials and Methods 236
5.7.4 Results of short-term tests 238
5.8 Chapter Summary 242
CHAPTER 6 NUMERICAL MODELLING APPLICATIONS 249
6.1 Introduction 249
6.2 Modelling of Coated Shotcrete Disc 249
6.2.1 Modelling of coated rock materials with TSL revisited 249
6.2.2 Methodology for numerical modelling assessments 249

6.2.3 Model settings 251
Room condition 251
High temperature and humidity condition 252
6.2.4 Modelling results 253
Room conditions 253
High temperature and humidity conditions 255
6.3 Chapter Summary 256
CHAPTER 7 DISCUSSIONS 258
CHAPTER 8 CONCLUSIONS AND RECOMMENDATIONS 268
CHAPTER 9 FRAMEWORK TO A GUIDELINE FOR TSL'S LONG-TERM PERFORMANCE 274
REFERENCES 278
APPENDICES 294

LIST OF FIGURES

Figure 1-1 Cause of fatalities in the South African mining industry between 1995 and 2018 (*Minerals Council South Africa*, 2018) 1
Figure 2-1 Load versus displacement capacities from pull tests of various areal supports (Tannant, 2001)..... 8
Figure 2-2 TSL's tensile resistance to loading mechanism (Yilmaz, 2010)..... 18
Figure 2-3 Adhesion loss – tensile rupture mechanism of a TSL supporting the weight of a loose block (Tannant, 2001)..... 23
Figure 2-4 Relationship between VRT and depth for the BIC and the Witwatersrand Basin (Biffi *et al*, 2007) 25
Figure 2-5 ASTM D638 Shapes and dimensions for Type I and IV (ASTM D-638, 2010)..... 38
Figure 2-6 Valid failure location of a dog-bone specimen tested in tension (Yilmaz, 2010)..... 38
Figure 2-7 Classification of TSL's tensile strength (Yilmaz, 2010) 39
Figure 2-8 Dimensions of (a) Steel dolly (b) Perspex mould and (c) rock substrate (Yilmaz, 2013)..... 41
Figure 2-9 Membrane displacement test set-up (Spearing *et al*, 2001) 42
Figure 2-10 Aspect of MBT specimen after testing (Spearing *et al,* 2001)..... 43
Figure 2-11 (a) Force versus displacement capacity of TSLs and shotcrete (Morton *et al*, 2008); (b) Load versus displacement capacity of various areal supports (Tannant, 2001) 43
Figure 2-12 TSL's load – displacement behaviour (Morton *et al*, 2008) 44
Figure 2-13 Load-displacement plot of a TSL (Spearing *et al,* 2001)..... 44
Figure 2-14 Numerical modelling of BIT principal stresses along the loaded diameter due to: a) point load and b) strip load..... 47
Figure 3-1 Creep Behaviour..... 55
Figure 3-2 Relaxation Behaviour..... 56
Figure 3-3 Principle of operation of the CSIR creep testing machine (Malan *et al,* 1997)..... 56

Figure 3-4 Classic shear creep behaviour of a discontinuity (Drescher and Handley, 2003) 57
Figure 3-5 Typical fracture patterns relating the time-dependent processes around an underground slope (Gay and Jager, 1986) 58
Figure 3-6 Post-failure relaxation curves for more and less brittle rocks (Drescher and Handley, 2003) 59
Figure 3-7 Determination of long-term strength for Norite specimen in unconfined tests (Bieniawski, 1967) 61
Figure 3-8 Step-wise loading method for hard rock long time performance determination through uniaxial compression (Drescher and Handley, 2003) 62
Figure 3-9 Step-wise loading method for hard rock long time performance determination through shear loading on discontinuities (Drescher and Handley, 2003) 62
Figure 3-10 Time-to-failure plot for mottled Anorthosite (Nyungu and Stacey, 2014) 63
Figure 3-11 Example of long-term stress relaxation curve obtained by superposition (Osswald, 2015) 65
Figure 3-12 Creep rupture curves of a cement-based TSL under tensile loading (Guner and Ozturk, 2018) 66
Figure 3-13 Multi-step creep technique (Yang *et al*, 2018) 69
Figure 3-14 H-K rheological model 70
Figure 3-15 Burgers rheological model 70
Figure 3-16 (a) S type load cell (Covscale, n.d.) and (b) LVDT model ('ACT LVDT Displacement Transducer', n.d.) 72
Figure 3-17 Wheatstone bridge configuration 74
Figure 3-18 One-gauge bridge configuration 75
Figure 3-19 Two-gauge bridge configuration 76
Figure 3-20 Coupling of power supply with a data logger 78
Figure 3-21 Wheatstone bridge connection of a transducer 79
Figure 4-1 TSL's good performance aspect 94
Figure 4-2 Thin liners applied in a haulage passage 95

Figure 4-3 Aspect of TSL near the footwall in an active area 95
Figure 4-4 Case of TSL's loss of adhesion near the footwall 96
Figure 4-5 De-bonding of TSL at a borehole entrance 97
Figure 4-6 Loss of TSL's adhesion in a stable rock mass environment 98
Figure 4-7 Aspect of moisture conditions (a) halfway up the wall , and (b) near the footwall 98
Figure 4-8 Adhesion strength loss of TSL near the footwall 99
Figure 4-9 TSL used as stand-alone support close to an abandoned mining area 100
Figure 4-10 TSL used in combination with other conventional supports close to an abandoned mining area 101
Figure 4-11 TSL combined with other conventional supports in a disturbed mining zone 102
Figure 4-12 Adhesion failure of TSL on a roof 103
Figure 4-13 Adhesion failure of TSL on a wall 104
Figure 4-14 TSLs affected by humidity conditions (a) near the roof, and (b) on the sidewall 105
Figure 4-15 Young TSL bad performance near the footwall 106
Figure 4-16 Poor performance of "Young TSL" in dry and humid conditions 107
Figure 4-17 TSL1 applied close to the footwall 110
Figure 4-18 TSL combined with cable anchors and resin bolts 111
Figure 4-19 TSL applied in humid zone 112
Figure 4-20 TSL performance aspect in section 13 E 112
Figure 4-21 TSL applied on a pillar prone to scaling 113
Figure 4-22 TSL applied on a roof prone to falls of ground 114
Figure 5-1 MTS model 643.15A – 03 119
Figure 5-2 Amsler compressive testing machine 120
Figure 5-3 Load cell type S calibration 121
Figure 5-4 Details on circuit connectivity of load cell transmitter TR-3 shown through (a) snapshot of the input selection, and (b) circuit configuration 122

Figure 5-5 Proportionality between kilograms and millivolts readings from load cell S type 123
Figure 5-6 (a) Preparation of TSL mixture and (b) Electric mixer (Kanda and Stacey, in press)..... 124
Figure 5-7 Pouring and levelling down of TSL mixtures (Kanda and Stacey, in press)..... 126
Figure 5-8 Ongoing UTS test on the MTS 643 under room environmental conditions 127
Figure 5-9 Design of UTS creep testing machine (M3) – Perspective Solid.... 130
Figure 5-10 UTS creep testing machine (M3) in operation 130
Figure 5-11 Relationship between M3 input (kg) and output (mV) loads..... 131
Figure 5-12 Relationship between onset load and on-specimen load of M3 132
Figure 5-13 (a) Displacement transducer gripped to a dog-bone specimen, and (b) Sample of transducers' dummies for Wheatstone bridge 133
Figure 5-14 Relationship between displacement on M3 transducer's grips and output voltage 134
Figure 5-15 Sample of some TSL dog-bone specimens (TSL1, TSL2, and TSL3) tested on the MTS 643 at various environmental conditions 136
Figure 5-16 TSL1 tensile strength sensitivity to environmental conditions 136
Figure 5-17 TSL2 tensile strength sensitivity to environmental conditions 137
Figure 5-18 TSL3 sensitivity to environmental conditions..... 138
Figure 5-19 TSL1 stress-strain behaviours after various exposure periods in (a) room conditions, (b) saturated conditions, and (c) humidity and high temperature conditions. (d – Days; mstr – millistrain)..... 140
Figure 5-20 TSL2 stress-strain behaviours after various exposure periods in (a) room conditions, (b) saturated conditions, and (c) humidity and high temperature conditions. (d – Days; mstr – millistrain)..... 142
Figure 5-21 TSL3 stress-strain behaviours after various exposure periods in (a) room conditions, (b) saturated conditions, and (c) humidity and high temperature conditions. (d – Days; mstr – millistrain)..... 144
Figure 5-22 Impact of environmental conditions on (a) tensile strengths, (b) elongations and (c) moduli of TSL1..... 146

Figure 5-23 Impact of environmental conditions on (a) tensile strengths, (b) elongations and (c) moduli of TSL2 147
Figure 5-24 Impact of environmental conditions on (a) tensile strengths, (b) elongations and (c) moduli of TSL3 148
Figure 5-25 TSL dog-bone specimen failed at creep test 151
Figure 5-26 Semi-logarithmic graphs of TSL1 UTS creep behaviours tested in room condition (≈2days – 2896 min; ≈6days – 8624 min; ≈11.5days – 16572 min) 153
Figure 5-27 Semi-logarithmic graphs of TSL1 UTS creep behaviours tested in humid condition (≈8hours – 485 min; ≈2days – 2853 min; ≈6.25days – 8996 min; ≈10.5days – 15124 min) 155
Figure 5-28 Estimation of TSL long-term uniaxial tensile strengths through plotting of time-to-failure strengths from room and humid conditions (R-room condition; H-humid condition) 156
Figure 5-29 TSL coating on a sidewall with an extension crack 157
Figure 5-30 (a) cored disc of shotcrete, (b) Panel of precast shotcrete 158
Figure 5-31 Coating phase of shotcrete discs with TSL 159
Figure 5-32 Final aspect of a coated BIT specimen with shaped coating 160
Figure 5-33 Rubber sleeves used to mould TSLs 161
Figure 5-34 (a) Ongoing BIT test on the MTS 643 under room environmental condition, and (b) Shape of BIT stress-displacement curve 162
Figure 5-35 BIT creep testing machine M1 164
Figure 5-36 BIT creep testing machine M4 165
Figure 5-37 BIT Creep testing machines (a) M1, (b) M4 and (c) M5 at practical state 165
Figure 5-38 Proportionality between onset loads in kg and output mV for BIT creep testing machine M1 167
Figure 5-39 Load Factor and dead weight determination for BIT creep testing machine M1 167
Figure 5-40 Proportionality between onset loads in kg and output mV for BIT creep testing machine M4 168

Figure 5-41 Load Factor and dead weight determination for BIT creep testing machine M4 169
Figure 5-42 Proportionality between onset loads in kg and output mV for BIT creep testing machine M5 170
Figure 5-43 Load Factor and dead weight determination for BIT creep testing machine M5 170
Figure 5-44 Displacement transducer for BIT specimens 171
Figure 5-45 Gripping of the BIT displacement transducer to a shotcrete disc . 172
Figure 5-46 Displacement transducer's dummy 173
Figure 5-47 Relationship between horizontal displacements of M1 transducer's grips and output voltages 174
Figure 5-48 Relationship between horizontal displacements of M4 transducer's grips and output voltages 174
Figure 5-49 Relationship between horizontal displacements of M5 transducer's grips and output voltages 175
Figure 5-50 Samples of tested specimens of (a) uncoated shotcrete, (b) TSLs, and (c) coated shotcrete discs 177
Figure 5-51 Uncoated shotcrete discs sensitivity to environmental conditions 178
Figure 5-52 BIT strength sensitivity to environmental conditions for TSL1 179
Figure 5-53 BIT strength sensitivity to environmental conditions for TSL2 179
Figure 5-54 BIT strength sensitivity to environmental conditions for TSL3 180
Figure 5-55 Coated BIT shotcrete sensitivity to environmental conditions for TSL1 181
Figure 5-56 Enhancing strength effect of TSL1 on shotcrete BIT substrates in various environmental conditions 182
Figure 5-57 Coated BIT shotcrete sensitivity to environmental conditions for TSL2 183
Figure 5-58 Enhancing strength effect of TSL2 on shotcrete BIT substrates in various environmental conditions 184
Figure 5-59 Coated BIT shotcrete sensitivity to environmental conditions for TSL3 185

Figure 5-60 Enhancing strength effect of TSL3 on shotcrete BIT substrates in various environmental conditions..... 185
Figure 5-61 Comparisons of vertical displacements of shotcrete and TSL's BIT after 15 days of exposure in (a) Room, (b) Saturated and (c) HT conditions. 187
Figure 5-62 Comparisons of vertical displacements of shotcrete and TSL's BIT after 28 days of exposure in (a) Room, (b) Saturated and (c) HT conditions 187
Figure 5-63 Comparisons of vertical displacements of shotcrete and TSL's BIT after 112 days of exposure in (a) Room, (b) Saturated and (c) HT conditions 188
Figure 5-64 Failure shape of a coated shotcrete under creep loading..... 190
Figure 5-65 Creep behaviour of BIT coated shotcrete with TSL1 tested in room condition at 75% of the ultimate load..... 191
Figure 5-66 Comparison of long-term BIT strengths of coated shotcrete with TSL1 tested in room and humid conditions (R-room condition; H-humid condition) 196
Figure 5-67 (a) Pouring and levelling up of TSL mixture on an MBT substrate, (b) MBT specimen ready for testing 198
Figure 5-68 (a) Aspect of MBT specimen just after testing; (b) Aspect of MBT specimen tested in preparation for reutilization 199
Figure 5-69 Grinding of an MBT substrate surface for re-utilization..... 199
Figure 5-70 MBT specimen placed in the MTS 643 before testing..... 201
Figure 5-71 Membrane displacement test (MBT) load-displacement graph (Kanda and Stacey, 2019)..... 202
Figure 5-72 Design of MBT creep testing machine (M2) - Perspective Solid View 206
Figure 5-73 MBT specimen under creep test..... 207
Figure 5-74 Setting up of MBT creep machine loading calibration 208
Figure 5-75 Proportionality between onset loads in kg and output mV for MBT creep testing machine 209

Figure 5-76 Load Factor and dead weight determination for creep testing machine M2 209
Figure 5-77 Relationship between vertical displacements of M2 transducer's arms at contact points and output voltage 210
Figure 5-78 MBT strength sensitivity to environmental conditions for TSL1 . 212
Figure 5-79 MBT strength sensitivity to environmental conditions for TSL2 . 213
Figure 5-80 MBT strength sensitivity to environmental conditions for TSL3 . 214
Figure 5-81 Representative curves of MBT tests for TSL1 after 28 days of exposure in R and H conditions..... 215
Figure 5-82 Representative curves of MBT tests for TSL1 after 56 days of exposure in R and H conditions..... 215
Figure 5-83 Representative curves of MBT tests for TSL1 after 112 days of exposure in R and H conditions..... 216
Figure 5-84 Representative curves of MBT tests for TSL2 after 28 days of exposure in R and H conditions..... 217
Figure 5-85 Representative curves of MBT tests for TSL2 after 56 days of exposure in R and H conditions..... 217
Figure 5-86 Representative curves of MBT tests for TSL2 after 112 days of exposure in R and H conditions..... 218
Figure 5-87 Representative curves of MBT tests for TSL3 after 28 days of exposure in R and H conditions..... 219
Figure 5-88 Representative curves of MBT tests for TSL3 after 56 days of exposure in R and H conditions..... 219
Figure 5-89 Representative curves of MBT tests for TSL3 after 112 days of exposure in R and H conditions..... 220
Figure 5-90 Comparison of MBT curves of TSLs exposed to R condition for 112 days..... 221
Figure 5-91 Comparison of MBT curves of TSLs exposed to H condition for 112 days..... 222
Figure 5-92 MBT specimen failed at creep test..... 224
Figure 5-93 Semi-logarithmic graphs of TSL1 MBT creep behaviours tested in room condition..... 226

Figure 5-94 Semi-logarithmic graphs of TSL1 MBT creep behaviours tested in humid condition 227
Figure 5-95 Estimation of TSL long-term membrane displacement test strengths through plotting of time-to-failure strengths from room and humid conditions 228
Figure 5-96 Sample of UCS specimens of shotcrete (SN'P1) and TSLs (TC'C and TC'T) with glued-on strain gauges 230
Figure 5-97 Representative UCM stress-strain curves of Shotcrete (mstr – millistrain) 231
Figure 5-98 UCS behaviours of TSLs tested after various exposure times in room condition 233
Figure 5-99 Comparison of trends of TSL1 UCS after various exposure times in R and HT conditions 234
Figure 5-100 Comparison of trends of TSL2 UCS after various exposure times in R and HT conditions 234
Figure 5-101 Comparison of trends of TSL3 UCS after various exposure times in R and HT conditions 235
Figure 5-102 Hoek cell used for Triaxial compressive strength 236
Figure 5-103 Aspect of TSL specimens tested to triaxial compressive strength 238
Figure 5-104 Measurement of the value of the beta angle 238
Figure 5-105 Mohr envelopes of shotcrete's Triaxial compressive strength test results from R and HT conditions 239
Figure 5-106 Mohr envelopes of TSL1 Triaxial compressive strength test results after 28 days of exposure in R and HT conditions 240
Figure 5-107 Mohr envelopes of TSL1 Triaxial compressive strength test results after 112 days of exposure in R and HT conditions 240
Figure 6-1 Snapshot of a coated BIT model 251
Figure 6-2 Snapshot of RSM staging for PoF determination of room coated BIT disc 254
Figure 6-3 PoF chart for Room coated BIT disc created through Oracle Crystal Ball 254

Figure 6-4 RSM staging for PoF determination of HT coated BIT disc..... 255
Figure 6-5 PoF chart for HT coated BIT disc created through Oracle Crystal Ball 256
Figure A-1 tensile creep testing machine (M3) – Solid Perspective 295
Figure A-2 Tensile creep testing machine (M3) - Front View..... 296
Figure A-3 Tensile creep testing machine (M3) - Right View 297
Figure A-4 Tensile creep testing machine (M3) - Top View..... 298
Figure B-1 Brazilian indirect tensile creep testing machine (M1)-Perspective solid view..... 299
Figure B-2 Brazilian indirect tensile creep testing machine (M1)-Perspective drawing view 300
Figure B-3 Brazilian Indirect Tensile creep testing machine (M1) – Front View.. 301
Figure B-4 Brazilian Indirect Tensile creep testing machine (M1) – Right View.. 302
Figure C-1 Brazilian Indirect Tensile creep machine (M4) for high temperature testing – Perspective solid View..... 303
Figure C-2 Brazilian Indirect Tensile creep machine (M4) for high-temperature testing – Front View 304
Figure C-3 Brazilian Indirect Tensile creep machine (M4) for high-temperature testing – Top View 305
Figure D-1 Membrane displacement testing machine (M2) – Perspective solid View 306
Figure D-2 Membrane displacement testing machine (M2) – Perspective drawing View 307
Figure D-3 Membrane displacement testing machine (M2) – Front View..... 308
Figure D-4 Membrane displacement testing machine (M2) – Right View..... 309
Figure F-1 Calibrating equation of M3 displacement transducer 313
Figure F-2 Calibrating equation of M1 displacement transducer 313
Figure F-3 Calibrating equation of M4 displacement transducer 314
Figure F-4 Calibrating equation of M5 displacement transducer 314
Figure F-5 Calibrating equation of M2 displacement transducer 315

Figure J-1 Comparative charts of performances of shotcrete and TSLs combined BIT strengths and elongation after 15 days of exposure to various environmental conditions 328
Figure J-2 Comparative charts of performances of shotcrete and TSLs combined BIT strengths and elongation after 28 days of exposure to various environmental conditions 328
Figure J-3 Comparative charts of performances of shotcrete and TSLs combined BIT strengths and elongation after 112 days of exposure to various environmental conditions 329
Figure K-1 Young's modulus behaviour of TSL1 after exposures in R conditions 330
Figure K-2 Poisson's ratio behaviour of TSL1 after exposures in R conditions 330
Figure K-3 Young's modulus behaviour of TSL2 after exposures in R conditions 331
Figure K-4 Poisson's ratio behaviour of TSL2 after exposures in R conditions 331
Figure K-5 Young's modulus behaviour of TSL3 after exposures in R conditions 332
Figure K-6 Poisson's ratio behaviour of TSL3 after exposures in R conditions 332
Figure L-1 UTS creep behaviour of TSL1 specimens tested in room condition at 92% of the ultimate load..... 333
Figure L-2 UTS creep behaviour of TSL1 specimens tested in room condition at 82% of the ultimate load..... 333
Figure L-3 UTS creep behaviour of TSL1 specimens tested in room condition at 78% of the ultimate load..... 334
Figure L-4 UTS creep behaviour of TSL1 specimens tested in room condition at 62% of the ultimate load..... 334
Figure L-5 UTS creep behaviour of TSL1 specimens tested in room condition at 58% of the ultimate load..... 335

Figure L-6 UTS creep behaviour of TSL1 specimens tested in room condition at 55% of the ultimate load..... 335
Figure L-7 UTS creep behaviour of TSL1 specimens tested in humid condition at 34% of the room ultimate load 336
Figure L-8 UTS creep behaviour of TSL1 specimens tested in humid condition at 29% of the room ultimate load 336
Figure L-9 UTS creep behaviour of TSL1 specimens tested in humid condition at 22% of the room ultimate load 337
Figure L-10 UTS creep behaviour of TSL1 specimens tested in humid condition at 18.2% of the room ultimate load 337
Figure L-11 UTS creep behaviour of TSL1 specimens tested in humid condition at 16.8% of the room ultimate load 338
Figure M-1 MBT creep behaviour of TSL1 specimens tested in room condition at 98% of the ultimate load..... 339
Figure M-2 MBT creep behaviour of TSL1 specimens tested in room condition at 95% of the ultimate load..... 339
Figure M-3 MBT creep behaviour of TSL1 specimens tested in room condition at 85% of the ultimate load..... 340
Figure M-4 MBT creep behaviour of TSL1 specimens tested in room condition at 67.1% of the ultimate load..... 340
Figure M-5 MBT creep behaviour of TSL1 specimens tested in room condition at 54.3% of the ultimate load..... 341
Figure M-6 MBT creep behaviour of TSL1 specimens tested in room condition at 52.1% of the ultimate load..... 341
Figure M-7 MBT creep behaviour of TSL1 specimens tested in room condition at 50.8% of the ultimate load..... 342
Figure M-8 MBT creep behaviour of TSL1 specimens tested in humid condition at 58% of the room ultimate load 342
Figure M-9 MBT creep behaviour of TSL1 specimens tested in humid condition at 47% of the room ultimate load 343
Figure M-10 MBT creep behaviour of TSL1 specimens tested in humid condition at 45% of the room ultimate load 343

Figure M-11 MBT creep behaviour of TSL1 specimens tested in humid condition at 41% of the room ultimate load 344
Figure M-12 MBT creep behaviour of TSL1 specimens tested in humid condition at 34% of the room ultimate load 344
Figure M-13 MBT creep behaviour of TSL1 specimens tested in humid condition at 32% of the room ultimate load 345
Figure M-14 MBT creep behaviour of TSL1 specimens tested in humid condition at 29% of the room ultimate load 345
Figure O-1 Generation of rock properties through RocData package 349

LIST OF TABLES

Table 2-1 List of TSL products and their compositions (Modified after Yilmaz, 2011)..... 17
Table 2-2 Technical Properties of TSL2..... 21
Table 2-3. TSL3 Strength Properties after 28 Days..... 22
Table 2-4 Equations of TSL Tensile Mechanical Behaviour (Guner and Ozturk, 2016)..... 24
Table 2-5 Some TSL applications in Underground mines (Guner and Ozturk, 2016)..... 28
Table 2-6 TSLs testing methods (Modified after Potvin *et al,* 2004; Yilmaz, 2011) 35
Table 2-7 Comparison of TSL tensile strengths obtained from suppliers 40
Table 2-8 MBT results from various TSLs..... 45
Table 3-1 Constitutive and creep equations for some rheological models under single-step loading (Yang *et al*, 2018) 69
Table 3-2 Description of employed strain gauges 73
Table 3-3 Characteristics of power supply for the research..... 77
Table 4-1 Field Enquiries..... 82
Table 4-2 Summary of feedback from interviews with TSL's suppliers and users (Kanda and Stacey, 2019)..... 86
Table 4-3 Case of interaction between a supplier and a geotechnical inspector regarding an applied TSL (Kanda and Stacey, 2019)..... 90
Table 5-1 Specification of the electric mixer..... 125
Table 5-2 Weighing parameters of tensile creep machine..... 132
Table 5-3 Determination of average 100% creep load for TSL1 UTS in room condition..... 152
Table 5-4 Determination of average 100% creep load for TSL1 UTS in humid condition..... 154
Table 5-5 Weighing parameters of BIT creep testing machine M1..... 168
Table 5-6 Weighing parameters of BIT creep testing machine M4..... 169
Table 5-7 Weighing parameters of BIT creep testing machine M5..... 171

Table 5-8 Converting equations of voltage outputs into specimen displacements for BIT creep testing machines..... 176
Table 5-9 Statistics of representative BIT strengths for specimens exposed in room, humid, and humidity and high temperature conditions..... 181
Table 5-10 Determination of average 100% creep strength for shotcrete coated with TSL1 and tested in room condition on the BIT creep testing machine “M1” (SCLT_R: S-shotcrete, C-coated, LT-long-term, R-room condition) 192
Table 5-11 Determination of average 100% creep strength for shotcrete coated with TSL1 and tested in humid condition on the BIT creep testing machine “M4” (SCLT_H: S-shotcrete, C-coated, LT-long-term, H-humid condition) 192
Table 5-12 Recorded data from BIT creep tests on shotcrete specimens coated with TSL1 and exposed to room condition (N/A- Not available), (SCLT_R: S-shotcrete, C-coated, LT-long-term, R-room condition) 194
Table 5-13 Recorded data from BIT creep tests on shotcrete specimens coated with TSL1 and exposed to humid condition (N/A- Not available), (SCLT_R: S-shotcrete, C-coated, LT-long-term, H-humid condition)..... 195
Table 5-14 MBT results from various TSLs (Modified after Kanda and Stacey, 2019)..... 203
Table 5-15 Some invariant parameters of the MBT..... 205
Table 5-16 Weighing parameters of MBT creep testing machine 210
Table 5-17 Determination of MBT indicators for TSL1 after R and H exposures. 216
Table 5-18 Determination of MBT indicators for TSL2 after R and H exposures. 218
Table 5-19 Determination of MBT indicators for TSL3 after R and H exposures. 220
Table 5-20 Comparison of MBT indicators for 112 days of exposure under R and H conditions..... 223

Table 5-21 Determination of average 100% creep load for TSL1 MBT in room condition 225
Table 5-22 Determination of average 100% creep load for TSL1 MBT in humid condition 227
Table 5-23 Averages of UCS tests on shotcrete material for R conditioning... 232
Table 5-24 Averages of UCS tests on shotcrete material for HT conditioning 232
Table 5-25 Resulting cohesions and angles of internal friction of various liners tested in R and HT conditions (TCS-Triaxial compressive strength, R-room condition, HT- Humid and high temperature condition) 241
Table 6-1 Input parameters of the coated BIT model for room conditions (N/A – Not available) 252
Table 6-2 Input parameters of the coated BIT model for HT conditions (N/A – Not available) 253

Table E-1 Result of trials for calibration of load cell type S readings on the data logger 310
Table E-2 Result of trials for M3 creep testing machine calibration 310
Table E-3 Result of trials for M1 creep testing machine calibration 311
Table E-4 Result of trials for M4 creep testing machine calibration 311
Table E-5 Result of trials for M5 creep testing machine calibration 312
Table G-1 Statistics of TSL1 UTS under various environmental conditions ... 316
Table G-2 Statistics of TSL2 UTS under various environmental conditions ... 317
Table G-3 Statistics of TSL3 UTS under various environmental conditions ... 318
Table H-1 Uniaxial tensile strengths, strains at failure and moduli of TSL1, TSL2 and TSL3 after various exposure times in room condition (R - room condition; mstr - millistrain)..... 319
Table H-2 Uniaxial tensile strengths, strains at failure and moduli of TSL1, TSL2 and TSL3 after various exposure times in humid condition (H - humid condition; mstr - millistrain)..... 319

Table H-3 Uniaxial tensile strengths, strains at failure and moduli of TSL1, TSL2 and TSL3 after various exposure times in humid and high temperature condition (HT – humid and high temperature condition; mstr - millistrain)..... 320
Table I-1 Statistics of uncoated BIT of shotcrete under Room condition..... 321
Table I-2 Statistics of uncoated BIT of shotcrete under saturated condition.... 322
Table I-3 Statistics of uncoated BIT of shotcrete under combined humid and high temperature condition..... 322
Table I-4 Statistics of shotcrete BIT specimens coated with TSL1, exposed to room condition..... 323
Table I-5 Statistics of shotcrete BIT specimens coated with TSL1, exposed to humid condition..... 324
Table I-6 Statistics of shotcrete BIT specimens coated with TSL1, exposed to humid and high temperature condition..... 324
Table I-7 Statistics of shotcrete BIT specimens coated with TSL2, exposed to room condition..... 325
Table I-8 Statistics of shotcrete BIT specimens coated with TSL2, exposed to humid condition..... 325
Table I-9 Statistics of shotcrete BIT specimens coated with TSL2, exposed to humid and high temperature condition..... 326
Table I-10 Statistics of shotcrete BIT specimens coated with TSL3, exposed to room condition..... 326
Table I-11 Statistics of shotcrete BIT specimens coated with TSL3, exposed to humid condition..... 327
Table I-12 Statistics of shotcrete BIT specimens coated with TSL3, exposed to humid and high temperature condition..... 327
Table N-1 Results of Triaxial compressive tests of shotcrete for R and HT conditions 346
Table N-2 Results of Triaxial compressive tests of TSL1 for R and HT conditions 347
Table N-3 Results of Triaxial compressive tests of TSL2 for R and HT conditions 348

Table N-4 Results of Triaxial compressive tests of TSL3 for R and HT conditions 348
Table P-1 Sample showing the extent of data collected from a UTS creep test through channel 5 (CH5), and with failure time of 2 minutes 23 seconds 350

LIST OF SYMBOLS AND ACRONYMS

σc: Compressive strength (MPa)

σt: Tensile strength (MPa)

σ1: Major principal stress (MPa)

σ2: Intermediate principal stress (MPa)

σ3: Minor principal stress (MPa)

c: Cohesion (MPa)

ϕ: Angle of internal friction (°)

%: Percent

ASTM: American Society for Testing and Materials

BIC: Bushveld Igneous Complex

BIT: Brazilian Indirect Tensile

CoV: Coefficient of variation

CR: Containment Ratio

CS: Containment Strength

CSIR: The Council for Scientific and Industrial Research

EFNARC: European Federation of National Associations Representing for Concrete

FLAC: Fast Lagrangian Analysis of Continua

FOG: Fall of ground

FoS: Factor of Safety

G: Shear modulus (GPa)

GSI: Geological Strength Index

H: Humid condition

HPU: Hydraulic Pump Unit

HT: Humid and high temperature condition

Hz: Hertz

ISRM: International Society of Rock Mechanics

K: Bulk modulus (GPa)

LVDT: Linear Variable Displacement Transducer

MBT: Membrane Displacement Test

MBTS: Membrane Displacement Test Strength

MCS: Moment of containment strength

MIROC: Mining Industry Research Organisation of Canada

MTS: Material Testing Systems

MPa: Mega Pascal

mV: millivolt

PGM: Platinum Group Metals

PoF: Probability of Failure

R: Room condition

RCS: Relative Containment Strength

RMR: Rock Mass Rating

RS3: Rock and Soil 3-dimensional (analysis program)

RSM: Response Surface Methodology

SANIRE: South African National Institute of Rock Engineering

TCS: Triaxial Compressive Strength

TSL: Thin Spray-on Liner

UCS: Uniaxial Compressive Strength

UTS: Uniaxial Tensile Strength

VRM: Vertical Retreat Mining

VRT: Virgin Rock Temperature

CHAPTER 1 INTRODUCTION

1.1 Background

Geotechnical hazards in deep-level mining environments are closely linked to rock-related accidents (Potvin *et al*, 2004; Szwedzicki, 2003). This also applies in South African underground mines where, for the year 2018 alone, the number of fatalities was 81, compared with 90 fatalities in the previous year (Minerals Council South Africa, 2018). The year 2017 saw a fatality increment due to rockburst and its consequent fall of ground (FOG) incidents. There is, however, a general declining trend of fatalities. The reduction in mining fatalities represents about 88% since 1993. Nevertheless, although rock-related fatalities have also generally decreased since 1997, as can be seen in Figure 1-1, they remain the highest cause.

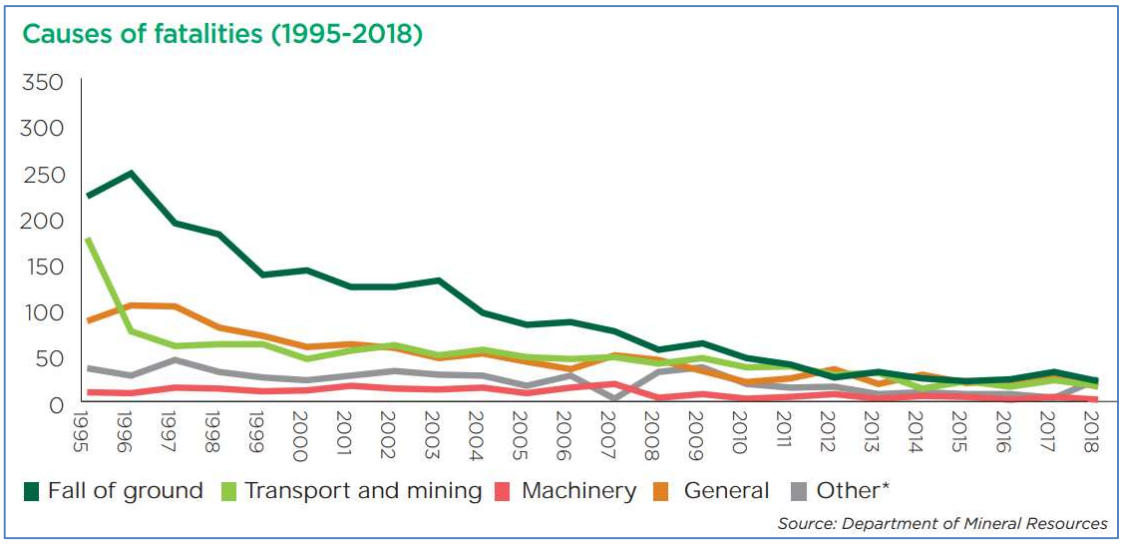


Figure 1-1 Cause of fatalities in the South African mining industry between 1995 and 2018 (*Minerals Council South Africa*, 2018)

Although the statistics from the Department of Mineral Resources, published by the Minerals Council South Africa, formerly called Chamber of Mines of South Africa, show a general decrease in the contribution of FOG related fatalities, the belief is that there still room for improvement.

For many years, in the quest of mitigating rock-related accidents, various techniques have been adopted and used to improve safety in the mining environment. Rockbolts-and-mesh support has been one of the rock mass stabilization methods widely used in the mines and has shown good performance. However, although the installation of rock-bolts can be mechanized, this is much more difficult in the case of wire mesh, and this difficulty of mechanization has led to miners opting instead for shotcrete, especially steel-fibre reinforced shotcrete. Yet shotcrete usage also has constraints, such as the logistics associated with the transportation of large quantities, which is not always easy to handle. Additionally, it is argued that the use of shotcrete in deep tunnels is inefficient since the rock deformations may exceed its displacement capacity (Potvin, Stacey and Hadjigeorgiou, 2004). As an alternative to shotcrete, some mines have made use of Thin Spray-on liners (TSLs), introduced more than 25 years ago, which are also referred to in this thesis's research as thin sprayed membranes, multi-component polymeric (based) liners, thin coatings (materials), or thin liners. This type of areal support can be defined as a polymer-based fibre, employed to span large cracks in the rock mass since it bonds tenaciously with the rock surfaces (Tannant, 2001). TSLs have given satisfactory results, particularly due to their characteristics of high tensile and bond strengths (Potvin *et al*, 2004).

1.2 Statement of the Problem

Although TSL's mechanical behaviours have shown promising results, and clear benefits, which have been evidenced by their extensive usage, these liners are not unanimously accepted and used in the mining industry. The fact that they are not structural supports, and probably when performing in extreme environmental conditions has resulted in some scepticism about their wider usage in the mining environment. This scepticism has increased since there is no documented, convincing reported information regarding TSL performance in the mines where it has been employed. This lack of suitable evidence on TSL applications constitutes a limitation to the perceived reliability of TSLs, an opinion held by many mining companies.

1.3 **Aim and Objectives**

This thesis's research intends to fill the gap identified by researchers such as Tannant (2001) and Mpunzi *et al* (2015) who stipulated that there is a need for documenting the performance of TSLs from actual mining experiences.

The thesis's research aims to produce evidence of TSL performance from actual mine experiences such that its reliability might be assessed and well known. Thus the study intends to assess the performance of TSLs, especially for long-term usage. The following are the specific objectives of the thesis research:

- To provide documented evidence of TSL performance in practice, including the identification of those field activities that may enhance or inhibit the good performance of TSLs, and the provision of information that will represent good practice guidelines for the application of TSLs to promote stability.
- To identify conditions in which TSLs can replace shotcrete applications or conditions when TSLs need to be combined with shotcrete (and/or other surface support elements such as wire mesh) for optimal support in underground mines.
- To investigate the long-term effectiveness and value of TSLs in supporting deep underground excavations.
- To conduct numerical models that will assist to understand TSLs performance in underground mines and may provide information for the design of rock support using TSLs.

The proposed research is essentially an assessment of the possibility of using TSLs as permanent supports. This may increase the interest in using polymeric liners, as they have generally been employed only as temporary supports. They might then be recommended for wider underground usage, and sometimes as a substitute for wire mesh, the latter being a laborious and time-consuming methodology that could be hazardous to the personnel working in the mine. Furthermore, the research

should also be capable of defining the limitations of TSL supports, and therefore prevent their applications wherever their performance might be prejudicial to mine safety as well as to the amounts budgeted for the mine's support systems.

1.4 **Research Methodology**

The methodology opted for this thesis's research is detailed as follows:

- Detailed review of relevant literature that connects the proposed research to previous works

- Collection of data from the mining industry through questionnaire and interaction that aims to identify the practical factors capable of influencing TSL performances, as observed by the mines' users

- Visual survey of specific zones where TSLs have been applied, particularly the zones that are prone to weathering, spalling, and high-stress conditions, etc.

- Collection of information from the mines' suppliers about the available TSL types and analysis of the mines' databases on their performances; and collection of TSL material from suppliers/manufacturers for laboratory testing

- Preparation of Uniaxial Tensile Strength (UTS), Brazilian Indirect Tensile (BIT), and Membrane Displacement Test (MBT) specimens for short-term and long-term tests

- Exposure of the prepared specimens to various environmental conditions for scheduled periods

- Laboratory trials of UTS specimens of TSLs after various exposure times, and to various environmental conditions, using the traditional short-term testing procedure (through a Material Testing System (MTS) equipment)

- Laboratory testing of BIT specimens of TSLs, the substrate (shotcrete) and coated substrates after various exposure periods, and to various environmental conditions, using an MTS for short-term trials

- Laboratory testing of MBT specimens after various exposure times, and to various environmental conditions, for short-term trials

- Long-term UTS testing of TSL specimens under various environmental conditions, using creep testing machines

- Long-term trials of BIT specimens coated substrates under various environmental conditions, using creep testing machines

- Creep trials of MBT specimens under various environmental conditions, using creep testing machines

- Uniaxial Compressive Strength (UCS) and Triaxial Compressive Strength (TCS) tests of TSLs and shotcrete (substrate) to understand the mechanical behaviour of the used materials, and for collection of data to be used for numerical modelling

- Numerical modelling of TSL behaviour using the properties that are characteristic of TSL's underground mines properties

- Data analyses and assessment of long-term performance of TSLs for usage as underground mining support

- Recommendations for TSL good performance when used as long-term support in underground mines

1.5 Envisaged Contribution to Knowledge

The current research intends to provide information concerning TSL performance in real mining environments with consideration given to the practical environmental conditions of deep underground mines. The latter information does not currently exist. Indeed, to our knowledge, humidity and temperature impacts on TSL performance — taking into account a relatively longer exposure — will be presented in the literature for the first time through this endeavour. These parameters will be included in some traditional TSL tests to approximate the real mechanisms of TSLs in underground mines. They will also be considered in creep tests, which have just recently been introduced in literature by Guner and Ozturk (2018). The proposed information could serve as guidelines to further decisions-making on the application of thin spray-on membranes, and it is expected to dissipate the scepticism around the use of TSLs in the mining industry. The proposed research outcomes should also be able to provide the means of quantifying the reliability of TSLs in underground mines, which is a powerful index for TSL users to confidently decide on whether to use them.

1.6 Layout of the Thesis

As introduced earlier, the research aim of this thesis is to assess the long-term performance of TSLs for use as permanent support in underground mines. To meet this aim, CHAPTER 1 introduced the subject matter of this work by mentioning the reasons for embarking on the research, the aim, a brief explanation of the methodology and the contribution to knowledge. In CHAPTER 2, the characteristics of thin spray-on liners and other areal supports are presented. CHAPTER 2 also discusses relevant work done on TSL performance for usage in underground mines. CHAPTER 3 elaborates on the time-dependency concepts in the mining environment and proposes some designs of long-term easy-to-handle testing machines that should be used later in this thesis's research. CHAPTER 4

presents the undertaken fieldwork that aimed to assess TSLs in-situ performances. All the laboratory trials of TSL performances are described in CHAPTER 5. CHAPTER 6 analyses the numerical modelling applications of TSLs when used in underground mines-like conditions. CHAPTER 7 and CHAPTER 8 respectively present the discussions and conclusions on the findings, followed by CHAPTER 9, which proposes a framework to a guideline for TSL's good performance, especially as long-term support in underground mines.

CHAPTER 2 CHARACTERISTICS OF THIN SPRAY-ON LINERS AND OTHER AREAL SUPPORTS

2.1 General Statement on Ground Support Tools

For many years, rock-bolts and wire mesh have been used as underground supports in the mining industry (Hoek, Kaiser and Bawden 2000; Stacey, 2001b; Tannant 2001; Zhenjun *et al*, 2014). They have widely contributed to minimizing geotechnical disasters related to rock mass instability. However, the time taken for installation of rock bolts and wire mesh support is considered high, and the installation is hazardous and laborious (Tannant, 2001). To overcome these constraints, miners have resorted to other types of supports such as shotcrete (Potvin *et al*, 2004), with the steel reinforced shotcrete being the most common (Tannant, 2001). This areal support has seen its reliability increasing, especially in Canada in the 1990s (Spearing and Champa, 2000; Tannant, 2001; Morton, Thompson and Villaescusa, 2008; Mpunzi, 2012). But its adoption is constrained by the difficulty of transporting large quantities of material to active underground areas and by its limited ability to withstand deformations (Potvin *et al*, 2004). Its performance may be perceived from Figure 2-1, which illustrates the deformation behaviour of various support types under loading conditions.

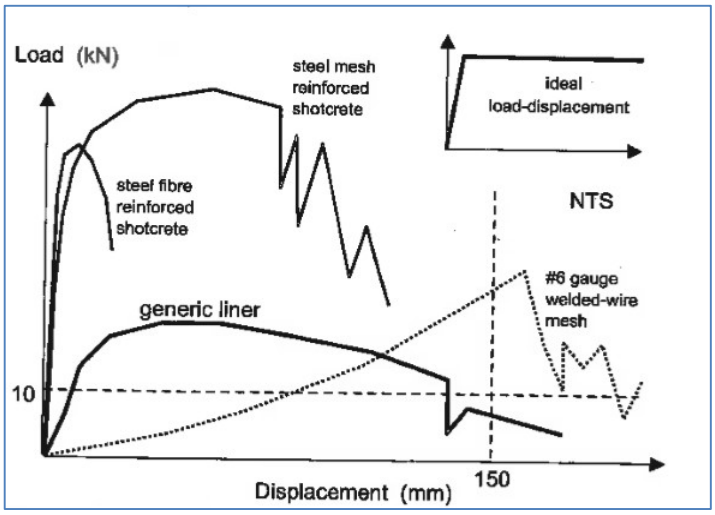


Figure 2-1 Load versus displacement capacities from pull tests of various areal supports (Tannant, 2001)

Figure 2-1 shows the limited ability of shotcrete to resist deformation. It is noticed that the reinforcement of shotcrete enhances its ability to resist displacements, but this ability cannot be compared with welded wire mesh or the generic liners, which can perform much better. Generic liners were then investigated as an alternative to the use of shotcrete by organizations such as MIROC (Mining Industry Research Organisation of Canada) (Tannant, 2001; Yilmaz, 2011). However to date, no conclusive and particularly reliable outcomes have been produced for the use of thin membranes in replacement of shotcrete.

Originally, the adopted type of TSL was Mineguard (Archibald, Mercer and Lausch, 1992; Masethe, 2015; Potvin *et al*, 2004), which is a polyurethane-based product. Then came Rockguard. The latter TSL is a hybrid polyurethane mixture of Mineguard (Espley, O'Donnell, Thibodeau and Paradis-Sokoloski, 1996; Lacerda, 2004; Tannant, 1997; Tannant, Swan, Espley and Graham, 1999). Besides these polyurethane-based products, other TSLs were used, such as the latex-based liner called Everbond (Wojno and Kuijpers, 1997), assessed by South African researchers from the year 1996. The latex liner then evolved into the product Evermine (Potvin *et al*, 2004). Nowadays there are numerous different TSL products available in the market.

TSLs have proven to have a particular characteristic not found in shotcrete behaviour, which is the caisson effect, as described by Gyenge and Coates (1972). These researchers defined it as an effect of creating an impermeable barrier to differential pressures. These pressures might generate sufficient pressure disequilibrium resulting in the prevention of gravity falls of rocks. Finn, Teasdale, and Windsor (1999) followed the same trend, researching on the caisson effect. They characterized it as an air tightness capable of limiting rock mass dilation and failure.

Despite the growing interest in TSL coatings, mines are still sceptical regarding their usage (Mpunzi *et al*, 2015). Researchers such as Spearing *et al* (2001), Stacey (2004) and Mpunzi *et al* (2015) underlined TSL incapacity to operate as a structural

support, and others such as Pappas, Barton, and Weiss (2004) suggested that, depending on their types, TSLs should not be used for a period exceeding three to six months. Otherwise, the consequent decrease of their strength might be prejudicial to the mining supports. However, the broad opinion from researchers leads to the conclusion that TSLs usually perform even better than expected. Since there is not enough evidence of their real performance, such as systematic published reports that have assessed the performance of coating supports throughout different types of mines, the lack of confidence regarding TSL applications persists (Mpunzi *et al*, 2015).

In the attempt of getting better support conditions, and since mining supports are often used in conjunction, Dirige and Archibald (2009) suggested that TSL performance should also be evaluated when associated with other types of supports.

2.2 Active and Passive Supports

Mining supports can be active or passive (Hoek *et al*, 2000). Although acting differently, both types are all used to enhance the self-supporting capability of rock masses and therefore inhibit their loosening, leading to the formation of dead weight loading, which is usually difficult to support (Tannant, 2001). And the choice of the type of support depends on the extent of the looseness in the rock mass zones (Hoek *et al*, 2000). The most commonly used areal mining support types include wire mesh, shotcrete, fibre-reinforced shotcrete and most recently, thin spray-on liners (Spearing *et al*, 2001; Lacerda, 2004; Zhenjun *et al*, 2014; Mpunzi *et al*, 2015). Wire mesh and shotcrete are very common and still have their applicability justified by the number of advantages they offer (Tannant, 2001; Stacey, 2001b). Hoek *et al,* (2000) also mentioned that among the active support types, though unable to be tensioned, grouted or friction anchor dowels can show greater advantages than mechanically anchored rock-bolts. They have the particularity of providing support even after the anchor has slipped or the face plate has broken off, and they can also be combined with passive areal support (Hoek *et al*, 2000). However, they also have some limitations, depending on the type and mechanisms of the mobilizing rock masses, and thus might require alternative supports such as TSLs.

Thin Spray-on membranes are multi-component polymeric materials (Tannant, 2001). TSLs are mostly cement-polymer based, but they may also be polyurethane, polyurea or methacrylate-based materials (Yilmaz, 2011). Two particular issues bother people who are dealing with or have to deal with TSLs (Yilmaz, 2007): The manufacturers want to certify whether their products are good and the users want to know what the best TSLs are before using them. To respond to these matters, Yilmaz (2007) suggested that a series of parameters should be assessed. This researcher stipulated that, instead of only looking at a few common parameters, one should develop a variety of testing procedures, to provide a large number of parameters capable of rating the TSL products. And for this, TSL manufacturers are well placed to perform in-depth tests since they are aware of the material properties (Yilmaz, 2007). However, independent trials should also be performed for validation purposes. The outcomes of the TSL trials should assist in knowing a TSL's ability and the conditions when it can be employed as stand-alone or in combination with other supports, either passive or active (Dirige and Archibald, 2009). Each support has qualities and limitations. The next sections will focus on briefly comparing the performances and limitations of some of these supports with TSL supports.

2.3 Comparison between Wire Mesh and TSLs

As a passive support, wire mesh requires displacements of the failed rock mass in the order of hundreds of millimetres before offering any resistance to the failure process (Tannant, 1995; Tannant *et al*, 1997; Hoek *et al*, 2000; Zhenjun *et al*, 2014). When comparing this support to TSL, it can be observed that although mesh supports are efficient when it comes to catching and holding falls of small rocks, they are passive at the initiation stage of a rockfall (Hoek *et al*, 2000). This is not the case with multi-component polymeric liners, which are sensitive to small displacements, offering resistance in the case of potential rockfalls at an early stage and preventing their occurrence (Hoek *et al*, 2000; Tannant, 2001). Wire mesh support is more likely to resist extensive deformations than TSLs, as presented in Figure 2-1, (Tannant, 2001). Another areal support, widely used in the mining

environment, is shotcrete. The choice of TSL utilization over shotcrete should also depend on the in-situ mechanical behaviours of unstable rock masses.

2.4 Comparison between Shotcrete and TSLs

Shotcrete has already proven its ability in civil engineering and in the mining sector. One of its limitations has to do with the constraints faced for transporting larger quantities of material to the underground. And concerning its behaviour, some theory emerges suggesting that TSLs might accommodate larger displacement before failure than shotcrete (Tannant, 2001). This might be one of the reasons to investigate the conditions where TSL is more performant than shotcrete.

Rather than assessing the best performing liners between TSL and shotcrete, Masethe (2015) tested TSL-coated shotcrete and uncoated shotcrete, and compared their percentage strength gain. He defined this percentage using the following ratio:

$$\%\ Strength\ gain = \frac{Coated\ strength\ (Mean) - Uncoated\ strength\ (Mean)}{Uncoated\ strength\ (Mean)}.100\% \qquad (I)$$

This author found that reinforced shotcrete shows a greater increase in strength than unreinforced shotcrete. Mpunzi *et al* (2015) indicated that this finding might be justified by the fibre-reinforced shotcrete having a ductile post-failure characteristic, while unreinforced shotcrete is less ductile. Nevertheless, this liner requires thorough care during preparation. And the factors that are essential to produce good quality shotcrete include a skilled nozzleman, care in the preparation of the surface to be sprayed, control of the thickness and the material delivery rate (Masethe, 2015; Moser and Girmscheid, 1999). Another factor is to ensure that shotcrete is not exposed to temperatures below 9ºC at the time of its application and for at least 96 hours thereafter (Pappas *et al*, 2004).

To compare TSL and shotcrete, Dirige and Archibald (2009) assessed the performances of TSLs when applied in tunnels under high stress and rockburst conditions. The outcomes confirmed that TSLs highly contribute to suppressing

rock deterioration that occurs in highly stressed and rockburst conditions. In their endeavour, the same authors undertook a comparing study of TSLs and shotcrete effectiveness when used as rock support. The study showed that TSL products might perform equally to shotcrete materials in supporting the rock mass.

The applicability of shotcrete linings and TSLs may vary depending on their intrinsic mechanical properties. Shotcrete is semi-rigid while TSLs are highly deformable (Guner and Ozturk, 2016). According to these authors, stiff support systems, which are semi-rigid, are stable without a need for any interaction with the rock mass. These supports are deformable and therefore can react as structural supports by redistributing the stress applied by the rock mass; which justifies the use of shotcrete as final supports, either as temporary or permanent supports. In contrast, supports that are weak in bending are highly deformable, such as TSLs. These supports are therefore not stable to stand alone but need to interact with the neighbouring rock mass. They have mostly been used as temporary supports but should be investigated in the current research for long-term performance to be used as permanent supports.

In the comparison of shotcrete with TSL, the support resistance generated by reinforced shotcrete is higher than that obtained from TSLs (Tannant, 2001). However, Potvin *et al* (2004) advocate for the use of TSLs in place of shotcrete since they can offer extensive deformations and can resist significant dynamic shock impacts. These authors found that thin liners contribute to improving the self-supporting capacity of rock masses, and hence have a performance very close to that of shotcrete. Shotcrete coated with TSL can display a strength increase of about 40% compared to the uncoated shotcrete (Masethe, 2015). And there is a similarity in the failure modes from both the polymeric liners and shotcrete (Golser, 1977; Masethe, 2015; Stacey, Mason, and Fowkes, 2009; Potvin and Hadjigeorgiou, 2008). Both liners fail under shear through or diagonal tensile rupture at initial confinements accompanied by some millimetres of rock mass displacement (Tannant, 2001). This latter author, however, specified that these similar failure modes are likely to occur when the adhesive and tensile strengths are similar. He

also pointed out one of the advantages of TSL-supports is their ability to identify major geological structures and major joints in the rock mass even after the liner has been applied. But he mentioned that there also exist opaque TSLs that do not offer this advantage. Nevertheless, whenever this advantage is applicable, it should be very helpful in ensuring that blast holes are not collared near the joints (Tannant, 2001).

After comparing the two latter-mentioned liners, support designers are called to choose which one is to be used for specific rock mass geotechnical conditions. The decision might also be, instead of replacing a mining support tool by TSL, to combine various supports that include these thin liner coatings.

2.5 Replacing and Combining Mining Support Tools

2.5.1 Replacing some mining support tools

Espley, Gustas, Heilig, and Moreau (2001) stipulated that the interest in TSL's research is motivated by the need to replace the traditional supports used in underground, mainly wire mesh and possibly rock bolts. Actually, liners (shotcrete and TSLs) can adhere to rock and thus are capable of mobilizing rock interactions at small deformations (Mpunzi *et al*, 2015). This is not the case with wire mesh, which are passive supports in the sense that instead of offering resistance to rock displacements, they accommodate them to a certain extent before offering resistance through the basket mechanism (Kuijpers, Rangasamy and Sellers, 2004). And when they interact with the rock mass, it is to ensure the carrying of the dead weight of rock mass blocks that have fallen between the rock bolts (Stacey, 2001a). This holding ability of wire mesh can also be performed by thin liners, making them more complete supports, since they become multifunctional (Tannant, 2001).

A particular TSL product, the polyurea type, has been documented as capable to operate as mesh replacement, and also probably capable to sensibly reduce the amount of (or replace) rock bolts (Espley *et al*, 2001). According to the same authors, this TSL product has a capacity of curing under moist conditions. Espley

et al (2001) further suggested that if proven as effective supports in high-stress conditions, TSLs should also be investigated as a replacement of shotcrete support. However, to date, thin-spray membranes have mostly been used because of their fast development cycle rather than as stand-alone structural supports since the latter capacity is limited. And contrary to the latter cited authors, Myrvang, Stjern, Kompen, Opsahal and Berg (1993) in Finn (2004) recommended TSLs only as a replacement of mesh supports, not of rock bolts and cables, since the deep anchoring effect and structural reinforcement provided by these cannot be provided by thin membranes. Morton *et al* (2008) also do not advocate the attempt of replacing shotcrete with TSLs.

The variety of opinions on TSL's practical performance in the mining sector has led some researchers to suggest the use of this liner in conjunction with other supports, rather than as permanent stand-alone support — as will be presented in the next section.

2.5.2 Combining TSLs with other mining support tools

The deepening of mining activities brings about more stability challenges due to high stress and rockburst conditions. Guner and Ozturk (2016) thought on the supports adequacy in these new mining conditions. They suggested that the use of the combination of bolts, mesh and shotcrete in deep levels and under high stress and rockburst conditions requires the addition of a more deformable but tougher support such as TSL. This suggestion conforms with recommendations by Haile (1999) in Kuijpers (2004), who, after back analyses of fatal accidents and support failure due to rockburst, stipulated that it was practical to combine rock bolts with areal support such as TSLs to extend the supporting effect of rock bolts beyond their immediate vicinity and cover the space between them.

Espley *et al* (2001) suggested that, until strong validation of TSL's high reliability as stand-alone support in high-stress conditions is made, this thin liner should be used in conjunction with rock bolts. The same authors insisted on the importance of applying these combined supports immediately after the advancing of the headings or after a shorter period. Additionally, they recommended that the

distances between the bolts be varying according to the type of rock mass that is planned to be supported. Tannant (2001) and Mpunzi *et al* (2015) also promoted the combination of TSLs with other mining supports. They suggested that, although expensive, the combination of wire mesh and/or shotcrete with TSLs should offer higher strength resistance and deformation properties. Dirige and Archibald (2009) also suggested that the variant layer combination of TSLs may perform as well as conventional mining supports such as shotcrete, or even perform better than them when employed for rockburst mitigation or in highly stressed mine conditions. They added that when TSLs are associated with shotcrete, they form the product called "Super-Liner". Here, the thin liner serves as a coating on shotcrete support and constitutes a very tough combined support capable to oppose high rockburst effects. And according to Guner and Ozturk (2018), it is the combination of TSLs and wire-mesh that could result in an equal or even higher strength than that of reinforced shotcrete.

2.6 Types of Thin Spray-on Liners

TSL types vary depending on their compositions. TSL compositions usually vary between manufacturers (Yilmaz, 2011). However, it should not be excluded that extra assessments be undertaken to validate or complete provided TSL characteristics. The current research also intends to complete this task. Only a few of the most used TSLs will be assessed in this thesis's research depending on their availability.

Table 2-1 presents a list of TSLs, each associated with its manufacturer.

Table 2-1 List of TSL products and their compositions (Modified after Yilmaz, 2011)

TSL Product Name	Composition
Mayco Super lining; BASF white TSL	Cementitious polymer
A-Seal; V-Seal	Cement-polymer-sand-polypropylene fibre
Superseal	Cementitious polymer
CHC TSL	Acrylate polymer
D21H; Concor Standard TSL	Cementitious polymer
Rockguard	Polyurethane/polyurea hybrid
Tekflex	Cementitious polymer
Geo-Mining TSL	Cementitious
Diamondguard	Polyurethane
Polyurethane TSL	Polyurethane
MasterSeal 840R01A; 850C	Methacrylate resin and filler mixture
Masterseal CS1251; 845A; CE1286; CT1266	Acrylate polymer
Capcem KT (grey, white); Raplok; Tekflex white	Cementitious polymer
Rock Hold	Methacrylate mixed with water
Super lining	Cementitious polymer
Conseal	Cementitious polymer
Tunnelguard (grey, yellow, white); TGNC; TGNT; TGC	Cement-polymer-sand-polypropylene fibre
Polyurea TSL	Polyurea
RockWeb	Polyurethane/polyurea hybrid
Everbond; Evermine	Water-based polymer-cementitious filler
Mineguard	Polyurethane

Some of these TSL types have special characteristics, but others are no longer produced. Besides the polyurea product, which has a noticeable tensile strength of 15.5 MPa and a capability to cure under moist conditions, there is another type of

TSL with a special characteristic, namely the zeolite-based material. Although not a polymer base product, this mineral-based TSL is characterized by high adhesive strength and a noticeable high performance in moisture conditions. It also has the benefit to quickly set. However, it is also known to be brittle with low tensile strength and low elasticity (Espley *et al*, 2001).

2.7 TSL Properties

2.7.1 Generic thin spray-on liners

Several properties may dictate the TSL behaviour, however only three of them are considered very important: tensile strength, elongation and tensile bond strength (Potvin *et al,* 2004), with the tensile strength possibly making the greatest contribution in supporting the rock mass (Stacey and Yu, 2004). Additionally, other TSL strengths properties are shear bond strength, shear strength, shear tear and tensile tear strengths, impact strength, compressive strength, bend strength, and deformation modulus in tension and compression (Potvin *et al*, 2004; Yilmaz, 2007). In practice, TSLs are subject to tension after the pulling action of loose rocks has overcome the TSL's adhesive strength or when cracks dilate. The mechanism will endure until the acting load of the rock mass overcomes the liner's tensile strength, at which point failure will occur (Yilmaz, 2010). Figure 2-2 illustrates the mechanism associated with TSL tensile strength property.

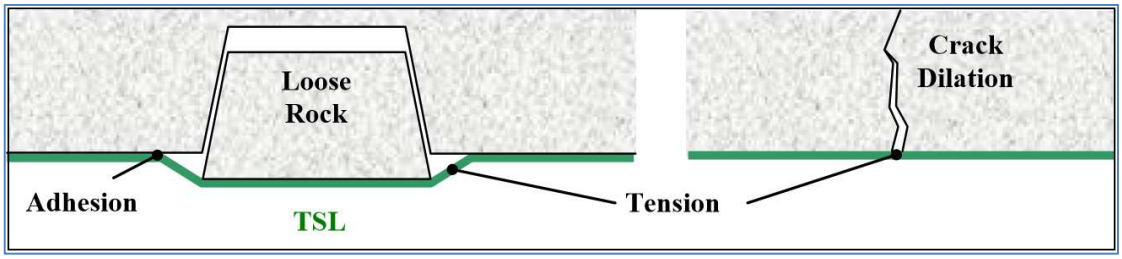


Figure 2-2 TSL's tensile resistance to loading mechanism (Yilmaz, 2010)

The tensile strength of TSL is likely to be greater than that of most rocks and shotcrete (Yilmaz, 2014), and its shear strength has a high probability of being similar to the tensile strength (Tannant, 2001). For this reason and due to the lack of test data, when the shear strength of a liner is not known, it is assumed to be

equal to the tensile strength (Tannant, 2001). Guner and Ozturk (2016) also confirmed that the tensile strength test has been widely used and stands as the most employed mechanical testing method for thin liners. Additionally, these last cited authors found that a TSL's tensile strength is strongly dependent on its curing time and that this relationship could be expressed through a logarithmic function. Besides the tensile strength, TSL adhesive strength is also crucial to the determination of its performance, since the efficiency of thin coatings depends on how strong the bond is between them and the underlying rock mass (Potvin *et al*, 2004). All the above-cited properties are active when TSLs are subject to various loading mechanisms, mostly due to the loosening of rock blocks. Guner and Ozturk (2016) also recommended the study of the mechanical properties and constitutive relationship of TSLs older than 28 days, and under various temperature and humidity conditions, since they believed that the results should be different from those obtained for TSLs younger than 28 days. This recommendation shall be investigated in this research.

Additional research on TSL's properties has exposed other characteristics. Among them are the following:

- TSLs can be used to protect steel support elements (wire mesh, rock bolts, etc.) against corrosion (Espley *et al,* 2001; Yilmaz 2010)
- Thin liners can also be applied in boreholes where they contribute to maintaining the collar integrity (Espley *et al,* 2001)
- There is a correlation between the surface moisture condition and the TSL's adhesion strength. And research has shown that, although more data is needed to define the acceptable moisture limit values, if the moisture value is less or equal to 60%, TSLs could still perform satisfactorily (Espley *et al,* 2001)
- TSLs are unable to adhere to chloritic joint planes (Potvin *et al,* 2004)
- When TSLs are applied in burst-prone environments or sections with frequent blasting, these materials should require additional assessment regarding their mechanical behaviour under dynamic conditions (Potvin *et al,* 2004).

Based on the abovementioned TSL properties and characteristics, it is clear that the characterization of TSLs behaviour will also vary from one product to another, depending on their specificities, which are dependent on the manufacturer formulas. Therefore, a review of the available liners for this research is necessary before their utilization. Three TSLs from three different manufacturers shall be assessed, and these are coded for the sake of confidentiality as TSL1, TSL2 and TSL3. These three TSLs were among the most applied in the visited mines.

2.7.2 **TSL1**

TSL1 is a thin liner support composed of a cementitious product mixed with additives. This TSL is composed of cement-polymer-sand-polypropylene fibre. Specifically, these constituents are the synthetic latex binder, a cementitious material, silica sand, and the propylene fibre. The technical document from the supplier shows that the mixing material is effective in preventing unravelling and oxidation as well as in affording some lateral constraints to the rock mass. Further details could not be availed for confidentiality reasons, as it was agreed with the manufacturer.

2.7.3 **TSL2**

TSL2 is a cementitious material employed as a sealant coating. The raw material comes in a bag as a single component powder, to which clean tap water is added to form the mixing to be used for coating. The recommended proportion for the mixing product is 10.8 litres of clean water per 50 kg of raw material to be handled in temperature conditions between 20ºC and 30ºC. Some of the technical properties of this TSL are presented in Table 2-2.

Table 2-2 Technical Properties of TSL2

Age	Compressive Strength (MPa)	Tensile Strength (MPa)
24 Hours	17.2	1.4
7 Days	31.1	2.1
28 Days	44.7	3.1

Suggestions from the technical data sheet are: the setting time of this TSL type should be in the range of two to three hours, and its expected fresh wet density is 2040 kg/m^3. The same technical sheet stipulates that, in principle, 14.9 litres of the mixing yields 2.9m^2 at 5 mm thick, but the actual coverage should depend on the texture and porosity of the surface to be covered. This fibre reinforced product has a property of being non-toxic and non-flammable. It is also believed to have a shelf life of 12 months when stored in cool, dry conditions.

2.7.4 **TSL3**

TSL3 is identified as a plasticiser free aqueous copolymer emulsion and it is composed of acrylic acid esters. Besides, it is constituted of wetting agents mixed with a cementitious binder. The provided technical data of this product are:

- White liquid binder
- Solid Content: 46% per volume
- PH 8-9
- Boiling point: 100ºC
- Non-flammable
- Non-toxic
- Non-corrosive
- Cementitious
- Silica sand and fillers

The technical sheet suggests that, after 28 days, the material strength is as described in the following Table 2-3.

Table 2-3. TSL3 Strength Properties after 28 Days

Property	Strength (MPa)
Shear strength via Flexural	10.4
Shear bond strength via pull off	6.54
Tensile strength	9.75

For this particular fibre reinforced thin liner, the expected setting time is in the range of one to two hours. In principle, a 25kg bag can cover an area of about $3m^2$ at a thickness range of between 3 and 5mm depending on the rock factor that is influenced by the texture and porosity of the surface to be coated. The recommended proportion of the mixing product is 2 litres of binder and 10.5 kg of the cementitious material. The shelf life of this product is 3 months when stored in cool, dry conditions, and preferably away from sunlight. This TSL is non-toxic, bio-degradable and with easy application. Its other claimed advantages are the ability to bond to dusty, wet and fatty surfaces; easy handling, superior bond strength, ability to bond to any type of rock including coal, cost-effective, environmentally friendly.

2.8 Mechanical Behaviour of TSLs

Tannant (2001) suggested that, when there is an expectation of ground convergence and enough relative or shear displacements between blocks, the support designer should consider using supports with significant deformation capability, like TSLs. In this case, one should bear in mind that the elongation capability of ductile liner types is inversely proportional to the liner's tensile strength (Guner and Ozturk, 2016). Finn (2004) defined the TSL's mechanical behaviour as a stabilizing process in which the liner's intrusion into the rock mass cracks is contributing to oppose the inter-blocks movements and thus increasing their cohesion and friction angle. The same TSL also has the capability of preventing the rockfalls and thus contributing to the opening stability. Another TSL ability, promoted by Tannant (2001), is its resistance to small deformations (<1mm) of rock mass blocks, and this resistance

should be considered as a combination of shear, adhesion, and tensile strength, which are characteristics of the mechanisms of TSLs behaviour.

Stacey (2001b) suggested that there are several mechanisms of TSL behaviours, among which are basket mechanism, slab mechanism, mechanical protection, wedge and block loading, distributed surface loading, stress-induced loading, water pressure loading, bending loading, etc. These mechanisms generally occur in underground mines; and to avoid uncontrolled TSLs failure, stringent requirements are demanded whenever liners are chosen as the option for support (Potvin *et al*, 2004). One of the most referred TSL's practical behaviour is the "adhesion loss – tensile rupture". This behaviour is common to most of the liners, either shotcrete or TSLs. This will be fully observed from one of the testing methods to be adopted: the Membrane Displacement Method (MBT). This property intervenes in the process of the support failure, as the membrane starts by stretching simultaneously with some adhesion strength loss (Tannant, 2001). Previously illustrated in Figure 2-2, this mechanism is much elaborated through the following Figure 2-3 (after Tannant (2001). In this illustration, a rotation (θ) of a portion of the liner is caused by the downward movement of a loose block of weight (W). The liner adhesion loss will continue until W becomes greater than the vertical component of the tensile strength (T). At this point, the rupture of the liner occurs (Tannant, 2001).

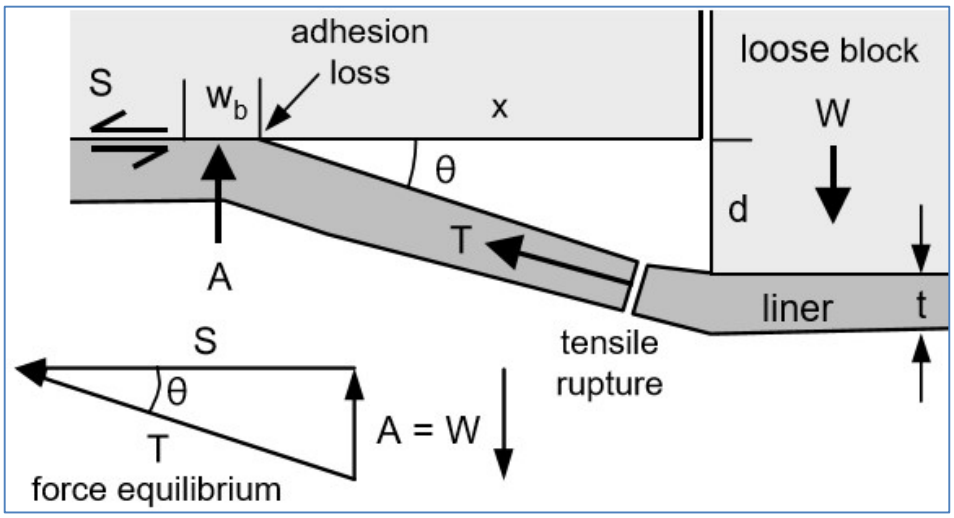


Figure 2-3 Adhesion loss – tensile rupture mechanism of a TSL supporting the weight of a loose block (Tannant, 2001)

When a liner adhesion strength is less than its tensile strength, there should be a progressive adhesion failure around the displacing block, and the thin liner should start acting in tension to resist the weight of the moving block (Tannant, 2001). And depending on whether the type of TSL is relatively ductile or brittle, the general curves that illustrate its mechanical behaviour can be constructed through the following equations and correlation coefficients proposed by Guner and Ozturk (2016) and displayed in Table 2-4.

Table 2-4 Equations of TSL Tensile Mechanical Behaviour (Guner and Ozturk, 2016)

Equation name (Y)	**Liner 1 (ductile)**		**Liner 2 (brittle)**	
	Equation	**R^2**	**Equation**	**R^2**
Tensile strength	$Y = 1.31\ln(x) + 0.54$	0.91	$Y = 0.98\ln(x) + 2.17$	0.71
Elastic modulus (Extensometer)	$Y = 230.27\ln(x) - 58.03$	0.65	-	-
Elastic modulus (LVDT)	$Y = 22.13\ln(x) + 4.04$	0.71	$Y = 23.68\ln(x) + 62.7$	0.61
Elongation at break % (Extensometer)	$y = 47.85\ x^{-0.92}$	0.75	-	-
Elongation at break % (LVDT)	$y = 57.87\ x^{-0.61}$	0.8	-	-

Nevertheless, this table should only serve as guidance, since each TSL has its particular stress-strain behaviour (Guner and Ozturk, 2016).

Among the factors that can influence a TSL's mechanical behaviour, time, temperature and humidity are believed to be relevant (Tannant, 2001). In the mining sector, the time-dependent behaviour of rocks and rock masses has already captured the attention of researchers such as Malan *et al* (1997). These researchers focused

their studies on rock creep behaviours. Creep behaviour is a continued deformation generated by constant stress applied to a material such as rock.

It is only in the recent past that TSL's time-related behaviour has been presented in the literature (Guner and Ozturk, 2018). This mechanical behaviour will largely be presented in CHAPTER 3. Temperature and humidity related behaviour of TSLs is yet to be found in the literature. However, TSL behaviours in such environmental conditions should imperatively be investigated since these liners are usually applied in underground mines characterized by these conditions. For instance, Donoghue (2004) studied the relationship between virgin rock temperature (VRT) and depth. He said that this proportional relationship is caused by factors such as the geothermal gradient as well as the auto-compression of the air column. Biffi, Stanton, Rose, and Pienaar (2007) in Oniyide (2015) undertook in-depth studies on the VRT and depth relationship of the Bushveld Igneous Complex (BIC) rock masses. And the outcome of their research showed that the VRT in the BIC rock mass can reach temperatures higher than 90°C, as displayed in Figure 2-4, which shows the geothermal gradient trends of the BIC East, the BIC West and the Witwatersrand Basin.

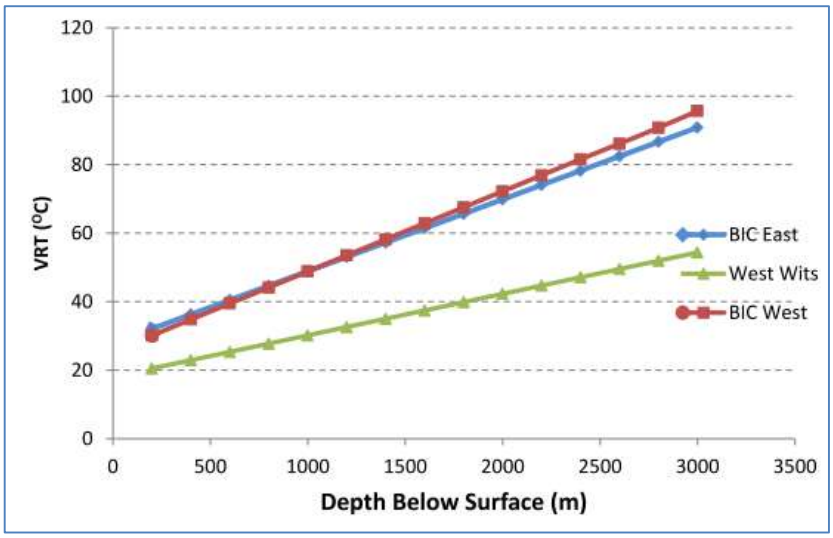


Figure 2-4 Relationship between VRT and depth for the BIC and the Witwatersrand Basin (Biffi *et al*, 2007)

From this literature, there is a need to incorporate the temperature parameters in the assessments of thin liners, which are also coated in deep mines. Therefore, this thesis's research will investigate and present the effects of both humidity and temperature on TSL mechanical behaviour for the first time in the literature.

Apart from the abovementioned factors capable of influencing TSL mechanical behaviour, the TSL's proper design is of considerable importance as it can dictate the mechanical behaviour.

2.9 **Design Principles**

Mpunzi *et al* (2015) have demonstrated that the amount of thickness of a TSL applied on a Brazilian specimen does not significantly influence the overall tensile strength, but only the Brazilian specimen's thickness should be influential. However, concerning the adhesive strength, Ozturk and Tannant (2011) have proved earlier that the TSL's thickness has an impact on this property. These authors went further in their research, showing that the increase of TSL thickness weakens its adhesive strength, yet the overall substrate's supporting capability should increase with a thicker coating, as per the suggestions by Stacey and Yu (2004). Although the aim of the current research is not to investigate the thickness effect on substrate strength, this parameter will, at best, be kept constant. Yet even with this proposition, Guner and Ozturk (2016) found that a TSL thickness, carefully adjusted in the preparation phase, can still vary during the curing period. Its size might decrease depending on the chemical compositions of the liner. They stipulated that mixing and curing times of TSLs, also dependent on their chemical compositions, are variable, leading to TSL's shrinkage, particularly for water-based liners. And this shrinkage also influences the decrease of the liner's durability.

Another TSL design parameter is the bond width. This parameter plays an important role in dictating the amount of area on which TSLs may act when subjected to tensile loads (Tannant, 2001). In practice, good site preparation is needed so that the optimal bond width is exploited, otherwise, some of TSL's characteristics will

not fully function as predicted in the laboratory (Kuijpers *et al*, 2004b). However, caution should also be considered when defining the thin liners' characteristics from the laboratory, because some of them may not be reached in practice. For instance, the assumption of full adhesion between a liner and a rock is generally not reflecting reality. The scenario is different because of the occurrence of progressive failure of the bond between the two materials (Tannant, 2001). TSLs' field behaviour should, therefore, be assessed with sufficient details before attempting to reproduce them through numerical modelling techniques.

2.10 Application and Assessment of TSLs in the Mining Sector

2.10.1 Functions of a TSL in the mining sector

In practice, TSLs have been preferred to other spray-on liners in hard rock mines, especially in some mines in Canada, Australia and South Africa (Tannant, 2001). They have also been employed in underground coal mines (Laurence, Galvin and Beer, n.d.). Some of the TSL's applications are presented in Table 2-5.

Table 2-5 Some TSL applications in Underground mines (Guner and Ozturk, 2016)

Applications	References
Reducing the permeability of shotcrete coatings	Hawker (2001)
Used as anti-corrosion for steel	Espley *et al* (2001); Komurlu, Kesimal and Colak (2014)
Temporary support in Tunnel Boring Machine tunnels	Archibald (2001); Lacerda and Rispin (2002); Potvin *et al* (2004); Pickett and Thomas (2013)
Suitable with the installation of permanent supports at a very early stage	Hawker (2001)
Primary support, just after blasting	Espley *et al* (2001); Potvin *et al* (2004)
Ground alteration such as humidity, moisture, chemical contamination	Espley *et al* (2001); Potvin *et al* (2004); Kuijpers (2001)
Preventing weathering, rock fall, or rock mass mobilization	Espley et *al* (2001); Lacerda and Rispin (2002); Laurence *et al* (n.d.); Lewis (2001); Pappas *et al*, (2004); Tannant (2001)
Gas management tool in underground coal mines	(Li, Saydam, Mitra, and Chalmers, 2016)

These functions will later be detailed by evidencing the advantages of resorting to TSLs. But before that, the equipment used for TSL application will be presented.

2.10.2 Field testing of TSL

Generally, rock mass behaviour under stress confinement is assessed either from in situ or laboratory tests. TSLs have also been assessed in the field as well as in the laboratory. The laboratory tests aim to predict the true behaviour happening in the field. Kuijpers *et al* (2004b) indicated that the test results of TSL behaviour in the

field are not generally the same as those obtained through laboratory tests**.** And since the mechanisms of support behaviour and support loading play a major role in the choice of the testing method, care should be taken to reproduce them (Stacey, 2001a).

TSL support performance from field testing

From field observation, TSL can act as a membrane at an excavation surface or as glue if forced between two blocks of the rock mass (Kuijpers *et al*, 2004b). And when acting as a glue, the support performance of TSL mostly depends on how many rocks are involved in the failure process and what the magnitude of the displacement is between the blocks (Tannant, 2001). The efficiency of a thin membrane, however, is higher when applied just after excavating an opening and before the movement of the rock mass takes place (Tannant, 2001). Therefore, the ability of a TSL type to support the rock mass depends on the load of the rock mass, the number of mobilized blocks and the magnitude of their displacement within the rock mass (Tannant, 2001). The polymeric multicomponent liners function well when used as superficial supports, usually coupled with rock bolts (Potvin *et al*, 2004). These authors also suggested that a good TSL is that which adheres tenaciously to the rock surface. It also cures quickly and is characterized by high tensile strength.

TSLs fit well in hard rock mines, where they can replace the use of the traditional wire mesh supports or shotcrete. And when applied on surfaces supported by rock bolts, they constitute a much better support (Tannant, 2001; Mpunzi *et al*, 2015). However, Mpunzi *et al* (2015) specified that this is not the behaviour observed on porous rocks where a coating of TSL had an initial effect of weakening the tensile strength of the rock. Therefore, as validated by the experience, before the application of a thin liner coating, thorough site preparation accompanied by removal of loose rocks is imperative for better adhesion between the liner and the exposed surface (Kuijpers *et al*, 2004b). Consequently, polymeric liners should not be recommended for rock-mass with surfaces that are difficult to clean or have a crumbly texture (Tannant, 2001). In observing recommendations such as those cited earlier, the TSL's capabilities should be fully functional.

Advantages of TSL application

Some TSL attributes are crucial for its behaviour and should always be taken into account for assessment and design purposes (Tannant, 2001). The advantages of using thin membranes have been widely promoted in the literature, some of them being:

- Application near or at tunnel faces (Nagel and Joughin, 2002; Tannant, 2001)
- Sensitivity to blasting: Thin liners are believed to be less affected by blasting events (Lacerda and Rispin, 2002; Spearing and Champa, 2000)
- Timing of liner application**:** When thin liners are applied on a newly blasted heading, and even before the removal of the dead block, they prevent the loosening of the rock mass. TSL has the attribute of quickly supporting the ground before the occurrence of severe deformations (Archibald, 2001; Borejszo and Bartlett, 2002)
- Continuous coverage versus web**:** Instead of applying the liner on the overall surface, the liner's consumption may be reduced by using intelligent equipment capable of spraying the liner only on the localized jointing zones, simulating a spider's web (Tannant, 2001)
- Long-term performance**:** This characteristic was previously assessed by researchers such as Pappas *et al* (2004) who looked at their site behaviour before recent studies by Guner and Ozturk (2018) who investigated the thin liners' creep performances
- Reduced time of equipment installation, handling, and field clean-up (Archibald, 2001; Hawker, 2001)
- Increased mobility and easier application procedures than for conventional mesh and bolts installation (Borejszo and Bartlett, 2002; Finn, 2001; Lacerda and Rispin, 2002; Tannant, 2001)
- Simple spraying equipment that is easy to repair (Espley *et al*, 2001; Laurence, 2001)

- Productivity increase when applying TSL concurrently with the drilling process (Lacerda and Rispin, 2002; Spearing and Champa, 2000)
- Possibility of continuous spraying (Henderson and Louw, 2001, in Yilmaz, 2011)
- Wasted material due to rebound is very negligible (Finn, 2001; Lacerda and Rispin, 2002; Laurence, 2001, in Yilmaz, 2011)
- Safety**:** Contrary to meshing, liners can resort to robotic applications and therefore avoid the hazardous conditions observed for mesh supports (Spearing and Champa, 2000). The incidence of injuries due to rockfalls should thus be reduced
- Rock visibility**:** Though not applicable to all the thin liners, there is still the possibility of seeing the geological structures on the rock surface after TSL application (Tannant, 2001).
- Some thin membranes, especially the white TSLs, can improve the illumination through light reflection (Potvin, 2002)
- TSLs such as the Polyurea can cure and perform well in moisture conditions (Espley *et al*, 2001; Hepworth and Lobato, 2002, in Yilmaz, 2011)
- Contamination of ore**:** It is believed that mining in a TSL supported zone will not negatively impact on the milling and mineral recovery as does shotcrete (Tannant, 2001).

The author plans to assess the consistency of these advantages at a long-term view in the mining sector. Further observations will be made on how TSL attributes may be compromised, hence its performance affected, and whether this might be due to a non-fulfilment of the recommendations or to other factors.

Apart from the abovementioned advantages, some researchers have also demonstrated that the application of TSL contributes in changing the rock post-failure behaviour from brittle behaviour to smooth and ductile behaviour due to the confinement of the failed rock with a limited resistance ((Espley-Boudreau, 1999; Archibald and DeGagné, 2000; Mpunzi *et al*, 2015). Mpunzi *et al* (2015) highlighted the TSL characteristic of increasing the capacity of energy absorption in the failure process, while Stacey and Yu (2004) emphasized the major

contribution of its tensile strength to better-support the rock mass. It is this high capability of the tensile strength that gives TSL materials a huge advantage over other liners in sustaining large deformations before rupture (Tannant, 2001). The height of a moving block can thus be predicted and in consequence, hazardous areas are likely to be identified and remedial actions taken prior to any fall of ground (Tannant, 2001). However, there are also disadvantages associated with the use of TSLs.

Disadvantages of TSL usage

The use of thin coatings is also accompanied by disadvantages that may be associated with their design requirements, cost, composition, storage conditions, etc. The following are few of them:

- TSLs are not structural supports (Mpunzi *et al*, 2015) and are prone to extensive impact damage when hit by trackless machinery, particularly in the earlier stage after their application (Laurence, 2001)
- The tear strength of most polymeric multicomponent liners is poor (Nagel and Joughin, 2002)
- The gaps encountered in very fractured zones are unlikely to be covered with TSLs (Archibald, 2001)
- Specialized workers are needed for the mixing of TSL because the process is complex and may result in weaker material if not properly done (Lewis, 2001; Nagel and Joughin, 2002). Additionally, improper TSL mixing with sand will result in degrading and weakening the coating (Tannant, 2001)
- There is severe limitation in gauging thin spray-on membranes' thicknesses, unless proper training is provided on how to properly move the nozzle and at what speed to advance; this is practically difficult to be asserted, which leads to divergence of results when compared with those expected (Pappas *et al*, 2004; Potvin, Stacey and Hadjigeorgiou, 2004a)
- The good performance of thin liners is very delicate and cannot always be fully monitored since it highly depends on the cleanliness and roughness of the rock surface (Tannant, 2001)

- It is not always easy to prepare the rock surfaces before TSL coating and some TSLs such as Polyurea and Polyurethane need to be applied on relatively dry surfaces since they underperform by not sufficiently adhering to the humid rock (Finn, 2001; Lacerda and Rispin, 2002; Potvin, 2002, in Yilmaz, 2011)
- Some of the thin membranes can set quickly, thus delays in spraying them on the rock surface can result in pipe blockage, alteration of the liner's texture and unsuitable mixture for adequate support (Espley *et al*, 2001; Nagel and Joughin, 2002, in Yilmaz, 2011)
- Some logistics such as compressed air, water, storing conditions, etc. are required before spraying of thin membranes (Pappas *et al,* 2004; Yilmaz, 2011)
- Though yet to be demonstrated, it is believed that the performance of TSLs may decrease due to high and freezing temperatures, in the same way that these factors affect the liners' shelf life (Spearing *et al*, 2001)
- The preparation and application of some TSLs may be detrimental to health conditions since they can cause the following effects: vapour generation, antimony trioxide emission, coughing, eye and skin irritation, allergy, asthma, skin adhesion, etc. (Archibald, 2001; Laurence, 2001, in Yilmaz, 2011)
- The high cost of the polymeric liner materials (Hepworth and Lobato, 2002; Tannant, 2001)

In the preparation and application of TSLs, care should be taken to minimize some of the disadvantages as much as possible. This recommendation should also be observed during laboratory testing.

2.11 **Laboratory Testing of TSL Materials**

The choice of adequate support elements is imperative for successful support designs, and before their utilization, sufficient knowledge of their mechanical properties should be attained. This is accomplished through methods such as laboratory testing. For TSLs also, laboratory testing is an essential procedure to determine the material properties as well as to know their behaviour when

interacting with the rock mass. And to achieve this, a well-designed TSL test procedure requires that tests be simple, practical, repeatable, cost-effective and able to quantify relevant properties and behaviour (Potvin *et al*, 2004). Although it is reported that an accepted TSL testing standard is yet to be established, some of the testing methods, such as tensile and tensile bond strength tests, have gained acceptance (Kuijpers *et al*, 2004). Tensile failure mechanisms are parts of the common occurring mechanisms observed in the underground, and for this reason, much focus has been on them. However in general, a range of laboratory testing methods aiming to assess TSL mechanical properties have been undertaken by several researchers such as Swan and Henderson (1999); Spearing, Ohler and Attiogbe (2001); Naismith and Steward (2002); Yilmaz, Saydam and Henderson (2003); Ozturk and Tannant (2010); Yilmaz (2010); Ozturk and Tannant (2011); Yilmaz (2014), etc. Tannant (2001) and later on Mpunzi *et al* (2015), demonstrated that a TSL tensile strength slowly improves to a maximum strength after a curing period of 28 days. TSL mechanical properties are also assessed for a different purpose; instead of testing isolated properties, other researchers have opted for "Representative Testing", which consists of testing a combination of properties supposedly representative of the TSL's behaviour. Some of the people who have dealt with this matter are Swan and Henderson (1999); Espley, Tannant, Baiden and Kaiser (1999); Archibald and DeGagné (2000); Naismith and Steward (2002); Stacey and Kasangula (2003); etc. Thus, Table 2-6 presents a number of TSL testing methods and their corresponding references.

Table 2-6 TSLs testing methods (Modified after Potvin *et al,* 2004; Yilmaz, 2011)

Class of tests	TSLs Testing Methods	References
Isolated property tests	Tensile strength testing	Yilmaz (2010); Guner and Ozturk (2016), Guner and Ozturk (2017) Guner and Ozturk (2018)
	Bond strength testing	Lewis (2001); Tannant and Ozturk (2003); Yilmaz (2013)
	Torque test	Yilmaz *et al* (2003)
	Coated Panel Testing	Kuijpers (2001)
	Shear bond test	Yilmaz (2007); Qiao et. al. (2015)
Representative tests	Asymmetric core punching test	Stacey and Kasangula (2003)
	Tensile strength and elongation testing	Tannant *et al* (1999); Archibald (2001); Yilmaz (2010)
	Large scale plate pull test (Deformation tests on coated panels simulating a jointed rock mass surface, brick panels, interlocking paving blocks, etc.)	Tannant (1997); Espley *et al* (1999)
	Punch Testing	Kuijpers and Toper (2002)
	Baggage load	Swan and Henderson (1999)
	Point loaded tests on coated concrete slabs/paving slabs	Kuijpers (2004); Naismith and Steward (2002).
	Coated core tests, to determine the strength and behaviour enhancement provided by the TSL coating	Espley *et al* (1999); Archibald and DeGagné (2000); and Kuijpers (2004)

Since TSL testing standards are yet to be established, some testing methods rely on already-established standards which were originally adopted for other materials,

and are likely to have similar properties with the thin liners (Kuijpers *et al,* 2004). In the case of TSL's tensile strength testing, the testing method follows the ASTM D638 standard, which was initially established for plastic and resin material, and not explicitly for TSLs. The variety of TSL types may raise concerns whether the same details of this particular standard should apply to all the thin liners. Another concern is related to the TSL tensile testing procedure. Guner and Ozturk (2016) noted that so far, most of the researchers have been measuring the displacement of the tested specimens by considering their total lengths and not the sample's gauge length as recommended by the ASTM D638 standard. In addition to the previous observation, people usually measure sample displacements with a Linear Variable Displacement Transducer (LVDT) and consider the length from the machine grips. The recommendations from Guner and Ozturk (2016) stipulated that instead of these practices, people should use the sample's gauge length, which guarantee better results in the evaluation of the TSL's Young Modulus and the tensile strength. Moreover, the same authors recommended that the strain in the elastic regime should be accurately identified because the lack of this could result in large errors when calculating the Young Modulus. They also suggested the usage of an extensometer or a bonded strain gauge to better evaluate a specimen strain rate. However, if the study is about the comparison of elongations as it will be done further in this endeavour, this observation might be bypassed. Besides, it was observed that although Guner and Ozturk (2016) pointed out these poor practices, the same authors still resorted to some of them by not considering only the length of the specimen gauge (Guner and Ozturk, 2018). Another more important aspect is that thorough care is taken during the specimen preparation stage (Yilmaz, 2011), to avoid inconsistent results caused by the uncertainty and variability of TSL tensile properties, very dependent on the specimen preparation, mixing speed and testing environment (Guner and Ozturk, 2016). Therefore, these authors recommended that all samples should always be prepared the same way in comparative testing materials. They also suggested that a maximum degree of uniformity should be secured by taking much care when comparing materials behaviours within any determined series of specimens.

To meet the purpose of this thesis's research, three of TSL mechanical properties and representative properties will be reviewed in detail. These are the tensile strength, the adhesion strength, here assessed as the factor of enhancement of the strength of a Brazilian indirect tensile (BIT) specimen, and the representative properties encountered in the MBT. In this particular testing method, the elongation, tear, tensile and adhesive properties are believed to be among the main acting mechanical properties (Kanda and Stacey, 2019; Spearing *et al*, 2001).

2.11.1 Uniaxial tensile strength

The preparation of TSL dog-bone specimens for the tensile test can be performed through moulds made of perspex or steel (Yilmaz, 2010). Another mode of dog-bone preparation is by resorting to the stamping process through die cutting moulds suggested by Tannant *et al* (1999), Archibald and DeGagné (2000) and Guner and Ozturk (2017). The last-mentioned researchers recommended that the use of die cut dog-bone specimens be favoured, especially for tensile creep tests, since they offer high reliability index and high strength results as compared to specimens prepared through moulding. However, their tests were performed on ductile TSLs rather than on more brittle specimens that were used by Yilmaz (2010). Thus, based on their outcomes, one can say that brittle TSLs might be better prepared through the moulding process while ductile TSL specimens should be better-performing if prepared through die cutters.

TSLs and shotcrete tensile strengths are generally tested through the use of dog-bone specimens. The thicknesses of these shaped specimens are generally chosen in similarity with the in-situ applied thicknesses. And the testing process for UTS specimens follows the descriptions recommended by ASTM D-638 (2010), which are sometimes slightly modified to adapt to the practical experiments as suggested by researchers such as Yilmaz (2010). Figure 2-5 presents the TSL specimen dimensions for types I and IV, as proposed by the ASTM D638.

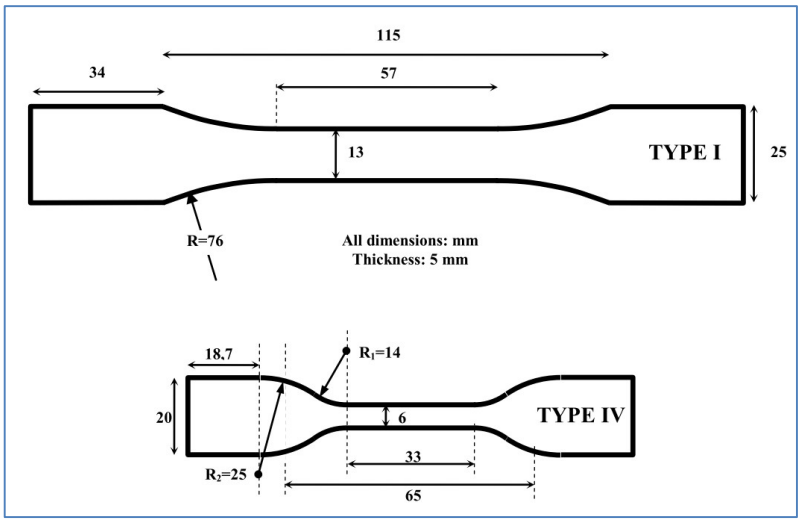


Figure 2-5 ASTM D638 Shapes and dimensions for Type I and IV (ASTM D-638, 2010)

Yilmaz (2010) recommended that the thickness of TSL specimens is to be uniform, and there should not be any eccentricity between the direction of the specimen axis and the pull. And a tensile test will only be validated when the specimen fails at the narrow section as shown in Figure 2-6.



Figure 2-6 Valid failure location of a dog-bone specimen tested in tension (Yilmaz, 2010)

Nevertheless, before adopting these guidelines, some basic requirements have to be observed concerning specimen preparation and test execution (ASTM D-20, 2010; Yilmaz 2010):

a. TSL performance is highly dependent on diligence during mixture preparation until halting once a proper texture is obtained. It is also dependent on the timing between the preparation of the thin liner and its coating. The environmental conditions observed at the time of application

also play an important role in the performance of a thin membrane coating: Two technicians can use a TSL product from the same supplied bag and prepare their specimens in the same laboratory, yet the resulting strengths might be different.

b. Only consider the results from tensile tests where dog-bone specimens failed at the narrow section.
c. For better tensile testing outcomes from a testing machine, an initial loading rate of about 2.5N/s should be applied for approximately 40 seconds before the start of the tensioning process at the rate of 5N/s until failure occurs. However, from experiments, a preload of about 15N followed by a maximum rate of 5N/s produced the same results (Yilmaz, pers. Comm., 18 April 2017)

Following these requirements, Yilmaz (2010) suggested that the expected strength of strong and very strong TSLs, after 28 curing days, should range from 3.5MPa to 9MPa, respectively. Therefore, a TSL direct tensile strength might be classified as described in Figure 2-7.

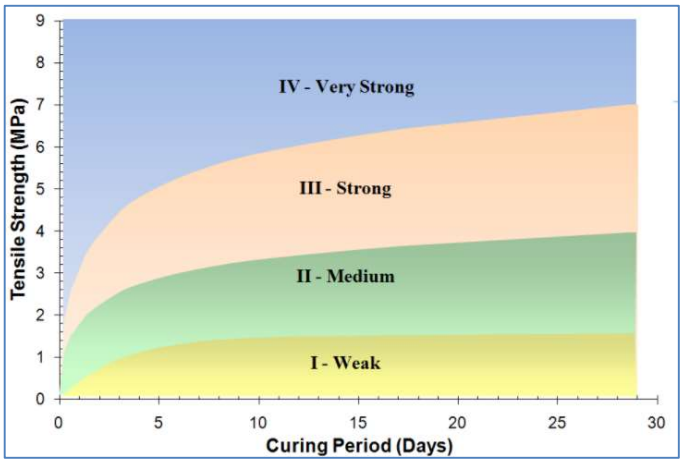


Figure 2-7 Classification of TSL's tensile strength (Yilmaz, 2010)

As introduced earlier, throughout this research, three TSLs will be assessed. The technical sheets from the manufacturers provide the strengths that are expected after 28 days of curing time in room environmental conditions. These values are listed in Table 2-7.

Table 2-7 Comparison of TSL tensile strengths obtained from suppliers

TSL ID	TSL's type	Tensile strength (after 28 days) provided by suppliers and laboratory (MPa)
TSL1	Cement-based	9.7
TSL2	Cement-based	3.1
TSL3	Cement-based	9.75

Although the UTS of the three liners were provided by the manufacturers, supplementary UTS tests will be performed for validation and usage of the practical strength obtained in the specific conditions used during this endeavour.

Besides the direct tensile strength, another property that is highly characteristic of TSLs is the tensile bond strength.

2.11.2 Tensile bond strength

Since TSL is used as a coating, it generally fails under tensile adhesion loss and shear bond loss. The aim in reviewing the adhesive strength property is to highlight its contribution to the substrate's tensile strength — as has been initiated by Mpunzi *et al* (2015). This thesis will include deep underground-like environmental conditions in the latter review, also taking into account the long-term parameter, which will be explained later in CHAPTER 5.

Investigations on the tensile adhesion loss mechanism proved to be imperative. Another objective is to reproduce almost the same conditions as those encountered in the mine by using a coated TSL rather than testing it as a stand-alone as was explained for UTS tests. The tensile bond strength test proposed by Yilmaz (2013) consists of a pull mechanism using the same types of rocks as substrates, the same types of TSLs, and the same humidity conditions, if possible for all the tests. Yilmaz (2013) resorted to ASTM D4541, DIN 1048-2, involving a steel dolly that is pulled away from the rock substrate. To eliminate an over-coring process, a Perspex mould was used. Figure 2-8 displays the equipment necessary for these tests.

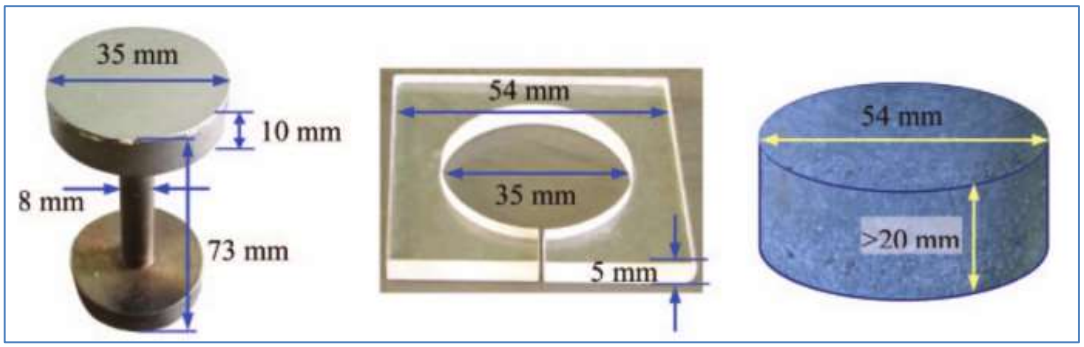


Figure 2-8 Dimensions of (a) Steel dolly (b) Perspex mould and (c) rock substrate (Yilmaz, 2013)

The current research, however, will assess the tensile bond strength, not from the pull mechanism, but rather from a coated BIT test as developed by Mpunzi *et al* (2015). However, a similar bonding methodology presented by Yilmaz (2013) should be followed. Although Guner and Ozturk (2016) argued that there is a positive effect of bonding strength when TSL is sprayed rather than when moulding is used, the constraints of spraying small amounts of liners and achieving almost identical thicknesses are definitely higher for sprayed liners than moulded liners.

Mpunzi *et al* (2015) assessed the strength-enhancement factor of thin coatings applied on a Brazilian substrate in tension. From their testing, they demonstrated the positive impact of using thin coatings, which enhance the substrate's tensile strength by 30% to 40%. However, they did not simulate deep and ultra-deep mines, which involve temperature and humidity conditions which will be considered in this research. The TSL's properties considered by these authors were: UCS TSL: 35MPa and σt: 5MPa.

It is believed that the representativeness of TSL's behaviour through this proposed technique by Mpunzi *et al* (2015) is higher than that from UTS tests. However, the MBT method can produce other resulting behaviours not identified in the coated Brazilian specimens. The latter is one of the main reasons for also reviewing the MBT method.

2.11.3 **Membrane displacement test**

The MBT is a representative punch-through testing technique used to assess the tensile, elongation, tear and adhesion strengths of thin coating materials (Spearing *et al,* 2001). These researchers designed the MBT testing method as illustrated in Figure 2-9.

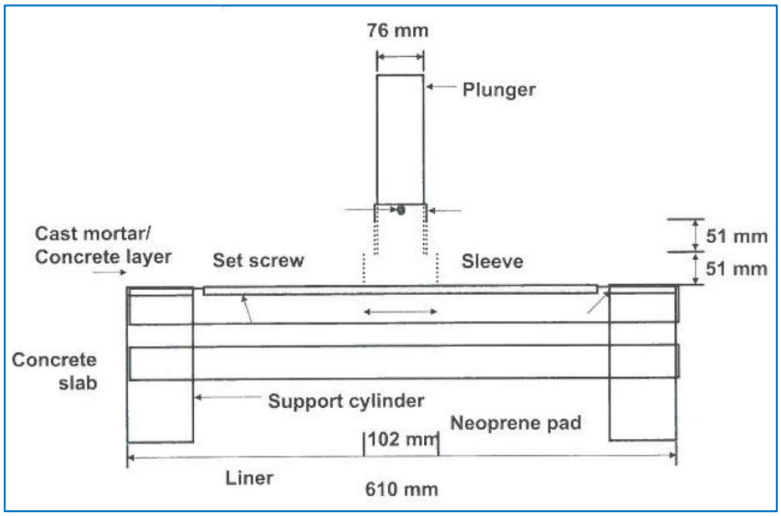


Figure 2-9 Membrane displacement test set-up (Spearing *et al*, 2001)

The principle of this test consists of applying a force through the plunger, which is vertically positioned, passing through a hole produced at the centre of the concrete slab. This should cause transmission of this force onto a thin coating that has been earlier applied to the surface of the patio slab. Following this, data of the applied force versus displacement are recorded for further analyses (Spearing *et al,* 2001).

The look of an MBT specimen after testing is as presented in Figure 2-10.

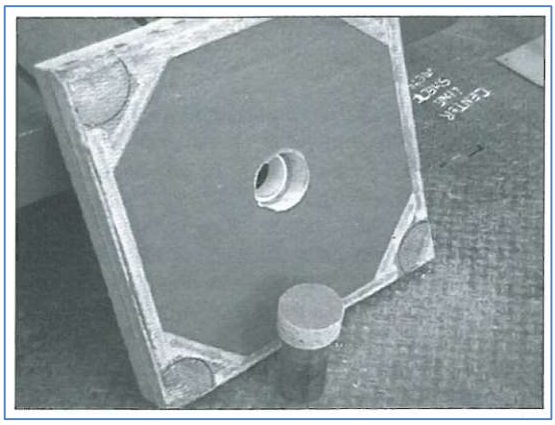
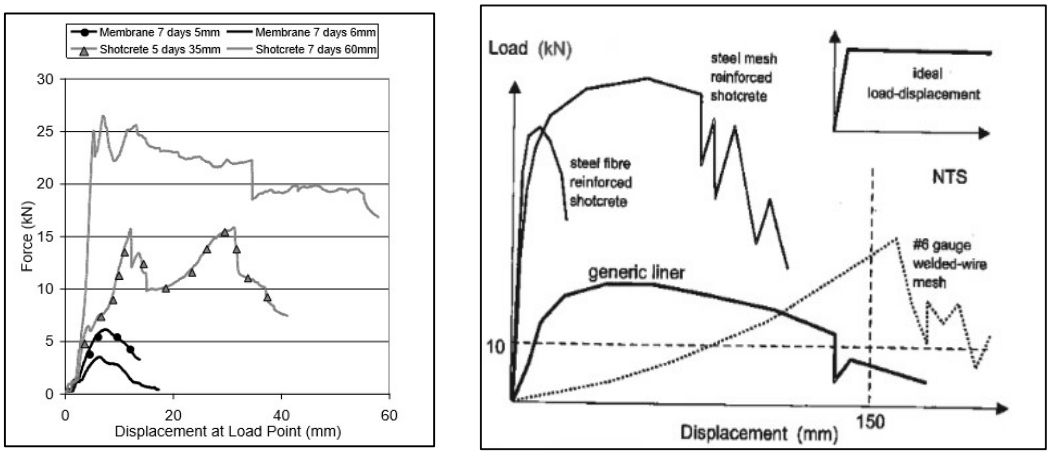


Figure 2-10 Aspect of MBT specimen after testing (Spearing *et al,* 2001)

Thin membranes are capable of accommodating large deformations compared to shotcrete (Tannant, 2001; Yilmaz, 2014). This ability makes them first choice over other types of areal supports when this property is concerned (Stacey 2001), thus they should perhaps be on par with meshing supports (Yilmaz, 2011). However, this possibility does not meet absolute approval, because contradictory results exist in work done by Archibald (2004), Morton *et al* (2008), Spearing *et al* (2001), and Stacey and Kasangula (2003). The main discording point is the potentially high containment capability of TSLs, which makes them better than shotcrete. This claim is not supported by other researchers who, on the contrary, tend to demonstrate TSL limitations, particularly in the case of high deformations, and they rather suggest that shotcrete should be preferred to thin liners, even when the areal support is aimed to accommodate large deformations. Figure 2-11 (a) and Figure 2-11 (b) illustrate these two tendencies.



(a) (b)

Figure 2-11 (a) Force versus displacement capacity of TSLs and shotcrete (Morton *et al*, 2008); (b) Load versus displacement capacity of various areal supports (Tannant, 2001)

For a better understanding of the MBT behaviours, as well as of the assessment of these behaviours, a comparative review of a few of the MBT results from literature is presented. This piece of study will examine work done by Kuijpers (2004), Morton *et al* (2008) and Spearing *et al* (2001). Their resulting load-displacement graphs are displayed in Figure 2-12 and Figure 2-13. No graph was found for Kuijpers (2004), who, instead, presented the results in words.

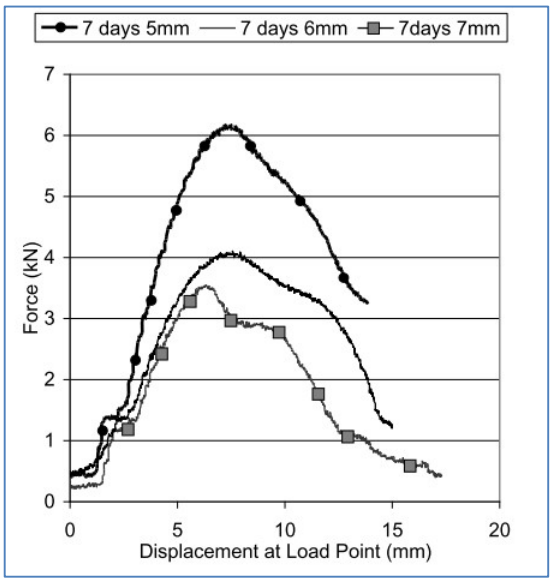


Figure 2-12 TSL's load – displacement behaviour (Morton *et al*, 2008)

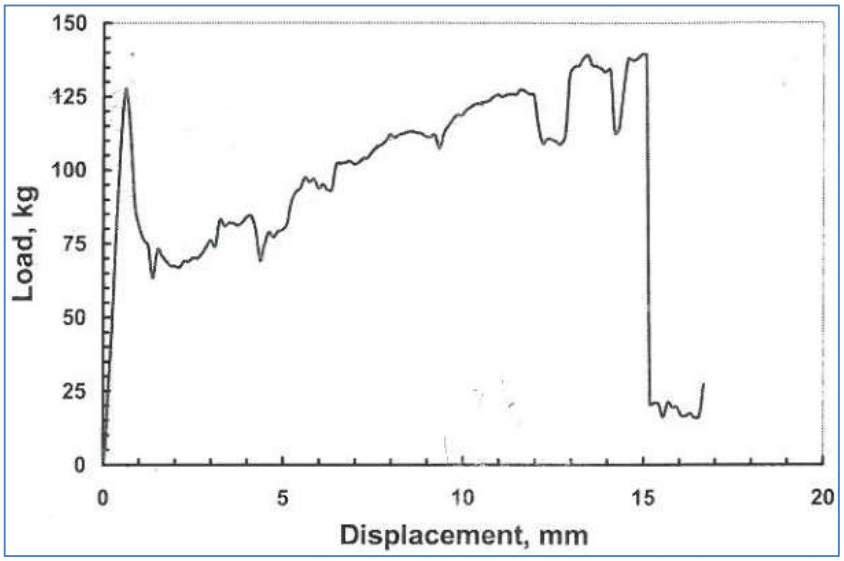


Figure 2-13 Load-displacement plot of a TSL (Spearing *et al,* 2001)

The comparative review of the MBT results is presented in the following Table 2-8.

Table 2-8 MBT results from various TSLs

Reference	Membrane thickness	Substrate size (m^2)	Substrate area (m^2) (A)	Piston diameter (m) (B)	Peeled distance (m) (C)	Contact point Area (m^2) ($D=\pi *B^2/4$)	First peak load (KN) (E)	Load capacity (KN/m) (F=E/C)
Spearing et. al (2001)	6 mm	0.15 × 0.15	0.0225	0.102	0.175	0.00817	1.3	7.43
Kuijpers (2004)	–	0.2 × 0.2	0.04	-	0.142	-	–	–
Morton *et al* (2008)	5 mm	1.5 × 1.5	2.25	0.5	–	0.19625	6.2	–
Morton *et al* (2008)	6 mm	1.5 × 1.5	2.25	0.5	–	0.19625	4.1	–
Morton *et al* (2008)	7 mm	1.5 × 1.5	2.25	0.5	–	0.19625	3.4	–

The table shows that, from the parameters proposed by each author, not all the results can be compared using the load capacity parameter defined by Spearing *et al* (2001). Therefore, an effort should be made to express the MBT results through standardized parameters, particularly for the results obtained from an MTS machine, since there is a way of monitoring the load and tracing the displacement behaviour before and after the maximum load. As noticed, the outcome values are not standardized, which causes difficulties in the comparison of the different studies, thus a standardized parameter applicable to all the tests is imperative. The current research has been investigating a number of those parameters and preliminary results have been published (Kanda and Stacey, 2019). These authors suggested the use of the containment strength (CS) and the relative containment strength (RCS), as they can be adapted to most of the MBT results. The authors justified this choice by the fact that from the literature, no standardized technique is set to compare the performances of liners tested using the MBT method, but the

initial peak load is mostly referred to. Other researchers investigated focussing on the released energy (Kuijpers, 2004), but this technique requires significant effort to assess the energy. Besides, the method does not necessarily highlight how significant the containment capability of the liner is.

But, rather than assessing the results based on the maximum bearing load or by using the various non-standardized parameters, the liners should be assessed based on their capacity of containing the rock mass (Stacey, 2001b). This matter will be dealt with later in this thesis. Nevertheless, the results from laboratory assessments should provide data on rheological rock mass deformation, as stipulated by Drescher and Handley (2003). This data should then serve as inputs for numerical modelling of rock masses under high-stress conditions. That logic will be applied in this research as well.

2.12 **Numerical Modelling of TSLs**

Numerical modelling (NM) techniques are tools used to validate the results obtained from field assessments (Itasca, n.d.) and laboratory trials of support performance (Guner and Ozturk, 2016). Dirige and Archibald (2009) simulated TSL supports using a numerical modelling package, Flac3D, under highly stressed conditions and yielded positive results. The NM assessment verified and completed both field and standard material characterization test results. Similarly, the current research intends to simulate the field and laboratory mechanisms of TSLs, to identify or predict the behaviour trends and to validate their behaviours through comparison with the results from numerical modelling.

The performance of TSL in underground excavations was successfully simulated through NM methods by Guner and Ozturk (2016), and these techniques exhibited the liner capabilities of availing adequate areal support to potential loose blocks of the rock mass. These potentially unstable zones are evidenced by the stalling of deformations at tunnel crowns under high-stress conditions and mining-induced rockburst environments. These findings concerned a cured TSL which was assessed for periods not longer than 28 days after its application. TSL mechanical behaviours

should also be assessed for periods relatively longer than the traditional curing time of 28 days. And the outcome should provide details of the magnitude of TSL performance since Guner and Ozturk (2016) have already shown that with longer curing times of 28 days, a liner's tensile strength and Young's Modulus increase at break, while its elongation decreases.

However, the same authors underlined the importance of calibrating the numerical models. For this, they resorted to Particle Flow Code software (PFC2D) models, with laboratory tests to determine the constitutive behaviour of TSLs. Through the calibration of their inputs, they came up with a scaling coefficient that they believed can serve as guidance to model larger-scale TSL support behaviour.

The current research should resort to NM analyses, particularly when assessing the coating impact on BIT substrates from different scenarios. In this aspect, Yuan and Shen (2017) have shown that the differences in stress distributions due to the contact between the specimen and the jaws are less significant at the centre of the specimen disc than at the perimeter of the specimen. They therefore suggested the assessment of the stress-strain curve from the centre rather than the specimen edge, to minimize the error of wrong positioning of a BIT specimen in the steel jaws. Figure 2-14 illustrates the consistency of results at the BIT centre regardless of whether the loading is a point load or a strip load.

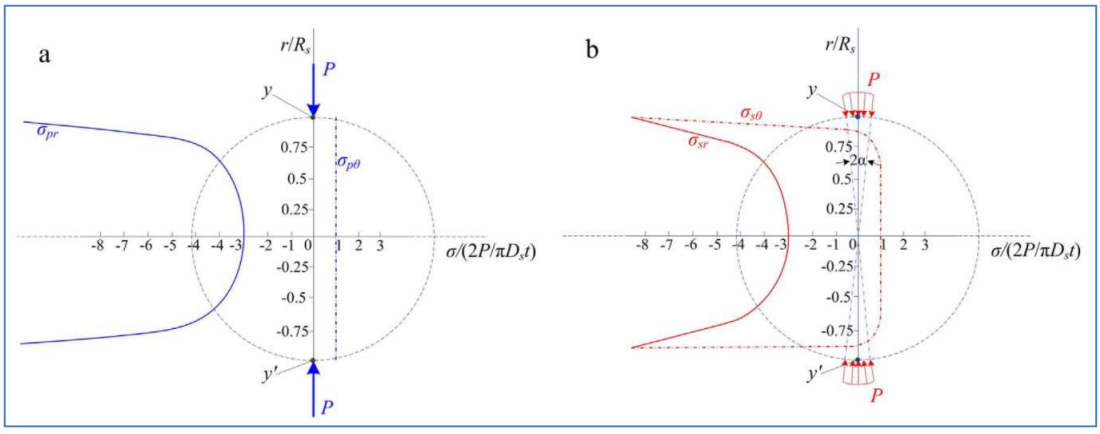


Figure 2-14 Numerical modelling of BIT principal stresses along the loaded diameter due to: a) point load and b) strip load

They then proceeded by glueing the strain gauges at the BIT centres to assess the strain-stress curves. However, although the technique is resorted to by several researchers, it is subject to critics from others. This is because the process of gluing strain gages on a BIT specimen is elsewhere seen as a reinforcement of the specimen tensile strength, yet to be determined (Stacey, pers. Comm., 2 March 2017). The reinforcement can be caused by the glue and by the tensile strength of the gauge.

The outcomes of NM analyses should validate and provide a better understanding of TSL's mechanical behaviours. And the understanding of the behaviours, together with the different observations made throughout the whole handling of TSLs, should assist in producing a series of guidelines for better utilization of thin coatings. Some of these guidelines are already available in the literature and are reviewed in the next section.

2.13 Sample of Available Guidelines for Application of TSLs to Promote Stability

2.13.1 General guidelines for TSL utilization

A sample of some relevant existing guidelines for TSL utilization is presented as follows.

- Care should always be taken whenever the shelf life of thin liners is involved. Usage of liners whose shelf life is older than their allowed maximum will negatively impact their performance (Yilmaz, 2010). In addition to this, Pappas *et al* (2004) compared the shelf lives of Shotcrete and TSLs. They pointed out that, contrary to the indefinite shelf life of the first cited liner when stored in a warm and dry location, thin coating materials only have limited shelf life, varying from 3 to 6 months, but capable of extending to 12 months in particular circumstances. And Lacerda and Rispin (2002) noticed that the liners that are stored in warmer conditions have shorter shelf lives than those stored in colder conditions.

- The timing between the obtaining of an adequate TSL mixture and its application should never be exceeded, since the liner would begin setting before being applied, which can negatively impact on its texture, thus on its overall performance (Yilmaz, 2010).

- An excessive mixing of water or binder fluid should be avoided since it might cause shrinkage distortion of the specimens while curing, consequently affecting the laboratory test results or the in-situ TSL performance (Kanda and Stacey, 2019; Yilmaz, 2010).

- The mechanical behaviour a TSL is dependent on whether the liner is ductile (plastic) or brittle (mostly cement-based). Furthermore, even within the same type of TSL, from the same manufacturer, the performing results can differ if the proportions of constituents are not followed. Therefore, care should be taken when mixing a TSL material. This must be done by rigorously following the manufacturer's suggested proportions, either in the underground or in the laboratory (Yilmaz, 2011).

- Due to difficulty in maintaining a uniform thickness during the TSL application, it is essential that this operation is executed by a skilled nozzle-man for the obtaining of the expected results (Yilmaz, 2011).

2.13.2 **Guidelines for laboratory testing of TSLs**

A few of the guidelines on how to handle the laboratory testing of TSLs were collected from the literature and are presented here:

- When assessing TSL strengths, the most important mechanical properties that one should look at are tensile strength and elongation, shear strength, adhesion strength, tear strength, compressive strength, bend and abrasion strength (Yilmaz, 2011)

- Laboratory testing of TSLs should be sustainable by satisfying the following requirements (Yilmaz, 2011):
  - Manageable specimen size: Specimen sizes should be relatively small in order to meet preparation-time stipulations, at an affordable cost, as well as allowing its easy handling
  - Simple test method: the simpler the test method, the easier will be the specimen preparation procedure, test execution, data analyses and consequently the timing of the test
  - Time management: Three minutes are understood to be sufficient for the completion of the main test cited earlier, and for this the specimen preparation and the testing process should be kept easy to execute
  - Affordability of the test: The testing method should be kept at the lowest cost possible, which would be partly fulfilled through the design of smaller specimen sizes and shorter time of specimen preparation
  - Repeatability: All the factors related to the test should be manageable to allow its reproduction, the comparisons of results, and thus, to make the test statistically valid
  - Relevance: In as much as possible, the representability of in situ support and loading mechanisms of TSL should be included in every testing method
  - Re-use of test components: As a matter of cost-effectiveness, apart from the proper thin liner supplied materials, all the components that intervene in the performing of a TSL test should be manufactured in a way that they can be indefinitely re-utilized
  - Adaptability: Ease of transferring a testing method from one laboratory to another

- The smooth handling of a testing machine and the care regarding its alignment during TSL tensile strength testing should be emphasized on. These processes should, therefore, be thoroughly handled to avoid premature failure of a specimen (Yilmaz, 2010)

- Reliable tensile testing results require that, when using a testing machine, initial loading rate should be of approximatively 2.5N/s, applied for about 40 seconds, after which shall begin the tensioning stage at the rate of 5N/s until the specimen fails (Yilmaz, 2010)

- The condition of a substrate's surface from laboratory should be similar to that from an underground rock mass. In addition, this prepared surface should be free of dust, cleaned down with water, and put in approximatively the same environmental conditions with underground substrates. And it is recommended that these surfaces be prepared through the use of a diamond saw (Yilmaz, 2010)

- It is not advisable to apply a TSL on weaker substrates such as shale, mudstone, etc. because these substrates may fail earlier than the coating material. Besides, it is recommended to avoid the use of substrates with cracks or structural discontinuities (Yilmaz, 2011)

- The results from the tensile test will only be considered valid if the UTS specimen fails at the narrow section — also called gauge of the dog-bone (Kuijpers *et al*, 2004)

- In the assessment of TSL performance, it is poor practice to directly compare results of specimens that have different curing times (Kuijpers *et al*, 2004)

2.13.3 **Guidelines for *in situ* application of TSLs**

Guidelines for *in-situ* application of TSL were collected from the literature and are presented as follows:

- Before applying a TSL in an underground mine environment, care is needed to be observed during the surface preparation because a poorly-prepared surface can be a major contributor to a TSL's bad performance (Yilmaz, 2011)

- To avoid failure in reaching proper texture and to avoid causing shrinkage effect, the mixing liquid should not be used in deficit or in excess. Moreover, it must be understood that a shrinkage phenomenon may lead to detachment of coating from a substrate (Kuijpers *et al*, 2004)

- It is advisable to apply a thin membrane on a newly blasted heading, even before the removal of the muck, since this liner can start providing the support that can prevent the loosening of the rock mass (Tannant, 2001)

- TSL can be applied in web coverage: Instead of applying the liner in a continuous way, covering the whole substrate's surface, thin membranes consumption may be reduced through the usage of intelligent equipment that can spray the product only on localized jointing zones, appearing like a spider's web (Tannant 2001)

- Since good adhesion is needed for a TSL to perform, the area of contact between the liner and the substrate should be well cleaned, and small loose rocks should always be removed before the spraying of the liner (Tannant 2001)

2.14 **Chapter Summary**

From the selected literature, it has been noticed that TSL is an emerging and significantly performing areal support, which is characterized by impressive tensile and bonding strengths, placing it in a good position to complete or substitute some traditional areal supports. However, its mechanical behaviour can be affected by several factors such as its category, whether it is a ductile or brittle liner, by the cautions taken during the specimen preparation, the type of mechanisms, the structural conditions of the rock mass to be supported, etc.

Yet throughout this literature review, questions related to TSL's practical effectiveness in underground mines-like conditions as permanent support through

in-depth and specific assessments remained unanswered. The effect of humidity and temperature on TSL mechanical performance is still not investigated although these factors are believed to be characteristics of some deep mines, as observed in the South African mines, where these coatings are used, though with caution. The provision of answers to these questions has therefore been the key reason to embark into the current research, so that proper understanding of TSL's mechanical behaviours in underground mines can be established, and whether this type of liner can be relied on for long-term usage.

Since the long-term performance of TSLs in underground mines is a concern for this research, there was a need for reviewing the time-dependency concept in the mining environment. This is elaborated in CHAPTER 3.

CHAPTER 3 TIME-DEPENDENCY CONCEPTS IN THE MINING ENVIRONMENT

3.1 Introduction

Time-dependency behaviour of materials encompasses concepts such as creep, rate-dependent behaviour, delayed fracturing and long-term performance (Malan *et al*, 1997). In the current research, creep and long-term concepts will be considered as substitutable, since it will be through the means of creep tests that the long-term performance will be established. However, each terminology should be well presented for a better understanding of the upcoming studies. The current chapter will review the time-dependency concepts in the mining sector. Rock time-dependency behaviour will be looked at first, followed by review of some of the studies on polymer-based time-dependency, then followed by focus to TSLs.

This particular piece of study is supported by the findings from Kanters, van Erp, van Drongelen, Engels and Govaert (2017) who stated that creep rupture, namely a plasticity-controlled failure, is a failure mechanism capable of limiting the lifetime of polymer-based materials under loads, alongside two other failure mechanisms, namely the slow crack growth and the molecular degradation.

3.2 Creep and Relaxation Behaviour in the Rock Mass Environment

Malan *et al* (1997) defined creep behaviour as a continued deformation generated by a constant stress applied to a material such as rock. They emphasized that the constant stress test should be used solely for intact rocks or rocks that can be handled in laboratories and that do not contain large scale discontinuities. Drescher and Handley (2003), on the other hand, defined the creep process as a measure of complex interaction responsible for material damage and which occurs between the material loadings. They added that this mechanism is not a driving process of failure, but rather a perceptible consequence of failure processes occurring in a stressed material. Another definition, by Kanters *et al* (2017), is that creep trials

usually result in a flow rate that depends on temperature and stress in the material. They then added that this flow is sustained for a definite period until the occurrence of failure. These authors also suggested that the prediction of creep test is feasible, and it finds its origin from practical observations showing that the product of the failure time and the strain rate is constant even when varying the loads. Additionally, it is relevant to define another behaviour that also occurs in the mining sector where creep is a matter of concern, namely the relaxation.

In conjunction with creep assessments, rock relaxation behaviour is often studied since it is much easier controlled, for the rock mass point of view. The process represents a behaviour wherein a material is under compressive stress while the strain is maintained constant for a certain period. The rheological material behaviour is assessed afterward. Concerning the relaxation process on rock materials, Drescher and Handley (2003) stated that this mechanism is observed on failed rocks, and the studies undertaken so far only focussed on uniaxial compression of a specimen. However, the same authors recognized that a trial of a tri-axial post-failure relaxation was already done by Malan *et al* (1997). The following Figure 3-1 and Figure 3-2 illustrate the behaviours of materials under creep or relaxation conditions.

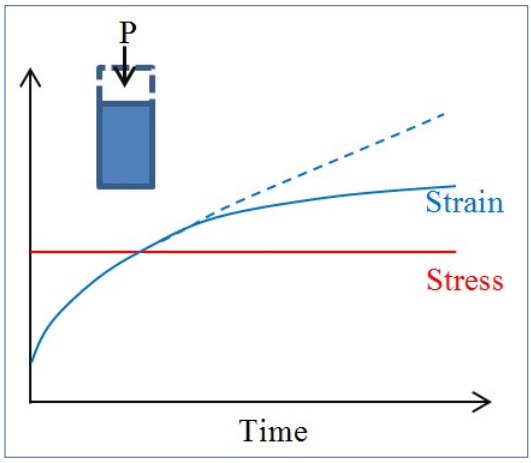


Figure 3-1 Creep Behaviour

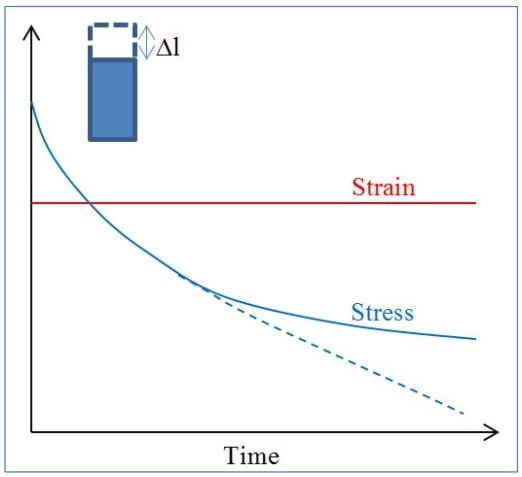


Figure 3-2 Relaxation Behaviour

An example of a creep testing machine from the CSIR is illustrated in Figure 3-3.

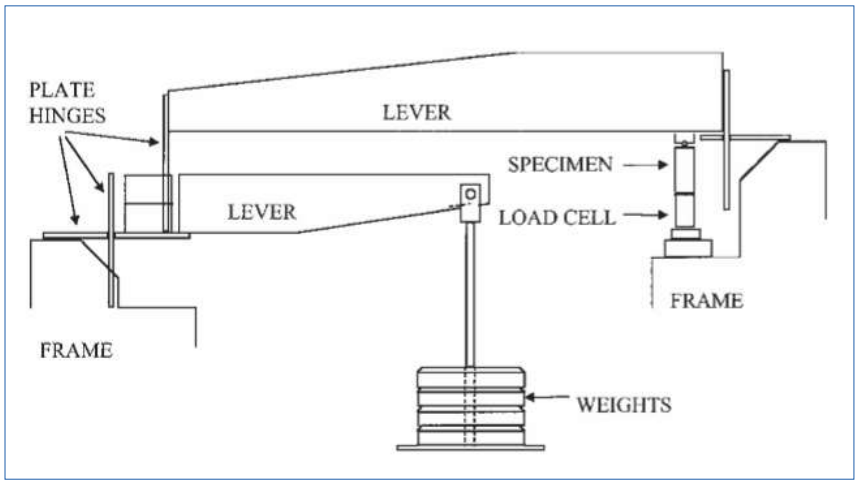


Figure 3-3 Principle of operation of the CSIR creep testing machine (Malan *et al,* 1997)

According to Drescher and Handley (2003), rheological rock properties are well determined for softer and less brittle rock types. These are the cases of rocks such as potash and rock salt. They have shown the ability to dissipating a considerable percentage of the applied energy during a creep cycle. And consequently, mines with these kinds of rock masses are not prone to highly stressed conditions and rockburst. However, when hard rocks are in study, creep results show less behaviour than when soft rocks are involved. Classic shear creep behaviour of a

discontinuity was illustrated by Drescher and Handley (2003), as shown in Figure 3-4.

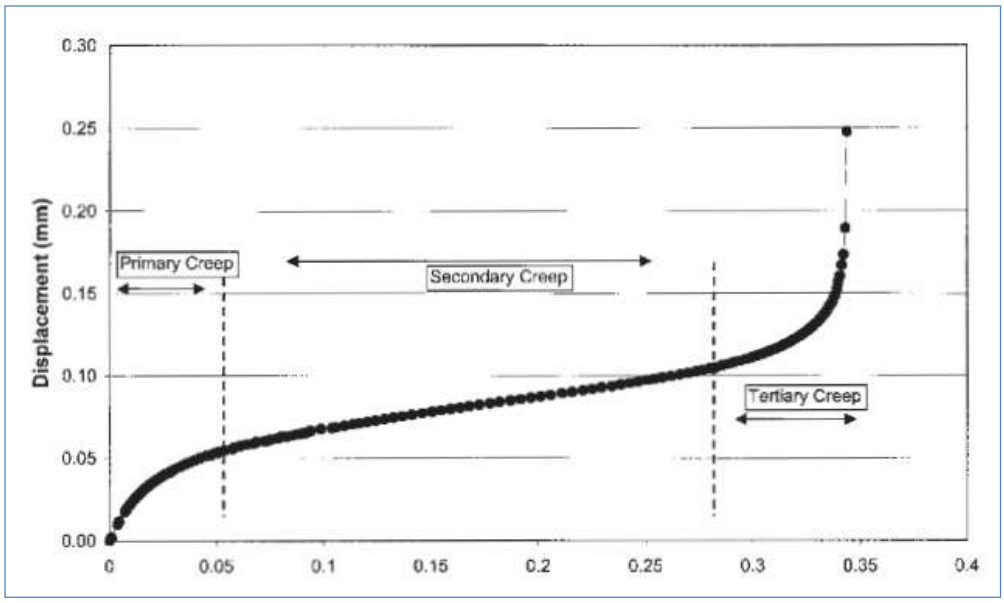


Figure 3-4 Classic shear creep behaviour of a discontinuity (Drescher and Handley, 2003)

Figure 3-4 encompasses three phases, namely primary, secondary and tertiary creep stages. The primary stage is also called decelerating creep, the secondary is the steady-state creep, while the tertiary phase is known as the accelerating creep (Wang *et al*, 2016).

Drescher and Handley (2003) believe that the reason behind the creep behaviour is the lack of enough release of energy in the opening stage of a stope. The release of energy that occurs sometime after a shift is resumed is generally sudden, in the form of rockburst. This theory is seen as the basis of the latter-mentioned authors' assertions, which emphasize that it is difficult to carry out hard rock creep measurements underground or in the laboratory, though a few studies have previously been done on the topic. Figure 3-5, suggested by Gay and Jager (1986), illustrates the typical fracture patterns of the creep/relaxation results obtained from the laboratory and underground.

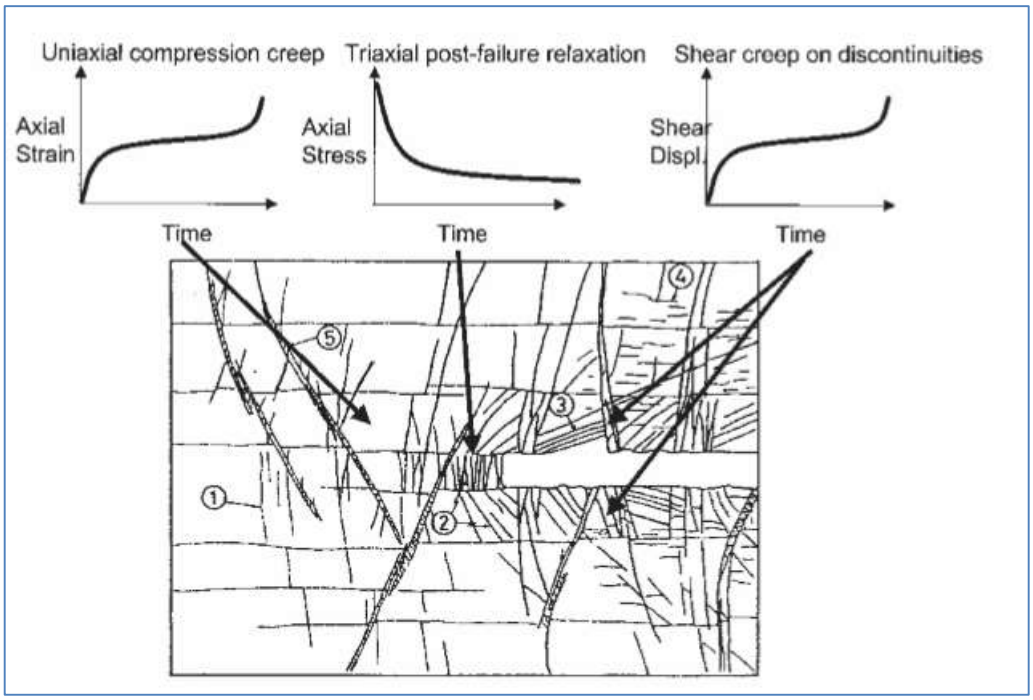


Figure 3-5 Typical fracture patterns relating the time-dependent processes around an underground slope (Gay and Jager, 1986)

Where (1), (2) and (3) are the most significant creep, namely:

(1) : Discontinuities in uniaxial compression

(2) : Axial relaxation

(3) : Shear creep on discontinuities

Figure 3-5 shows that considering an underground stope model, creep mechanisms occur in the intact rock encountered ahead of the stope face and on the discontinuities surrounding the stope, respectively under compression creep deformation and shear displacement. Besides, the fractured rock mass immediately ahead of the stope is in tension, undergoing a stress-relaxation resulting in some creep displacements (Drescher and Handley, 2003). These researchers then concluded that shear displacement on discontinuities combined with discontinuity dilations are the main driving time-dependent mechanism leading to stope closure, while compression creep deformation has a slight impact or an insignificant contribution to the stope closure. Here, it is believed that since there is only a slight influence of the intact rock creep on stopes closure, which only happens for few

hours or days, other mechanisms such as the rheological properties of discontinuities might be the main causes of time-dependent behaviour of hard rocks (Tan and Kang, 1980; Bowden and Curran, 1984; Malan, 1999). The occurring rock material dilation caused by rock damage is also not a major stope closure contributor. Since TSLs are the liners in study, the research should assess their time-dependent behaviour and whether this might influence the rock mass rheological deformation.

3.3 Time-dependent Deformation in Jointed Rock Masses

3.3.1 Time-dependency of ductile and brittle rocks

Time-dependent deformation in more ductile rock masses has been assessed by authors such as Drescher and Handley (2003) and Hudson and Brown (1972). The first authors worked on the post-failure relaxation behaviour of a Quartzite rock, while the latter studied the post-failure relaxation of a Cherokee Marble. This rock is weak and very plastic. It was reported to be less brittle than the Quartzite or the Lava but is the strongest rock that had been tested for post-failure relaxation (Drescher, 2006). This latter statement was based on the experimental outcomes from Drescher and Handley (2003), represented in Figure 3-6.

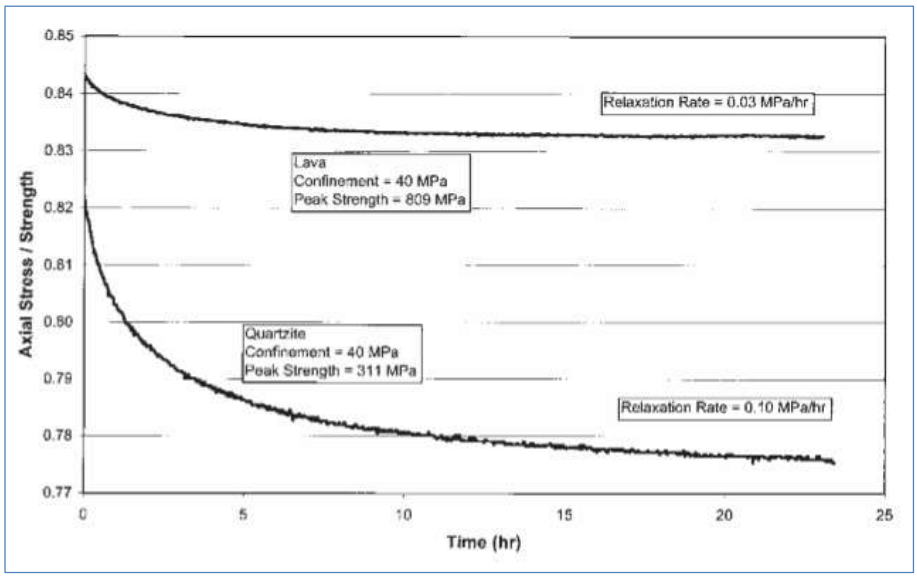


Figure 3-6 Post-failure relaxation curves for more and less brittle rocks (Drescher and Handley, 2003)

Figure 3-6 illustrates the post-failure relaxation of a more ductile rock, represented by the Quartzite curve, as well as a more brittle rock, here represented by a Lava type of rock.

3.3.2 Comparison of the results of post-failure relaxation behaviour of different types of rock materials

Similarly to the explanation in section 3.2, the released amount of relaxation stress is small in the Lava (a more brittle rock), which is understandable since the rock is capable of retaining a large amount of energy. This large amount of retained energy is likely to be suddenly released, thus predisposing the material to rock-burst conditions.

Figure 3-6 showed that the amount of relaxation stress is higher for the Quartzite than for the Lava. A large amount of energy was dissipated during the post-failure relaxation process, making larger the creep displacements in soft rocks in contrast to hard rock creep displacement behaviours, which remain small even for large volumes of assessed rocks. This makes it easier for a study of post-failure relaxation behaviour for a more ductile rock material (Drescher and Handley, 2003).

3.3.3 Long-term performance of rocks

Long-term strength (LTS) behaviour of rocks may be determined for uniaxial compressive strength trials, tensile trials or a tri-axial compression test (Bieniawski, 1967). This cited researcher stipulated that the plot should be axial stress versus volumetric strains, as illustrated in Figure 3-7 representing an unconfined trial of a Norite specimen.

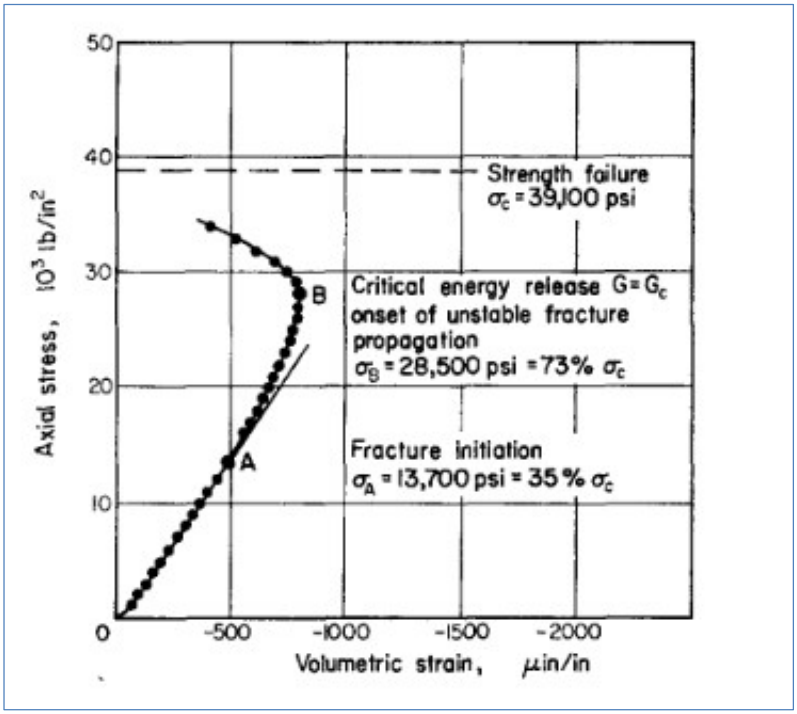


Figure 3-7 Determination of long-term strength for Norite specimen in unconfined tests (Bieniawski, 1967)

The long-term rock strength corresponds to the onset of unstable propagation, represented by point B in the graph. And in addition to Bieniawski's (1967) research, Drescher and Handley (2003) used the step-wise loading method to also determine the long-term performance of hard rock in a shorter time than it is required with the traditional constant creeping load. They considered a uniaxial compression creep wherein an initial applied load was 60% of the expected failure load. And a step by step increment of approximately 5% was applied after every 48 hours until the rock failure, the span time being obtained by the method of trial and error.

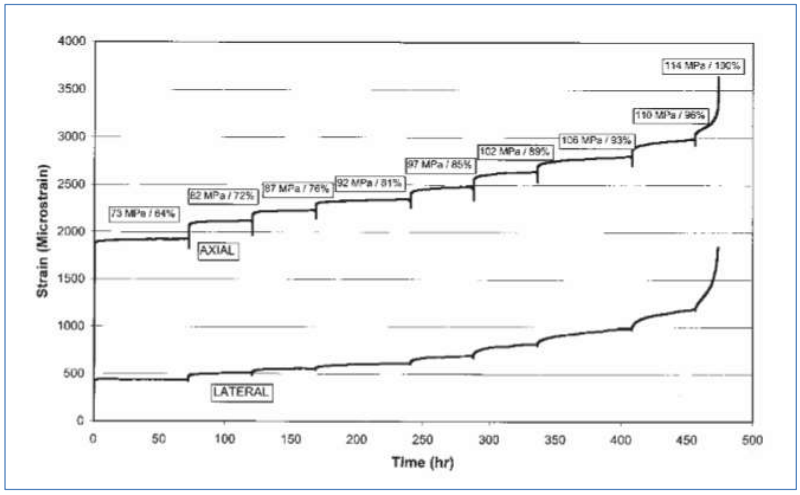


Figure 3-8 Step-wise loading method for hard rock long time performance determination through uniaxial compression (Drescher and Handley, 2003)

These same researchers emphasized the need to understand the stress relaxation rate of a failed rock mass, which could influence the mining rate, since a stress relaxation rate lower than the mining rate makes the rock mass prone to rockburst. The shear displacement behaviour on discontinuities is also being of significant importance in the mining environment, as explained in section 3.2. Its step-wise loading process was determined as illustrated in Figure 3-9, as proposed by Drescher and Handley (2003).

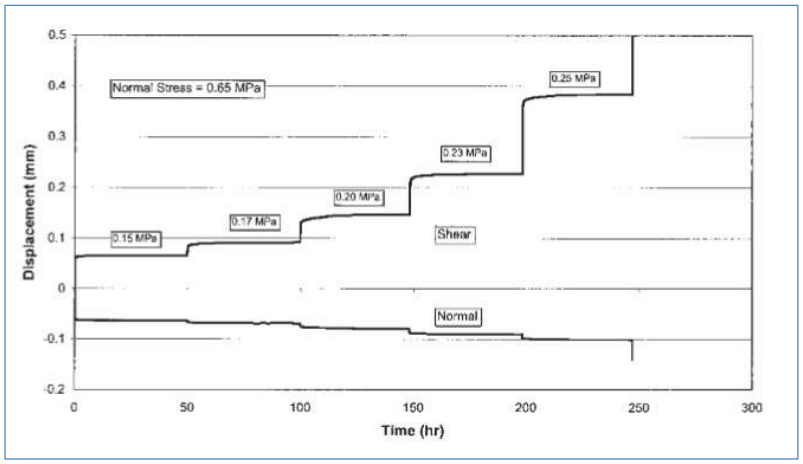


Figure 3-9 Step-wise loading method for hard rock long time performance determination through shear loading on discontinuities (Drescher and Handley, 2003)

Although this loading method will not constitute the core technique to be used for the rock-like specimens that will be used later in this work, due to the controversy behind the method, it should, however, be employed for few cases just for the sake of hypothetical predicting outcomes.

The overall long-term strength of rocks will follow the paths described by Nyungu and Stacey (2014) and presented in Figure 3-10.

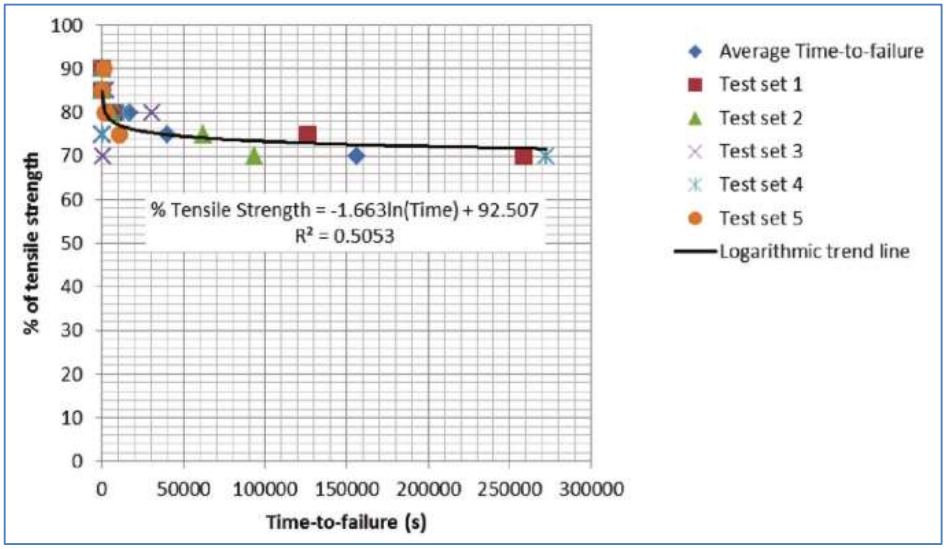


Figure 3-10 Time-to-failure plot for mottled Anorthosite (Nyungu and Stacey, 2014)

Similar to several other research initiatives, the long-term strength is found as the percentage of the tensile or compressive strength that coincides with the asymptote of the plotted time-dependent strength. However, since this endeavour is focused on studying the long-term behaviours of TSLs, which are generally polymer-based materials, rather than investigating any particular rock, it is worth investigating the time-dependency behaviour of those materials

3.4 Time-Dependent Deformation of Polymer-Based Materials

The mechanical characteristics of polymeric materials are mostly dictated by its viscoelasticity (Osswald, 2015). This should justify why a polymer material has different behaviours depending on whether it is subjected to long or short term

loadings (Osswald, 2015). Microscopically speaking, the latter cited author explains the behaviour as follows: When loading the polymeric material on a short-term basis, the molecules will not have enough time to move and easily slide to occupy new positions. This phenomenon results in them returning to their initial positions after the load has been removed; the occurring deformation is thus recovered, and the material is considered perfectly elastic. However, if the applied load is maintained for on a long-term basis, the extended time of deformation is microscopically seen as sufficient to allow the moving molecules to slide past each other. Therefore, they will occupy new positions, resulting in permanent deformation.

For slow deformations, Osswald (2015) suggested that polymeric material behaviours should be explained through the Boltzmann superposition principle. As illustrated in Figure 3-11 (Osswald (2015)), various curves of stress relaxation tests were performed at different temperatures. Bearing in mind that the relaxation time parameter (λ) dictates the duration of stress relaxation, high-temperature conditions shorten the time of molecular relaxations while low-temperature conditions extend the relaxation time, with these temperatures not affecting the shapes of the stress relaxation curves (Osswald, 2015). The same author then explained that after choosing a temperature of reference (T) for the master curve, which was 25ºC, and after determining the corresponding relaxation time, equivalent to 100 hours, the various curves of stress relaxation are shifted horizontally to the right and left of the curve of 25ºC, for higher and lower temperatures than T respectively. The resulting curve obtained after superposition is the master curve at the temperature of reference T.

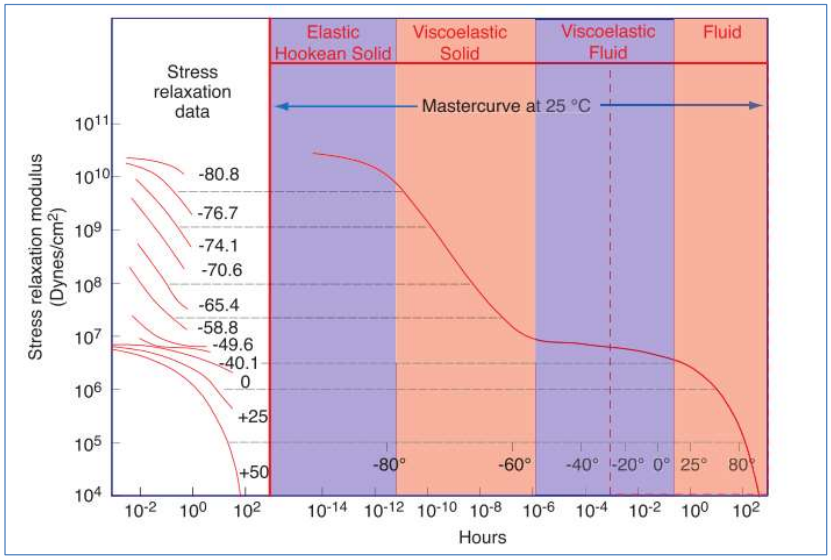


Figure 3-11 Example of long-term stress relaxation curve obtained by superposition (Osswald, 2015)

The same author then recommended a way of retrieving the horizontal shift, log a_T, through the means of the William-Landel-Ferry (WLF) equation expressed as follows. However, the WLF needs to be adjusted to the stage when it fits the experimental data.

$$\log a_T = \frac{-C_1(T - T_{ref})}{C_2 + T - T_{ref}} \qquad \text{(II)}$$

Where

C_1= 17.44 C_2=51.6

C_1 and C_2 are called universal constants

log a_T : Horizontal shift

T_{ref} : Temperature of reference

T : A relaxation response temperature

The importance of determining a master curve is to allow tracing of the rheological behaviours of the polymeric materials for much longer periods than those established experimentally (Osswald, 2015). Some of these theories will be of great value in creep studies, and would possibly assist the current research to determine how TSLs behave over longer loading periods.

3.5 Creep Tests on TSLs

There is no broad information on the creep behaviour of TSLs in the literature. Actually, if no study was yet done on TSL's creep behaviour at the time of the conception of this thesis's project, little has been done since then and to our knowledge, this subject was very-recently developed for the first time in the literature by Guner and Ozturk (2018). In their work, these researchers assessed the long-term tensile performance of a cement-based TSL that has been cured for one, seven and fourteen days. Their creep loadings and creep rupture envelopes were as presented in Figure 3-12.

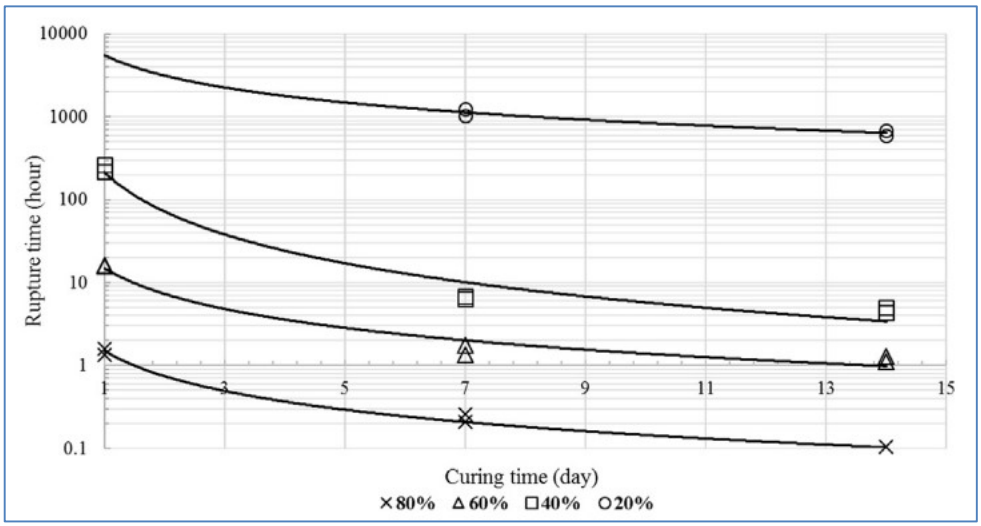


Figure 3-12 Creep rupture curves of a cement-based TSL under tensile loading (Guner and Ozturk, 2018)

The same authors have carried on investigating TSL's behaviour under creep loading and have proposed some models that can define these behaviours (Guner and Ozturk, 2019; Ozturk and Guner, 2019).

The outcomes from the work by Guner and Ozturk (2018) have shown that the ultimate tensile strength parameter should not be considered as a design reference or for prediction of service life, since TSL showed much lower long-term strength as compared with the ultimate strength. They also advised that TSLs should be resorted to as temporary supports until the installation of permanent supports. It was

observed that their research was only limited to the direct tensile mode of failure and all the tests were in room conditions, rather than in underground mines-like conditions. And in their recommendations, these researchers suggested that other failure modes be investigated, different environmental conditions be considered, and a variety of TSLs be investigated to complete their research; and this is exactly what the current research is aiming to achieve.

The other type of creep study, developed by Guner and Ozturk (2019) and Ozturk and Guner (2019) involved the establishment of a rheological model for TSLs, that should assist in understanding and predicting TSL's creep behaviours. The outcomes should particularly be used in building and running numerical models. Although this technique will not be applied in the current research, as it constitutes an entire subject of an investigation on its own, a review of the fundamental concepts will be necessary for understanding the modelling background.

3.6 Rheological model concepts

Two loading techniques are mostly used for creep testing, these being the single-step and multi-step loadings. When testing a rock material, unlike the single-step loading, the multi-step technique (Cao, Youdao, Yixian, Haiping and Bingxiang, 2016; Yang, Hu, Ranjith, and Xu, 2018) has the advantages of being time-efficient as well as avoiding the isolated influence of rock specimens on creep strain (Yang *et al*, 2018). The inconvenience of the multi-step technique, however, is that the subsequent loadings are affected by the previous ones, since the creep strains of the later steps encompass the earlier ones unless two conditions are observed (Kolařík and Pegoretti, 2008; Xia and Zhong, 1989):

- The loading history is taken into consideration and
- The creep curve reaches the steady-state stage where the strain rate is constant

Although the multi-step loading method will not be resorted to in the current research, it is a powerful creep procedure on condition that the stress and strain behaviour histories (laws) are well represented to avoid wrong interpretations.

These laws can be explained in detail through mathematical expressions of multi-step creep loading that will be detailed in this paragraph. The first expression is given through the equation III.

$$\sigma(t) = \Delta\sigma_1.\theta(t-t_1) + \Delta\sigma_2.\theta(t-t_2) + \Delta\sigma_3.\theta(t-t_3) + \cdots + \Delta\sigma_i.\theta(t-t_i) + \cdots + \Delta\sigma_n.\theta(t-t_n) \quad \text{(III)}$$

Where:

For $t - t_i \geq 0$, $\theta.(t - t_i) = 1$

And for $t - t_i < 0$, $\theta.(t - t_i) = 0$

And based on the Boltzmann superposition, the creep strain equation becomes:

$$\varepsilon(t) = \frac{\sigma(t)}{E} + \int_{-\infty}^{t} \sigma(\tau)\frac{\partial J(t-\tau)}{\partial \tau}d\tau = \frac{\sigma(t)}{E} + \int_{-\infty}^{t} \sigma(\tau)K(t-\tau)\,d\tau \quad \text{(IV)}$$

Where: $J(t-\tau)$: $Creep\ compliance$ and $K(t-\tau)$: $Creep\ Kermel\ function$

And assuming: $\theta(t-t_1) = \theta_1$,

$$\varepsilon(t) = \frac{\Delta\sigma_1.\theta_1 + \Delta\sigma_2.\theta_2 + \Delta\sigma_3.\theta_3 + \cdots + \Delta\sigma_i.\theta_i + \cdots + \Delta\sigma_n.\theta_n}{E} + \int_0^t (\Delta\sigma_1.\theta_1 + \Delta\sigma_2.\theta_2 + \Delta\sigma_3.\theta_3 + \cdots + \Delta\sigma_i.\theta_i + \cdots + \Delta\sigma_n.\theta_n)K(t-\tau)\,d\tau \quad \text{(V)}$$

And if $(t - ti) \geq 0$, the creep strain equation of a single-stage creep deduced from a multi-stage creep is believed to be:

$$\varepsilon(t) = \frac{\Delta\sigma_1 + \Delta\sigma_2 + \Delta\sigma_3 + \cdots + \Delta\sigma_i + \cdots + \Delta\sigma_n}{E} + \int_{t_1}^{t} \Delta\sigma_1 K(t-\tau)\,d\tau + \int_{t_2}^{t} \Delta\sigma_2 K(t-\tau)\,d\tau + \int_{t_3}^{t} \Delta\sigma_3 K(t-\tau)\,d\tau + \cdots + \int_{t_i}^{t} \Delta\sigma_i K(t-\tau)\,d\tau + \cdots + \int_{t_n}^{t} \Delta\sigma_n K(t-\tau)\,d\tau \quad \text{(VI)}$$

This is illustrated in Figure 3-13.

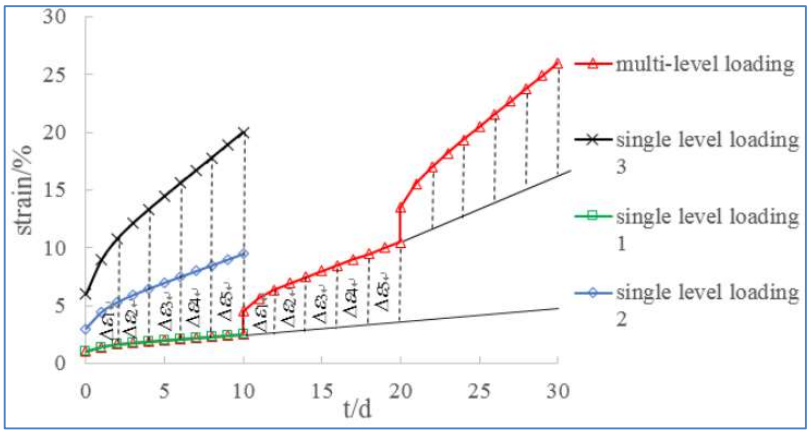


Figure 3-13 Multi-step creep technique (Yang *et al*, 2018)

The single-level loading 2 represents the creep strain curve obtained by the superposition of the strains produced by the application of $\Delta\sigma_1$ and $\Delta\sigma_2$ in the multi-step creep method. And some constitutive equations are presented in Table 3-1.

Table 3-1 Constitutive and creep equations for some rheological models under single-step loading (Yang *et al*, 2018)

Rheological model	**Constitutive equation**	**Creep equation**
Maxwell	$\dot{\varepsilon}=\frac{\dot{\sigma}}{E}+\frac{\sigma}{\eta}$	$\epsilon=\frac{\sigma_0}{E}\left(1+\frac{E}{\eta}t\right)$
Kelvin	$\sigma=E\epsilon+\eta\dot{\epsilon}$	$\epsilon=\frac{\sigma_0}{E}\left(1-e^{-\frac{E}{\eta}t}\right)$
H-K	$\sigma+\frac{\eta}{E_1+E_2}\dot{\sigma}=\frac{E_1E_2}{E_1+E_2}\varepsilon+\frac{\eta E_1}{E_1+E_2}\dot{\epsilon}$	$\epsilon=\frac{\sigma_0}{E_1}+\frac{\sigma_0}{E_2}\left(1-e^{-\frac{E_2}{\eta}t}\right)$
H\M	$\sigma+\frac{\eta}{E_2}\dot{\sigma}=E_1\varepsilon+\frac{E_1+E_2}{E_2}\eta\dot{\epsilon}$	$\epsilon=\frac{\sigma_0}{E_1}\left(1-\frac{E_2}{E_1+E_2}e^{-\frac{E_1E_2}{(E_1+E_2)\eta}t}\right)$
Burgers	$\sigma+\left(\frac{\eta_2}{E_1}+\frac{\eta_1+\eta_2}{E_2}\right)\dot{\sigma}+\frac{\eta_1\eta_2}{E_1E_2}\ddot{\sigma}=\eta_2\dot{\epsilon}+\frac{\eta_1\eta_2}{E_2}\ddot{\epsilon}$	$\epsilon=\frac{\sigma_0}{E_1}+\frac{\sigma_0}{E_1}\left(1-e^{-\frac{E_1}{\eta_1}t}\right)+\frac{\sigma_0}{\eta_2}t$
Bingham	$\sigma=E\epsilon$ for $\sigma<\sigma_s$ $\sigma+\frac{\eta}{E_2}\dot{\sigma}=\sigma_s+\eta\dot{\epsilon}$ for $\sigma\geq\sigma_s$	$\epsilon=\frac{\sigma_0}{E}$ for $\sigma<\sigma_s$ $\epsilon=\frac{\sigma_0}{E}+\frac{\sigma-\sigma_s}{\eta}t$ for $\sigma\geq\sigma_s$
Nishihara	$\frac{\eta_1}{E_1}\dot{\sigma}+\left(1+\frac{E_2}{E_1}\right)\sigma=\eta_1\dot{\epsilon}+E_2\epsilon$ for $\sigma<\sigma_s$ $\ddot{\sigma}+\left(\frac{E_2}{\eta_1}+\frac{E_2}{\eta_2}+\frac{E_1}{\eta_1}\right)\dot{\sigma}+\frac{E_1E_2}{\eta_1\eta_2}(\sigma-\sigma_s)=E_2\ddot{\epsilon}+\frac{E_1E_2}{\eta_1}\dot{\epsilon}$ for $\sigma\geq\sigma_s$	$\epsilon=\frac{\sigma_0}{E_1}+\frac{\sigma_0}{E_2}\left(1-e^{-\frac{E_2}{\eta_1}t}\right)$ for $\sigma<\sigma_s$ $\epsilon=\frac{\sigma_0}{E_1}+\frac{\sigma_0}{E_2}\left(1-e^{-\frac{E_2}{\eta_1}t}\right)+\frac{(\sigma-\sigma_s)}{\eta_2}t$ for $\sigma\geq\sigma_s$

3.6.1 H-K creep model

This model is used to simulate the stable creep behaviour of materials such as hard rocks that are submitted to low loads or stresses which are below the yield stress surface σ_s (Yang *et al*, 2018). It is illustrated through Figure 3-14.

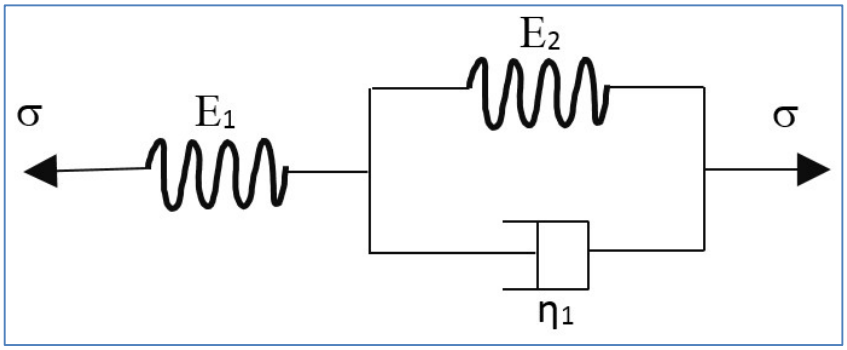


Figure 3-14 H-K rheological model

But as noticed by Yang *et al* (2018), although the deduced single-step and multi-step loadings have the same stable creep strain after some days, their transient creep lines diverge due to time influence on the multi-step creep curve. Therefore, these authors proposed the correction of the effect of the former loadings in a multi-step loading process. Before that, it is worth also looking at the Burgers model, mostly used in rheological studies.

3.6.2 Burgers model

The Burgers model is believed to be very useful for steady-state creeps (Yang *et al*, 2018). This model is equivalent to the previous cited, to which a dashpot has been connected in series. Its illustration is shown in Figure 3-15.

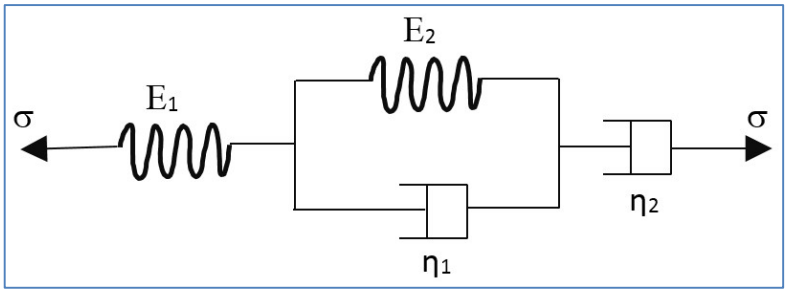


Figure 3-15 Burgers rheological model

These rheological models diverge in their abilities and limitations in describing the real material properties. Some of them draw attention, namely the Burgers and Nishihara rheological models, capable of describing:

- The creep behaviour
- The relaxation behaviour
- The transient deformation
- The elastic after-effect behaviour
- The viscous flow

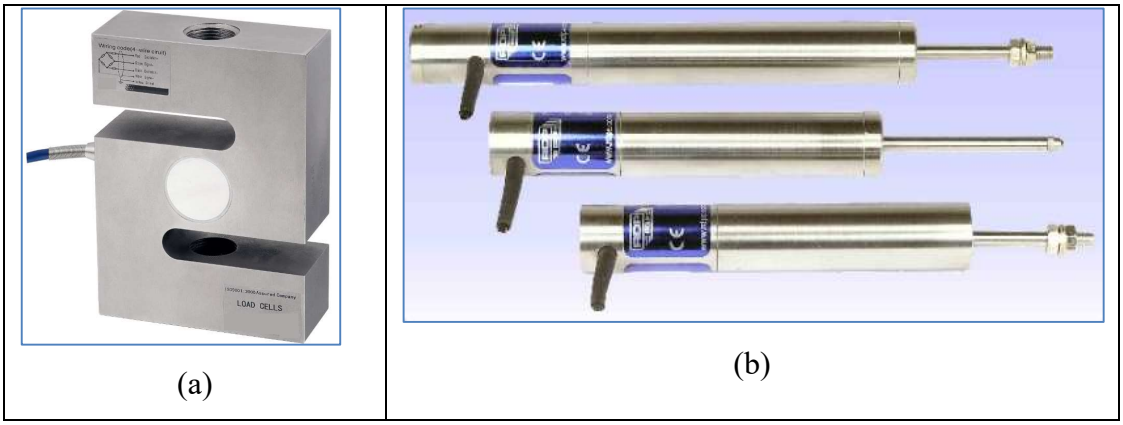
But these two models are not able to provide the deformation limit, likely available in Kelvin, H-K and H\M, whereas they possess some advantages that these latter cannot provide. In light of the complexity of these models, in-depth and exclusive studies should be recommended for the use of TSL creep behaviours. This research will follow the traditional methodology of creep assessment by running full single-step loading creep tests and finding the strains and creep times instead of using the multi-step loadings to assess the expected strains and times.

3.7 Accessories for Stress and Strain Measurement

3.7.1 Load cells and linear variable differential transformers

Load cells are instruments used for weight measurement. Similarly, the LVDT is an electrical instrument that is used to measure linear displacements. Both instruments are made of a spring element on which strain gauges have been attached so that the resulting deformation can be read and converted into the proportional onset loading or displacement (Riley *et al*, 1993).

Different types of load cells are available, such as the shear beam load cell, the compression load cells, the tensile S type load cells, etc. Figure 3-16 illustrates (a) an S type load cell (Covscale, n.d.) and (b) an LVDT instrument (*ACT LVDT Displacement Transducer*, n.d.).



(a) (b)

Figure 3-16 (a) S type load cell (Covscale, n.d.) and (b) LVDT model ('ACT LVDT Displacement Transducer', n.d.)

If an S type load cell will be used for calibration of all the creep testing machines, adapted LVDTs will be made, as will be presented later in CHAPTER 5. Nevertheless, since these measuring instruments are expected to detect any small deformation from the built-in strain gauges, they will need to be configured in a Wheatstone bridge circuit.

3.7.2 Wheatstone Bridge configuration

Introduction

Conceived in 1843 by Sir Charles Wheatstone, the Wheatstone bridge configuration is a bridge circuit resorted to for measurements of electrical resistances (Hoffmann, 1974). This circuit aims to compare unknown resistances to well-defined ones. It also has the particularity of measuring small changes of resistance such as those observed in strain gauges. Thus it is an ideal tool for the measurement of static strains (Hoffmann, 1974; Omega, 1999) and could be useful in the configuration of the displacement transducers to be used in this research.

Strain gauges

Strain gauges are grid-shaped sensing elements, used to measure surface strains. They are generally made of thin metallic resistive foil (Kyowa Electronic Instruments Co., Ltd, n.d.). They are set on a thin plastic film and are also laminated

with a thin film (Kyowa Electronic Instruments Co., Ltd, n.d.). They are based on the principle of bearing a mechanical elongation (or contraction) to observe the output change in electric resistance. Therefore, the strain is measured through the resistance change; with each strain gauge having its characteristic defined by the gauge factor (GF) (Kyowa Electronic Instruments Co., Ltd, n.d.). The gauge factor is defined by the equation:

$$K = \frac{\Delta R / R}{\Delta L / L} \quad \text{(VII)}$$

Where

K: Gauge Factor

R : Gauge Resistance in Ohm

ΔR: Resistance change in Ohm

$\Delta L / L$: Gauge strain, also expressed as ε

For the present research, two types of strain gauges were used as presented in Table 3-2.

Table 3-2 Description of employed strain gauges

Type	Lot No	Gage Factor (K) (24ºC, 50%RH)	Gage Length	Gage Resistance	Temperature coefficient of Gage Factor
KFG-20-120-C1-11	Y4533S	2.12±1.0%	20 mm	119.8±0.2 Ω	+0.008%/ºC
K-10-A1-11	Y756-046	2.00±1%	10 mm	120±0.3 Ω	0.015%/ºC

The strain tension limit is estimated in the range of 1000 με to 10 000 με, with experimental results generally approximating 3000 με (Omega, 1999).

Wheatstone bridge structures

Balanced and unbalanced bridges

To form a bridge, four resistors were combined as illustrated in Figure 3-17.

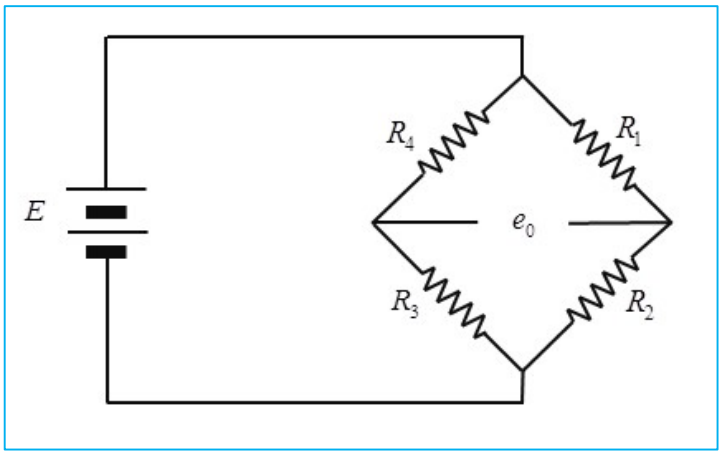


Figure 3-17 Wheatstone bridge configuration

Where

E: input voltage

e_o : Output voltage

R_1, R_2, R_3, and R_4: Resistors; in this thesis's research they are strain gauges

If these resistors are equal and not under the effect of any resistance change, the output voltage e_o will remain zero for whatever might be the input voltage. And in this case, the bridge will be in balance, represented by the following equation:

$$\frac{R_1}{R_2} = \frac{R_4}{R_3} \qquad \text{(VIII)}$$

However, any resistance change (also called active gauge) on one or more of the resistors will make the bridge lose its balance, and the output voltage e_o will no longer be zero, as per the following inequality, except when the changes nullify themselves.

$$\frac{R_1}{R_2} \neq \frac{R_4}{R_3} \qquad \text{(IX)}$$

And the general equation when all four gauges are active is:

$$e_o = \frac{1}{4}\left(\frac{\Delta R_1}{R_1} - \frac{\Delta R_2}{R_2} + \frac{\Delta R_3}{R_3} - \frac{\Delta R_4}{R_4}\right)E$$ (Kyowa Electronic Instruments Co., Ltd, n.d.) (X)

And if the strain gauges are of the same types, with the same gauge factors, then the equation XV can be written as follows:

$$e_o = \frac{1}{4} K(\varepsilon_1 - \varepsilon_2 + \varepsilon_3 - \varepsilon_4)E \qquad \text{(XI)}$$

When only one gauge is active, the bridge is a 1-gauge system. In this particular research, the change could be observed on two arms of the bridge, also called a 2-gauge system. However, for a better explanation, a 1-gauge system will be briefed before showing the actual case concerning this research.

One-gauge system

The one-gauge system is represented by the following configuration.

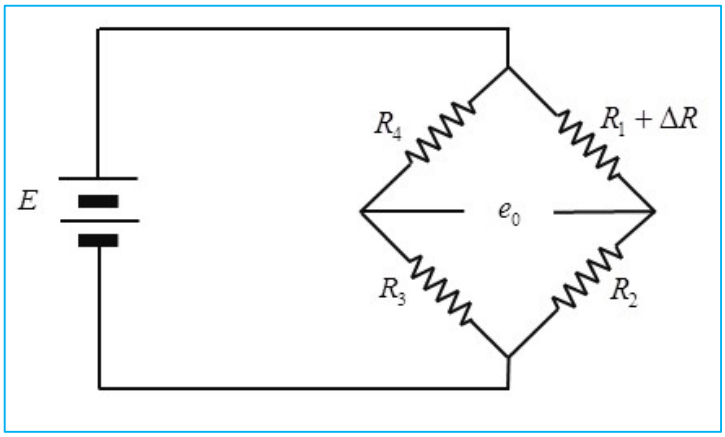


Figure 3-18 One-gauge bridge configuration

Since the resistance change only occurs in R_1 (in tension), the strains ε_2, ε_3 and ε_4 will be equal to zero, and the equation of the output voltage is therefore:

$$e_o = \frac{1}{4} \frac{\Delta R_1}{R_1} E \qquad \text{(XII)}$$

Or

$$e_o = \frac{1}{4} K(.\varepsilon_1).E = e_1 \qquad \text{(XIII)}$$

For a 1-gauge system, $e_o = e_1$. This structure is also called a quarter bridge.

Let's compare a 2-gauge system with a 1-gauge system.

Two-gauge system

The configuration to be used is displayed in Figure 3-19.

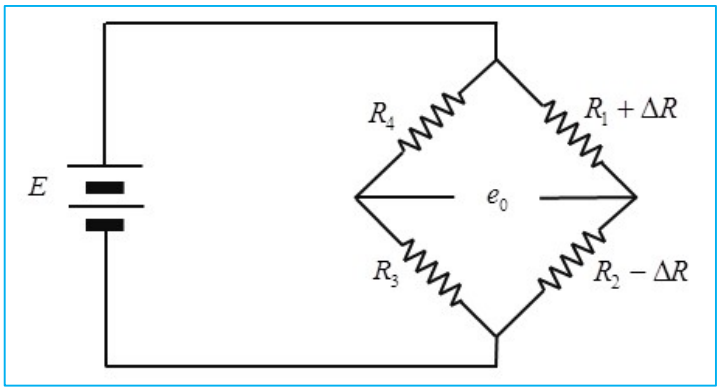


Figure 3-19 Two-gauge bridge configuration

Two active gauges or pairs of gauges will be placed in the circuit of the displacement transducer or the load transducer, respectively. And to complete the bridges, two inactive gauges or pairs of gauges will be added to the rest of the arms of the bridge, respectively. These gauges are also called dummies. The output voltage equation will therefore be:

$$e_o = \frac{1}{4}\left(\frac{\Delta R_1}{R_1} - \frac{\Delta R_2}{R_2}\right)E \qquad \text{(XIV)}$$

Knowing that one of the active gauges will be in tension (R_1) and the other in compression (R_2), the expression in the bracket will, in reality, be an addition of the values instead of subtraction because the change of resistance in compression is negative. And since the strain gauges are of the same types with same gauge factors, the previous equation (XIX) can be displayed as follows:

$$e_o = \frac{1}{4}K\left(\varepsilon_1 - \varepsilon_2\right)E \qquad \text{(XV)}$$

And since R_1 is in tension and R_2 in compression, then

$$\varepsilon_1 = \varepsilon = -\varepsilon_2\,; \qquad \text{(XVI)}$$

$$e_o = \frac{1}{4}K\left(\varepsilon_1 + \varepsilon_1\right)E \qquad \text{(XVII)}$$

$$e_o = \frac{1}{4} K(2\varepsilon_1)E = \frac{1}{2} K\varepsilon_1 E = 2e_1 \quad \text{(XVIII)}$$

This circuit is also called half-bridge, and its output voltage is twice the output voltage of the quarter bridge, provided that the gauges are of the same types, with the same gauge factor, and one gauge (or a pair of gauges) should be in tension while the other gauge (or pair of gauges) is in compression or vice versa.

Similarly, a full bridge might be set with all the gauges being active, but this was not applied in this thesis's research.

Input voltage

Since the bridge needs to be excited with an input voltage *E*, a switching power supply was used, with the following characteristics:

Table 3-3 Characteristics of power supply for the research

Data	Characteristics
Model	RS-15-5
Input voltage	100-240VAC
Output voltage	+5V CC
Current intensity	3.0A

The output voltage of the power supply was regulated at more or less 4.5V, which is the input voltage of the Wheatstone bridge. Figure 3-20 illustrates a sample of the employed power supplies as well as the connection to a data logger, used to display the output voltages.

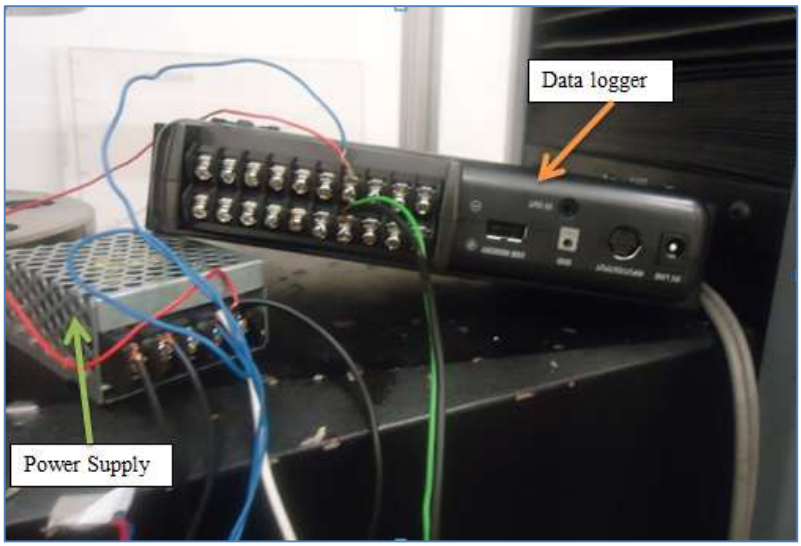


Figure 3-20 Coupling of power supply with a data logger

Adopted Wheatstone bridge circuit

Figure 3-21 presents a better illustration of how the connections were made between the power supply instrument, the transducer, the dummy, and the data logger.

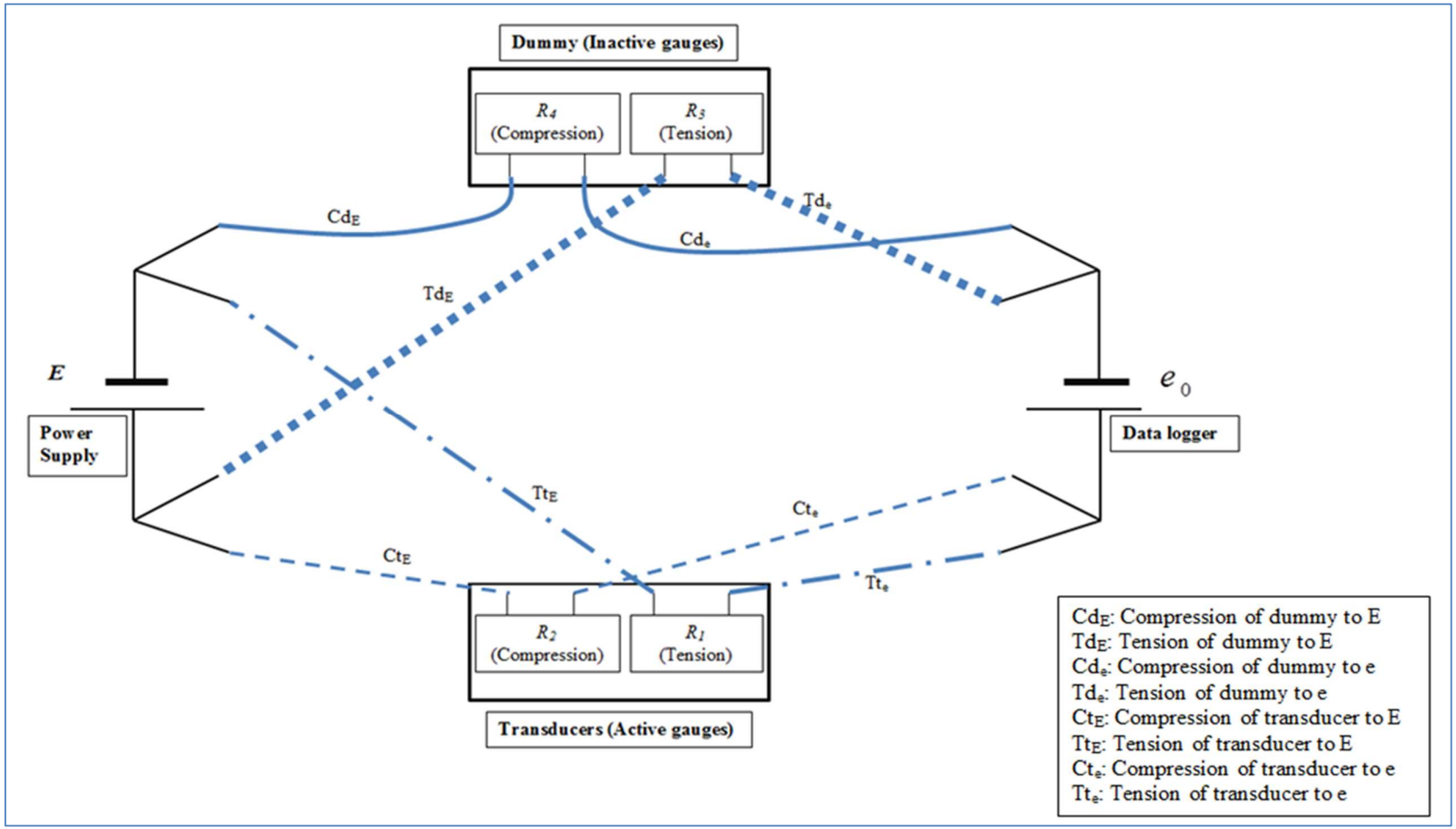


Figure 3-21 Wheatstone bridge connection of a transducer

3.8 Chapter Summary

The fact that very-limited literature information is available on TSL long-term performance, indicates that, due to its lower long-term strength, TSL's ultimate tensile strength should not be the design indicator or a reference for prediction of service life. Although preliminary rheological models are also being developed for a better understanding of TSL creep behaviour, much is still to be done to acquire sufficient knowledge on the practical effectiveness of thin membranes, particularly in underground mines. From the literature, it was also found that there is still a need to diversify the TSL materials, the testing mechanisms, and possibly to vary the environmental conditions. The current research will attempt to provide such information in CHAPTER 4, which will investigate the practical in-situ behaviours of TSLs from some underground sites through field observation, and data collection, and analysis. Following this, CHAPTER 5 and CHAPTER 6 will attempt to complete the field information by assessing TSL long-term performance through laboratory trials and numerical modelling applications, respectively.

CHAPTER 4 FIELD ASSESSMENT OF TSL PERFORMANCE

4.1 Introduction

Most of the information on TSL performance is based on laboratory experiments. Very few field assessments have been made and reported thus far, which has caused difficulty in practically evaluating the statistics concerning TSL good performance. This lack of sufficient field data on thin membranes has prompted the fieldwork within this thesis. The key concept for such assessments of support performance was to characterize the field behaviour of various TSLs. This method of assessment is highly valued since it may assist in a better evaluation of the real behaviour of these membrane supports. And to achieve this, two South African mines were visited: a relatively deep mine (deeper than 1500 metres) and a shallow mine (approximately 350 metres). These were the only ones to express interest in TSL assessment and to facilitate this endeavour. Other mines had very few areas where TSLs were applied, or were not prepared for field inspection due to internal reasons. In the visited mines, visual TSL assessments were performed according to a pre-established method. This method is presented in the following paragraph.

4.2 Methodology of Field Assessment

The field assessment was undertaken following three steps:

- Collection of data through a questionnaire and opinion
- The undertaking of in situ investigations on specific sites, and for a variety of thin liners
- Data analyses of TSL's field performance

4.2.1 Collection of data through a questionnaire and opinion

The objective in proceeding with this kind of study was to identify the practical factors that can influence TSL performances, based on the feedback from the mine technicians. These performances had to subsequently be validated through laboratory tests and numerical modelling. The study intended to start from an

enquiry addressed to some selected experienced workers. The enquiry included the following non-exhaustive list of questions displayed in Table 4-1.

Table 4-1 Field Enquiries

Number	Questions
1	When did the mine start using the TSL products?
2	Which types of rocks have TSLs been applied on?
3	What was the adopted TSL thickness?
4	What equipment was used for the TSLs application?
5	What were the moisture conditions of the surfaces where TSLs were applied?
6	What is the temperature level in the sectors where TSLs are used?
7	Which other supports were combined with TSLs for better stabilization of the rock mass?
8	What were the characteristics of the combined supports to TSLs?
9	What are the surface types where TSLs have been applied?
10	What type of infrastructure have TSLs been applied on?
11	What are the infrastructures where TSLs were/are successful?
12	In which conditions have TSLs supports started showing signs of failure?
13	What are the site types where TSLs have underperformed?
14	What are the geotechnical characteristics of the sites where TSLs have underperformed?
15	What are the loading mechanisms leading to TSLs' failure?
16	How long have the underperforming TSLs lasted?
17	What were/are the observed signs of TSLs failure?
18	What methods are used for field assessments?
19	What were the measured pieces of evidence (properties) of TSL failure?
20	Were the surfaces coated with TSLs initially well prepared?
21	What are the characteristics of the rocks where TSLs performed well?
22	For how long have the successful applied TSLs been performing?

This section will also highlight the views of an applied TSL from a supplier and a geotechnical inspector, followed by a discussion between them over its effectiveness (Kanda and Stacey, 2019). Since TSL is subject to varying opinions depending on the angle from which it is scrutinized, discussion between a supplier and an inspector based on evident facts proved to be meaningful for understanding the dual conception of its performance. The latter discussion can probably alert on the cautions to take in the interpretations of the questionnaire feedback, and it also emphasizes the importance of a thoroughly-independent assessment to provide proven evidence on TSLs performance, particularly for a long-term purpose. These opinions are not considered to be representative of all aspects, but are referred to because they reflect the leanings of the interviews from the visited mines' perspectives, and thus may lead to understanding the diversified views on TSL performance, thus could assist in decision-making for thin coatings utilization.

4.2.2 *In situ* inspection of TSL performance

By performing the field assessments, the author intended to compare, confirm or complete the data collected through the questionnaire and interaction. A visual survey of specific zones where TSLs were applied was undertaken. Studies were focused on sites that are prone to weathering, spalling, high-stress conditions, and wave propagation effects. Where possible, mapping of the selected sites, together with the geological databases were provided, and this could assist in the analyses of the observed mechanisms of TSL failure, namely: basket mechanism, slab mechanism, mechanical protection, wedge and block loading, distributed surface loading, stress-induced loading, water pressure loading, bending loading (Kanda and Stacey, 2019). Through these mechanisms, the losses of TSL properties could be investigated. The most targeted losses of properties were:

- Tensile strength loss: This property generally accompanies the failure of a thin liner due to the loosening of rocks (Tannant, 2001) or due to crack dilation in the rock mass (Yilmaz, 2010). In this endeavour, the author targeted some known unstable zones, and characterized the loading effect of loosened rocks so that the bond strength could be assessed, namely whether it was still effective or already overcome (loss of adhesion or failure

of tensile bond strength). And based on the performances of TSLs described in the literature review, some failed TSLs were assessed on whether there were cracks just behind them that could lead to tensile failure. Similarly, on some specific known unstable zones, observations were made on whether there were areas where TSLs were still holding the rock mass even after this latter had failed

- Tensile bond strength loss: In this case, the author intended to observe whether there were sites where TSLs were no longer bonded to the rock or shotcrete. Some barring processes, when allowed, were performed to check on the bonding strength, knowing that a slight triggering factor, a weak bond will lead the coating to detach.

- Shear bond strength loss: This property was expected from TSLs that had penetrated the cracks, thus such cases were assessed on whether the TSLs had then loosened or showed some incapacity in bonding to the rock mass.

It is worth noting that substrate strength, wholeness, and cleanliness are among the major factors for a better performance of the coating. In this aspect, the *in-situ* uniaxial compressive strength (UCS) of the rock mass or shotcrete was also assessed through the use of the Schmidt hammer. The anvil calibration assisted in converting the rock hardness into the UCS. Along with the Schmidt hammer, a geologist's hammer was also used to detect hollowness, indicating the presence of cavities behind the liner.

TSL performance can be affected by factors such as the environment. Therefore, underground tracking of temperature and humidity were also undertaken. In this, data obtained from enquiries should be compared with observed information for the sake of validation.

4.2.3 Analysis of field data on TSL performance

Prior to the assessment of any support performance, plans of all sites where the thin spray-on membranes had been applied were acquired where such were available. These included the geotechnical and geological plans of sites where TSL was used. All the information about the available TSL types was recorded and the information on their performances analysed.

Here, the ideal procedure should have been to first analyse the data of the initial and progressive design plans of the mine supports, and then to assess and analyse the periodic reports of the supports' performance, and finally to characterize the various practical TSL behaviours. But there was a limitation in acquiring enough data mentioned on the two first steps: Generally, no systematic reports of periodic TSL assessments were provided, and the initial and progressive design plans of TSLs supports were not availed. This led this research to mainly rely on the availed data (which was mostly incomplete) to characterize the coating sites.

4.3 Feedback from the Inquiry

4.3.1 Responses to the questionnaire on TSL performance

The summary of the interviews with the TSL users and the suppliers is presented in Table 4-2.

Table 4-2 Summary of feedback from interviews with TSL's suppliers and users (Kanda and Stacey, 2019)

Topic	Feedback from a deep mine	Feedback from a shallow mine	Feedback from a supplier of TSL1	Feedback from supplier of TSL2
Average time of performing TSL (years)	11	6	17	11
Types on rock where TSL is applied	Igneous and metamorphic, with an average RMR of 60	Igneous, with an average RMR between 52 and 77. Some other scaled pillars were characterized with an RMR of 43	Igneous, metamorphic and sedimentary	Igneous and Metamorphic
Type of TSL	Polymer cement	Polymer cement	Polymer cement	Polymer cement and Polymer only
TSL's thickness (mm)	> 4	> 4	> 4	> 4
Other Supports usually combined with TSL	Friction Rockbolts of 2.4m (used as primary support) and wire mesh added to compensate a de-bonding TSL	Rockbolts (18mm, 1.6m resin bolts to bear 14t capacity)	Rockbolts and Wire-mesh (mostly used when the dynamic stresses characterize the rock mass)	Rockbolts and wire mesh

Topic	Feedback from a deep mine	Feedback from a shallow mine	Feedback from a supplier of TSL1	Feedback from supplier of TSL2
Infrastructures where TSLs were performing	None	Unknown	Tunnels, stopes, high stress and stress changing areas	Tunnels, ore passes
Observed failure properties	Adhesive failure	Tensile failure, Adhesive failure	Adhesive failure due to application in excessive water dripping and dampness in wall	Adhesive failure, shear bond failure
Frequent loading mechanism	Water pressure loading	Slab mechanism	Unknown	Unknown
Moisture conditions	Humid (unavailable percentage)	Dry	Variable: Dry, humid or very wet	Variable: Dry, humid or very wet
Underperforming moisture conditions areas	Humid (unavailable percentage)	Dry, because of the only one available moisture condition	Very wet	Dry, unless cleaned before the thin liner application
Surface preparation prior to TSL's application	Yes	Unknown	Yes	Not sure
Temperature conditions	Unknown	Unknown	30 – 40ºC	Variable

Topic	Feedback from a deep mine	Feedback from a shallow mine	Feedback from a supplier of TSL1	Feedback from supplier of TSL2
Geological structures highly influential for TSL's failure	Joints	Scaling pillar	Unknown	Normal
TSL's time of effectiveness	Variable, can fail even less than an hour after the recommended curing time	variable	10 to 20 years	Unknown
Major principal stress	Less than 70MPa	Less than 70MPa	100-140MPa	Unknown
Most common difficulties during TSL's application	TSL sprayed on easily but failed during the installation of bolts or after blasting operations	Difficult to get the homogeneity of the mixture	Blockage of the mixture caused by its rapid setting time.	-------

Comments on the above table will be made following the presentation of another type of feedback, which presents the views from a TSL supplier and a geotechnical inspector on a TSL performance:

4.3.2 Briefing on a discussion between two technicians concerning a TSL performance

The following opinions were made by two technicians, a TSL supplier and an external geotechnical inspector, over the performance of a TSL that was applied in a certain underground mine characterized by the presence of hypersaline water. The applied liner was the Evermine TSL, known as a flexible liner. It was coated in an underground mine's drive wall. And it was a few weeks after the traditional curing time that its performing assessment had to be undertaken. Table 4-3 presents these results.

Table 4-3 Case of interaction between a supplier and a geotechnical inspector regarding an applied TSL (Kanda and Stacey, 2019)

Technicians	Geotechnical conditions of the infrastructure before the coating	Opinions on TSL effectiveness	Recommendations based on TSL's observed performance
TSL supplier and in charge of coating	Not indicated	Impressive results observed from the liner application. This was also the impression from the on-site geotechnical engineer.	The results from TSL performance in the mining environment advocate for its expansion over the mines. Since this liner is a very good supporting material and easy to handle, it could be used as an alternative to shotcrete which has heavy logistic manoeuvres.
Geotechnical Inspector	Stable just because there are no unstable blocks	Disappointed on the supplier's feedback regarding his liner's performance. The supplier's comments would be misleading and may constitute a dangerous reference for the mining industry. One particular negative observation from the applied liner was that it performed poorly when hit by the underground loaders, and consequently should not be recommended to replace shotcrete.	Based on the observed TSL performance, this type of liner should not be recommended for the mining sector. Another thing is that thin coating materials are believed to be very hazardous in underground mines. Therefore, despite other positive claims of their performances, these materials should not be suggested by the geotechnical engineers based on the fact that some are difficult to spray, easy to tear, toxic and expensive. Alternatively, the resort to shotcrete should mostly be favoured for areal supports based on its advantages to highly absorb energy. It is though, with relatively high tensile and compressive strength. It is also durable, time-dependent and can transfer loads under static and dynamic conditions.

4.3.3 Analysis of the responses to the questionnaire and the opinions on a TSL performance

The overall feedback obtained from Table 4-2 shows that the causes of TSL's underperformance cannot be attributed to a single triggering factor. It is, however, a combination of factors and conditions that are contributors to lowering its supporting capability. Therefore, an optimal TSL design should be one that takes into consideration a variety of parameters that practically perform in the working environments.

The analysis of the interaction between the two technicians can be done as follows:

- The supplier's opinion on the applied TSL:

  This opinion was made based on a simple observation done just a few days after the expected curing time. Praising the good performance of a liner on a short-term basis would not be ideal since this TSL is intended to perform for a considerably long period. And besides the recommendation of assessing this support performance for a longer period before providing any sustainable opinion, it is advisable to apply this liner in relatively unstable zones or in zones susceptible to trigger the TSL supporting capabilities. The current work should look into this aspect through field assessments of some TSLs that were coated in some known underground undisturbed zones

- The geotechnical inspector's opinion on the applied TSL:

  The statement of disappointment expressed by the inspector regarding the supplier's comments can be partially understood for the reasons elaborated in the analysis of the supplier's opinion. Actually, based on the liner's properties of flexibility, it should have behaved better than it did. Nevertheless, the absolute rejection of TSL utilization as underground mine support is very harsh and not fully supported. And the advanced reason from the inspector of TSL not being able to perform well when hit by an underground loader may be justified when it comes to comparing thin membranes to shotcrete since the earlier are not structural supports. But there is a need for more

investigation before supporting that TSL cannot substitute shotcrete, the reason being that this suggestion is available in the literature as was presented earlier in this work. Therefore, the additional investigation should be able to demonstrate that, contrary to some suggestions proposed by some organisations such as the Australian Centre for Geomechanics (ACG), in all means, shotcrete is better than TSL. This comparison is valid for properties that include the air-tightness effect, tensile strength, toxicity, cost-effectiveness, in dynamic conditions, etc. Another factor that should be assessed has to do with environmental conditions. In the case of the mine where this assessed TSL was applied, it is known to host hypersaline water, though not accounted in the previous comments, but which may be a contributor in the noted underperformance of the liner.

Besides the collection of data of TSL performance through the questionnaire and from the interaction between a supplier and the inspector, a personal investigation was done from underground visits.

4.4 Inspection Report: Union Richard Shaft (relatively deep mine)

4.4.1 Introduction

The first mine that was visited for TSL's visual assessment was a platinum deep mine. The field assessment was done in January 2017. Located in the north-western section of the Bushveld Igneous Complex (BIC), this South African Platinum Group Metals (PGM) mine covers a total of 119km^2 and is currently deeper than 1500 metres. The PGMs are concentrated in two planar orebodies, namely the Merensky Reef and UG2 Reef. The composition of the rock-forming silicate minerals of the Merensky Reef is as follow: Orthopyroxene (60%), plagioclase feldspar (20%), pyroxene (15%), phlogopite (5%), and occasional olivine encountered in Bushveld-type rocks. The reef also contains occurrence of secondary minerals such as talc, serpentine, chlorite and magnetite. The composition of the base metal sulphides is as follow: Pyrrhotite (40%), pentlandite

(30%), chalcopyrite (15%), and trace amounts of millerite, troilite, pyrite and cubanite. The major PGM are composed of cooperite, braggite, sperrylite and PGE alloys. The UG2 Reef is characterised by the presence of abundant PGE sulphides that comprise laurite, cooperate, braggite and aggregates of PtRhCuS.

The commodity is essentially PGM, platinum, palladium, rhorium, iridium, ruthenium, gold, nickel and copper. The applied mining methods are the breast stoping with strike pillars and the hybrid mining applied at the declines. The mining operations were, at that time, performed at depths between 100 and 1500 metres below the surface. The density of the main reef is relatively high, and its ore is characterized by a high friability. No specific information on rock mass characterization was provided, except for the average rock mass rating (RMR) which is approximated to 60. There was no available in-situ stress data, but the mine is known to be seismically active. A few in-situ strength assessments were performed through the use of a Schmidt hammer. In this case, each estimation required at least 10 readings of the rebound numbers, and the average was then converted to the in-situ UCS by the means of the conversion curves of the hammer.

Three different sites were inspected at the Union Richard Shaft: the 14th, 15th and 17th levels. These sites were chosen based on the presence of TSL coatings. These products were either solely applied or combined to “whitewash” materials or also combined to other rock supports such as welded wire mesh, rock bolts or anchors. From the information collected from the mine’s tour guide, the polymer-based supports encountered in the 14th level may have been applied for 5 years and they cover an approximate distance of 500m. The thin liner support encountered in the 15th level was 11 years old at the time of the inspection. The extent of this thin membrane support is almost 600m. Besides, there were some TSLs applied close to an abandoned area since 2008 (about 9 years of age at the time of the field assessment). The 17th level hosts two TSL sites, namely an “old TSL” aged about 11 years and a “young TSL” that has been performing for 9 months at the time of the field visit. The TSL extents are respectively 750m and 200m. Critical field observation was undertaken, and different relevant aspects could be underlined.

4.4.2 **14th Level (690m below surface)**

The composition of the multi-component polymer-based membrane encountered at this level was not provided. At the time of the visit, it had already performed for four years. Generally, the observed performance was satisfactory, since there were no disturbing signs, except for a few areas. A sample of pictures from these sites is presented.

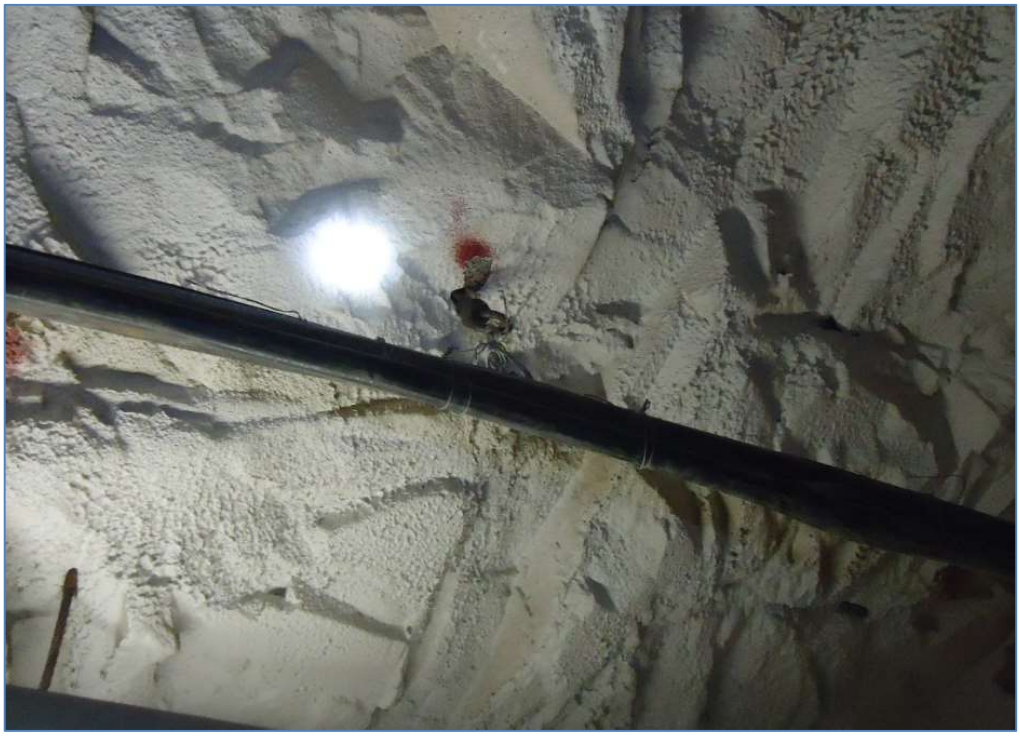


Figure 4-1 TSL's good performance aspect

Figure 4-1 shows a TSL applied on a roof of a blocky rock mass, but there was no alarming occurrence of falls of ground. This credit could also be attributed to the fact that the rock mass might be highly self-supporting on its own.

Close to the workshop, there was a moderate performance of the thin liners showing some losses of adhesion at few locations, and this may be due to the repetitive vibrations caused by the mine trolleys. The illustration of the observation from this site is shown in Figure 4-2.



Figure 4-2 Thin liners applied in a haulage passage

The TSL loss of adhesion was not very significant, only a few signs of localized losses of adhesion, definitely not provoked by an unstable rock mass, but rather made from an external tool that could have hit the coating or the haulage operations. A sample of this occurrence is illustrated in Figure 4-3.

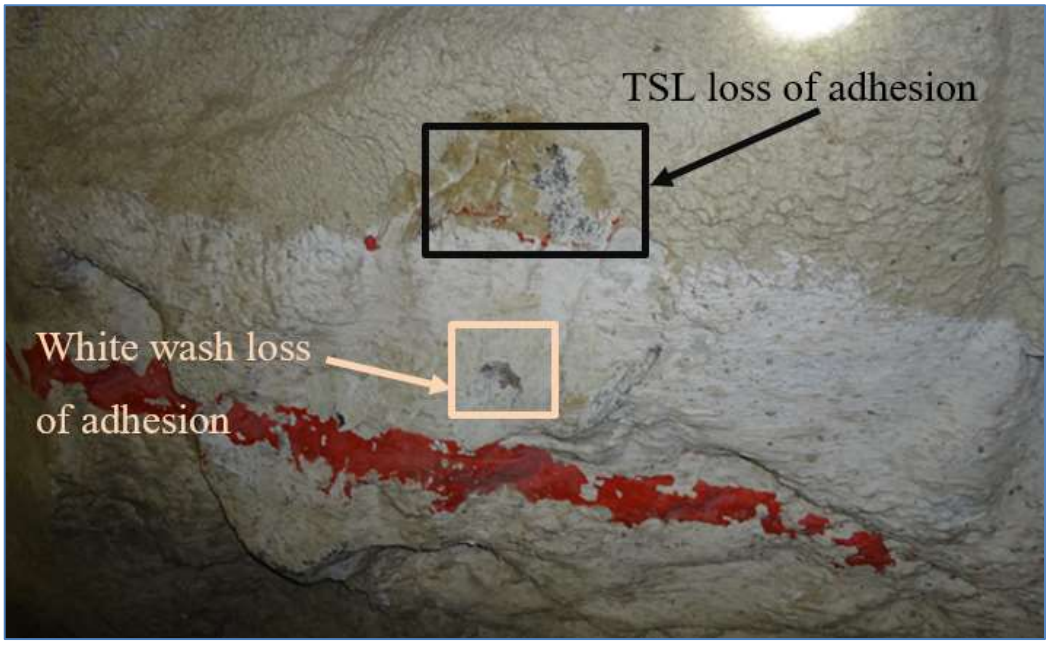


Figure 4-3 Aspect of TSL near the footwall in an active area

Since there is no presence of crack or signs of rock mass failure in the analysed sites, it can also be presumed that the loss could be caused by the effects of the mechanical manoeuvre near the coatings.

On some other sites, though in the same section with the previous case, much larger loss of adhesion could be observed (see Figure 4-4). The average from the rebound numbers was about 24, resulting in an approximated in-situ UCS of 20 MPa. The first presumption of the TSL failure might be its application very close to the footwall, whereas, in most sites of the mine, the lower parts of the walls near the footwall were rather coated with the whitewash material. TSL's application below the grade line could probably be a mistake.

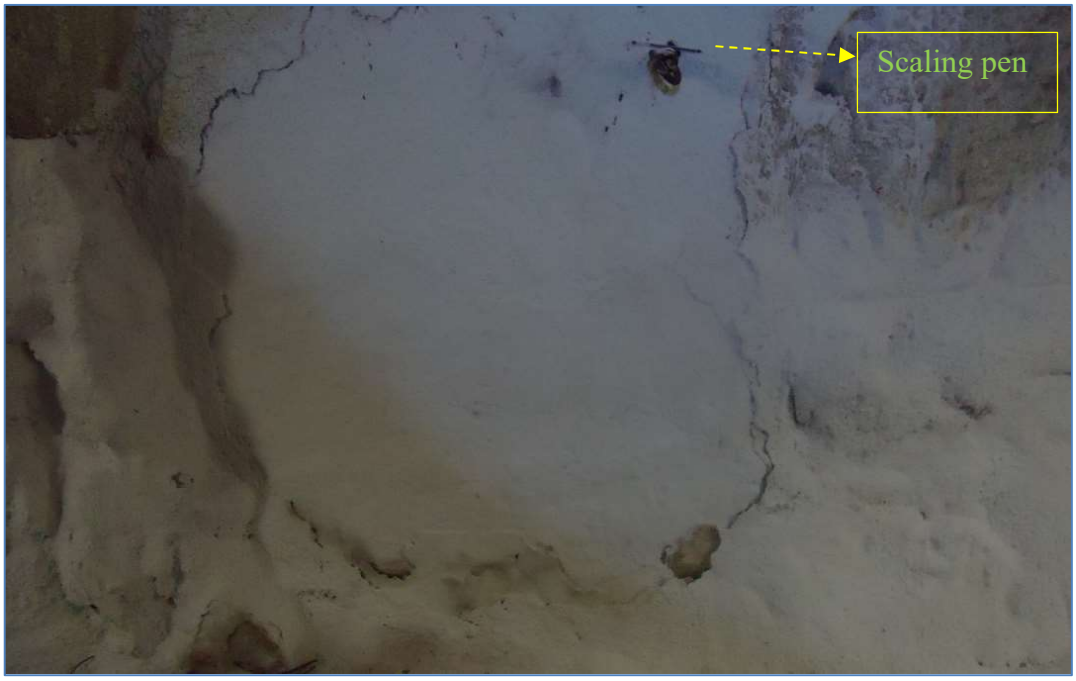


Figure 4-4 Case of TSL's loss of adhesion near the footwall

The large loss of adhesion of approximatively one square metre (a pen has been included for scaling purposes) could be caused by an unprepared surface or an underperforming TSL. The latter hypothesis might also be caused by a poor mixture in the preparation of the liner. Another reason might be the humidity presence since the liner failure happened near a humid footwall.

On the Eastern side of the 14th level, the observed performance of the 6 mm thick TSL was of good quality. The loss of adhesion was located only at the borehole entrances, see Figure 4-5, implying that it had been caused by the drilling mechanisms. The boreholes were made for blasting to widen the haulage passage. The surfaces of the rock mass appeared to be clean, not dusty or humid. The Schmidt hammer was used on these surfaces for in-situ UCS assessment. And sometimes it was used for scaling purposes; its length is approximately 27 centimetres. In this case, the estimated in-situ UCS was 41MPa from an average rebound of 39.



Figure 4-5 De-bonding of TSL at a borehole entrance

Similarly, other TSLs close to this site with boreholes were losing the adhesive strength, while the surfaces of the uncovered rock masses looked rough. There were also no records of field stress conditions, but the rebounds from the Schmidt hammer were on average equal to 39, hence an in-situ UCS of about 41MPa. And overall, it was observed that the proportions of the de-bonded areas were very small. It is worth noting that in some observed cases of TSL adhesion loss, such as that illustrated in Figure 4-6, the contour of the remaining liner could still show a TSL strong adhesion, with no indication of failure initiation.



Figure 4-6 Loss of TSL's adhesion in a stable rock mass environment

This particular case of failure could lead to the assumption of the failure being triggered by an external factor rather than by a geotechnical negative factor.Yet in the same mine level, there were other portions of the wall affected by moisture conditions. The failure signs were not very significant, but this could just be a matter of time. Figures 4-7 (a) and 4-7 (b) illustrate the observed moisture conditions halfway up the wall and near the footwall, respectively.



(a)



(b)

Figure 4-7 Aspect of moisture conditions (a) halfway up the wall , and (b) near the footwall

4.4.3 15th Level (750 m below surface)

The thin coating encountered at this level was applied 11 years earlier. It was mostly combined with wire mesh and rock bolts, and in some other circumstances, anchors were utilized instead of rock bolts. The types of mine supports showed that the rock mass is prone to slabbing/spalling, or is likely affected by the FOG incidents. For illustrative purposes, samples of some visited areas will be presented.

The next illustration displayed through Figure 4-8 concerns a 5mm thin membrane that was applied near the footwall. This TSL was identified as TSL1, earlier presented in this work. The reported main reason for its application was to prevent scaling.

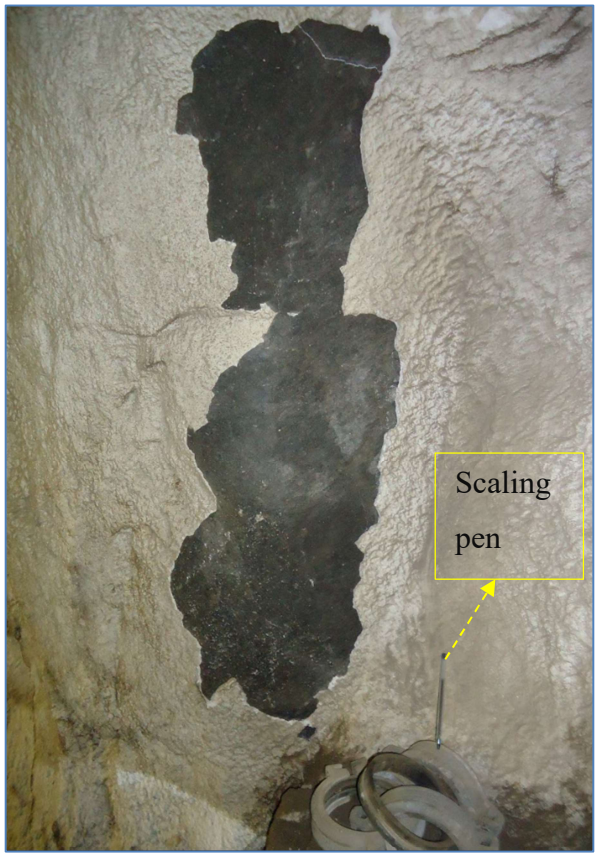


Figure 4-8 Adhesion strength loss of TSL near the footwall

This failure was localised, rather than extensive. The extent of the adhesion loss was elaborated through the use of a pen used for scaling and placed at the lower

right side of the examined surface. This showed that the adhesion failure happened on an area of approximately 1 x 0.2 m^2. The average rebound number was 35, equivalent to an in-situ UCS of 35MPa. The observed area of contact was characterized as smooth and friable, a probable reason for the adhesion-loss failure of the thin coating material.

Approaching an abandoned section of the mine, the rock mass structure was characterized by various discontinuities and indices of instability. Though TSL was used in a few areas as stand-alone support (Figure 4-9), a combination of various types of supports was more frequent as approaching the abandoned mining zone as presented in Figure 4-10.



Figure 4-9 TSL used as stand-alone support close to an abandoned mining area



Figure 4-10 TSL used in combination with other conventional supports close to an abandoned mining area

More serious damages could be observed along the way, in the disturbed rock mass area. And if a combination of supports was not used, the consequence could have been very disastrous with the employment of TSL alone as shown in Figure 4-11 (a, b, c and d)

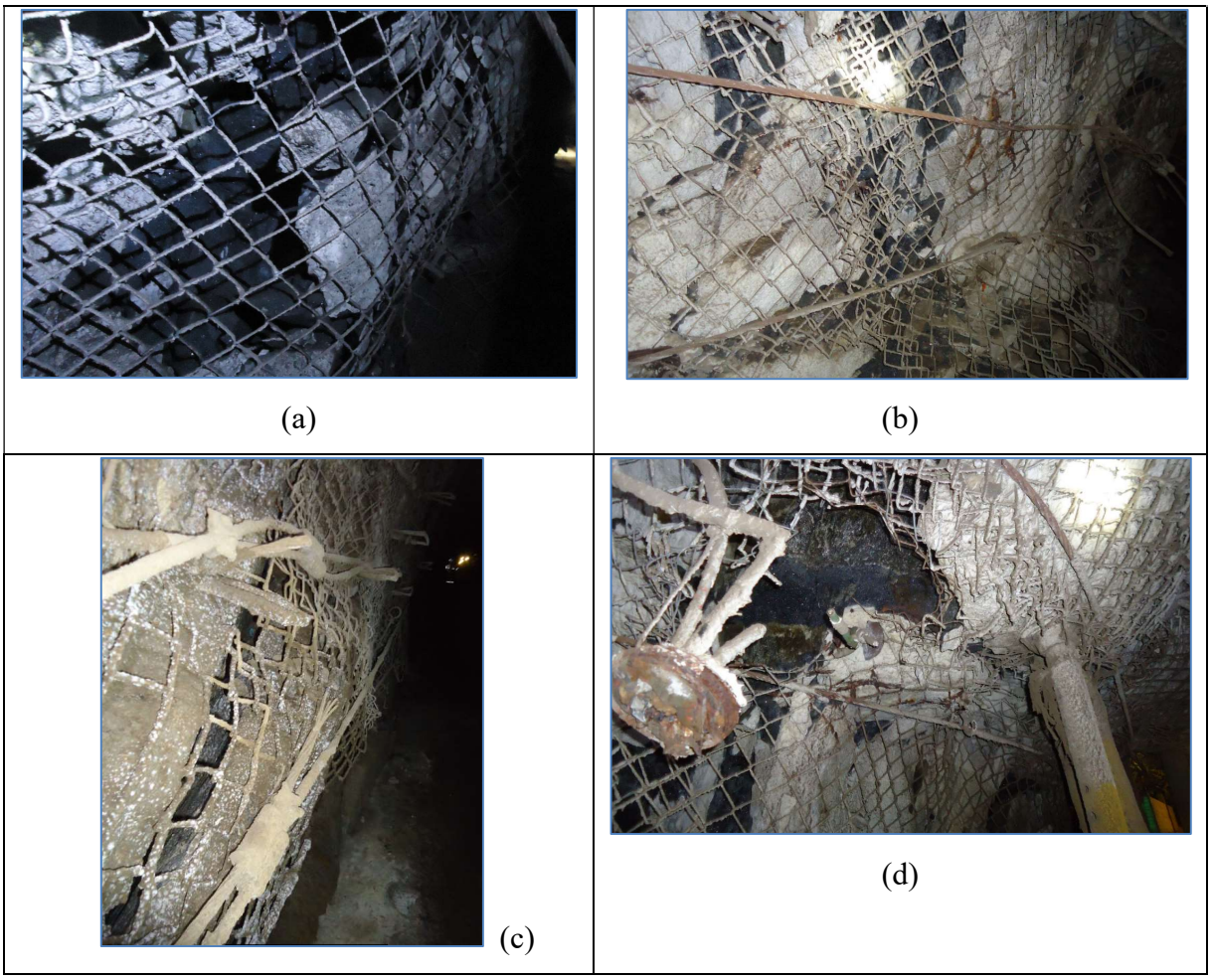


Figure 4-11 TSL combined with other conventional supports in a disturbed mining zone

From these figures, in addition to the thin coating materials, there is a presence of lining, anchors and wire mesh supports. These combined supports were applied on the Merensky reef to limit the damage of the abandoned mining zone.

4.4.4 17th Level (842 m below surface)

The multi-component polymeric liner was applied in the 17th level at two separate periods by the same supplier. The earlier applied TSL, also called "Old TSL" in this thesis, was applied eleven years before the visit, while the "Young TSL" was only applied nine months before undertaking this field assessment.

17th Level "Old TSL" (11 years old at the time of field assessment)

This section of the mine was characterized by an assessed in-situ UCS of 53 MPa, from an average rebound of 47. There was some observed loss of adhesion in the roof close to a pipe, as shown in Figure 4-12.



Figure 4-12 Adhesion failure of TSL on a roof

This failure might be due to unknown causes since the surface looked suitable for good adhesion, and there was no sign of rock mass failure in the neighbouring area. Probably, work related to the installation and/or maintenance of the pipe might have caused this adhesion loss. Almost the same circumstances are observed in the next illustration represented in Figure 4-13.



Figure 4-13 Adhesion failure of TSL on a wall

In this case, the adhesive failure is localized, with an estimated section of 25 x 15 cm^2, and the uncovered rock mass surface appeared to be clean, rough, and thus prone to a successful bonding of thin liners. It is believed that the portion of liner might have been purposely removed for a reason that remained unknown.

The moisture impacts on TSL performance were also assessed. Some roof areas and sidewalls in the 17^{th} level were observed to be humid as presented in Figures 4-14 (a) and 4-14 (b).

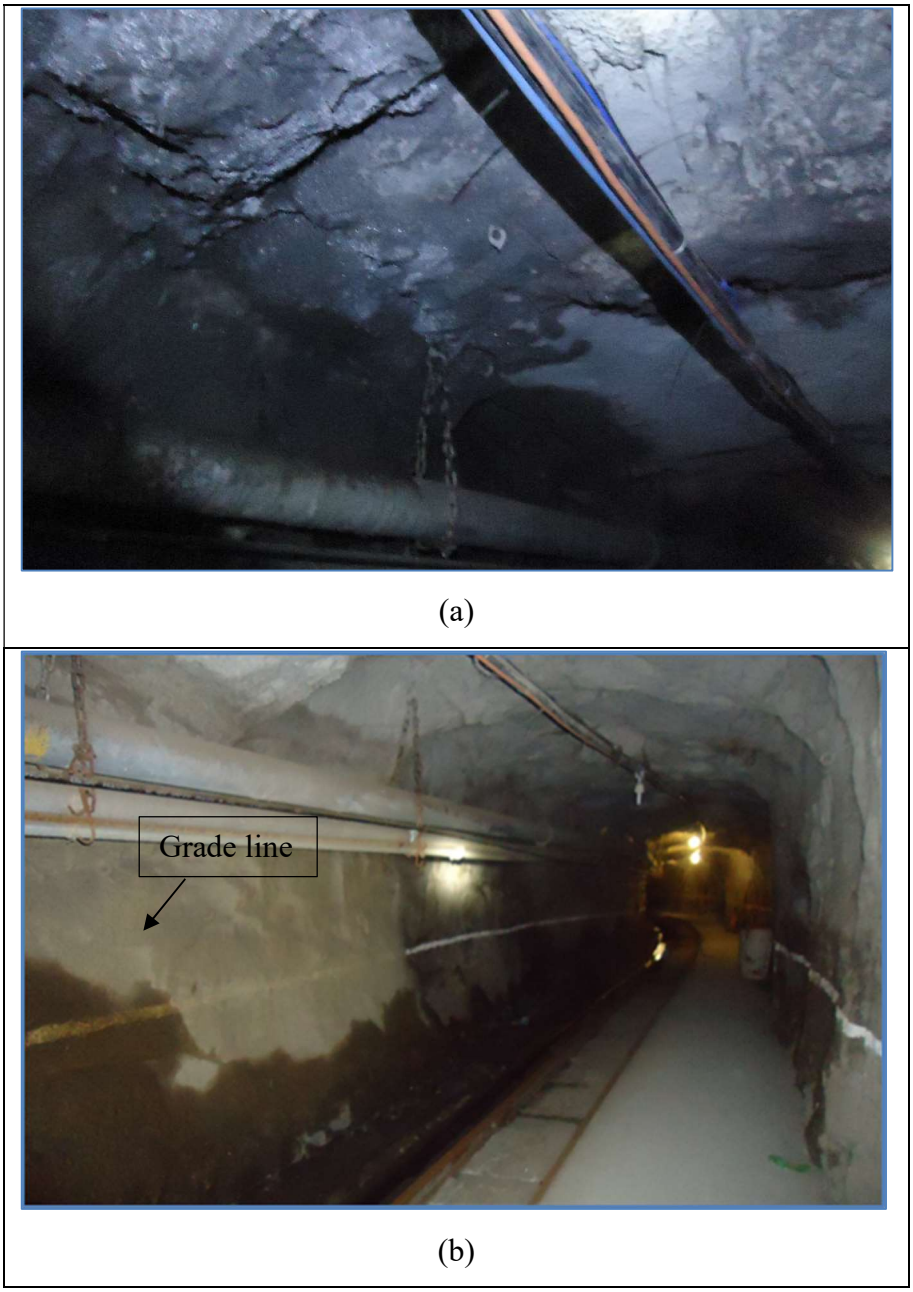


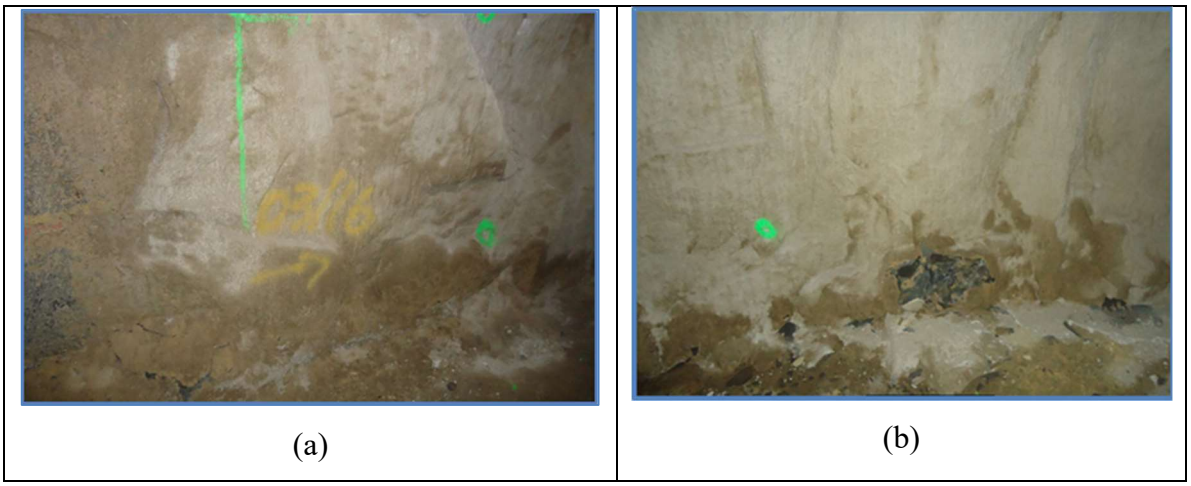
Figure 4-14 TSLs affected by humidity conditions (a) near the roof, and (b) on the sidewall

The observed area illustrated in Figure 4-14 (a) shows that although the humidity effect could be noticed, the thin liner did not show signs of failure. Based on the significantly longer period of that TSL performance (11 years), it is believed that this applied type of liner is adequate for humid conditions. And through Figure 4-14 (b) it can be seen a liner applied on a wall and a white horizontal line to demarcate the extent for the whitewash material that was still to be applied at the lower parts

of the railway walls to protect it against humidity negative influence. The timing between the thin liner application and the whitewash material application should be well studied to avoid its application when the thin coating material is already negatively affected.

17th Level "Young TSL" (9 months old at the time of field assessment)

The following Figures 4-15 (a) and 4-15 (b) show a poor performance of TSL which was applied on the walls, near the footwall only a few months earlier. The assessed in-situ UCS was found to be 42 MPa.



(a) (b)

Figure 4-15 Young TSL bad performance near the footwall

The observation made from this level, based on the illustrations in Figure 4-15 (a) and Figure 4-15 (b), was that the TSL applied close to the footwall did not perform well. This might be due in part to moisture presence. It was also observed that the coating could easily detach from the wall. The performance outcomes prove that either the surfaces were not well prepared beforehand or the thin coating is underperforming in humid conditions.

This TSL should not have been applied in these environmental conditions because it does not have the necessary characteristics to be used in wet zones. A recommendation should be to only apply TSL from at least a metre above the footwalls, especially when these are humid or with running water. Closer to the

footwalls, the application of calcimine or whitewash should be much suitable, but the tensile ability of the proposed material should fulfil the design criteria.

Another critical observation that was made concerned the overall performance of the “Young TSL”. This liner showed poor performance near the footwall (Figure 4-16 (d)), even in dry zones, as it can be seen in Figures 4-16 (a), 4-16 (b) and 4-16 (c).

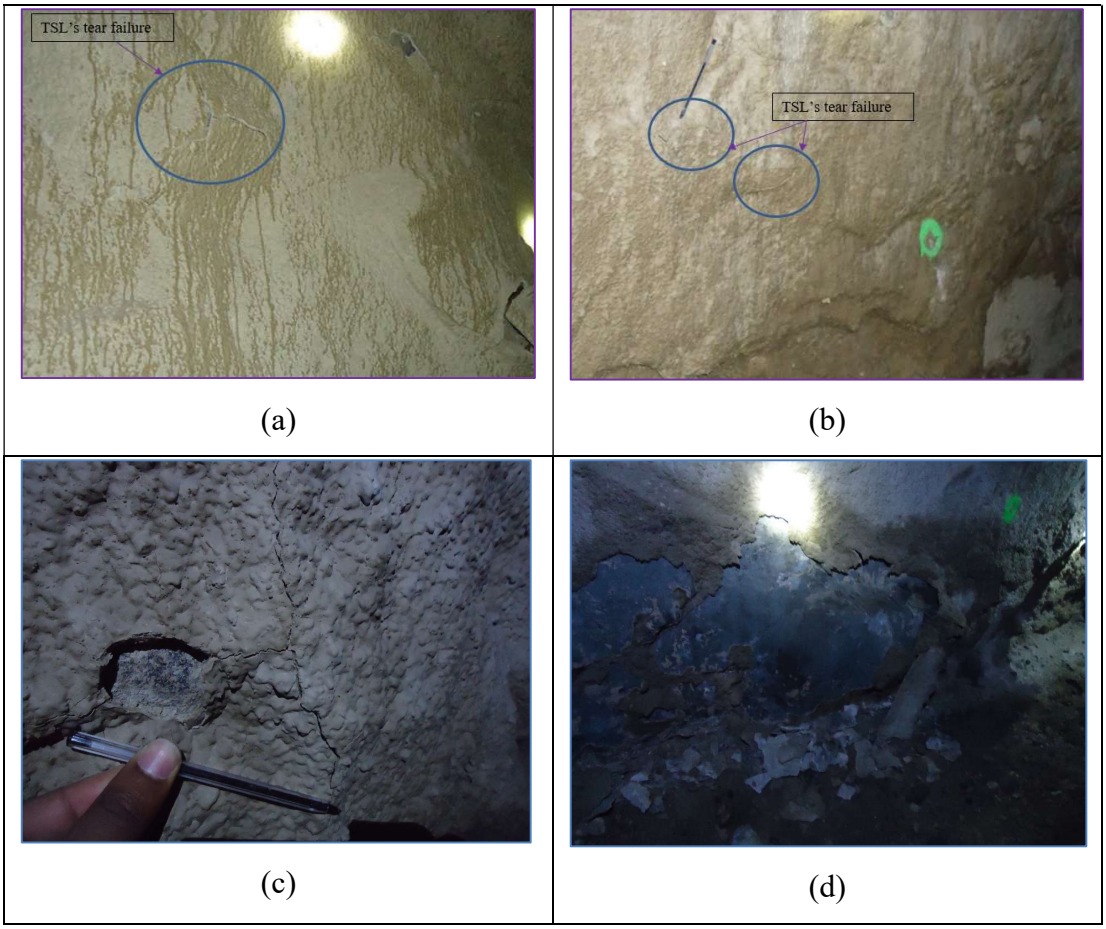


Figure 4-16 Poor performance of "Young TSL" in dry and humid conditions

Although applied only nine months before the mine visit, this thin liner performed badly compared to the “Old TSL” applied for 11 years. No records of mobilization of rock blocks or seismic activities were noted, and the observed longer space between the rock bolt sustain the hypothesis of a stable rock mass, yet the TSL was not performing well. The area being dry, it was assumed that either the TSL mixture was not well prepared or it was not sprayed in the required timing.

4.4.5 Interpretation of deep mine findings regarding TSL performance

The TSLs observed from the deep mine showed mixed results. Some behaved as expected, while others showed completely poor behaviour. There were cases of thin liners applied at lower depths not performing as well as those coated in much deeper levels, even though it is believed that in general, there should be high stresses in deep levels. However, the mining activities, which result in localized geotechnical disturbances, might highly contribute to the behaviour discrepancies. It was also noted that there is a need for proper knowledge of the characteristics of a liner before its application. Failing to do so could result in the liner performing poorly. Such performances were observed in humid conditions, but also in a few dry conditions. The preparation of the substrate surface and a proper mixture preparation of the thin liner were also pointed out as a factor that could dictate the thin coating performance. Near the footwalls, specifically in the section below the grade line, most of the TSLs did not show good performances. The whitewash material performed better in humid conditions than TSLs. However, the mechanical behaviours of this white material should require in-depth studies for stability purposes. Finally, it was found that in zones characterized by a poor self-supporting ability of the rock mass, a combination of TSL with other mining support was suitable to avoid the FOG effects.

4.5 Inspection Report: Bathopele Mine (shallow mine)

4.5.1 Introduction

The second visited mine was shallow, namely the Bathopele Mine. This mine was visited in March 2018. It is a mechanized bord and pillar platinum mine, relatively humid, and located in the Western section of the BIC. The middling between the Merensky and UG2 reefs is approximately 140 metres, with both reefs deeping at ~9° towards the northeast with relatively long-range grade consistency and predictability. The Merensky Reef is situated above the UG2 Reef and consist of pegmatoidal feldsphatic pyroxenite, having thin top and bottom contact chrome stringers with the UG2 Reef. This last cited Reef consists of a main chromitite seam

with an average thickness of 70 cm. The commodity of this magmatic deposit is essentially PGM, gold, platinum, palladium, rhorium, nickel and copper. Beside the Bord and pillar method, the other mining methods applied in this mine are breast mining and hydraulic mining.

Various sections were investigated regarding TSL performance, and the deepest section was located at 352.2 metres. No specific information on rock mass characterization was given, and the RMR varies between 52 and 77. The in-situ stress data were also not available. But the in-situ strengths could be recorded during the visit through the use of a Schmidt hammer. The field assessment concerned six different sites: Central shaft 3W-bord 11, Central shaft 3W-bord 10, Central shaft 13E, Central 14W, Central 15W and East 12E. These sites were chosen based on the presence of TSL coatings.

4.5.2 Central Shaft, section 3W, bord 11 – Ventilation crossing

This site is at a depth of 90.8 mm below the surface, along the ventilation crossing. It was reported being coated with TSL1, applied 38 months before the field visit, with an estimated thickness of 8mm. The reasons for TSL application were to support the wall and to prevent the need for barring whenever the excavations were too high to be easily barred. The illustration of the applied TSL is displayed in Figure 4-17.



Figure 4-17 TSL1 applied close to the footwall

The mixture appears in good shape, except at the footwalls where there were important losses of adhesion due to the friability of the substrate surface. On the wall, the coating was combined to a primary support constituted of 1.6 m resin bolts and a secondary support of 3.5 m cable anchors.

4.5.3 Central shaft strike, section 3 W, bord 10 – Belt drive

This belt drive is located at 76 m below surface and is coated with a mix of unknown TSL and shotcrete. The thin coating was reported been applied 37 months before the time of field assessment to compensate the need for barring. Its thickness varies significantly. Figure 4-18 illustrates the case of this coating.



Figure 4-18 TSL combined with cable anchors and resin bolts

Patches of exposed rock surfaces were noticed, and these were assumed being caused by mechanical operations. The combination of support observed in the ventilation crossing is also applicable in the belt drive. Two types of seams were observed: the Pyroxenite and Chromitite. The overall provided RMR was said to be greater than 65. The rebound number in the surrounding of the Pyroxenite is 35, resulting in a UCS of 35MPa, while the Chromitite rock mass strength was estimated at 51MPa, all this, through the resort to the Schmidt Hammer method.

Other portions in the same area have shown good performances, though humidity conditions were characteristics of the zone. This is displayed in Figure 4-19.



Figure 4-19 TSL applied in humid zone

4.5.4 Central shaft, section 13E, bord 7 – Belt drive and section 14E, bord 5 – Belt take-up

The thin coating applied in this section was reported to be TSL1. It was coated 25 months before the field inspection. The main reason for its application was to compensate the need of barring whenever high excavations were concerned. Although the environment was dry, the performance was not as good as in the previous case. This TSL performance is illustrated in Figure 4-20.



Figure 4-20 TSL performance aspect in section 13 E

The rock mass is composed of Norite, Anorthosite, and Pyroxenite. The overall observation is that this region has a stable rock mass condition, with a provided RMR being between 65 and 77 and the assessed in-situ UCS of 44 MPa. However, the liner was still combined with resin bolts and cable anchors. Its average thickness was assessed and found to be about 4mm.

The same observed conditions were noticed in the 14th W section, at the belt take up. This is situated at 344.1 m below surface and was coated with TSL1 about 34 months before the field visit.

4.5.5 Central shaft, section 15W, bord 6 – Belt drive

In this section, located at 350 m below surface, TSL1 was also reported to be the applied coating. The reason for its usage was to negate the scaling of the pillar. The RMR provided value was 57, and the TSL thickness was assessed to be between 5 and 6 mm. This liner was applied 10 months before the assessment and proved to have performed well, as presented in Figure 4-21.



Figure 4-21 TSL applied on a pillar prone to scaling

Although it was applied only a few months ago, which could imply the need to wait for more performing time before judging its performance, this preliminary

assessment gave good performing indications, since there was no index of adhesion loss due to the pillar scaling. Nevertheless, it is worth noting that this thin coating was combined with lacing support.

4.5.6 East shaft, section 12W, bord 8 – Bord

This section of the mine is situated at 204 m below surface. It is characterized by an RMR of 57. The reason behind the application of a multi-component polymeric-based liner is due to poor ground conditions, especially characterized by FOG occurrences. An illustration of this bord is shown in Figure 4-22.



Figure 4-22 TSL applied on a roof prone to falls of ground

This thin coating was applied 5 months before the field assessment and its thickness was between 5 and 6 mm. It was used in combination with rock bolts. The overall performance was judged satisfactory, though there could still be few portions of the hanging wall characterized by the FOG.

4.5.7 Interpretation of shallow mine findings regarding TSL performance

Similar to the deep mine, mixed results were observed regarding TSL performances in this shallow mine. This mine is relatively humid, and this environmental condition is believed to play an important role in the performance of some TSLs.

Nevertheless, there were other humid zones where TSLs seemed to have performed highly, some even 3 years after their application. Likewise, an unidentified TSL, applied on a blocky rock mass surface, showed good performance, which practically helped to prevent FOG occurrences. However, no further information was provided concerning the self-support ability of the rock mass.

In other circumstances, when the rock mass had poor stability conditions, the thin liners were combined with cable anchors and resin bolts to improve the support performance. Another critical condition where TSL performed well was when it was applied onto scaling pillars. In this case as well, the thin liner application on the scaling pillars was later combined with other supports, namely the lacing supports. This showed how contributing this thin liner can be for underground stability.

4.6 Chapter Summary

There has been a concern regarding the practical field performance of TSLs, which has led to scepticism over these liners' utilization. Although the mines where these thin coatings have been applied likely possess their performing data, this is not available in the literature. The task of collecting and availing TSL's behaviour feedback was therefore undertaken through this part of this research, though limited to only a few mines. The aim was to characterize the field behaviour of TSLs through the information on their performances obtained from two different mines: A relatively deep mine and a shallow mine. In practice, the methodology consisted of collecting the information of TSL performances through personal visual assessments, questionnaire addressed to the mines geotechnical engineers, and through the collection of opinions on an applied thin coating in a determined mine. All the obtained information was critically analysed.

From a series of established questions, addressed to the mines geotechnical engineers and to the suppliers, a sample of the feedback indicated that most of the employed TSLs were cement-based materials. The mine operators were still not sure where these liners were performing, but the suppliers highly advocated their

utilization in most of the mines' openings such as tunnels, stopes, ore passes, high stress and stress changing areas, etc. From the mines geotechnical engineers' perspective, the triggering structures for TSL's poor performance are the presence of discontinuities, scaling of pillars and FOG, whereas the suppliers claimed not to be aware of any specific structural condition capable to hinder the good performance of the thin coatings. The lifetime performance of TSL was said to be variable according to the miners. This performing period was quantified by the suppliers to vary between 10 and 20 years. Only a few TSL disadvantages were mentioned by the suppliers, the most common being the rapid setting of the mixtures during the preparation phase, often resulting in blockage during the spraying operation. The mine users presented quite an important number of disadvantages, among which were the observed failure of the thin coatings during the installation of the rock bolts, or the difficulty of reaching the mixture homogeneity without it beginning to set. Divergence of interpretations between the thin coating users and the manufacturers or suppliers was noticed when opinions were requested regarding an applied TSL in a mine, characterized by the presence of hypersaline water. Whereas the thin liner's suppliers, also in charge for the coating process, praised its performance and advocated expansion of its utilization, a geotechnical inspector lamented about the obtained results and claimed that the liner only performed well where the rock mass had good self-supporting ability, i.e. where the coating was not truly required.

Apart from the information collected from TSL manufacturers and users, personal assessments were undertaken by the thesis' author in shallow and deep mines. Mixed performing results were observed from the TSLs coated in the deep mine: Not all TSLs coated at lower levels performed better than those applied at deeper levels. This could be justified by the effect of localized geotechnical disturbances, the mixing condition of the liner, or by the mechanical properties of the applied liners and their predictable behaviour towards each physical and environmental condition of the substrate's surfaces. Better performance of whitewash material near the humid footwall was observed when compared to TSLs. And although more study is needed concerning the use of the whitewash in these environmental

conditions, these materials could be very useful to compensate for the action of thin liners in humid zones. But when the zones were characterized by poor stability and generally prone to FOG, it was observed that stabilizing-means were to combine TSLs to other traditional mining supports, either active or passive. Almost the same results were obtained from TSL's assessment in the shallow mine, which has a humid characteristic. Some particular TSLs performed well in practically humid zones. This was also the case observed in a blocky zone, though no further information was provided concerning the rock mass self-supporting capability. However, it is believed that a good choice of a thin liner based on the site of application might play a huge role in the stabilization of the mining infrastructures. Opting for a combination of TSL with lacing, meshing, bolting, etc., also proved to be efficient in zones prone to FOG or on scaling pillars.

CHAPTER 5 LABORATORY TRIALS OF TSL PERFORMANCES

5.1 Introduction

This chapter aims to investigate the mechanical behaviour that characterize TSL supports from a laboratory point of view, specifically for extended periods. Although many similar tests have already been mentioned in the literature, particularly for short term tests, it will be for the first time that TSLs will be trialled in temperature and saturation conditions, with emphasis on long-term exposure under these conditions. The basic TSL properties will be assessed through standardized methods such as defined by the American Society for Testing and Materials (ASTM), the International Society for Rock Mechanics (ISRM) and the European Federation of National Associations Representing for Concrete (EFNARC). These properties might furthermore serve as data input in the numerical modelling stage for validation and in-depth characterization of TSL support. The main tests to be undertaken are:

- Uniaxial Tensile Strength (UTS) test
- Brazilian Indirect Tensile (BIT) Strength
- Membrane Displacement Test (MBT)

It is worth noting that this latter method is yet to find universal consent concerning its representativeness and repeatability, since various techniques from the method have been developed, as presented earlier in this work, but none has yet been adopted to be the standard.

To these tests should be added:

- The Uniaxial Compressive Strength (UCS)
- The Tri-axial Compressive Strength (TCS)

All the tests were performed at the Wits Gold Fields laboratories, and the adopted main equipment for short-term UTS, BIT, UCS and MBT trials was the Material

Testing System (MTS) model 643.15A – 03, displayed in Figure 5-1. The incorporated load cell for UTS tests has a maximum capacity of 10 kN, while the equipped load cell for compressive tests, also included in the same apparatus, has a maximum capacity of 100kN. These loading capacities are large enough for testing TSLs and shotcrete strength, which behave like soft rocks.

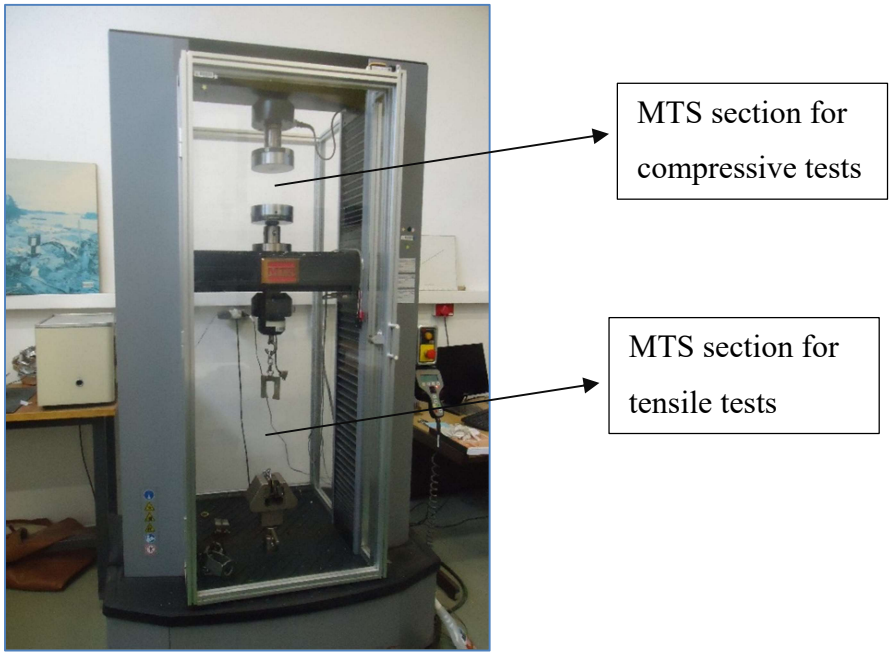


Figure 5-1 MTS model 643.15A – 03

Besides the earlier described tests, this multifunctional apparatus is capable of executing other tests such as punch tests, bond tests, etc. However, in the case of TCS, the AMSLER compressive machine was resorted to. This machine is a soft testing machine, equipped with a 500kN load cell, enough to handle the maximum strengths that can result from the TSL's triaxial tests. This machine is presented in Figure 5-2.

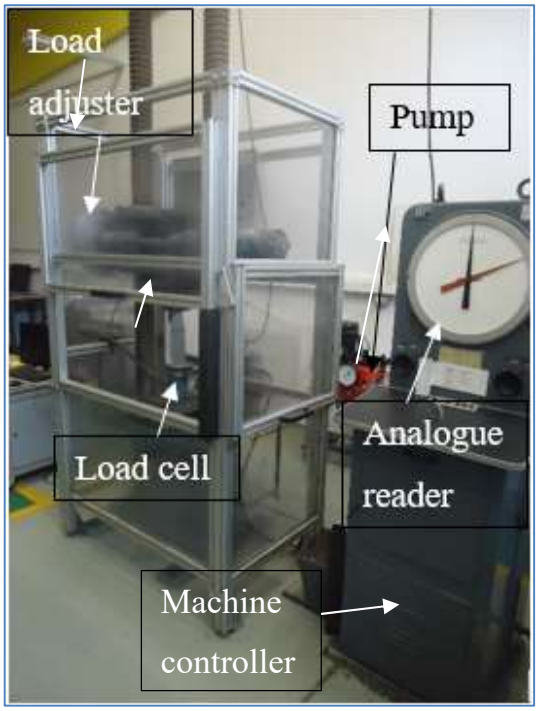


Figure 5-2 Amsler compressive testing machine

In conjunction with this equipment, used for the traditional short-term tests, other equipment needed to be used for long-term trials. These will be elaborated later in this chapter. However, since they are not standardized, there was a need for setting up, calibrating and validating their weighing components.

5.2 Setup of the Weighing System for Long-Term Tests

This section aims to calibrate the weighing system elaborated for long-term tests. A load cell type S was used for the calibration of all the creep testing machines. The following are some of its characteristics:

Brand name: LOADTECH

Model number: LT400

Capacity: 500kg

Sensitivity: 3mv/v

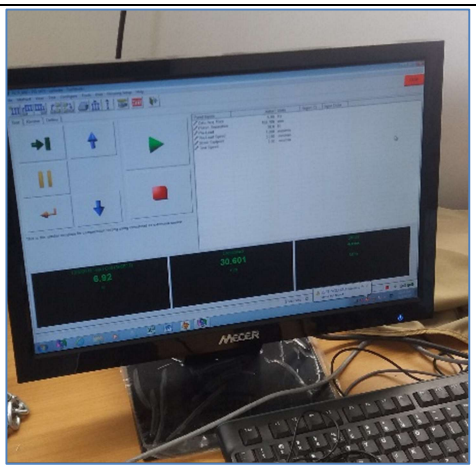
Impedance: 350Ω

Protection: IP66

This calibration intended to get the load cell readings in mV, using a multimeter (or a data logger type midi Logger GL220), and in N or kg by resorting to the MTS 643. With this, a conversion of the voltage readings into kilograms could be made. The process consisted of suspending the S load cell in the MTS 643 before the attachment of the weights (per Figure 5-3 (a)), and at the same time coupling it with a multimeter (or a data-logger) for the voltage readings as displayed in Figure 5-3 (c).



(a)



(b)

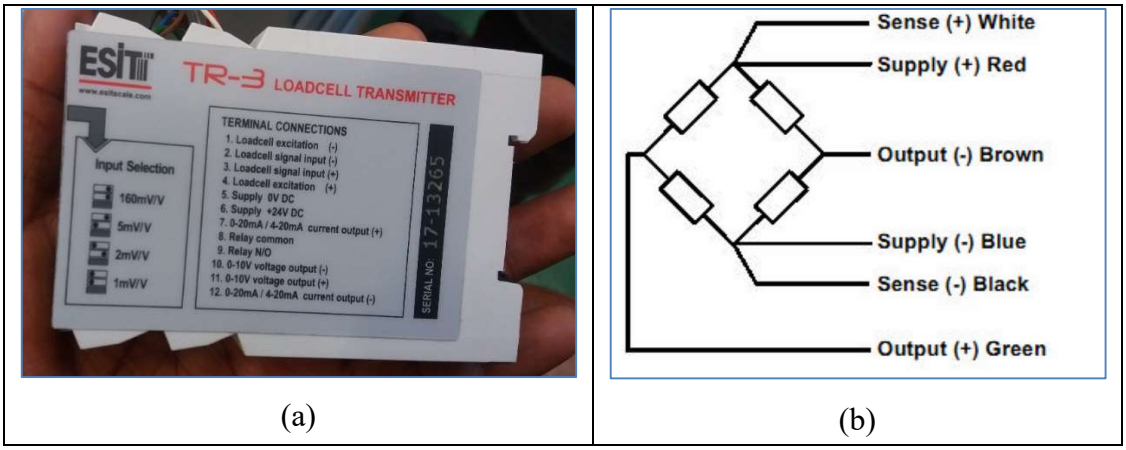


(c)

Figure 5-3 Load cell type S calibration

Figure 5-3 (b) shows the weighing readings from the MTS software. The load cell type S was associated with a transmitter model TR-3, which has a maximum output voltage of 10V. This transmitter was supplied with 24V CC from a power supply

unit. A snapshot of the transmitter TR-3 is displayed in Figure 5-4 (a) and the connections for tension are presented in Figure 5-4 (b) (Loadtech Load cells, n.d.)



(a) (b)

Figure 5-4 Details on circuit connectivity of load cell transmitter TR-3 shown through (a) snapshot of the input selection, and (b) circuit configuration

For this research, an input selection of the transmitter sensitivity was chosen from the available list (1mV/V, 2mV/V, 5mV/V, and 160mV/V), and the choice was made taking into consideration the maximum load capacity of the load cell, ensuring that the maximum weight capacity of the transmitter is closer to that of the load cell. The proportionality displayed in the following equation was observed:

$$\frac{\text{Max Weight Capacity of Load Cell S}}{\text{Sensitivity of Load Cell S}} = \frac{\text{Max Weight Capacity of Transmitter}}{\text{Sensitivity of Transmitter}} \qquad \text{(XIX)}$$

Through this expression, with a transmitter sensitivity of 5mV/V, the maximum weight capacity to be supported is 833.3kg, while 2mV/V sensitivity only supports 333.3kg. Although this latter sensitivity is appropriate for the UTS creep testing machine, the earlier sensitivity was adopted since it accommodates all the other creep testing machines that will be presented in the following sections. Therefore, if a maximum weight of 500kg is applied on the load cell, the maximum reading on the multimeter is found through the following expression:

$$\frac{\text{Output voltage}}{\text{Applied weight on load cell}} = \frac{\text{Max Output voltage of the Transmitter}}{\text{Max weight capacity of Transmitter}} \qquad \text{(XX)}$$

Or by using the available data, it is:

$$\frac{\text{Output voltage}}{500\text{kg}} = \frac{10\text{V}}{833.3\text{kg}}$$

After calculation, the highest output voltage from the transmitter was 6 volts.

The calibration of the load cell consisted of getting an accurate conversion between the applied weight (kg) and the voltage readings (mv). A sample of the results from the trials is given through Table E-1. The proportionality is expressed through the linear equation displayed in Figure 5-5.

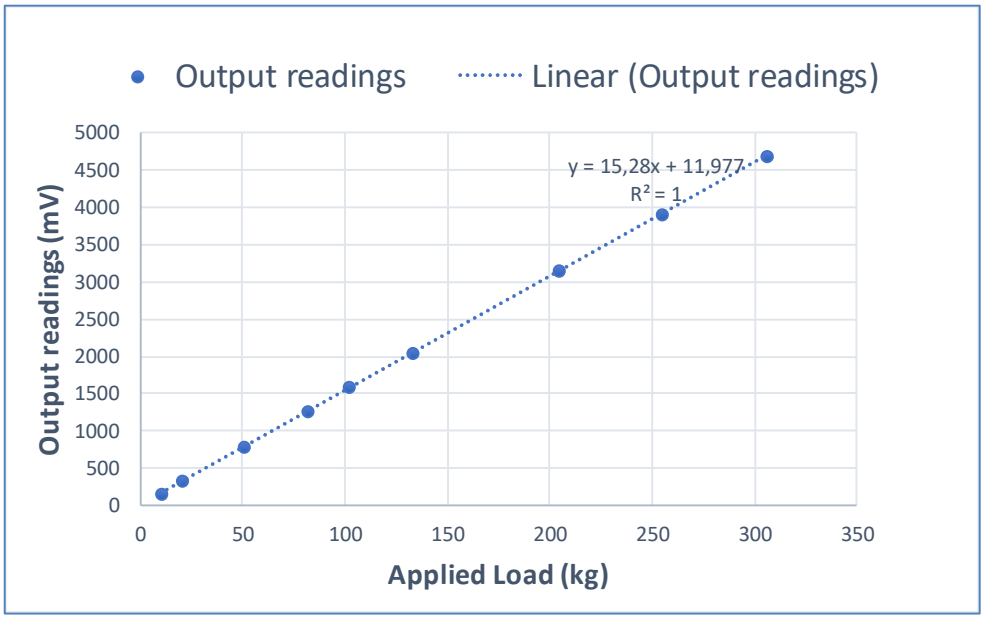


Figure 5-5 Proportionality between kilograms and millivolts readings from load cell S type

This figure shows a linear regression with a coefficient of determination R^2 equal to one; which validates the accuracy of the conversion from kilograms to millivolts when using the load cell type S. However, since the loadings on the creep machines were read from the data loggers, in millivolts, the inverse of the function expressed in Figure 5-5 could provide the equivalent reading in kilograms. This inversed function is:

$$y' = 0.06545x' - 0.78384 \quad \text{(XXI)}$$

Where,

x': Load readings from data logger (mV)

y': converted values of the load readings (kg)

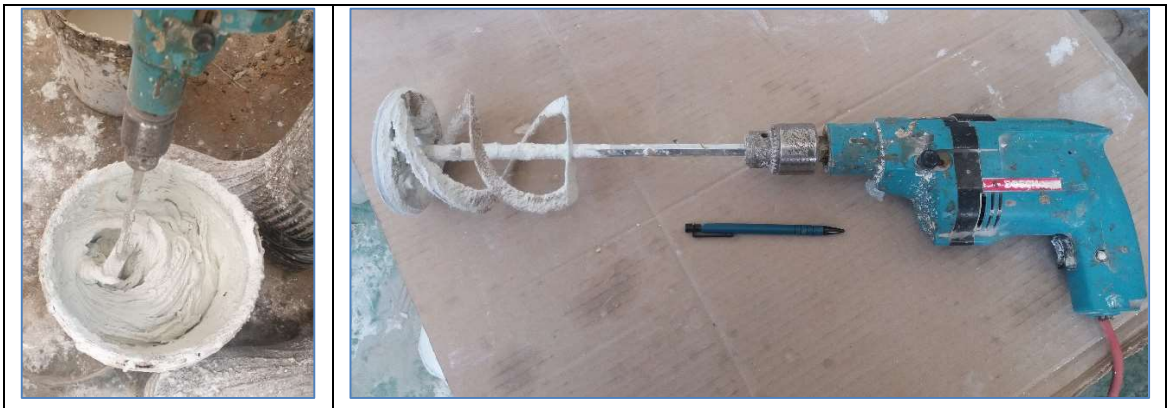
5.3 Uniaxial Tensile Strength Tests

5.3.1 Introduction

UTS is one of the most important mechanical properties of thin coating materials. A large number of tests (about 280 specimens) were undertaken to assess the environmental influences on this property, especially throughout an extensive period. This section will start by presenting the steps of the specimen preparation, followed by the employed materials and methodology. Finally, the results and analyses of the short-term and long-term tests will be presented.

5.3.2 Specimen preparation

TSL dog-bone specimens were prepared through the means of an electric mixer in room conditions, illustrated in Figure 5-6.



(a) (b)

Figure 5-6 (a) Preparation of TSL mixture and (b) Electric mixer (Kanda and Stacey, in press)

Some of the specifications of this mixer are presented in Table 5-1.

Table 5-1 Specification of the electric mixer

Specifications	**BOSCH n° 950/750/4700/3700**
Rated Power (W)	400W
Frequency (Hz)	50
Vibration level (drilling/chiselling)	13/6
Part number	0603151036

The adopted dog-bone shape is per the ASTM D-638 (2010) type I, whose sizes were earlier displayed in Figure 2-5. In practical, the gauge thickness of the moulded specimens varied between 4 to 6 mm, while the gauge width was between 12 to 14mm. The steps of the TSL preparation were all performed as follows (Kanda and Stacey, in press):

- Apply a release agent on all the elements of the mould sets
- Assemble each mould set and place them on a flat working place, previously covered with a plastic film to avoid direct contact between the thin liner and the working place — which would otherwise be capable of damaging the liner at the time of specimen releases
- Mix the components of the liners, according to the specifications provided by the manufacturers. The proposed ratios by the three manufacturers were presented in sections 2.7.2, 2.7.3, and 2.7.4
- Pour and level down the TSL mixture as displayed in Figure 5-7
- Use a plastic film to cover the mixture and gently level it down using a rock core to match the moulding set thickness of 5 mm
- Wait as long as two or three setting days before separating the mould elements and/or detaching the specimens
- Remove the few excesses of TSL around the dog-bone shape that can prevent the specimen from being in full contact with the grips during the testing phase



Figure 5-7 Pouring and levelling down of TSL mixtures (Kanda and Stacey, in press)

5.3.3 Materials and methods

The testing processes were performed separately depending on whether the adopted trials were short-term (resorting to the MTS) or long-term tests (using the creep testing machine). About 280 UTS specimens were prepared, in the ratio of 225 for short-term tests and 55 specimens destined to creep tests. About 75 specimens were allocated to the short-term testing methods, grouped into 25 specimens for each of the following three environmental conditions: Room (R), saturation or humidity (H), and humidity and high temperature (HT) conditions. The creep tests were performed only on TSL1 specimens due to time constraints. This thin liner was the most used TSL as from the visits feedback. It also gave balanced results compared with TSL2 and TSL3. Another restriction was to only resort to R and H conditions. The reason was that the preliminary displacement graphs from HT tests showed signs of fatigue of the displacement transducer's gauges, thus providing unrealistic data. A total of 55 tests were then performed, of which 29 concerned the R condition and 26 the H condition. Once a creep loading was chosen, the test was repeated four to five times to ensure the representativeness of the loading, following which the outliers were discarded and only two test results that were centred in terms of duration of the test and strain magnitude were selected.

Short-term tests

The tests were performed following the principles described in section 2.11.1. After recording the thickness and width values for each specimen, the tensile strength magnitude was directly calculated by the machine through the expression:

$$\sigma_t = \frac{F}{A} \quad \text{(MPa)} \qquad \text{(XXII)}$$

Where: F: Tensile load, expressed in Newtons (N)

A: Specimen cross-sectional area at the narrow section, expressed in square millimetres (mm^2).

The value of σ_t should assist in determining the capability of the support to resist the tensile's driving forces, and in characterizing the appropriate conditions of the liner utilizations. It should also be used for further analyses of the liner's behaviour. Figure 5-8 represents a TSL dog-bone specimen under a UTS trial.

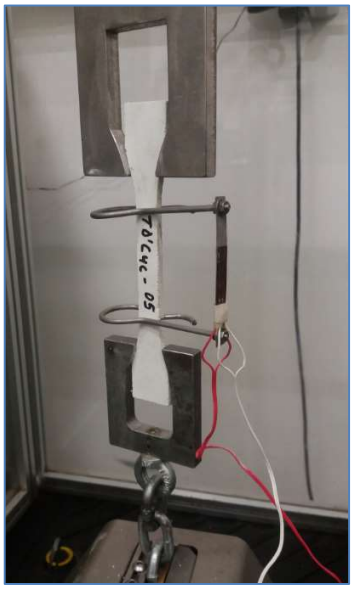


Figure 5-8 Ongoing UTS test on the MTS 643 under room environmental conditions

All the tests were performed, ensuring that the specimens were centred and well-adjusted in the grips. A pre-load of about 15 N was always set before the initiation of the tests that had to run at a loading rate of 5 N/s until failure occurrence.

The adopted method consisted of performing UTS tests on dog-bone specimens of three different TSLs. The aim was to assess the long-term influence of environmental conditions on TSLs' strength. To achieve this, a longer exposure of a thin liner in a determined environmental condition was observed before subsequent short-term testing through the MTS 643. The duration of the exposure had to be longer than the traditional 28 days of curing, but the specimens were also tested to shorter exposure time just for the sake of traceability of the strength over time. Therefore, the specimens were exposed to different environmental conditions and tested after the exposure durations of 15 days, 28 days, 56 days and 112 days.

The room condition consisted of storing the specimens in room temperature and humidity conditions. In saturated condition, the specimens were plunged into containers full of tap water under the room temperature condition. Finally, the humidity and high temperature condition consisted of placing the dog-bone specimens in containers of water and then storing them in an oven, calibrated at 50ºC. This temperature was chosen to reflect the deep mine temperature condition. Although higher temperatures could also be adopted, this value was preferred for uniformity purposes, since additional long-term tests were performed in a conditioned room for creep tests. Besides, the temperature needed to be limited to about 50ºC for the sake of the equipment safety, wiring protection against higher temperatures, and accuracy of the measurements, of which sensitivity could be affected by relatively higher temperatures. And practically, the adopted temperature can be validated, based on Biffi *et al* (2007) graph, displayed in Figure 2-4, which shows that the VRT for the visited deep mine should be around 60ºC if the coating was applied at the deepest level. However, this was not the case, with the deepest coated site not reaching 1000 metres below surface, or remaining below 50ºC.

Long-term tests

The trials were undertaken at the Wits Gold Fields laboratories, through the use to a UTS creep testing machine, conceived for the sake of the current research. The apparatus is mainly made of a lever for the transfer of loading (see APPENDIX A for the apparatus's dimension details). The reason for resorting to this equipment made of a lever was to use a lighter onset weight instead of applying a heavier weight directly on a specimen. This was based on understanding that the adopted machine should transmit the same final load applied on specimens, courtesy of a load multiplier, denominated Weight Factor (F). The long-term performance of UTS specimens was assessed on a limited number of TSL specimens. In effect, there were constraints related to the longer time taken to make and calibrate the creep machine, the exposure time of specimens to the adequate environmental condition prior to the testing, the duration of the tests, the limited allocated time to the doctorate program, etc. The H condition consisted of plunging UTS specimens in tap water containers for about 80 days before testing.

Design

The UTS creep testing machine was conceived to perform time-dependent direct tensile tests. This equipment, coded as "M3", was mainly built on the lever principle as presented in Figure 5-9. Through the lever "L" (load arm), a weight "W" placed at the onset point "A" shall be multiplied at point "C", with "B" being the pivot point. The real load applied to the tested specimen will be that on point C, also called "on-specimen load".A more detailed design of this machine with the related dimensions is presented in APPENDIX A.

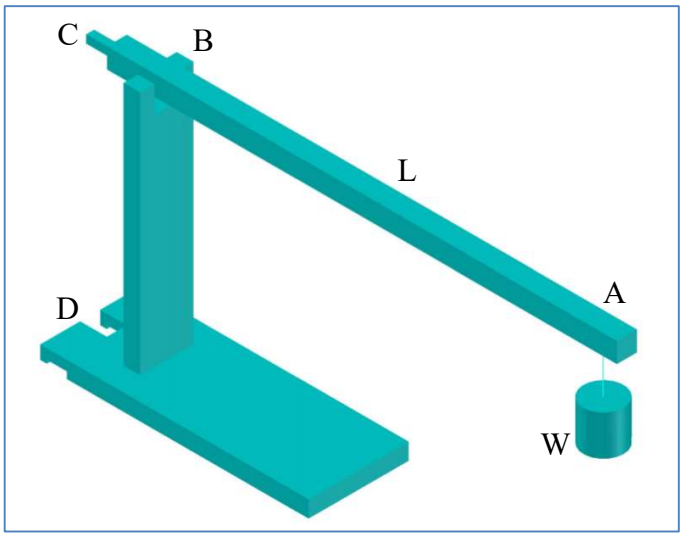


Figure 5-9 Design of UTS creep testing machine (M3) – Perspective Solid

In practice, the finished product included some modifications as presented in Figure 5-10, which also identifies the parts of the machine. The numbers in the description are the numbers stamped on the corresponding parts to ease their positioning.

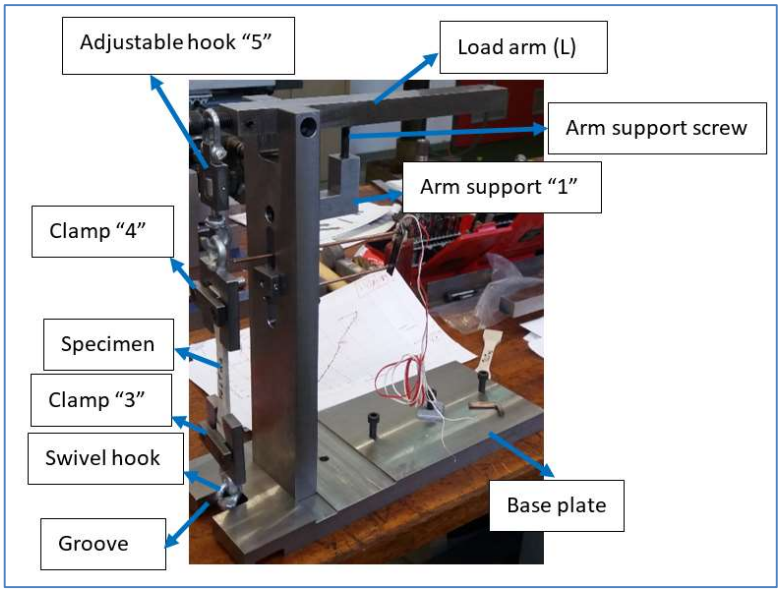


Figure 5-10 UTS creep testing machine (M3) in operation

The main part of the UTS creep testing machine is the load arm (L). It has the role of multiplying the applied weight. Although it was not imperative to multiply the weights for the UTS tests because TSL dog-bones fail at relatively lower

strengths than other strong materials, this machine might later be used to perform other material testing, not included in this specific work. Besides, every measuring weight projected to be used had to be calibrated before utilization. Knowledge of the exact weight would assist in determining the exact weight applied on the specimens.

Calibration of the weighing of the tensile creep testing machine "M3"

The calibration of the UTS creep testing machine consisted of determining the transferring weights from the onset load point to the specimen contact point. The dead load of the device and the weighing factor could then be determined. And since the readings from the data-logger were displayed in millivolt (mV), there was a need to convert them in kilograms. Figure 5-11 displays the UTS machine linear relationship between the input weights (in kg) and the output weights (in mV).

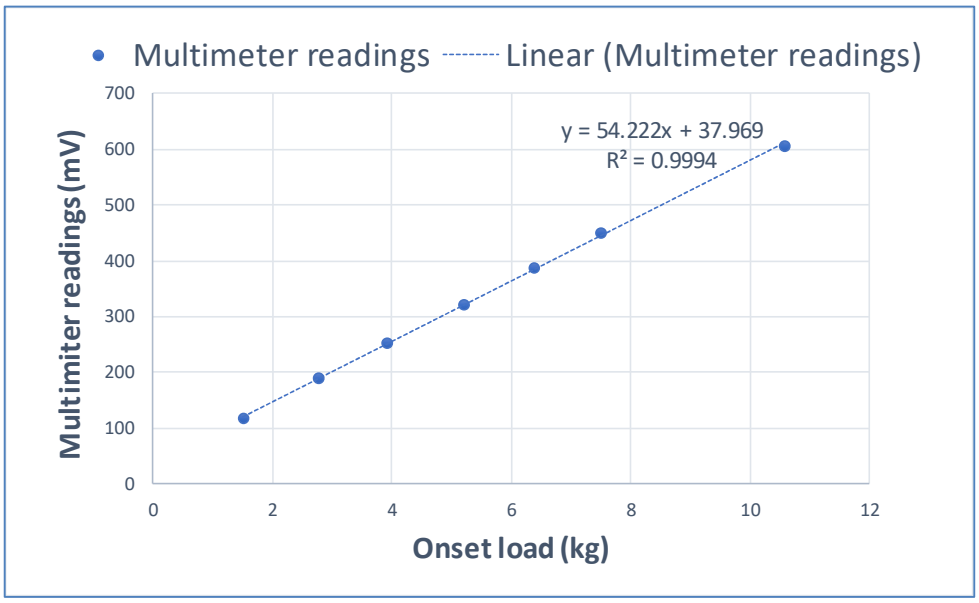


Figure 5-11 Relationship between M3 input (kg) and output (mV) loads

And, knowing the conversion relationship from mV to kg, calibrated from the load cell in section 5.2, the weight incremental effect from the onset to the on-specimen points was obtained, and here displayed through a linear expression in Figure 5-12.

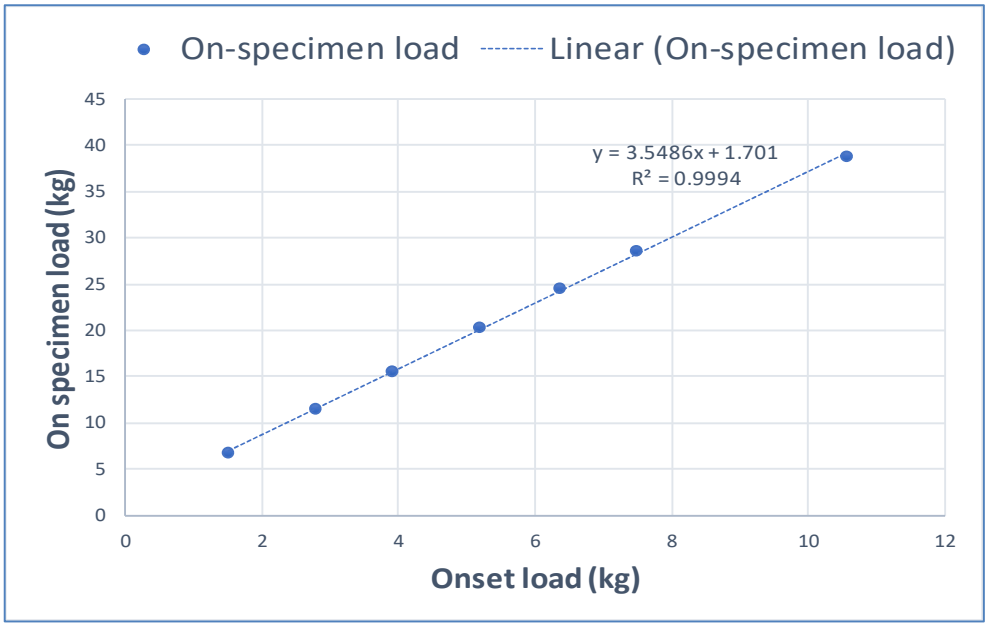


Figure 5-12 Relationship between onset load and on-specimen load of M3

Through the relationship found in the previous figure, the determination of M3 load factor and dead weight was done by extraction of the slope and the intercept. The first parameter is the load factor, while the second is the dead weight of the creep testing machine. And in the particular case of M3, these values are presented in Table 5-2.

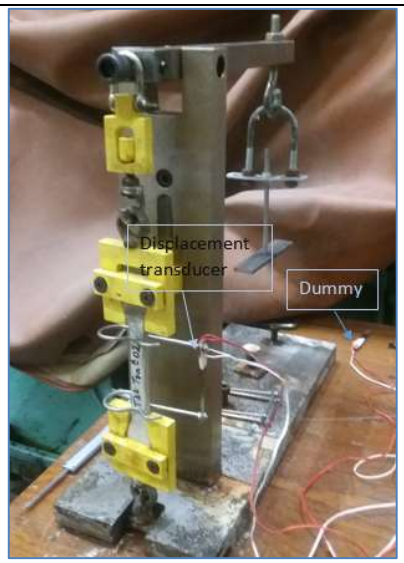
Table 5-2 Weighing parameters of tensile creep machine

Parameter	**Values**	**Units**
Load factor (F)	3.55	
Dead Weight	1.70	kg

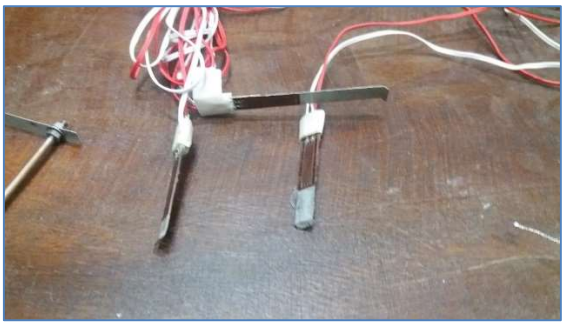
Calibration of the displacement transducer of the tensile creep testing machine "M3"

Similarly to the creep machine weighing calibration, the displacement transducers were also calibrated and validated early before the starting of the trial processes.

And this calibration and validation process was frequently repeated after small groups of tests to make sure that the strain gauges have not suffered any fatigue effect. Figure 5-13 (a) displays how the displacement transducer (also called LVDT) was attached to the dog-bone specimens, while Figure 5-13 (b) displays a sample of dummies, that were needed to complete the Wheatstone bridge configuration, as explained earlier in this research.



(a)



(b)

Figure 5-13 (a) Displacement transducer gripped to a dog-bone specimen, and (b) Sample of transducers' dummies for Wheatstone bridge

To calibrate the displacement transducer of the UTS creep testing machine, the distance between the holding points of the LVDT was varied and the readings from the data logger were recorded. The process was repeated for the sake of certainty of the outcomes. This was also periodically reassessed to check on the consistency of the results and to verify that the gauges had not suffered from fatigue. Figure 5-14 displays the calibrating equation of displacement transducer.

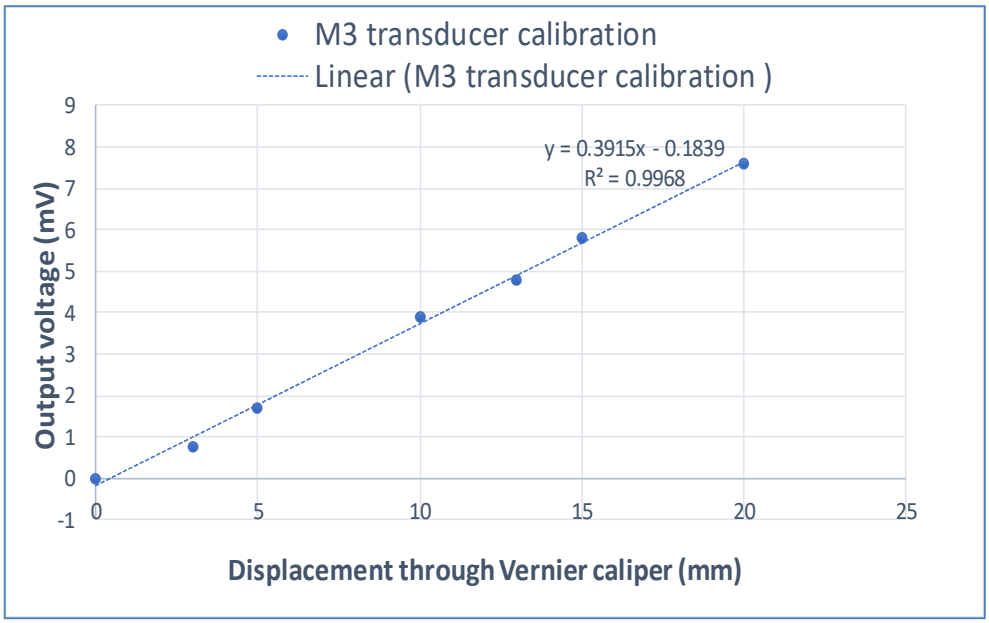


Figure 5-14 Relationship between displacement on M3 transducer's grips and output voltage

Since the data logger provided the resulting distances in millivolts (mV), the metric thresholds were obtained by inverting the coordinates. The plotting of the resulting equation is presented in APPENDIX F, Figure F-1, of which analytical expression is as follows.

$$x = 2.5462y + 0.4986 \quad \text{(XXIII)}$$

Where,

x: displacement of the dog-bone specimen until failure, in millimetres

y: displacement readings from the data logger, in millivolts

Having determined the metric displacements until failure, the corresponding elongations will be determined by dividing these by the initial lengths. And it was always ensured that the initial length between the grips was 66 mm.

Mode of operation of the UTS creep machine

A proper UTS creep test that is to be performed on the creep machine displayed in Figure 5-10 should be done according to the following steps:

1. Ensure that the load arm is lying parallel to the base plate. If not, adjust it by using the adjusting screw on the arm support marked "1"
2. Place the adjustable hook "5" at the edge of the load arm
3. Fit the swivel hook into the locating groove at the back and bottom of the base plate and ensure that it is centred
4. Attach the holding clamp "3" to the swivel hook
5. Suspend the holding clamp "4" on the adjustable hook "5"
6. Grip the displacement transducer onto the specimen gauge as shown in Figure 5-13 (a)
7. Fit the test piece in the top holding clamp (grip) marked "4" and fasten it lightly
8. Fit the test piece into the bottom holding clamp (grip) marked "3" and fasten it lightly
9. Take up the slack by adjusting the screw on the adjustable hook marked "5"
10. Connect the displacement transducer to the Wheatstone bridge configuration described earlier
11. Switch on the data-logger
12. Start the recording process on the data-logger at a frequency of half a second
13. Gently place the onset load on the load arm hook
14. Wait until the failure occurs
15. Stop the data-logger recording process and gently remove the specimen from the grip
16. Transfer the data obtained from the data-logger to a personal computer for further analyses

5.3.4 Results from short-term tests

Only the results from the dog-bone specimens that broke at the gauge section were considered. Figure 5-15 displays a sample of those mentioned specimens.



Figure 5-15 Sample of some TSL dog-bone specimens (TSL1, TSL2, and TSL3) tested on the MTS 643 at various environmental conditions

As stipulated earlier in this section 5.3.3, numerous trials were performed to assess the thin liners UTS sensitivities to changes in environmental conditions.

TSL1 sensitivity to environmental conditions

The results for the TSL1 assessment are illustrated in Figure 5-16.

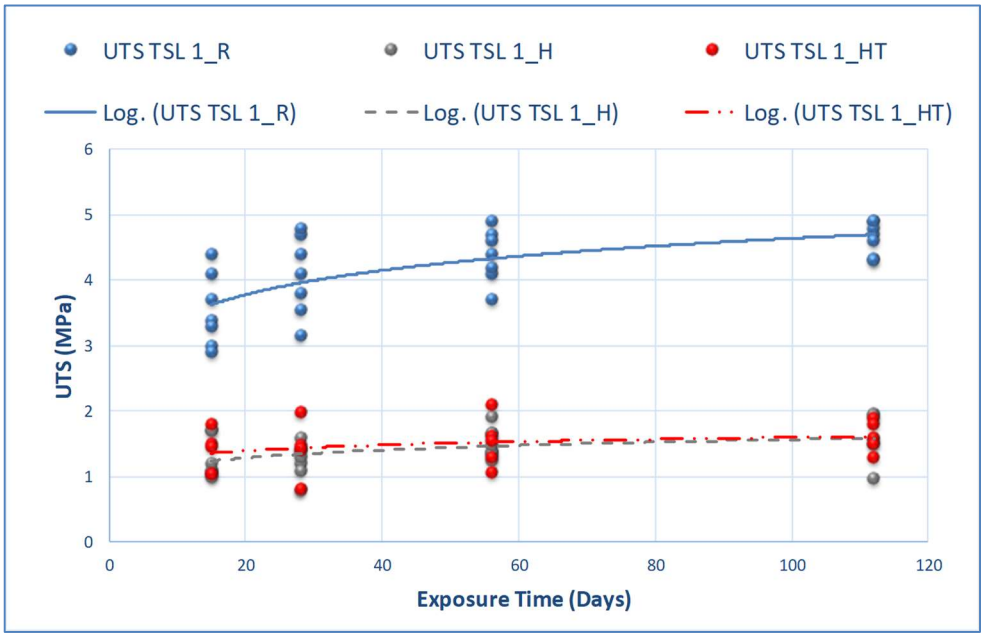


Figure 5-16 TSL1 tensile strength sensitivity to environmental conditions

According to these results, in room condition, TSL1 rapidly gains strength over time. The incremental rate is positive even after 28 days. However, if the ultimate

rate is assumed to be reached after 112 days, the strength after 15 days only represents about 76%.

In contrast, both humidity and the combined high humidity-temperature conditions show a very slight increment over time. These environmental conditions reduce the TSL1 tensile room strength by more than half its expected value. These results strongly show that it is a poor practice of simulating the replication of TSL1's Room behaviour in H or HT conditions. Additionally, it can be deduced from the same graph that temperature sole effect is less influential on the overall TSL1 tensile strength than humidity.

TSL2 sensitivity to environmental conditions

The results from TSL2 tensile testing are displayed in Figure 5-17.

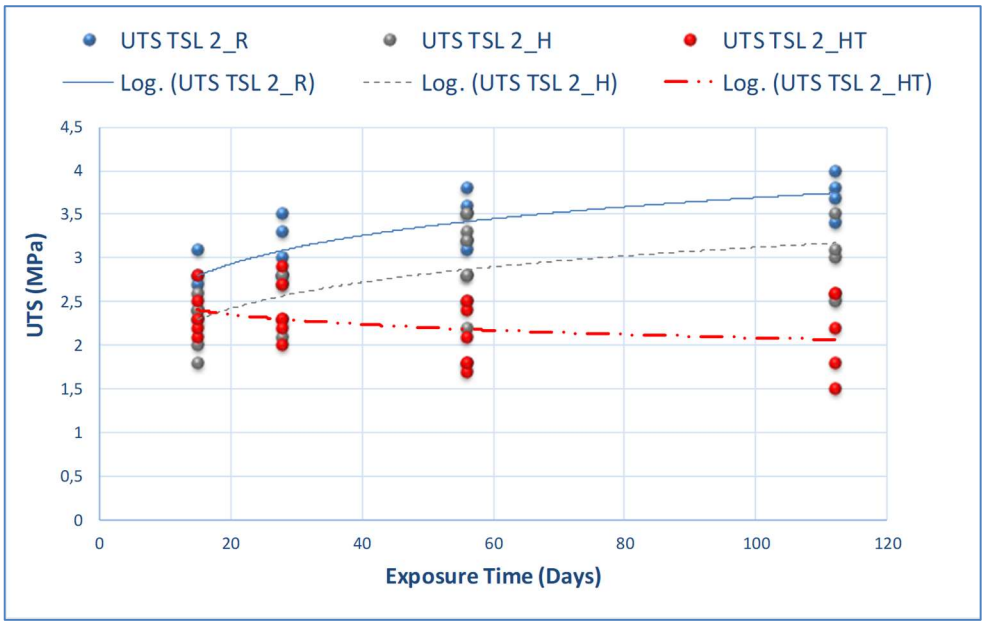


Figure 5-17 TSL2 tensile strength sensitivity to environmental conditions

TSL2 gains strength over time in room conditions. However, this strength is lower than for TSL1. And contrary to this cited liner, TSL2 still shows a clear strength increment when used in saturated conditions. Therefore, humidity contributes to strengthening this particular liner. One of the reasons might be that water is one of the constituents used during specimen preparation. Nevertheless, when associated

with heat, the effect is detrimental as there is a drop of strength over time. The temperature negatively impacts the integrity of TSL2. Here as well, it is not accurate to simulate the usage of TSL2 in saturated or HT conditions based on its performance from laboratory R condition.

TSL3 sensitivity to environmental conditions

The trends of TSLs getting stronger over time in room conditions have been observed for the previous two liners. However, it was not the case for TSL3 as shown in Figure 5-18.

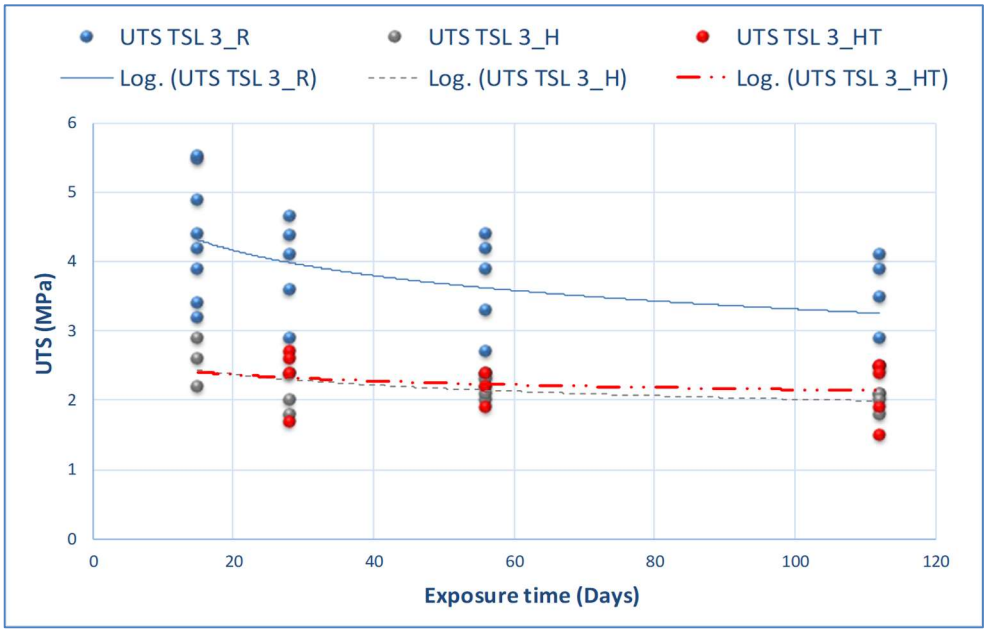


Figure 5-18 TSL3 sensitivity to environmental conditions

The technical sheet for TSL3 shows that this liner is the strongest out of the three tested in room conditions. This was partly true for shorter exposure times. However, the results surprisingly show a decrease in tensile strength over time. This should be a case of concern for TSLs behaving in this manner since this outcome was also observed in some tests performed by Yilmaz (2011). Actually, the supply of this particular thin liner was interrupted, if not terminated, just as more bag samples were requested to confront the results. The reason behind the supply interruption was however not elucidated, which is believed to be related to its bad performance. Also, this liner was tested after being stored in H and HT conditions. The trends

related to these two conditions show a slight decline over time. The effect of water on the liner performance is massive as it reduces by almost half the maximum strength.

Environmental impact on TSL elongation and modulus

From the literature, in room conditions, TSL tensile strength and modulus are proportional to exposure time and inversely proportional to elongation (Guner and Ozturk, 2018). This was also verified throughout the current research as shown in Figure 5-19 (a) and Figure 5-20 (a). Additionally, an investigation was done to assess whether this theory still prevails when the liners are exposed to different environmental conditions. But it is worth noting that before all these assessments, there was a need to determine the representative strength curves based on the averages of the strengths for the three adopted TSLs. And this was done taking into account the variation of the exposure durations, as presented through Table G-1 in APPENDIX G. Having determined the representative curves, the charts in Figures 5-19 (b) and 5-19 (c) displaying the strain-stress behaviours of TSL1 under H and HT conditions were also determined.

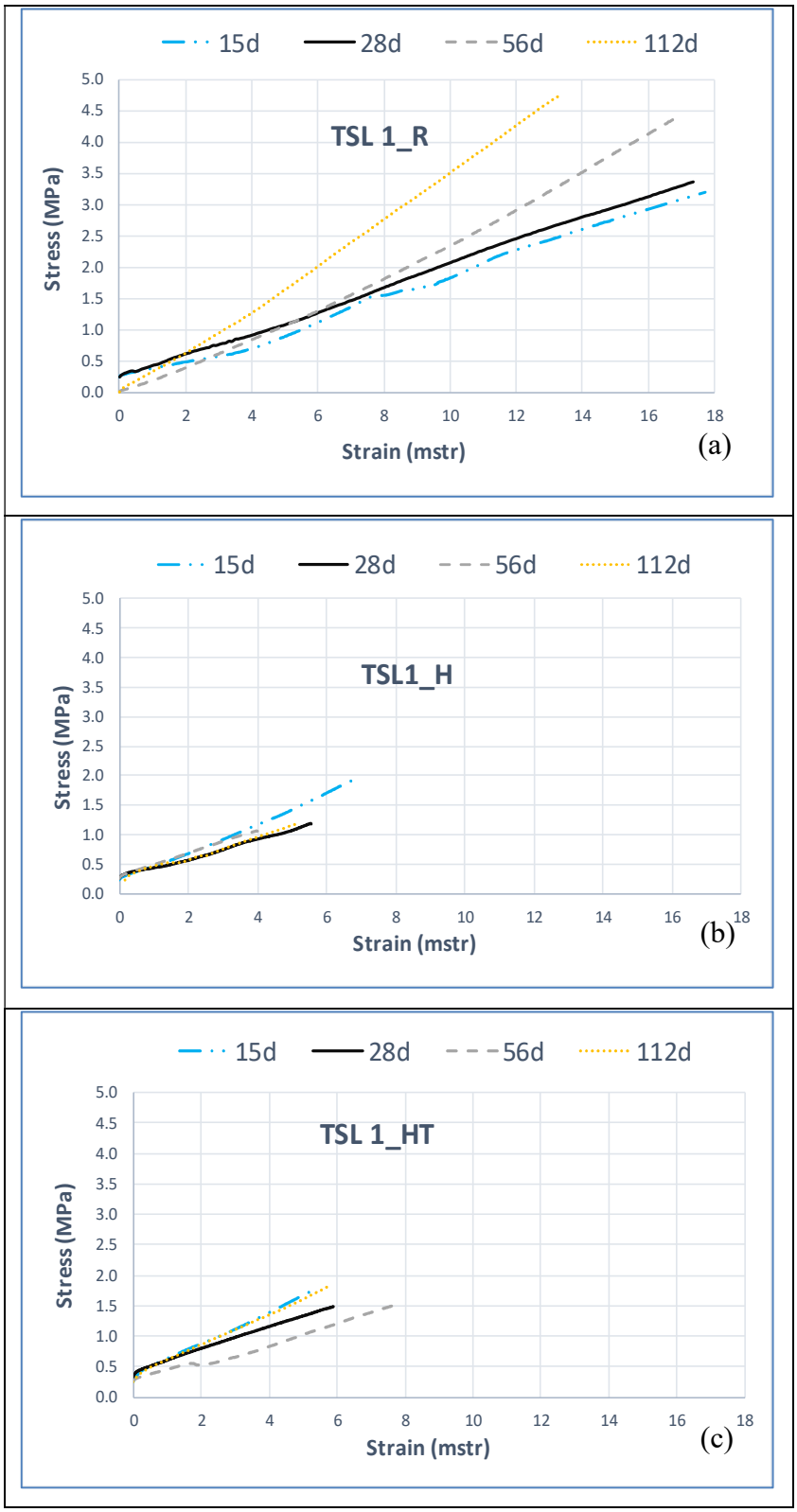


Figure 5-19 TSL1 stress-strain behaviours after various exposure periods in (a) room conditions, (b) saturated conditions, and (c) humidity and high temperature conditions. (d – Days; mstr – millistrain)

TSL1 elastic modulus is not demarcated with longer exposures in H and HT conditions as shown through Figures 5-19 (b) and 5-19 (c). However, longer exposures to saturated conditions tend to reduce the elongation of the liner, whereas the combined effect of humidity and high temperature perturbs the liner integrity, resulting in a non-conclusive statement regarding its elongation.

The assessment of elongation and modulus behaviour of TSL2 also required the establishment of referential values for the strength curves. These were obtained after the determination of the average strengths presented in Table G-2 in APPENDIX G. Afterward, the stress-strain behaviours of TSL2 were assessed, of which outcomes are illustrated through Figures 5-20 (a), 5-20 (b) and 5-20 (c).

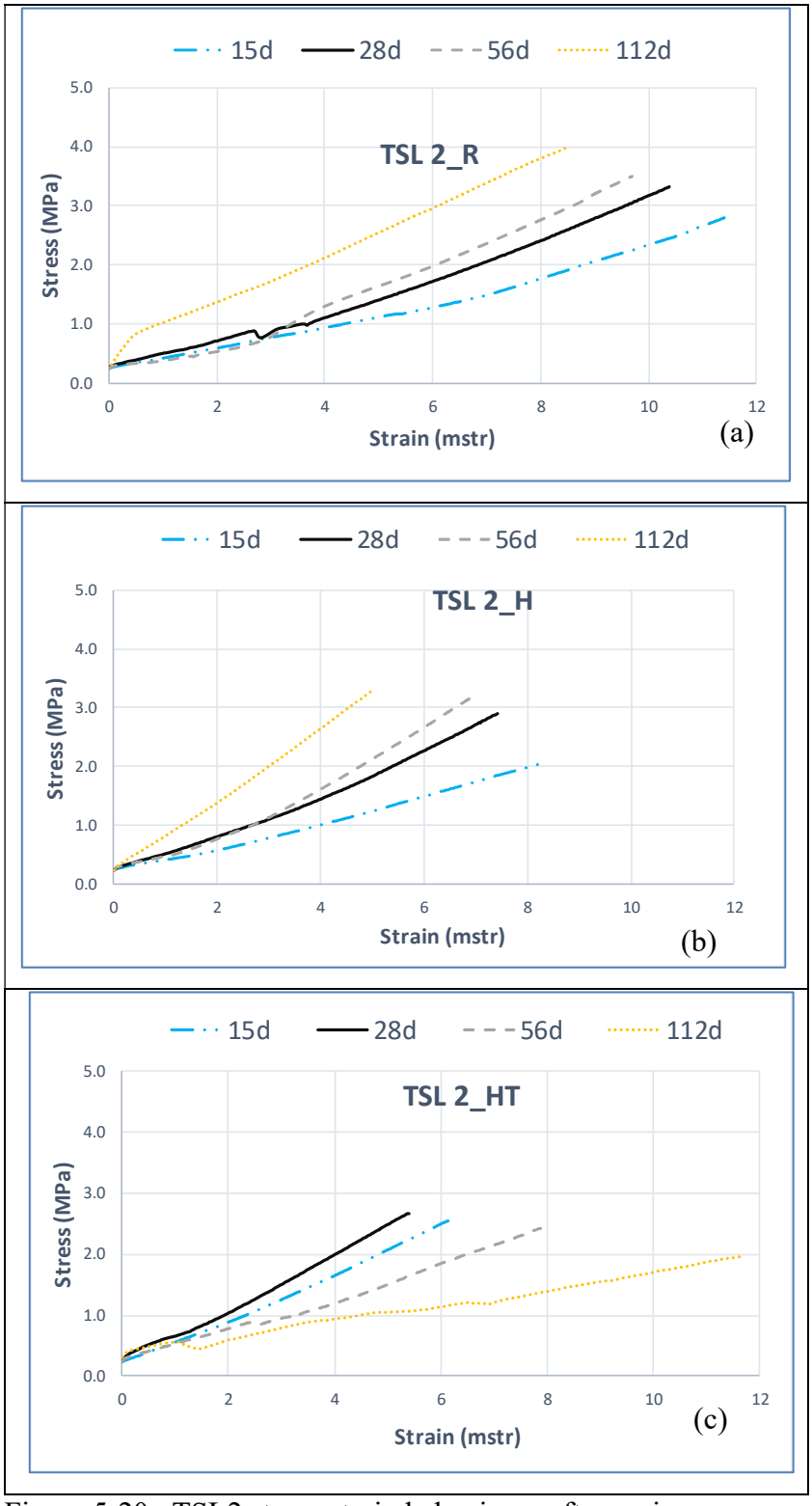


Figure 5-20 TSL2 stress-strain behaviours after various exposure periods in (a) room conditions, (b) saturated conditions, and (c) humidity and high temperature conditions. (d – Days; mstr – millistrain).

From a comparative study of Figures 5-20 (a), 5-20 (b) and 5-20 (c), longer exposure to room and saturated conditions strengthens TSL2 as well as it contributes to increasing its modulus while decreasing its elongation. Therefore, this liner should be preferred for usage in humidity conditions, though the strengths remain lower than the room strengths. And when humidity is combined to high temperature, an opposite effect takes place as the liner weakens and loses its stiffness, while gaining the plasticity characteristic, which is the ability to support high elongation before failure.

Considering TSL3, the average values for the representative strength curves behaviours were determined as shown in Table G-3 in APPENDIX G. From the behaviour presented in Figure 5-21, the exposure time to R, H and HT conditions does not impact on its elongation and modulus. The thin liner's strength is perturbed by these conditions, resulting in non-conclusive behaviours. Another reason to justify these behaviours might be the particularity of this liner strengthening behaviour in room conditions, which is opposite to the expected.

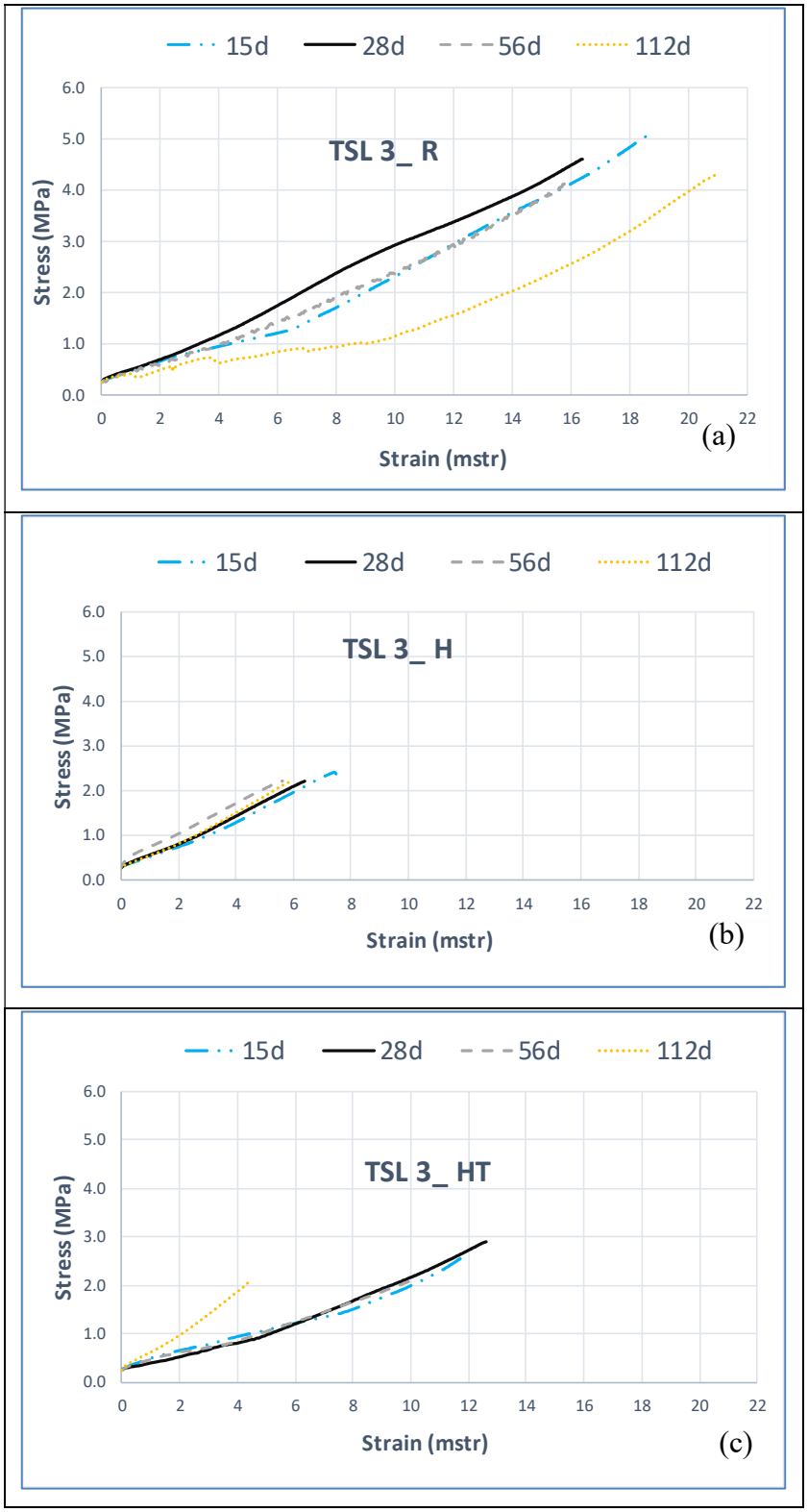


Figure 5-21 TSL3 stress-strain behaviours after various exposure periods in (a) room conditions, (b) saturated conditions, and (c) humidity and high temperature conditions. (d – Days; mstr – millistrain).

It is worth noting that this assessment process of the elongation and modulus behaviour could also be achieved through a comparison of their values. In this case, the strains at failure could be extracted from the stress-strain curves. The moduli could then be calculated as the ratio of stress to strain at 50% of the maximum stresses (Hudson and Harrison, 2000). The values of UTS, strain at failure and moduli for TSL1, TSL2 and TSL3 were assessed after exposure to the various environmental conditions and presented in APPENDIX G.

In summary, exposures in H and HT conditions prevent TSL1 and TSL3 UTS specimens from curing to their full room strengths, keeping their strengths almost constant throughout the time but lower than the room strengths. Non-conclusive statements can be made regarding the elongation and modulus behaviours of these liners as these environmental conditions significantly impact on their strengths, thus their integrity. TSL2, which is a water-based thin liner can perform in saturated conditions and shows distinctive behaviours of modulus and strength increment proportionally to longer exposures. The elongation is also clearly distinctive, behaving inversely proportional to longer H exposure. Nevertheless, this strength remains lower than in room conditions, similar to TSL1. In HT conditions, however, the TSL2 loses its composure observed in H conditions, weakening proportionally to the exposure time. Its stiffness also weakens while its elongation increases slightly. Therefore, high temperature has a detrimental effect on TSL2, even when it is combined with humidity conditions.

The latter results allowed assessing TSLs' elongation and modulus behaviours for various exposure times, considering a specified environmental condition at a time. Additional studies were required, which should focus on the impact of various environmental conditions on TSL tensile behaviours. Therefore, based on data displayed in APPENDIX G, a comparative assessment of the environmental conditions on the strength, elongation and modulus behaviours were performed, and the results are presented in Figures 5-22, 5-23 and 5-24.

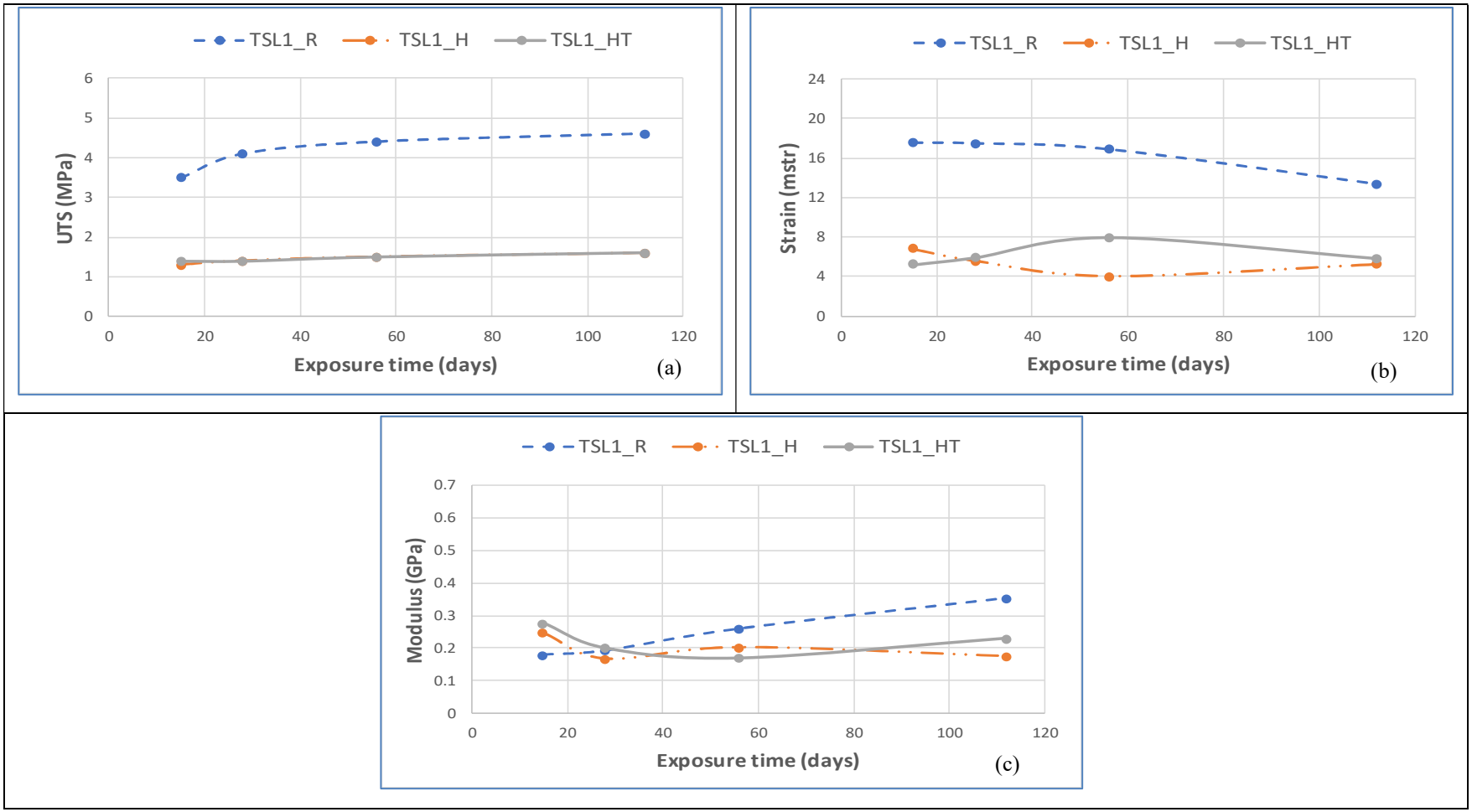


Figure 5-22 Impact of environmental conditions on (a) tensile strengths, (b) elongations and (c) moduli of TSL1

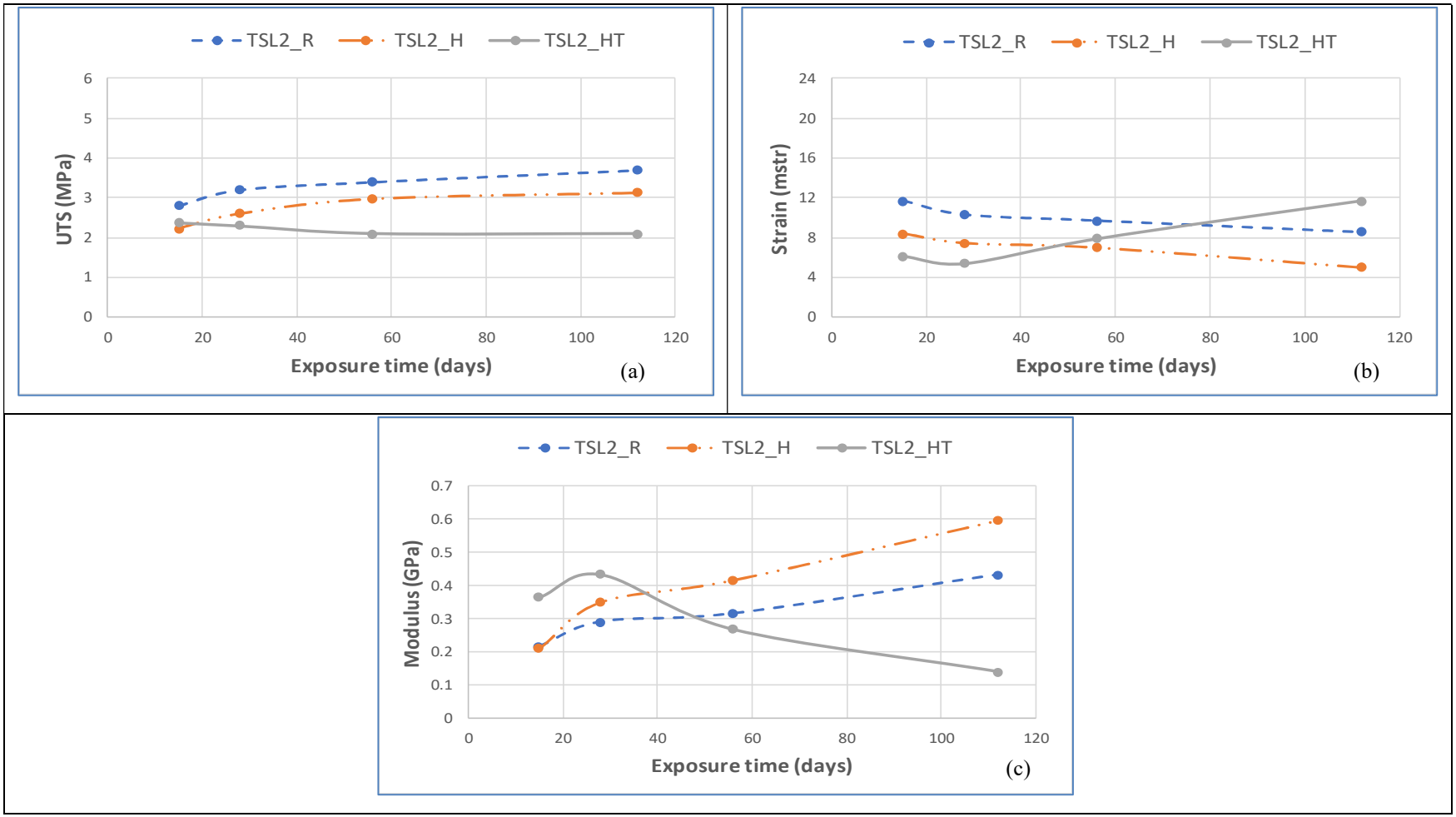


Figure 5-23 Impact of environmental conditions on (a) tensile strengths, (b) elongations and (c) moduli of TSL2

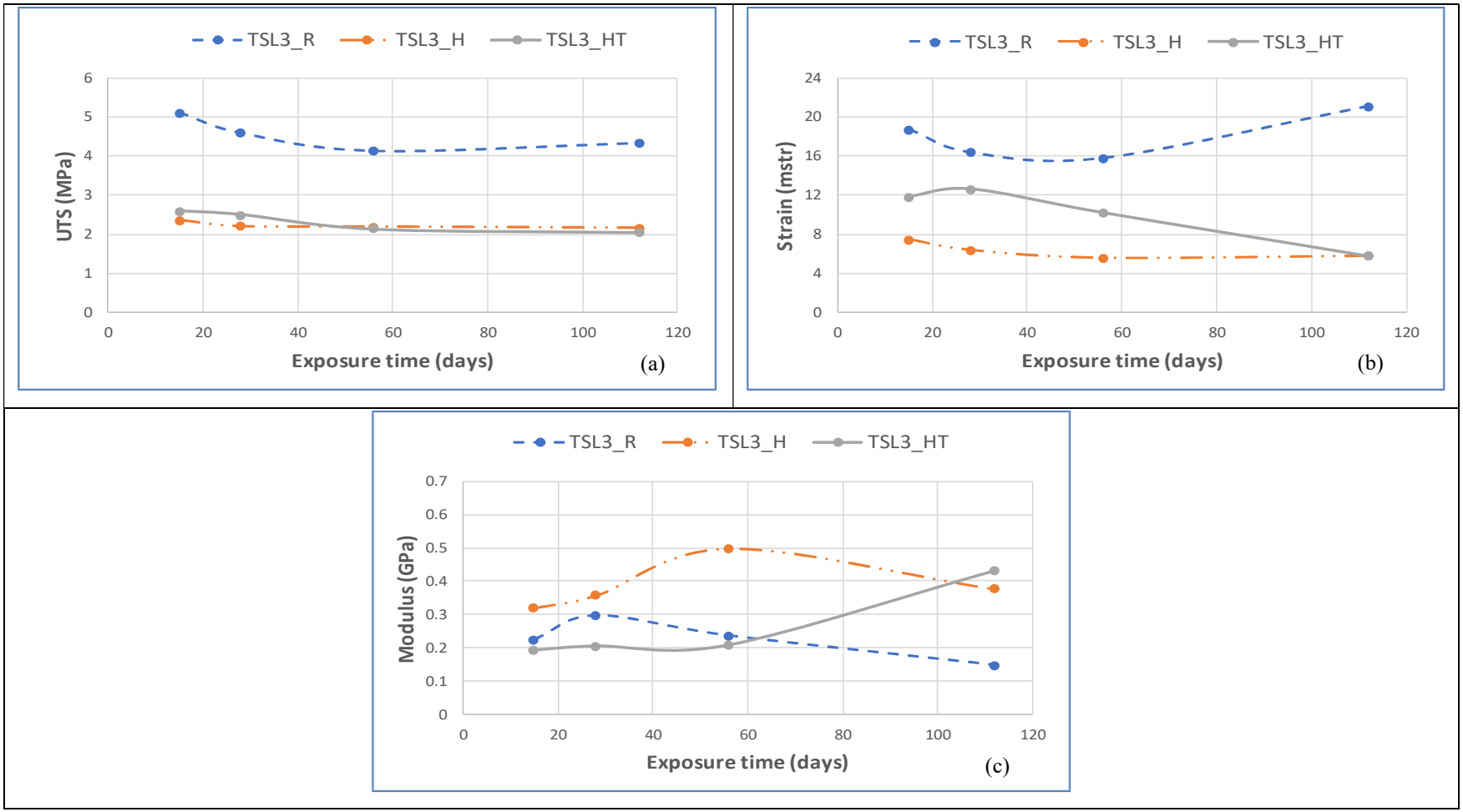


Figure 5-24 Impact of environmental conditions on (a) tensile strengths, (b) elongations and (c) moduli of TSL3

The graphs displayed in Figures 5-22 (a), 5-22 (b) and 5-22 (c) show that TSL1 strength and elongation are always lower in H and HT conditions compared to room conditions. Its stiffness also decreases or is irregular in these same environmental conditions proportionally to the exposure time. This shows that the risk of TSL1 failure is higher in H and HT conditions than in R conditions.

Figure 5-23 represents the behaviours of TSL2 UTS, elongation and modulus when facing changes in environmental conditions. As may be seen from Figure 5-23 (a), saturated conditions reduce TSL strength to less than its strength in room conditions. The strength from saturated conditions is also generally higher than that of the liner stored in HT conditions. The elongation follows the same path except for extensive exposures to HT conditions. The stiffness increases when this liner is exposed to humidity conditions but drastically decreases when exposed for longer periods in HT conditions. Therefore, this liner should not be recommended for HT conditions but should be preferred to TSL1 when called to be applied in saturated environments.

The graphs displayed in Figure 5-24 show that TSL3 strength and elongation are always lower in H and HT conditions than in room conditions. However, a concern for this TSL is that the room strength also decreases over the exposure time. The stiffness trend is irregular in R and H conditions but suddenly increases after long exposure in HT conditions, which might be a characteristic of a significant disturbance of its integrity due to a combined effect of temperature and Humidity. Based on the overall behaviour of TSL3, its risk of failure is expected to be significantly higher in H and HT conditions than in room conditions, thus precautions should be taken in the design of support using TSL3. This areal support should be thoroughly assessed to understand the reasons behind its strength decrease over time, observed even in room conditions.

Analyses of the influence of environmental conditions on TSL performance depending on the exposure time

The results obtained from UTS testing confirmed the strengthening of TSLs with longer exposure in room conditions, even beyond 28 days of exposure. There was an exception for a polymeric liner, TSL3, whose strength was decreasing with longer exposure, but its supply has been interrupted, probably due to its bad performance. The elongation is inversely proportional to TSL strengthening and its modulus in room conditions, except for TSL3 that produces inconclusive results. Only the water-based TSL abides by the same principle in H conditions, like TSL3 in HT conditions.

Humid conditions, however, negatively impact on tensile strengths of all three tested thin liners, causing those strengths to remain about half the values reached in room conditions. This might be one of the reasons behind some TSLs' underperformance in underground mines. However, out of the three TSLs, the water-based TSL2, though weaker than in room conditions, showed better strength and modulus incremental trends proportionally to longer H exposures. Its elongation is inversely proportional to H exposure time, unlike the inconclusive results of modulus and elongation trends observed for TSL1 and TSL3.

The trends of TSLs' performance when stored in HT conditions are of strength decline. For instance, if TSLs show a logarithmic trend of strength improvement over time in room conditions, except for TSL3, all three have shown a decline or lower incremental rate of their performances after extensive periods of exposure in HT conditions. Still in these latter conditions, the stiffness of the water-based liner is weakening while its elongation tends to increase, unlike TSL1 and TSL3 which showed non-conclusive stiffness and elongation trends. This finding shows that TSL's integrity is strongly perturbed by HT conditions.

In summary, the use of TSLs in H and HT conditions is very delicate and should be thoroughly investigated, ensuring that the support design considers the real TSL performances in these conditions. This strategy is needed to avoid under-evaluation

of the risks related to their utilization, and thus also to avoid exposure of opening stabilities, personnel and equipment to uncalculated risks. However, this statement is based on only three cementitious TSLs. Further similar studies on more TSLs, especially the ductile TSLs, could produce more representative conclusions.

5.3.5 Results from long-term tests

Like the short-term tests, only the results from the UTS specimens that broke at the gauge section and between the transducer's grips were considered, as displayed in Figure 5-25.

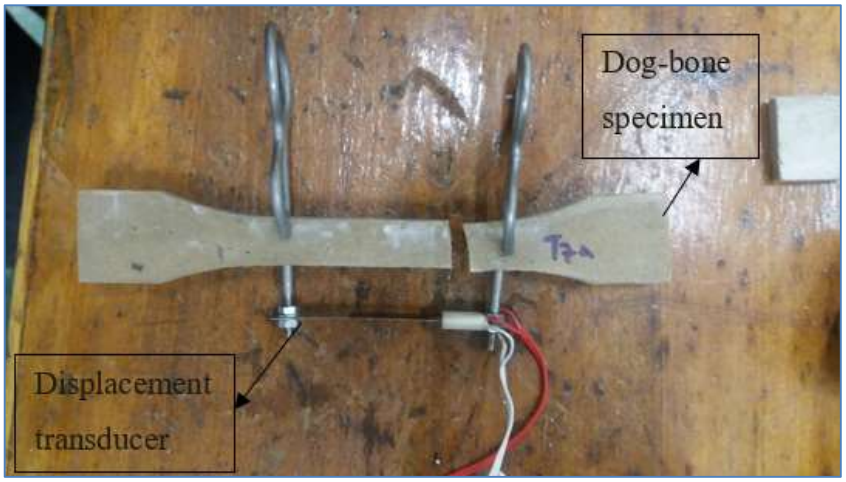


Figure 5-25 TSL dog-bone specimen failed at creep test

Only TSL1 specimens were assessed due to time constraints, and the results from the tests were plotted for both the R and H conditions as it will be presented in the following paragraphs. The data collected from the data logger were in millivolts, and they were mostly collected after every 500 milliseconds as shown in APPENDIX P which represents data collected from a single UTS creep test. Thus, the data points could reach a couple of millions of points depending on the duration of the test. And based on the proportionality equation suggested for the transducer calibration, these values could be converted to millimetres, thus in strains as explained earlier.

Room condition

The trials always began with the assessment of the 100% loading. The results of the trials are presented in Table 5-3

Table 5-3 Determination of average 100% creep load for TSL1 UTS in room condition

TSL1 specimen number	Environmental Condition	Exposure time (days)	Thickness (mm)	Width (mm)	Initial 100% Weight (kg)	Expected 100% On-specimen Load (N)	Expected 100% Strength (MPa)	Creep Strength (%)
1	**Room**	80	7	11.1	10.43	379.9	4.89	100
2	**Room**	80	6.5	13.5	11.1	403.2	4.60	100
3	**Room**	80	5.8	13.1	10.2	371.9	4.89	100
4	**Room**	80	6.4	12.8	10.6	385.8	4.71	100
5	**Room**	80	6.7	13.7	11.44	415.1	4.52	100
6	**Room**	80	5.6	13.8	10.1	368.4	4.77	100
Averages		***80***	***6.3***	***13***	***10.65***	***387.4***	***4.71***	***100***

From the previous table, the average initial onset weight of 10.65 kg was taken as a 100% representative load. This load was transferred and multiplied through the creep machine levers to become equal to 387.4 N (or 4.71 MPa) directly applied on specimens, such that it was capable of making a TSL1 UTS fail instantaneously. Subsequent lighter weights were used for UTS creep tests and their behaviours are displayed in APPENDIX L. For a comparative sake, however, these graphs could be superposed and presented in a semi-logarithmic graph as shown in Figure 5-26.

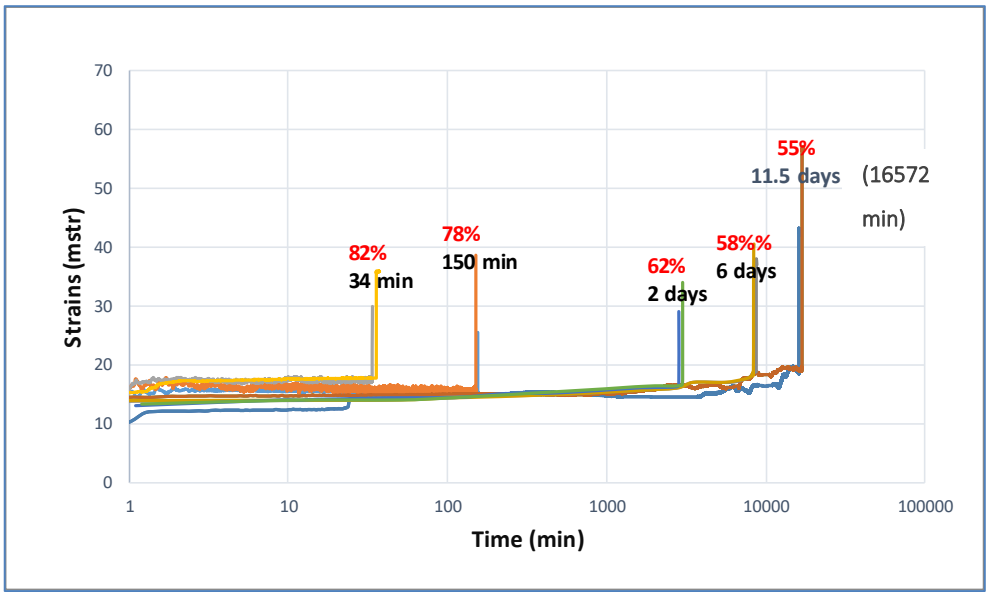


Figure 5-26 Semi-logarithmic graphs of TSL1 UTS creep behaviours tested in room condition (≈2days – 2896 min; ≈6days – 8624 min; ≈11.5days – 16572 min)

From the superposition of the TSL creep graphs in room condition, it is observed that the long-term strength is definitely below 55% of the short-term strength. Under greater creep loads, greater elongations occurred quickly but specimens broke after a short testing period. However, it was observed that the strains of the lighter creep loads, initially smaller than the strains of the heavier loads, could increase with the longer testing time and become greater than those under heavier loads as the testing time extended. This can be interpreted as a characteristic of TSL to practically accommodate higher displacements in room condition as opposed to its behaviour obtained through relatively short-term testing, since creep loading is a frequent mechanism that occurs in the rock mass. This constitutes an additional advantage of TSL for practical utilization. However, it only refers to room condition, therefore there is a need to assess this behaviour in an underground-like environment such as the humid condition.

Humidity condition

The initial tests were also performed to determine the loading that produces an instantaneous failure in humid condition, which corresponded to 100% of the

ultimate strength. Repeated tests were performed and the average 100% load was calculated. The results of the trials are presented in Table 5-4.

Table 5-4 Determination of average 100% creep load for TSL1 UTS in humid condition

TSL1 specimen number	Environmental Condition	Exposure time (days)	Thickness (mm)	Width (mm)	Initial 100% Weight (kg)	Expected 100% On-specimen Load (N)	Expected 100% Strength (MPa)	Creep Strength (%)
1	**Humid**	80	6.9	13.4	4.1	159.5	1.72	100
2	**Humid**	80	6.5	11.4	3.9	152.5	2.06	100
3	**Humid**	80	6.6	12.3	4.4	169.9	2.09	100
4	**Humid**	80	5.6	13.1	4	156.0	2.13	100
5	**Humid**	80	5.4	12.9	4.2	162.9	2.34	100
6	**Humid**	80	6.7	13.2	4.5	173.4	1.96	100
Averages		***80***	***6.3***	***12.7***	***4.2***	***162.4***	***2.03***	***100***

The latter table showed that the average load that represented 100% of the ultimate load applied on TSL specimens was about 162.4N, equivalent to 2 MPa. This strength represents 43% of the ultimate strength obtained in room condition. And since the long-term strength results from R and H conditions are to be compared, it was opted to represent the TSL's creep behaviours in humid condition with the percentage strengths related to room condition, as displayed in APPENDIX L. These TSL creep graphs from H condition were also superposed as presented in Figure 5-27 for the sake of comparison.

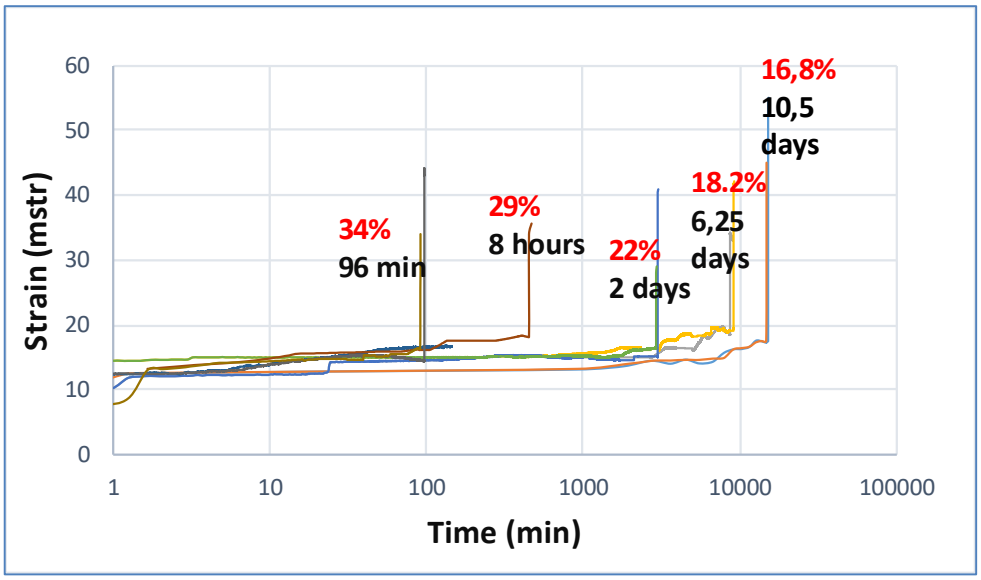


Figure 5-27 Semi-logarithmic graphs of TSL1 UTS creep behaviours tested in humid condition (≈8hours – 485 min; ≈2days – 2853 min; ≈6.25days – 8996 min; ≈10.5days – 15124 min)

Although the consistency of the strain behaviours in relation to the percentage loads and the time to failure was not fully observed, the trend is still of higher strains proportionally to the percentage creep loading. This is a confirmation of the results obtained from the room condition. However, the strain magnitudes at long-term strengths in humid condition are lower than in room condition. Therefore, the humid condition diminishes the containment effect of TSL offered in room condition, but still offers better containments than those assessed through short-term tests in the same environmental condition. Nevertheless, it is suggested that more creep trials be performed to investigate on the inconsistency of the strain behaviours and the containment capacity of TSL in underground-like condition.

Analysis of the influence of the environmental conditions on TSL for UTS long-term testing

Based on the resulting behaviours of TSL creep tests performed in R and H conditions, long-term uniaxial tensile strengths were assessed. This was done through the plotting of the averages of the percentage tensile strengths obtained from R and H condition, as displayed in Figure 5-28.

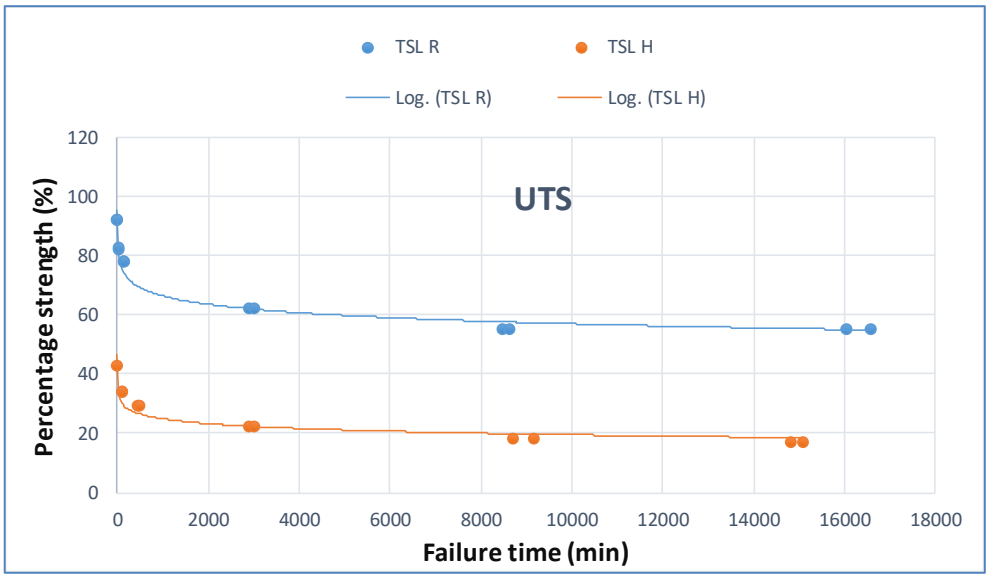


Figure 5-28 Estimation of TSL long-term uniaxial tensile strengths through plotting of time-to-failure strengths from room and humid conditions (R-room condition; H-humid condition)

The latter figure provides the long-term strengths of TSL equivalent to about 56% in room condition and 17% in humid condition. In light of this finding, TSL should not be resorted to for permanent support in humid underground mines. And based on the previous short-term behaviours of TSL in humid and high temperature conditions, it can be said that for underground mines that present this environmental condition, the long-term strengths should even be worse. Thus, TSL should not be used for permanent support in such conditions since its long-term capacity to oppose the tensile driving forces will be very small. But if the environmental condition is closer to the room condition, TSL utilisation can be motivated.

5.4 Brazilian Indirect Tensile tests

5.4.1 Introduction

BIT tests were resorted to for assessing the impact of coatings on substrates that are under indirect failure mechanisms and under various environmental conditions. Approximately 349 BIT specimens that included all three TSLs and 40 uncoated shotcrete discs were prepared. From the first group, 300 specimens were allocated to short-term tests (50 coated shotcrete specimens for each of the three TSLs and

50 TSL discs for each TSL) and 49 specimens allocated to creep tests of solely TSL1-related discs. The creep specimens only dealt with TSL1 due to time constraints, and they were grouped into 25 coated specimens for room tests and 24 coated specimens for the humid condition. In the second group, the uncoated shotcrete discs were prepared and tested in all three environmental conditions under the short-term BIT method after an extended exposure time. This section will look at TSL performances when used as a coating in underground-like conditions. It is believed that this approach will give a better view of TSL behaviour, since it does not act as a standalone dog-bone specimen under UTS tests, but rather performs as a coating on a mine wall, as illustrated in Figure 5-29.

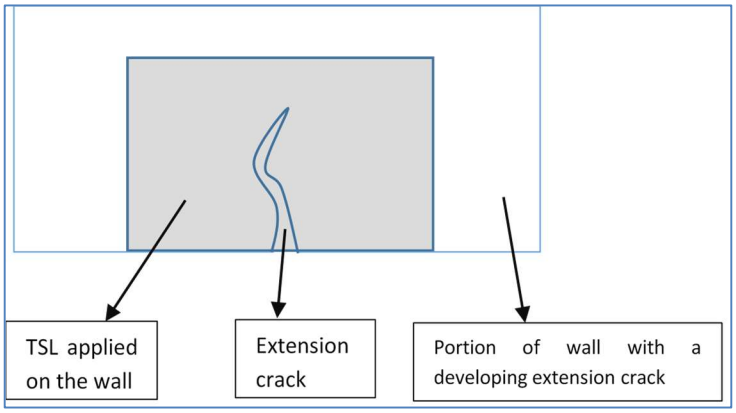


Figure 5-29 TSL coating on a sidewall with an extension crack

From Figure 5-29, TSL is coated on a wall with an extension crack. It is expected to oppose the crack expansion through its characteristics of tenacity in bonding on substrates and high tensile properties (Boeg-Jensen and Swan, 2014).

To assess the coated BIT specimens, the following steps will be developed: specimen preparation, material and employed methodology, and results and analyses of the short-term and long-term tests.

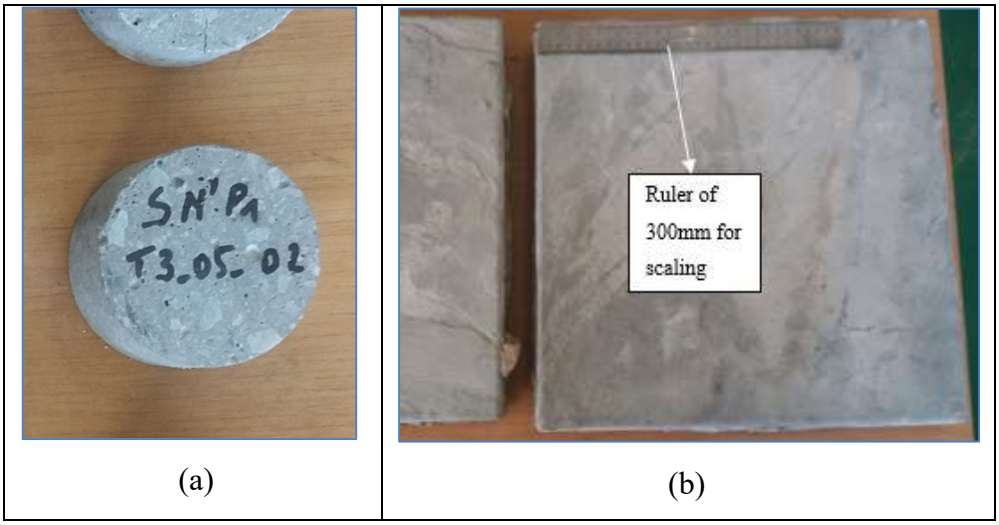
5.4.2 Specimen preparation

In this section, various specimens were prepared:

- Uncoated shotcrete BIT specimens
- TSL BIT specimens

- Shotcrete BIT discs coated with TSLs

The uncoated shotcrete and the TSL discs were prepared to be 21mm thick and 42 mm of diameter. A specimen of an uncoated shotcrete disc is presented in Figure 5-30 (a). The shotcrete discs were cored from panels of fibre-reinforced shotcrete (Wetcrete) of 450x450 mm^2 and 55mm thick. These were prepared, then cured in water containers for 30 days before their supply by Concrete Lining Products (CLP). A specimen of the supplied shotcrete panels is presented in Figure 5-30 (b).



(a) (b)

Figure 5-30 (a) cored disc of shotcrete, (b) Panel of precast shotcrete

The reinforced Wetcrete had the following specifications:

- Strength of 40MPa after 28 curing days
- Compressive strength penometer at 1.5hours is greater than 0.5MPa
- Absorbed energy is greater than 600 joules at a deflection of 2.5mm
- Resistance to high impact
- Anti-corrosive

The additional advantages of the adopted shotcrete are less rebound, less dust production, improved bonding, etc. TSL coatings were prepared via the electrical mixer presented in section 5.3.2. The cored discs were coated with TSL-thickness of 4 mm. Figure 5-31 displays the coating phase.



Figure 5-31 Coating phase of shotcrete discs with TSL

During the coating process, the mixture was poured in circular moulds of 4 mm thick and diameter of 50 mm. These moulds were placed on a working place covered with a plastic film and lubricated all-around their internal circumferences to allow smooth removal of the coated discs. After the pouring of TSL mixture, shotcrete discs, previously cleaned with tap water, were placed on and maintained for one to two days to allow a better TSL setting. The same process was repeated for the coating of the other face of the substrate. After a total of three to four curing days, the specimens were taken out of the moulds, and a diamond saw cutting machine was used to shape the coating contour, reducing its diameter to about a millimetre smaller than the substrate diameter, as presented in Figure 5-32. This was to ensure full contact between the steel jaws and the substrate during testing. However, it can be noticed that one of the faces was always one day younger in curing. But the difference curing time only slightly, if not, impacts on the overall long-term strength, which is the focus of the current research.



Figure 5-32 Final aspect of a coated BIT specimen with shaped coating

From experience, no more than 30 specimens could be coated from a single batch of the mixture since the timing of mixture pouring, levelling, and the substrate cleaning was to be kept short to avoid the formation of lumps in the mixture or its loss of integrity. Therefore, only small mixture quantity could be prepared, yet care needed to be taken to keep the mixtures identical throughout the entire process, and preliminary tests were undertaken to validate the consistency of the results.

The preparation of TSL discs adhered to the ISRM standards (ISRM, 2007). They were obtained by moulding the mixture in rubber sleeves of 42 mm diameter and 105 mm height (see Figure 5-33), previously lubricated in the inner part with a film of Vaseline to allow easy removal. After two setting days, the cylindrical TSL products were removed and cut into discs of 21mm thickness using a Diamond saw cutting machine.



Figure 5-33 Rubber sleeves used to mould TSLs

5.4.3 Materials and methods

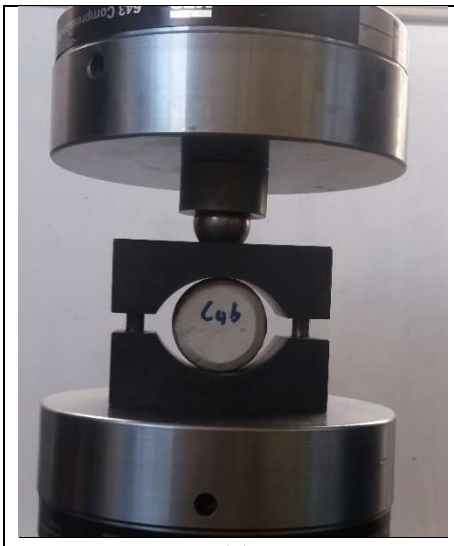
Two main test types were performed, namely the short-term (also called "instantaneous") and the long-term (creep) BIT tests. In both cases, the tests were performed for the primary purpose of assessing the practical enhancing capability of thin liners on a substrate strength, considering various environmental conditions, and particularly for longer-term. In this research, shotcrete was the adopted substrate for the following reasons:

- It is a rock-like material
- It has been used for similar research by Mpunzi *et al* (2015), thus the bases have already been laid and the outcomes of this research could provide additional information
- It is a soft material, thus should fail under lower applied loads than hard rocks. This property will help to simplify the complexity of the creep testing machine design.

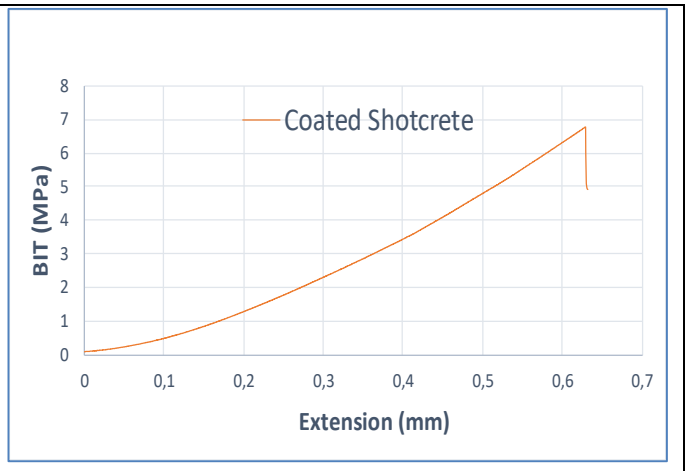
This research looked at the behaviour of BIT coated substrates after an extended exposure time in R, H and HT conditions. The assessment of the coating impact on the substrate performance was undertaken after the specimens had been stored in underground-like environmental conditions for periods up to 112 days.

Short-term tests

The method consisted of performing BIT tests on substrates coated with three different TSLs, namely TSL1, TSL2, and TSL3. Additionally, BIT specimens of TSL and shotcrete were tested separately. All the tests followed the ISRM standards (ISRM, 2007). The specimens were exposed to various environmental conditions for periods of 15 days, 28 days, 56 days and 112 days before being tested on the MTS 643, immediately after their removal from the environmental conditions at which the specimens were exposed. These conditions were: R, H and HT conditions. The conditioning of these environmental conditions followed the same principle explained in paragraph 5.3.3. And the short-term testing of the BIT coated specimens were performed on the MTS 643 as displayed in Figure 5-34 (a). The loading was realised in displacement control mode at a loading rate of 5 N/s. The shape of the resulting strength-displacement curves is also displayed in Figure 5-34 (b).



(a)



(b)

Figure 5-34 (a) Ongoing BIT test on the MTS 643 under room environmental condition, and (b) Shape of BIT stress-displacement curve

The indirect tensile strength was determined to the following formula built in the MTS:

$$\sigma_t = \frac{2F}{\pi t d}\ (MPa) \qquad \text{(XXIV)}$$

Where,
F: Compressive load vertically applied on the BIT specimen, and expressed in Newtons (N)
t: Thickness of the BIT specimen, without accounting the liner thickness, and expressed in millimetres (mm)
d: Diameter of the BIT specimen, also expressed in millimetres (mm)

For short-term tests, H and HT Specimens were tested in Room conditions for two reasons: firstly there was not appropriate logistic to test them in the same conditions of storage, and secondly the testing duration was usually less than 90 seconds, which is insignificant to dry a shotcrete specimen that has been stored for weeks or months.

The resulting BIT strengths from coated specimens were compared with those of uncoated shotcrete. The impact of the environmental conditions on the TSL enhancing capability was also assessed. And for a better understanding, a separate study of TSL behaviour when loaded in the same environmental conditions with the shotcrete substrates will be analysed. A comparison of the vertical displacements at peak strength between the TSL BIT and the uncoated shotcrete discs will be made to outline the thin liner with higher vertical displacement, thus higher elongation. Therefore, the characterization of each TSL on the overall enhancement will be determined based on the higher percentage of strength increase and the BIT higher vertical displacement at break.

Long-term tests

These kinds of tests aimed to assess the long-term performance of thin liners through creep tests. As with UTS long-term tests, only a limited number of 49 BIT tests were performed. This constraint was also dictated by the longer period during which a test can run, the variety of the types of the BIT tests and the limited allocated time of the doctorate program. Unlike the various short-term tests, only coated shotcrete discs were assessed through creep trials due to time constraints. The impact of the environmental conditions on the performance of coated shotcretes

was also assessed for R and H conditions. The specimens were exposed to room conditions as well as to humidity for about 80 days before being tested in a BIT creep testing machine under the same environmental conditions. It is worth noting that here as well, a few creep trials were performed in HT conditions, but the LVDT conceived for this thesis's research showed some limitations because its strain gauges became fatigued. The recorded data could show a decline in the displacement throughout time. This was contrary to the expected behaviour as observed for specimens tested in R and H conditions. Therefore, the outcomes will not be presented due to the lack of traceability.

Design

Three BIT creep testing machines were built. They were coded "M1", "M4" and "M5". M1 and M5 machines had almost the same shape, while M4 was previously conceived to fit in a heated container with enough water to keep the specimen humid. For illustrative purposes, M1 and M4 are presented in Figures 5-35 and 5-36. Detailed descriptions of all these creep testing machines are illustrated in APPENDIX B and APPENDIX C.

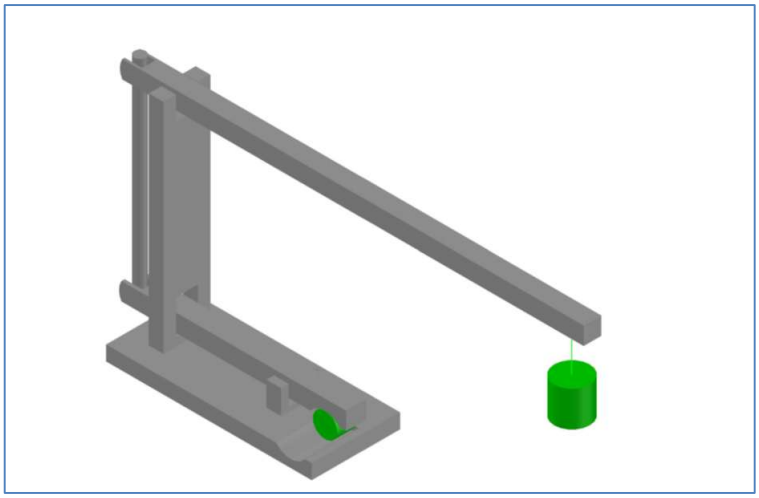


Figure 5-35 BIT creep testing machine M1

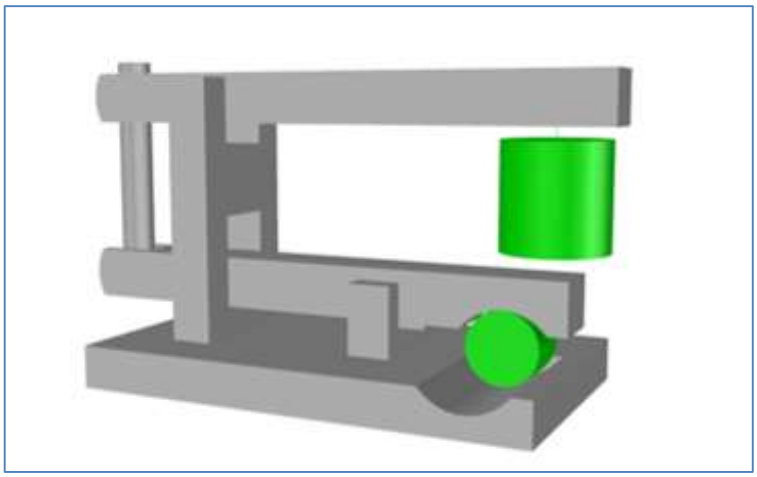
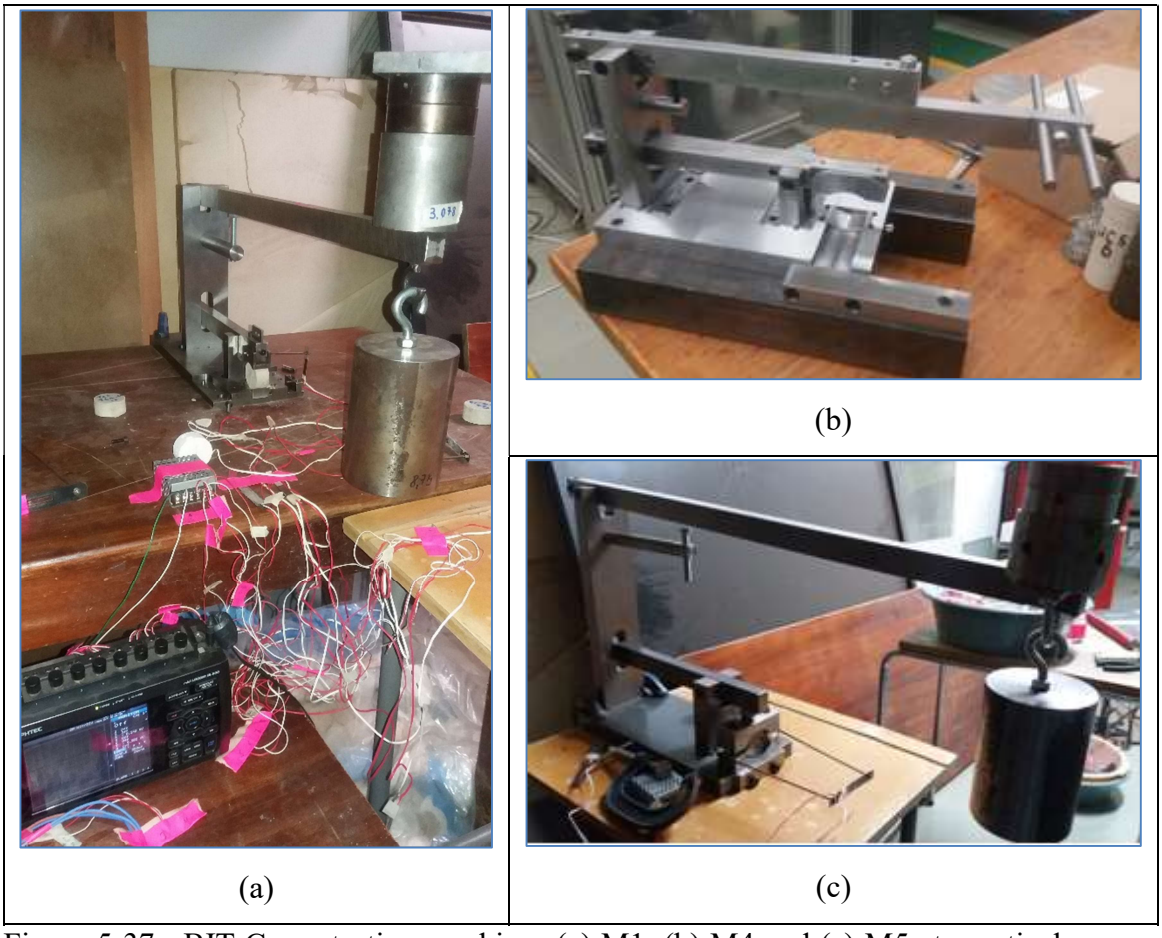


Figure 5-36 BIT creep testing machine M4

Practically, the finished products of all three BIT creep testing machines suffered few modifications as illustrated in Figures 5-37 (a), 5-37 (b) and 5-37 (c), which correspond respectively to M1, M4 and M5 finished-machines.



(a) (b) (c)

Figure 5-37 BIT Creep testing machines (a) M1, (b) M4 and (c) M5 at practical state

Unlike the UTS creep testing machine that only possesses one lever, this equipment needed a coupling of two arms (levers) since the specimens that are to be trialled here were expected to break at significantly higher failure loads than for UTS specimens. And the load factor from the onset point to the on-specimen point was assessed. Although Mechanics principles could be applied, they were not the adopted method since the effect of each machine part such as load, resistance in the joints, etc. needed to be well established. Instead, the load factor was determined as suggested in the case of UTS design by calibrating the overall creep testing machine weighing.

Calibration of Brazilian creep testing machines

The aim in this section is to establish, with the highest possible accuracy, the values of the dead weight and load factor. The available creep measuring devices were data-loggers (Graphtec midi Logger GL220 and Graphtec midi Logger GL 800), which provided the weight readings in mV. And the conversion from the data logger readings (mV) into the standard weight unit (kilogram) was based on the linear proportionality between these units obtained through the load cell type S calibration established in paragraph 5.2. The weighing characteristics of the three BIT creep testing machines that were manufactured are presented as follows:

a. Dead weight and weight factor of the Brazilian creep testing machine “M1”

The load cell type S was attached to the first BIT creep testing machine, M1, at the point where the specimen should be loaded. Incremental loadings were added on the onset of the machine and every reading was recorded. The plotting of this data provided a linear equation presented in Figure 5-38.

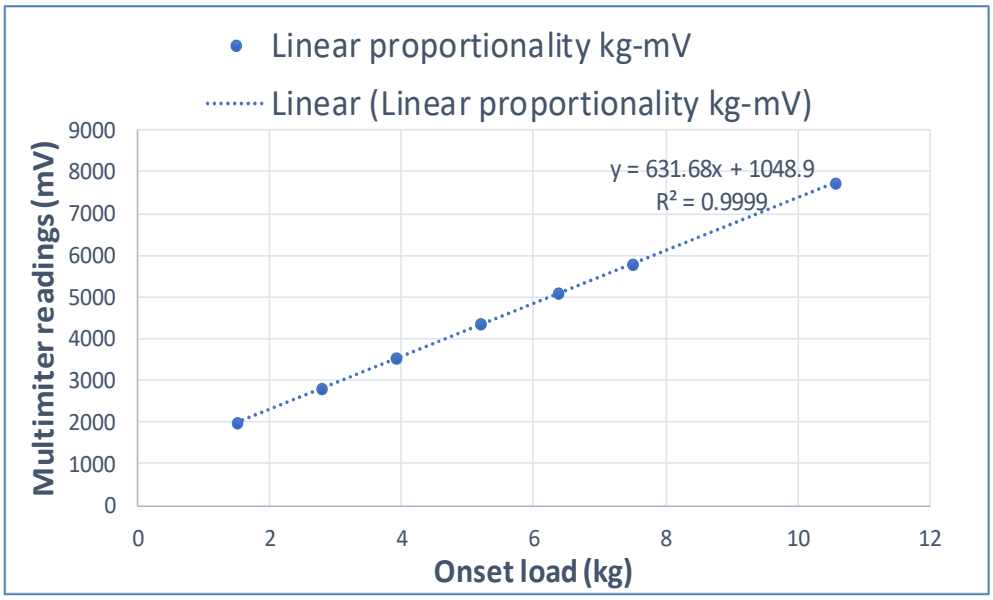


Figure 5-38 Proportionality between onset loads in kg and output mV for BIT creep testing machine M1

From the established proportionality, the ordinates were converted from millivolt readings into kilograms based on equation XXI. This resulted in the establishment of the equation shown in Figure 5-39, which provides the load factor and the dead weight of the machine.

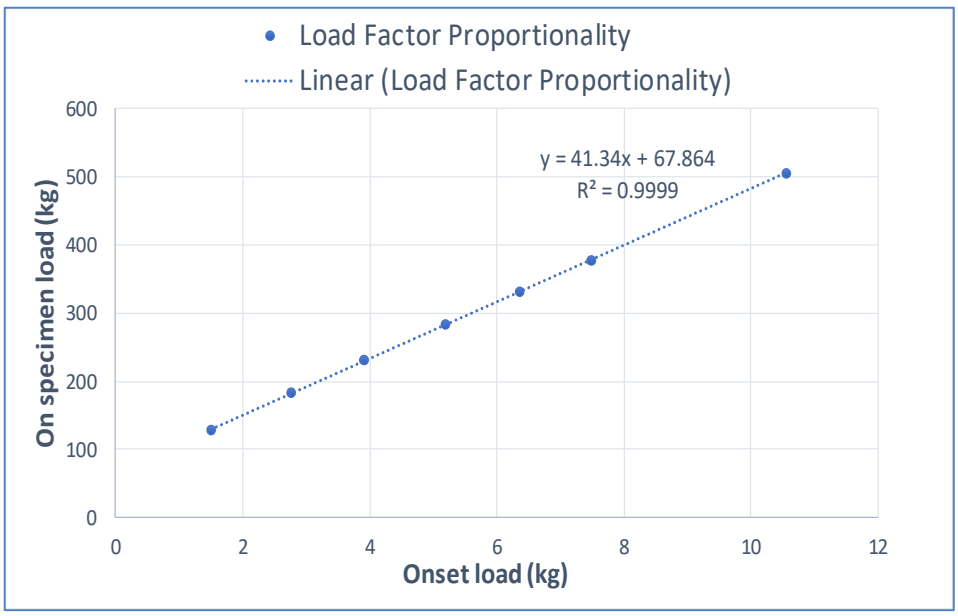


Figure 5-39 Load Factor and dead weight determination for BIT creep testing machine M1

The weighting parameters that were needed to undertake the loading of the creep testing machine M1 were extracted from the previous figure and are presented in Table 5-5.

Table 5-5 Weighing parameters of BIT creep testing machine M1

Parameter	Values	Units
Load factor (F)	41.34	
Dead Weight	67.86	kg

b. Dead weight and weight factor of the Brazilian creep testing machine "M4"

The process undertaken for the establishment of the dead weight and weight factor for the creep machine M1 was followed for M4. The resulting equation for the conversion of onset loading (kg) into on-specimen reading (mv) is presented in Figure 5-40.

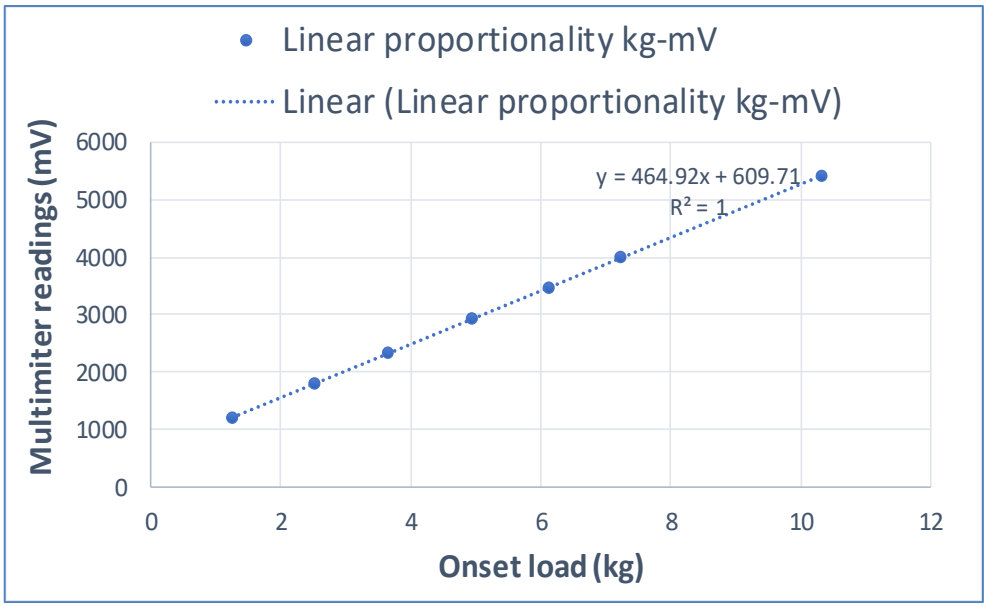


Figure 5-40 Proportionality between onset loads in kg and output mV for BIT creep testing machine M4

Similarly to the procedure in the previous section, the equation that provided the weight factor and the dead weight was established and is presented in Figure 5-41.

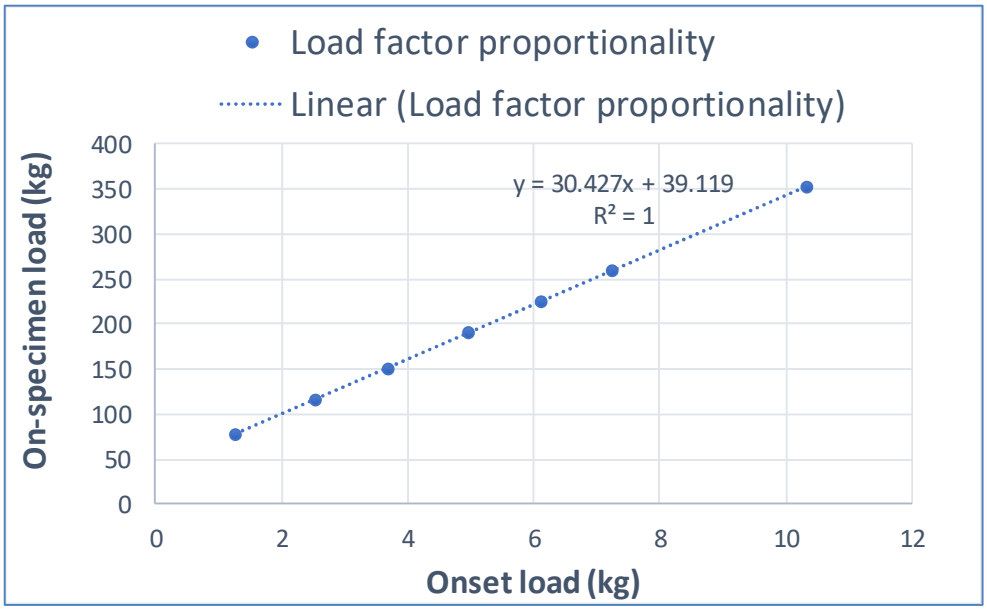


Figure 5-41 Load Factor and dead weight determination for BIT creep testing machine M4

Weighing parameters extracted from the previous figure are presented in Table 5-6.

Table 5-6 Weighing parameters of BIT creep testing machine M4

Parameter	Values	Units
Load factor (F)	30.427	
Dead Weight	39.12	kg

c. Dead weight and weight factor of the Brazilian creep testing machine "M5"

The procedure for the determination of the dead weight and weight factor for M5 provided the equations displayed in the following Figures 5-42 and 5-43.

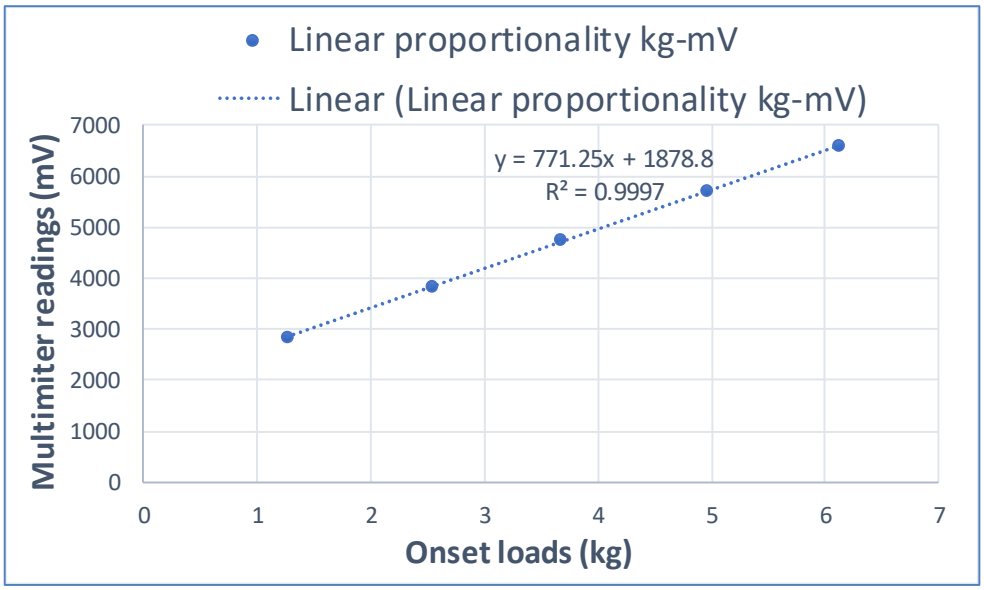


Figure 5-42 Proportionality between onset loads in kg and output mV for BIT creep testing machine M5

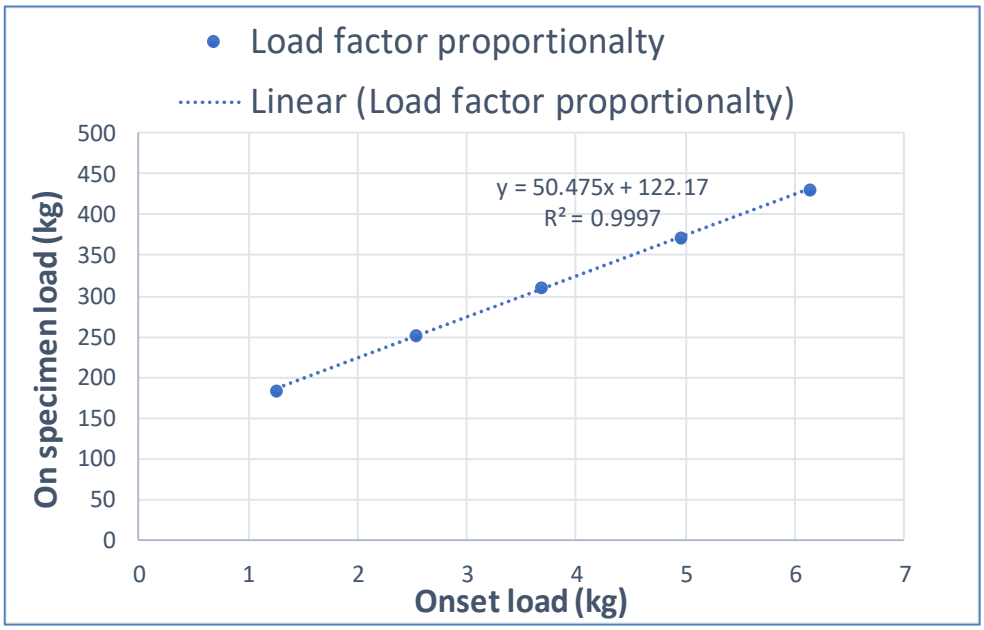


Figure 5-43 Load Factor and dead weight determination for BIT creep testing machine M5

Following the same procedure as in the previous sections, the weighing parameters for the creep testing machine M5 were obtained, and are shown in Table 5-7.

Table 5-7 Weighing parameters of BIT creep testing machine M5

Parameter	Values	Units
Load factor (F)	50.475	
Dead Weight	122.17	kg

Set up of displacement transducer

a. Design of the displacement transducer

Although the main task in creep testing was to record the time-dependency of specimens' failure for various static loads, this research also looked at the elongation behaviour of the coated BIT specimens. The aim was to understand the failure behaviour of coated shotcrete and to evaluate the influence of TSLs to oppose or delay the failure of such materials. A comparative study between the elongations at failure of the specimens tested at long-term and short-term conditions could also be performed. Thus this aspect brought in the use of a small device operating as a displacement transducer, as displayed in the following Figure 5-44.

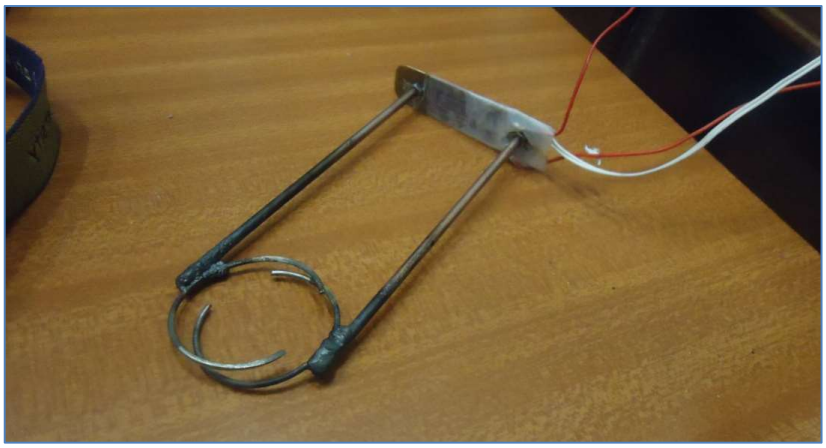


Figure 5-44 Displacement transducer for BIT specimens

The gripping of a BIT specimen was preferred to gluing of strain gauges onto the specimen for the reasons explained in section 2.12. In practice, this displacement transducer was attached to the specimen as shown in Figure 5-45, and the whole set

was placed in the testing machine. For the sake of recording very small displacements, a Wheatstone bridge configuration was used. The configuration of the employed bridge is similar to that which was earlier displayed in Figure 3-21, with two active strain gauges being centrally glued on both sides of the displacement transducer.

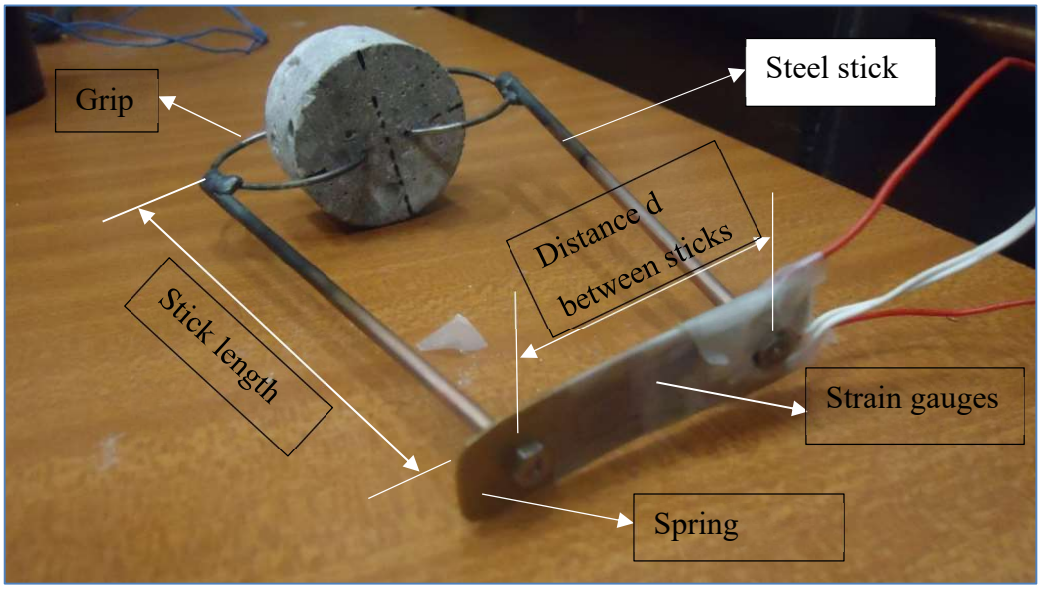


Figure 5-45 Gripping of the BIT displacement transducer to a shotcrete disc

As displayed in the previous figure, care was taken to ensure that the two grips holding the specimens were equally-distant from the centre and on a horizontal line of the specimen. They were also separated by a one-centimetre gap. The inactive gauges were centrally glued on the dummy made of the same type of spring material as the transducer for temperature compensation purposes (see Figure 5-46).



Figure 5-46 Displacement transducer's dummy

This dummy was incorporated in the Wheatstone bridge that included the active displacement transducer, a power supply, and a data-logger working as an output voltage, as it was earlier presented in Figure 3-21.

b. Calibration of the displacement transducer for BIT creep testing machines

Before their utilization, there was a need to calibrate and validate the BIT displacement transducers of M1, M4 and M5 for BIT creep tests. Various trials were performed, wherein the grips of the transducers were distanced one from another. Every distance was measured through a vernier caliper, and the output voltages were read from the data logger. The resulting linear functions displayed in Figures 5-47, 5-48 and 5-49 provided values of the coefficients of determination very close to unity, which is a validation of the accuracy of the readings.

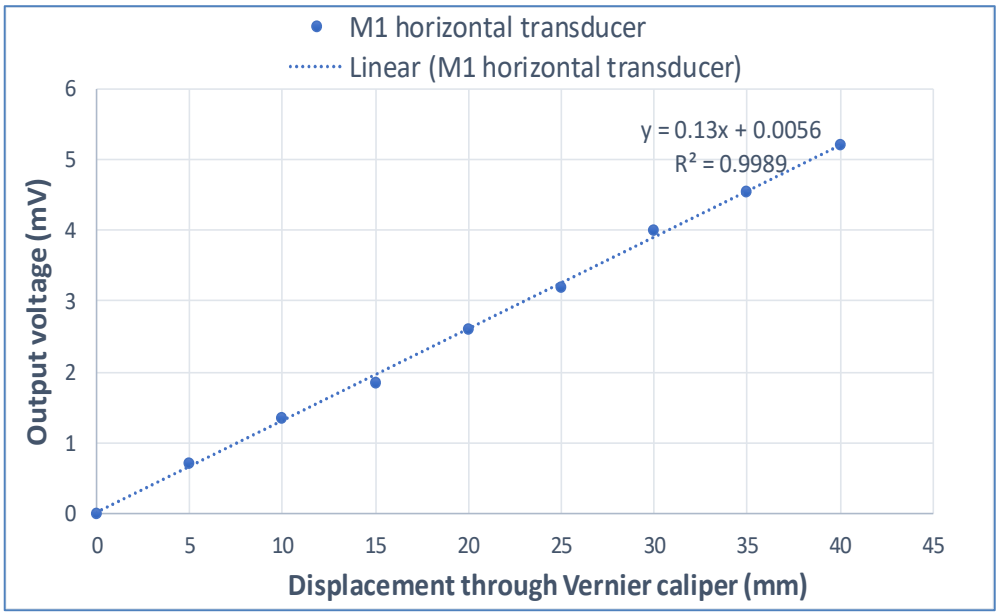


Figure 5-47 Relationship between horizontal displacements of M1 transducer's grips and output voltages

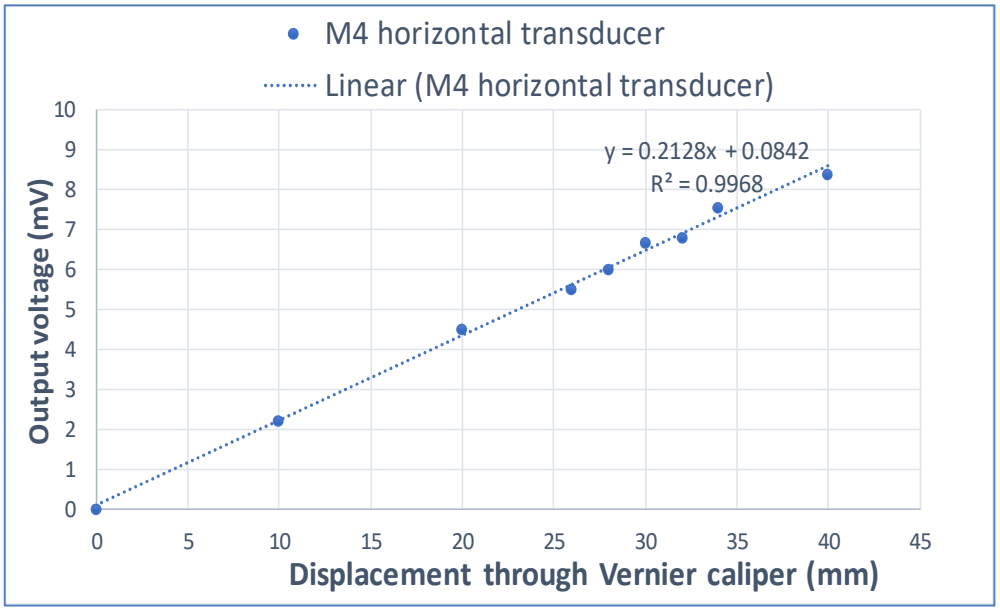


Figure 5-48 Relationship between horizontal displacements of M4 transducer's grips and output voltages

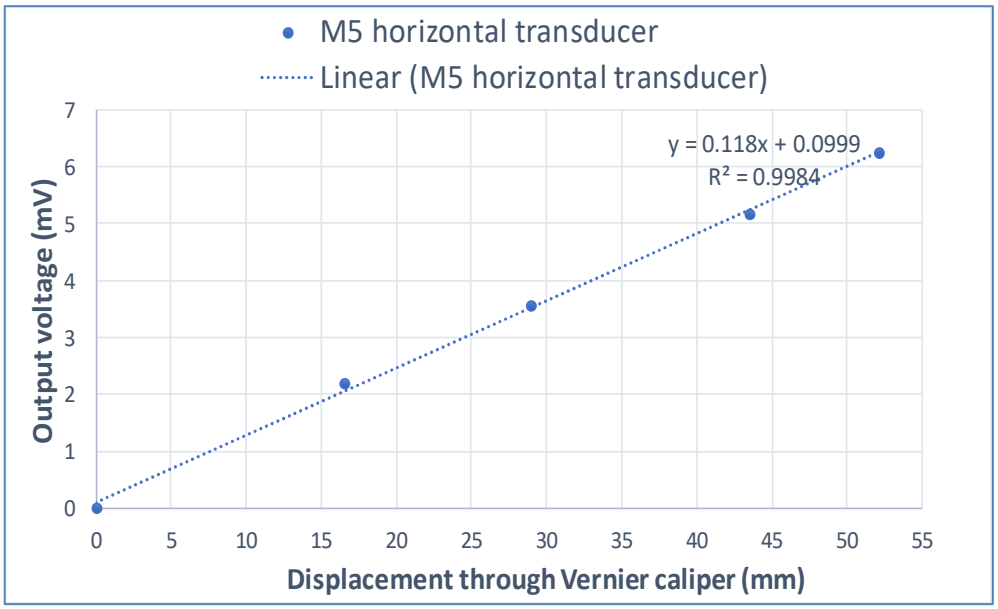


Figure 5-49 Relationship between horizontal displacements of M5 transducer's grips and output voltages

It was made sure that this process was frequently repeated to assess whether the strain gauges suffered any fatigue effect, thus requiring their replacement. But since the failure from the BIT tests was not accompanied by large cracks or the splitting of the specimens, there was no need for replacing the transducers.

And the determination of the specimens' displacements was made through the conversion of the recorded voltages from the data loggers, into metric units. The graphs showing the conversions of the voltages into millimetres are displayed in APPENDIX F. The linear equations provided by those graphs are presented in Table 5-8.

Table 5-8 Converting equations of voltage outputs into specimen displacements for BIT creep testing machines

Displacement transducer	**Converting equations from millivolts to millimetres**
M1 horizontal displacement	x = 7.6841y - 0.0212
M4 horizontal displacement	x = 4.6843y - 0.3154
M5 horizontal displacement	x = 8.461y - 0.8011

Where,

x: Resulting practical displacement in the specimen, in millimetres

y: Data logger recorded voltage values, in millivolts

The gripping of the displacement transducers to the BIT specimens was done in a way that the initial distance between the grips was kept constant for all the tests and equal to 14 mm.

Determination of onset creep weights

For every creep test, there was a need to determine the onset weight once the percentage loading was chosen. This was calculated only after having determined the on-specimen load. Therefore, the on-specimen load was deduced from the equation of determination of the BIT strength as follows:

$$P = \frac{\sigma_t.t.d}{0.6369} \qquad \text{(XXV)}$$

Where,

P: on-specimen load (N)

σ_t: Expected BIT creep strength (MPa)

t: Thickness of shotcrete disc without accounting the coating thickness (mm)

d: Diameter of the BIT specimen (mm)

After the determination of the on-specimen load, the onset weight to be applied on the creep machine load arm was calculated through extraction from the

corresponding equations of proportionality between the load factor and dead weight. This resulted in the following equation:

$$m = \frac{\left(\frac{P}{9.81} - w'\right)}{F} \qquad \text{(XXVI)}$$

Where,

m: onset weight (kg)

P: on-specimen load (N)

w': the dead weight of the creep machine (kg)

F: load factor

5.4.4 Results of short-term BIT tests

Samples of the tested BIT specimens are presented in Figure 5-50.



(a) (b) (c)

Figure 5-50 Samples of tested specimens of (a) uncoated shotcrete, (b) TSLs, and (c) coated shotcrete discs

Only the results from specimens that failed along the vertical diameter were considered. Since shotcrete panels were supplied more than 40 days after their preparation, the assessment of shotcrete strengthening trends could not be performed for earlier curing periods. Besides, rather than assessing the shotcrete intrinsic strength behaviour, the current study is focussed on determining its mechanical behaviour as a substrate. Knowing this, shotcrete discs were only tested

from about 100 days after their supply and showed an almost constant BIT strength of about 5.2 MPa in room conditions. This value was considered as representative for shotcrete BIT strengths in room environmental condition. For shotcrete assessed under H and HT conditions, only the time of exposure to those environmental conditions mattered.

Influence of the environmental conditions on uncoated shotcrete discs

The obtained results of uncoated shotcrete discs behaviour to environmental conditions are displayed in Figure 5-51.

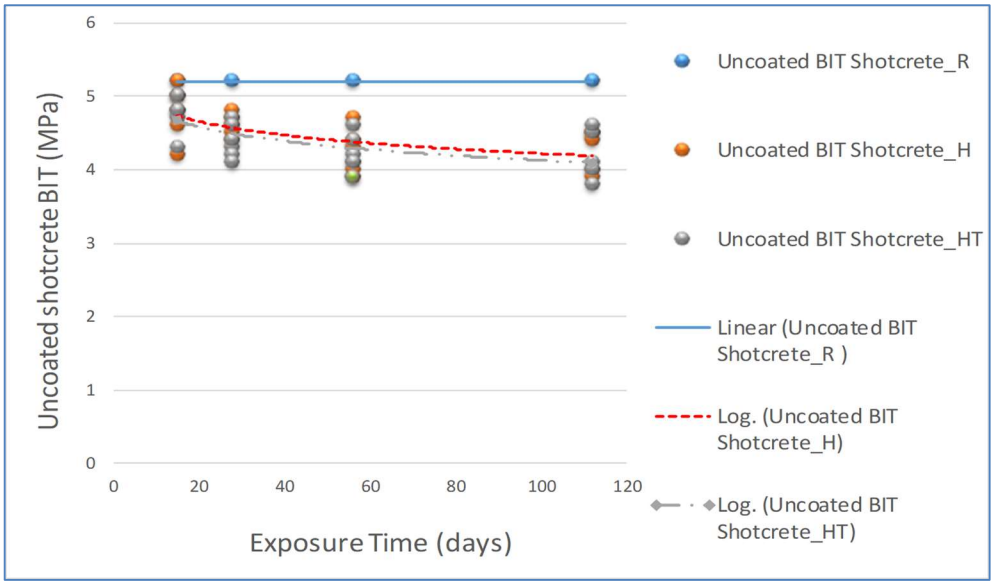


Figure 5-51 Uncoated shotcrete discs sensitivity to environmental conditions

Figure 5-51 shows that H and HT conditions negatively influence the uncoated shotcrete BIT strength. However, although it was expected that H condition would contribute to strengthening this liner since it is a Wetcrete, this was not the case when it was cured in saturated conditions. One of the reasons might be linked to the friability of shotcrete observed during the coring of specimens. The discs were shaped through the means of a diamond drilling machine. And during the process, tap water was supplied to lubricate and cool down the cutting operation. And as a result of water usage, a significant quantity of mud was produced. This liner therefore behaved as a mud-rock.

Besides the uncoated shotcrete behaviour, the knowledge of TSL BIT behaviour proved to be necessary.

Influence of the environmental conditions on TSL disc specimens

The understanding of TSL BIT behaviour can be fulfilled through the results displayed in Figures 5-52, 5-53 and 5-54.

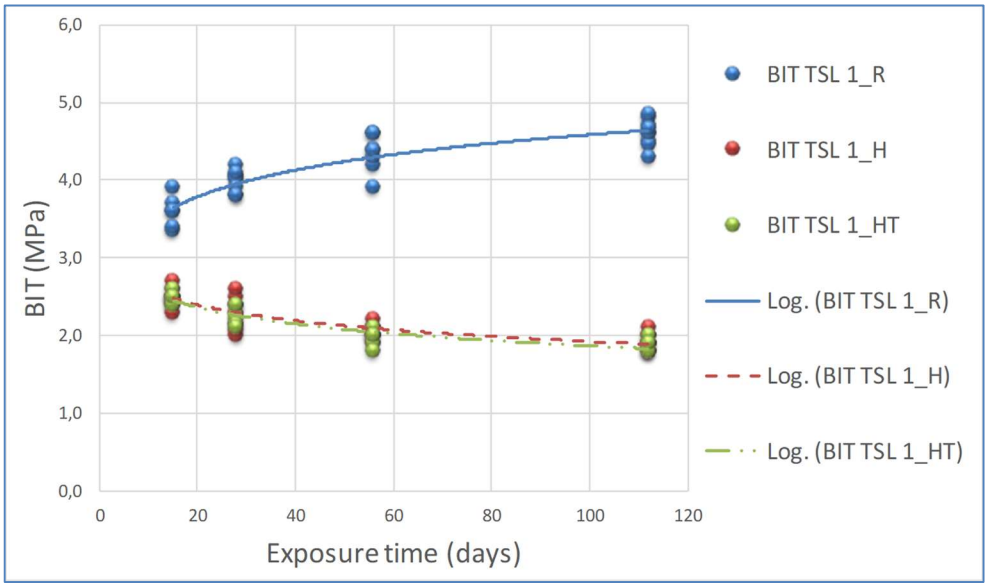


Figure 5-52 BIT strength sensitivity to environmental conditions for TSL1

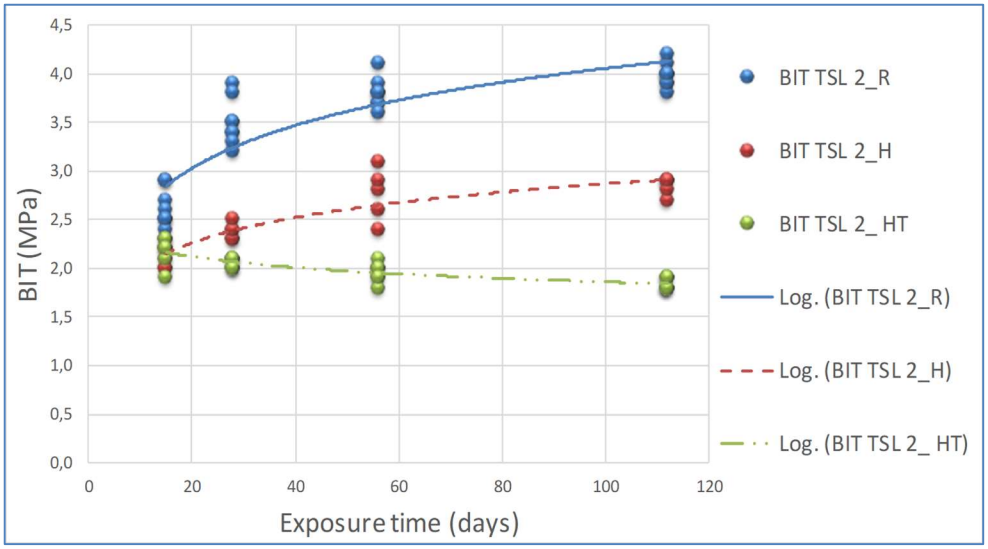


Figure 5-53 BIT strength sensitivity to environmental conditions for TSL2

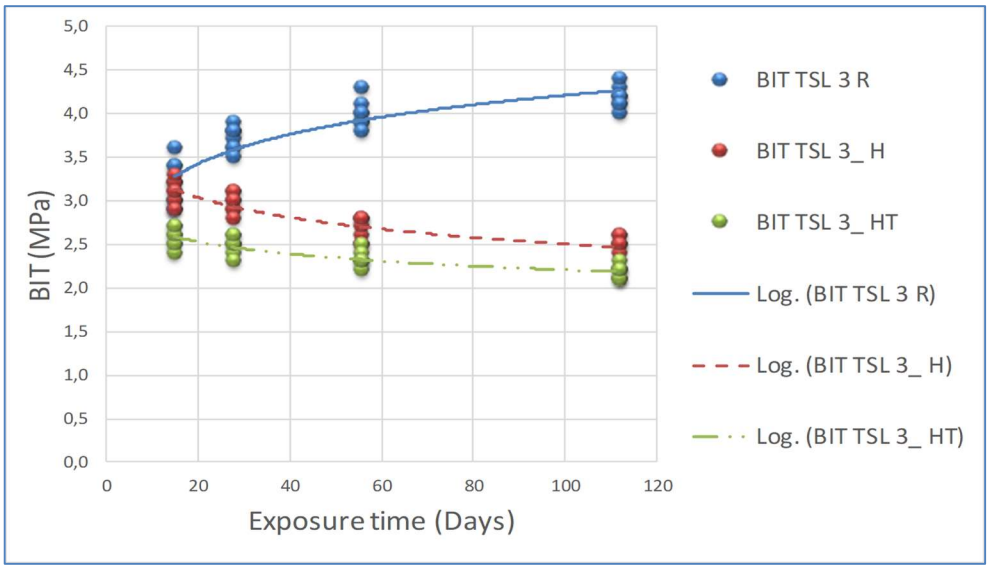


Figure 5-54 BIT strength sensitivity to environmental conditions for TSL3

Similar to UTS tests, TSL BIT strength increases over time after being stored in room conditions. However, TSL1 and TSL3 show a loss of BIT strength proportionally to the exposure time in saturated condition, while TSL2 BIT still strengthens throughout the time in the same environmental condition. Therefore TSL2, which is a water-based thin liner, should be the most effective liner to be used in underground saturated-like conditions with moderated temperature than the thin liners with properties closer to TSL1 and TSL3. And when HT condition is concerned, TSL generally underperforms. This might be a concern behind the use of TSLs in deep and ultra-deep underground mines where humidity and temperature are significantly high. But rather than investigating isolated TSL BIT behaviours, coated shotcrete with TSL should produce a closer behaviour to underground coated walls.

Influence of the environmental conditions on coated BIT specimens

The results displaying the behaviours of coated disc specimens tested to indirect tensile mechanisms are presented and analysed in this section. The impacts of each of the three TSLs on the substrate's overall strength are then compared. Table 5-9 presents the averages and coefficients of variation of uncoated and coated shotcrete

discs for different environmental conditions. More information on these specimens' statistics and periods of exposure can be found in APPENDIX I.

Table 5-9 Statistics of representative BIT strengths for specimens exposed in room, humid, and humidity and high temperature conditions

Type of specimens	Statistics	R		H		HT	
		15d	112d	15d	112d	15d	112d
Uncoated BIT	Mean (MPa)	5.2	5.2	4.76	4.26	4.77	4.22
	CoV	10%	10%	8%	7%	5%	7%
TSL1 Coated BIT	Mean (MPa)	5.38	6.30	5.38	5.00	5.40	4.38
	CoV	6%	5%	7%	6%	8%	8%
TSL2 Coated BIT	Mean (MPa)	5.28	5.66	5.35	5.25	5.07	4.60
	CoV	7%	8%	5%	7%	3%	10%
TSL3 Coated BIT	Mean (MPa)	5.59	6.07	5.43	5.03	5.40	4.98
	CoV	8%	6%	6%	8%	6%	6%

And Figure 5-55 presents the results obtained from testing substrates coated with TSL1.

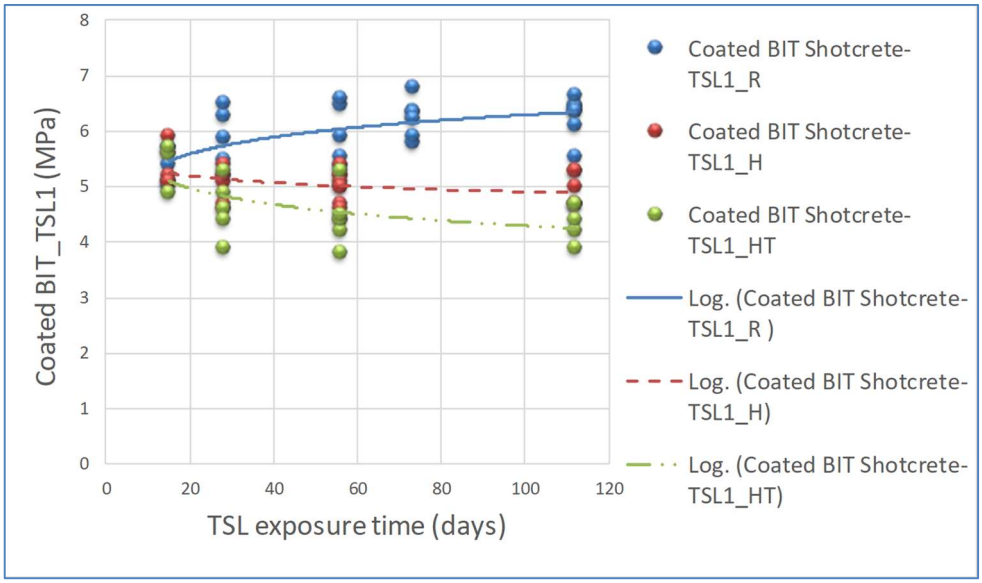


Figure 5-55 Coated BIT shotcrete sensitivity to environmental conditions for TSL1

From this figure, BIT specimens coated with TSL1 show strength increase over room exposure time, whereas there is a slight decrease of BIT strength observed when the specimens have been conserved in saturated conditions for periods up to 112 days. The strength decrease rate is even more significant in HT conditions. However, the observed strength rates are not only related to the coating performances in the various environmental conditions; the substrate is also affected by these environmental conditions.

To assess the sole impact of TSL1 on the overall specimen strength, Figure 5-56 is brought in. It displays the BIT strengths of uncoated and coated shotcrete, and the strength increase that is only due to TSL1. These BIT strengths correspond to the strength averages presented in APPENDIX I, except for the average BIT strength of uncoated shotcrete that was kept constant for room condition, as explained earlier.

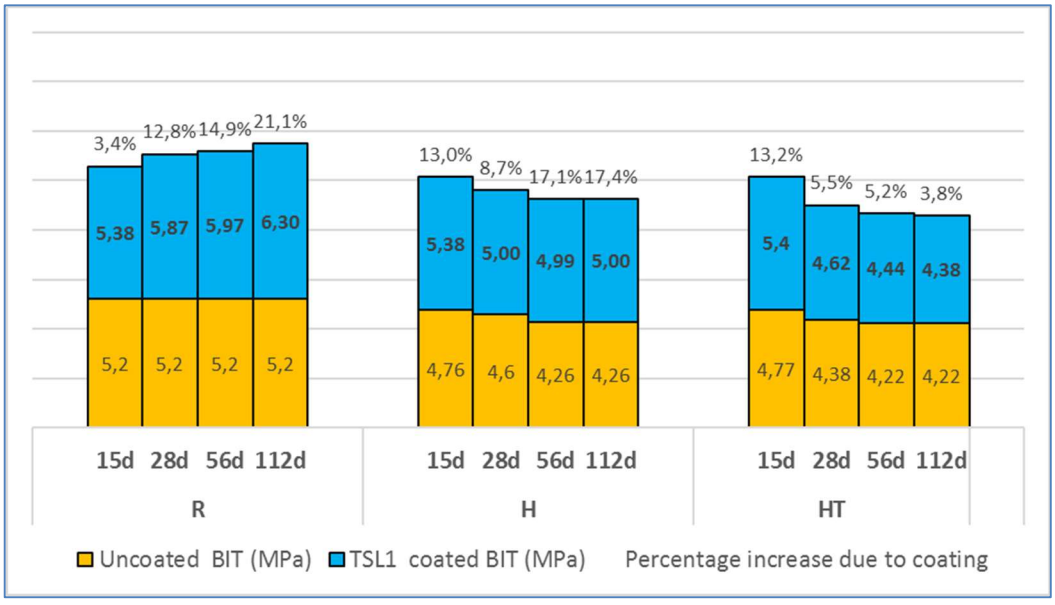


Figure 5-56 Enhancing strength effect of TSL1 on shotcrete BIT substrates in various environmental conditions

Figure 5-56 highlights that TSL1 contributes to strengthening shotcrete, independently of the environmental conditions. The strengthening rate is positive in room condition, characterized by a strength increment of 21.1% after 112 days

of exposure. Contrary to the overall coated specimen negative strength rate, TSL1 positively contributes to improving the coated specimen's strength in saturated condition. The thin liner's strengthening rate is also positive, reaching 17.4% of strength increase after 112 days of exposure. In HT condition, the declining strength rate is much bigger than in the previous condition, with the final strength increment of only 3.8% after 112 days. Therefore, there is no doubt that TSL1 should be effective to support underground mines' walls prone to extension cracks, located in environmental conditions close to room environmental conditions and of which surface is thoroughly cleaned prior to the thin liner application.

The results obtained from BIT shotcrete coated with TSL2 are characterized by the overall strengthening rates presented in Figure 5-57.

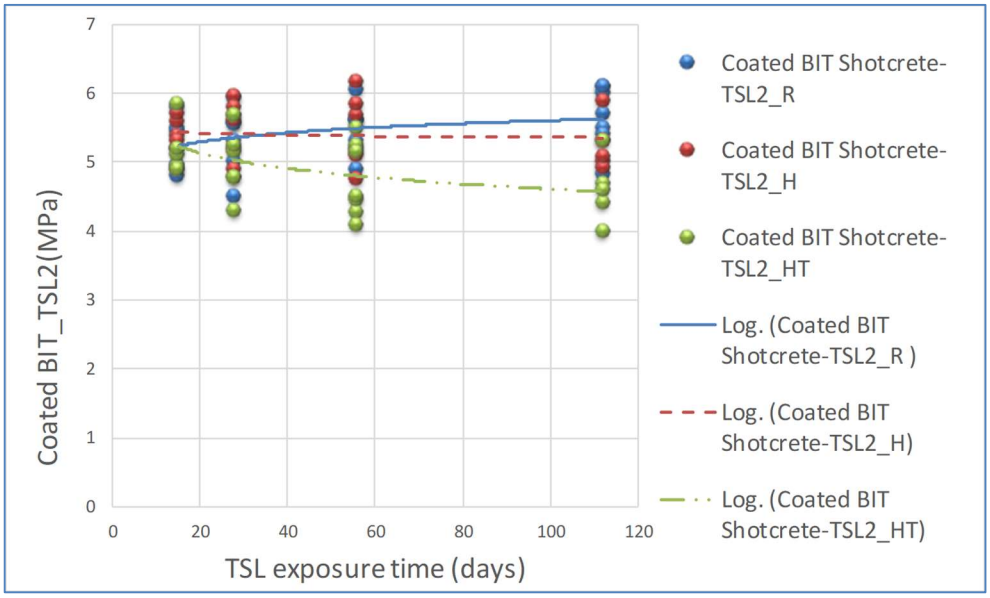


Figure 5-57 Coated BIT shotcrete sensitivity to environmental conditions for TSL2

From Figure 5-57, the strength of BIT shotcrete coated with TSL2 is increasing over exposure time in room conditions. The tendency is almost steady, with a very slight decline in saturated conditions. But in HT conditions, the decline is noted. The contribution of TSL2 in the strengthening or weakening of coated specimens exposed to various environmental conditions is distinctive in Figure 5-58.

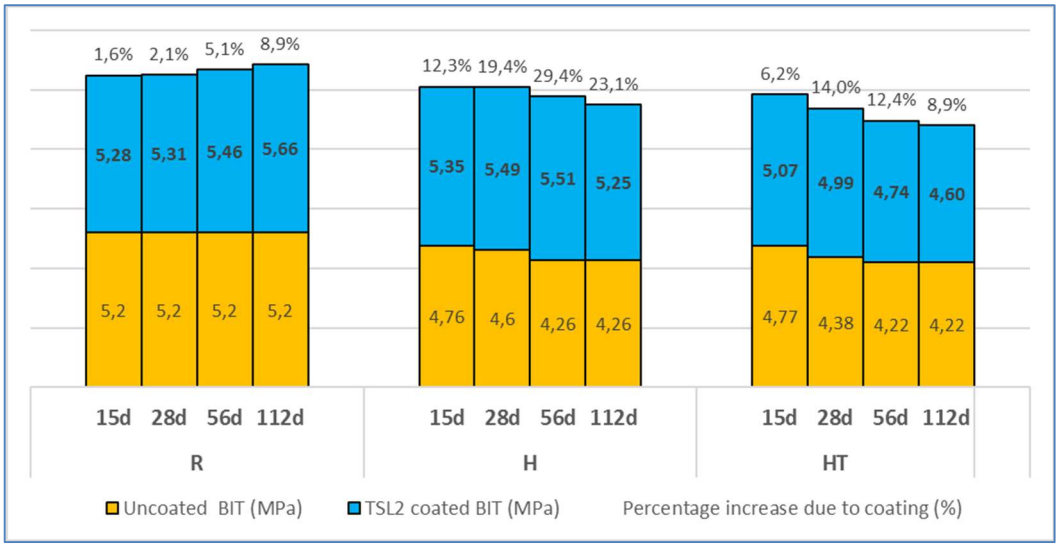


Figure 5-58 Enhancing strength effect of TSL2 on shotcrete BIT substrates in various environmental conditions

The strengthening trends provided by TSL2 are as follows: a positive strengthening rate in room condition, though significantly lower than of TSL1, with the strength increase reaching its peak (8.9%) after 112 days. In high humidity condition, the rate is still positive, with TSL2 enhancing the coated specimen's strength up to 23.1% after 112 days. However, in HT condition, the general trend of strength-increment shifts to negative; the final strength-increment value recorded after 112 days of exposure being of 8.9%. Therefore, TSL2 emerges as a potential reliable thin liner to be resorted to in underground mines characterized by high humidity condition but relatively low temperature neighbouring the room environmental temperature. This liner's capability to offer high resistance to the combined shear and tensile mechanisms could partially, if not totally, be justified by the liner being hydrophilic since it is a water-based material.

The assessment of the strengthening capability for TSL3 has produced the results presented in Figure 5-59.

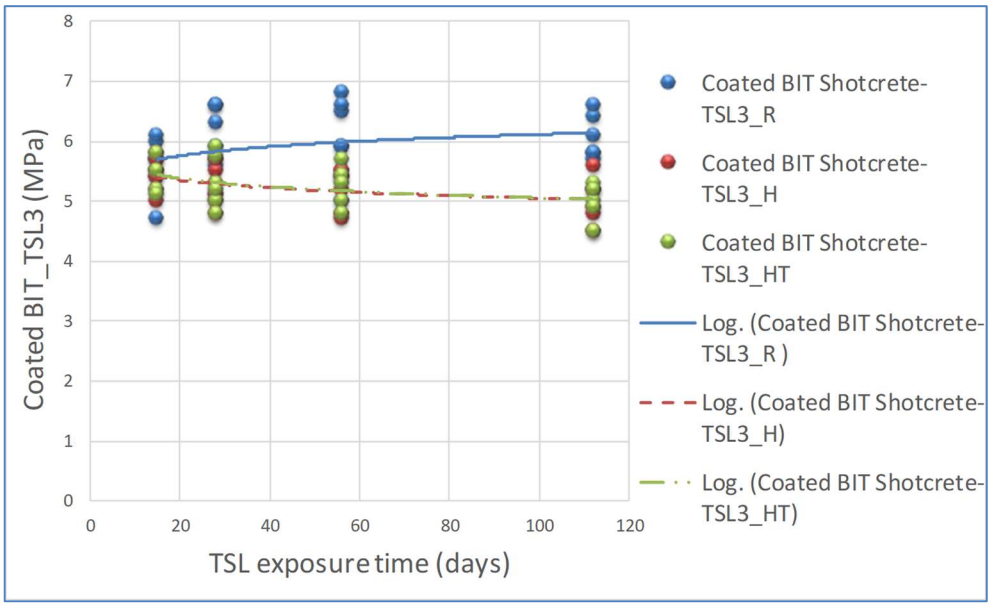


Figure 5-59 Coated BIT shotcrete sensitivity to environmental conditions for TSL3

Shotcrete strength increases over time if coated with thin liners with properties like TSL3, and stored in room environmental condition. The overall trend shifts to a decline of strength if the same specimen is stored over a significant amount of time in H and HT conditions. The strength's impact of TSL3 on coated shotcrete is elucidated through Figure 5-60.

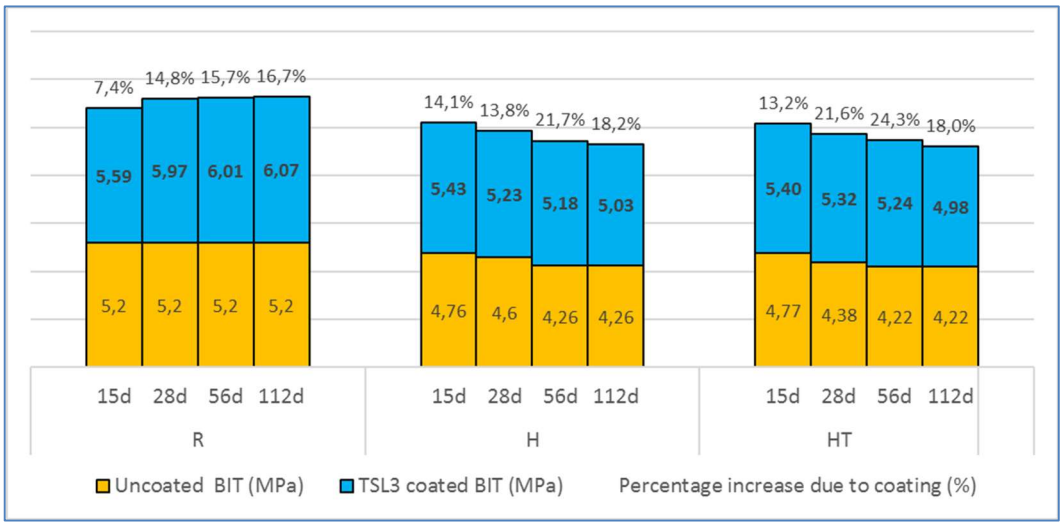


Figure 5-60 Enhancing strength effect of TSL3 on shotcrete BIT substrates in various environmental conditions

Figure 5-60 shows that if there is an increase of strength gain proportionally to the time of exposure for shotcrete specimens coated with TSL3 in room condition, the strengthening trend of TSL3 in H and HT conditions is not clearly defined. In these conditions, the results are inconclusive, though with a slight tendency to decrease. However, in HT condition, TSL3 contributes to strengthening the substrate by 18%, which is at least double that offered by the second-best performing coating in HT condition, namely the water-based TSL. It is worth stating that, out of the three tested TSLs, TSL3 is the most appropriate coating for walls in deep and ultra-deep mines, where the environmental conditions are closer to HT condition.

As stipulated by Guner and Ozturk (2016b), the characterization of a thin coating material should not only be based on its capability to support as much stress as possible before failure but also and mostly on its capability to offer a greater elongation. In effect, these parameters should be optimally chosen. Figures **5-61**, **5-62** and **5-63** display the results of TSLs' BIT strengths versus the maximum vertical displacement at break. This vertical displacement is believed to be proportional to that happening in the direction of crack development.

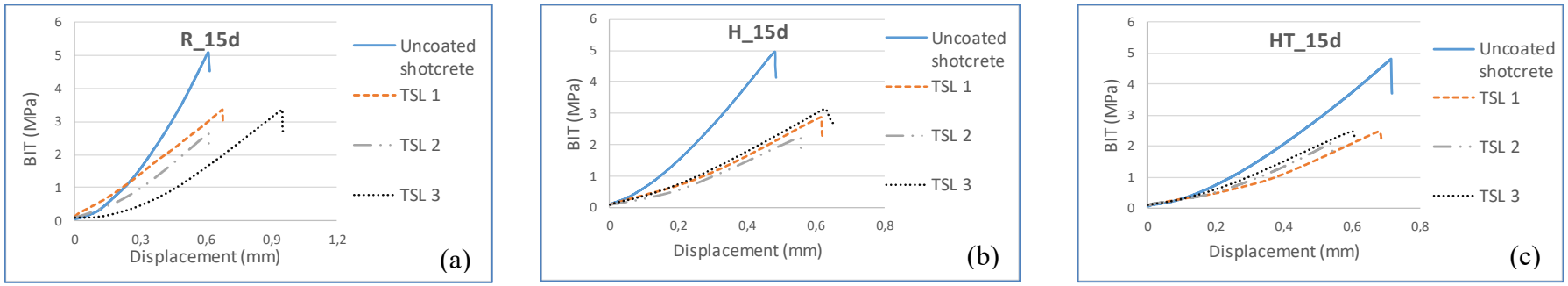


Figure 5-61 Comparisons of vertical displacements of shotcrete and TSL's BIT after 15 days of exposure in (a) Room, (b) Saturated and (c) HT conditions.

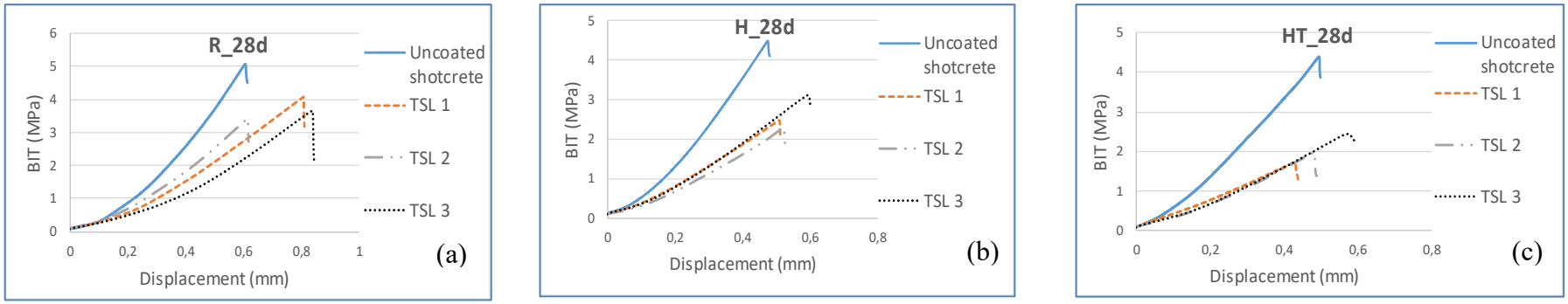


Figure 5-62 Comparisons of vertical displacements of shotcrete and TSL's BIT after 28 days of exposure in (a) Room, (b) Saturated and (c) HT conditions

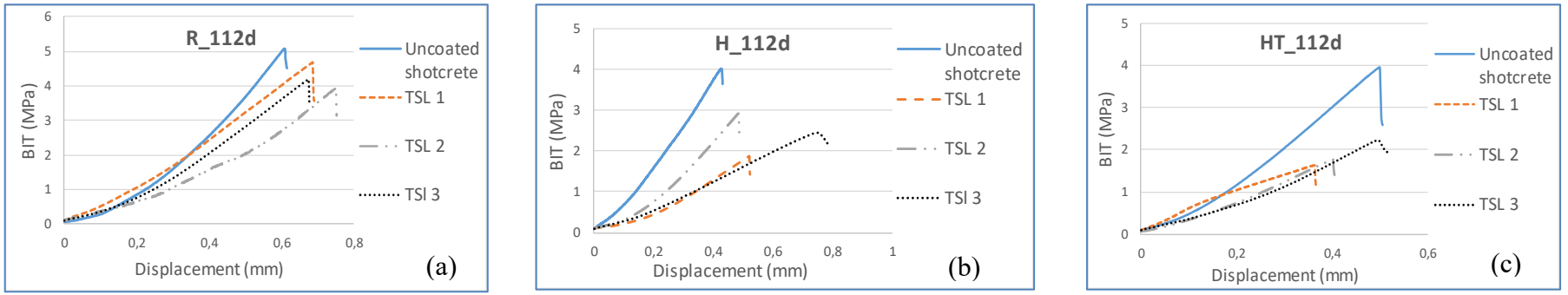


Figure 5-63 Comparisons of vertical displacements of shotcrete and TSL's BIT after 112 days of exposure in (a) Room, (b) Saturated and (c) HT conditions

The general trends show that TSL3 generally offers greater elongation than the other two. TSL1 is the second-best thin liner for this characteristic. The common characteristic of these two thin liners is that the mixture is prepared with the addition of a polymer fluid supplied as a binder by the manufacturer. The water-based liner, TSL2, is generally characterized by smaller elongations. Finally, for long-term assessment, the graphs in the previous Figures **5-61**, **5-62** and **5-63** confirm the suggestions of opting for TSL1 for room conditions, TSL2 for underground walls where the environmental conditions are like H conditions, and TSL3 for underground walls located in the environments similar to HT conditions. Details of the combinations of TSLs' BIT strengths and elongation values are presented in APPENDIX J.

Summary of BIT short-term test results

The coating of TSL on shotcrete, represented through Figures 5-56, 5-58 and 5-60, has shown that the overall BIT strength increases with time of exposure in room conditions. However, this overall strength decreases in H and HT conditions, except for the water-based TSL that still showed strength increment over time in H conditions. Since shotcrete discs were sensitive to environmental conditions, sole assessments of TSL impacts on coated BIT were undertaken and have resulted in TSL1 showing the greatest strength increase (21.1%) in R conditions. TSL2 proved to be the most efficient coating in offering the optimal BIT strength in H conditions, with 23.1% of strength increase. And TSL3, although not providing a distinctive trend of strength increment in HT conditions, remained the most efficient thin liner out of the three selected with 18% of strength improvement of the substrate after 112 days. These findings alone could not be the unique indicators in the choice of an optimal coating since they only relied on the liners' capacity of resistance to indirect tensile driving stresses. Another factor that needed to be considered is the liners' elongation. This factor, combined with TSL's BIT strength, was targeted in the choice of a better TSL. The TSLs mixed with the polymeric binder offered greater elongations than that mixed with water, but in sum, the optimal results confirmed and validated the choices done based on the liners' BIT strengths.

5.4.5 **Results of long-term tests**

From the tested long-term BIT specimens, only those that failed vertically along the diameter were considered valid. An illustration of a coated shotcrete that failed under creep loading is shown in Figure 5-64.



Figure 5-64 Failure shape of a coated shotcrete under creep loading

This particular testing method was very time consuming as compared to the UTS long-term testing method. And this was the main reason behind the making of three BIT creep machines instead of one. Another particularity of this creep method concerned the record of displacement until failure occurrence. Actually, unlike the UTS creep displacements of TSL that could be monitored, the BIT creep strains were constant from the initial point for almost the whole testing period until a sudden increase was observed at the time of failure, as illustrated in Figure 5-65.

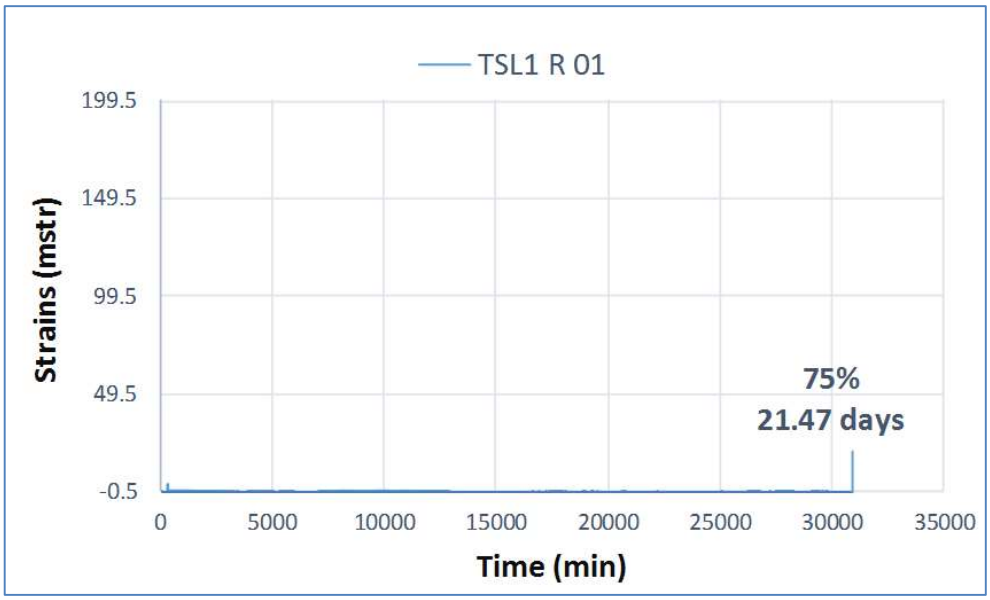


Figure 5-65 Creep behaviour of BIT coated shotcrete with TSL1 tested in room condition at 75% of the ultimate load

This figure does not provide information on the displacement behaviour of a BIT coated specimen that is under creep loading. It only allows the finding of the exact failure time. And for this reason, additional strain-failure time curves were not provided. Instead, it was opted to elaborate on the data related to the creep tests.

Determination of 100% creep strengths for coated shotcrete tested in room and humid conditions

Similar to the explanation provided for UTS creep tests, the BIT creep tests required prior knowledge of the onset weight that could equal the ultimate strength value. This was determined for both the room and the humid conditions as illustrated in Tables 5-10 and 5-11, respectively.

Table 5-10 Determination of average 100% creep strength for shotcrete coated with TSL1 and tested in room condition on the BIT creep testing machine "M1" (SCLT_R: S-shotcrete, C-coated, LT-long-term, R-room condition)

Item number	TSL Name	Environmental Condition	Exposure time (days)	Thickness (mm)	Diameter (mm)	Onset 100% weight (kg)	Expected 100% on-specimen Load (N)	Expected 100% Strength (MPa)	Percentage creep Strength (%)
1	**SCLT_R 01**	**Room**	80	21.5	41.9	21.4	9344.38	6.61	100
2	**SCLT_R 02**	**Room**	80	21.5	42	19.5	8573.84	6.05	100
3	**SCLT_R 03**	**Room**	80	21.5	41.9	21.4	9344.38	6.61	100
4	**SCLT_R 04**	**Room**	80	21.5	41.9	20.5	8979.39	6.35	100
5	**SCLT_R 05**	**Room**	80	21.5	42	19.8	8695.51	6.13	100
6	**SCLT_R 06**	**Room**	80	21.5	42.1	21.1	9222.72	6.49	100
7	**Averages**		***80***	***21.5***	***41.97***	***20.6***	***9026.70***	***6.37***	***100***

Table 5-11 Determination of average 100% creep strength for shotcrete coated with TSL1 and tested in humid condition on the BIT creep testing machine "M4" (SCLT_H: S-shotcrete, C-coated, LT-long-term, H-humid condition)

Item number	TSL Name	Environmental condition	Exposure time (days)	Thickness (mm)	Diameter (mm)	Onset 100% weight (kg)	Expected 100% on-specimen Load (N)	Expected 100% Strength (MPa)	Percentage Creep Strength (%)	Percentage in relation to R condition (%)
1	**SCLT_H 01**	**Humid**	80	21.6	41.6	21	6652.65	4.72	100	74.03
2	**SCLT_H 02**	**Humid**	80	21.7	41.6	21	6652.65	4.69	100	73.68
3	**SCLT_H 03**	**Humid**	80	21.6	41.9	20.5	6503.39	4.58	100	71.85
4	**SCLT_H 04**	**Humid**	80	21.6	42	21.2	6712.36	4.71	100	73.98
5	**SCLT_H 05**	**Humid**	80	21.1	41.8	22.1	6981.02	5.04	100	79.14
6	**Averages**		***80***	***21.52***	***41.78***	***21.16***	***6700.41***	***4.75***	***100***	***74.5***

Rather than focussing on the onset 100% creep weight, which could vary depending on the specimens' sizes, attention was directed to the averages of the ultimate strengths of the coated BIT specimens tested in room and humid conditions. These values are respectively 6.37MPa and 4.75MPa. Another parameter to bear in mind is the ratio of the humid BIT ultimate strength to the room BIT ultimate strength.

Its value is 74.5% and will constitute the starting point in the plotting of the long-term BIT strength trend in humid condition.

Influence of the environmental conditions on coated BIT specimens

19 additional BIT shotcrete specimens coated with TSL1 were prepared and tested on the creep machines. After choosing the percentage creep strengths, the onset weights were calculated and the resulting failure times of the creep tests were recorded for both the R and H conditions as presented in Tables 5-12 and 5-13, respectively.

Table 5-12 Recorded data from BIT creep tests on shotcrete specimens coated with TSL1 and exposed to room condition (N/A- Not available), (SCLT_R: S-shotcrete, C-coated, LT-long-term, R-room condition)

Item number	TSL Name	Environmental Condition	Exposure time (days)	Thickness (mm)	Diameter (mm)	Percentage creep Strength (%)	Expected creep Strength (MPa)	Expected on-specimen Load (N)	Onset weight (kg)	Time to Failure (min)
1	**SCLT_R 07**	**Room**	80	21.5	41.9	90	5.73	8108.92	18.4	6480
2	**SCLT_R 08**	**Room**	80	21.5	42	90	5.73	8128.28	18.4	5605
3	**SCLT_R 09**	**Room**	80	21.5	41.9	90	5.73	8108.92	18.4	9003
4	**SCLT_R 10**	**Room**	80	21.5	41.9	84	5.35	7568.33	17.0	12504
5	**SCLT_R 11**	**Room**	80	21.5	42	84	5.35	7586.39	17.1	11520
6	**SCLT_R 12**	**Room**	80	21.5	42.1	84	5.35	7604.45	17.1	10023
7	**SCLT_R 13**	**Room**	80	21.5	41.8	75	4.78	6741.31	15.0	36700
8	**SCLT_R 14**	**Room**	80	21.5	41.9	75	4.78	6757.44	15.0	34560
9	**SCLT_R 15**	**Room**	80	21.5	42	75	4.78	6773.56	15.1	31258
10	**SCLT_R 16**	**Room**	80	21.5	41.8	72	4.59	6471.66	14.3	47520
11	**SCLT_R 17**	**Room**	80	21.5	42.1	72	4.59	6518.10	14.4	50127
12	**SCLT_R 18**	**Room**	80	21.5	42.1	72	4.59	6518.10	14.4	44526
13	**SCLT_R 19**	**Room**	80	21.5	42	69	4.40	6231.69	13.7	N/A
14	**SCLT_R 20**	**Room**	80	21.5	41.8	69	4.40	6202.00	13.7	98828
15	**SCLT_R 21**	**Room**	80	21.5	41.9	69	4.40	6216.84	13.7	95042
16	**SCLT_R 22**	**Room**	80	21.5	41.9	68.4	4.36	6162.78	13.6	105120
17	**SCLT_R 23**	**Room**	80	21.5	41.7	68.4	4.36	6133.37	13.5	103259
18	**SCLT_R 24**	**Room**	80	21.5	41.5	68.4	4.36	6103.95	13.4	N/A
19	**SCLT_R 25**	**Room**	80	21.5	41.3	65	4.14	5772.58	12.6	N/A

Table 5-13 Recorded data from BIT creep tests on shotcrete specimens coated with TSL1 and exposed to humid condition (N/A- Not available), (SCLT_R: S-shotcrete, C-coated, LT-long-term, H-humid condition)

Item number	TSL Name	Environmental Condition	Exposure time (days)	Thickness (mm)	Diameter (mm)	Percentage creep Strength (%)	Expected creep Strength (MPa)	Expected on-specimen Load (N)	Onset weight (kg)	Time to Failure (min)
1	**SCLT_H 06**	**Humid**	80	21.5	42	66	4.20	5960.7	13.1	6369
2	**SCLT_H 07**	**Humid**	80	21.5	41.8	66	4.20	5932.5	13.0	7985
3	**SCLT_H 08**	**Humid**	80	21.5	41.7	66	4.20	5918.2	13.0	5521
4	**SCLT_H 09**	**Humid**	80	21.5	41.9	59	3.76	5315.9	11.5	13504
5	**SCLT_H 10**	**Humid**	80	21.5	42.1	59	3.76	5341.2	11.5	11521
6	**SCLT_H 11**	**Humid**	80	21.5	42	59	3.76	5328.5	11.5	10004
7	**SCLT_H 12**	**Humid**	80	21.5	42.1	50	3.19	4526.5	9.5	33694
8	**SCLT_H 13**	**Humid**	80	21.5	41.9	50	3.19	4505.0	9.5	36842
9	**SCLT_H 14**	**Humid**	80	21.5	41.9	50	3.19	4505.0	9.5	31441
10	**SCLT_H 15**	**Humid**	80	21.5	42.1	47	2.99	4254.9	8.9	47559
11	**SCLT_H 16**	**Humid**	80	21.5	42	47	2.99	4244.8	8.8	51005
12	**SCLT_H 17**	**Humid**	80	21.5	41.8	47	2.99	4224.6	8.8	47953
13	**SCLT_H 18**	**Humid**	80	21.5	42	41	2.61	3702.9	7.5	95040
14	**SCLT_H 19**	**Humid**	80	21.5	41.8	41	2.61	3685.3	7.4	92452
15	**SCLT_H 20**	**Humid**	80	21.5	41.8	41	2.61	3685.3	7.4	N/A
16	**SCLT_H 21**	**Humid**	80	21.5	41.9	40.7	2.59	3667.0	7.4	109120
17	**SCLT_H 22**	**Humid**	80	21.5	41.5	40.6	2.59	3623.1	7.3	105259
18	**SCLT_H 23**	**Humid**	80	21.5	41.7	39.5	2.52	3541.9	7.1	N/A
19	**SCLT_H 24**	**Humid**	80	21.5	42	39	2.48	3522.2	7.0	N/A

It is worth noting that the times to failure that are not available refer to testing that did not fail even after 90 days. The testing was then stopped to make way for other tests.

Analysis of the influence of environmental conditions on TSL for BIT long-term testing

The data collected from the creep tests were plotted on a percentage-BIT-strength-versus-time-to-failure graph. This was performed for both R and H tests as illustrated in Figure 5-66.

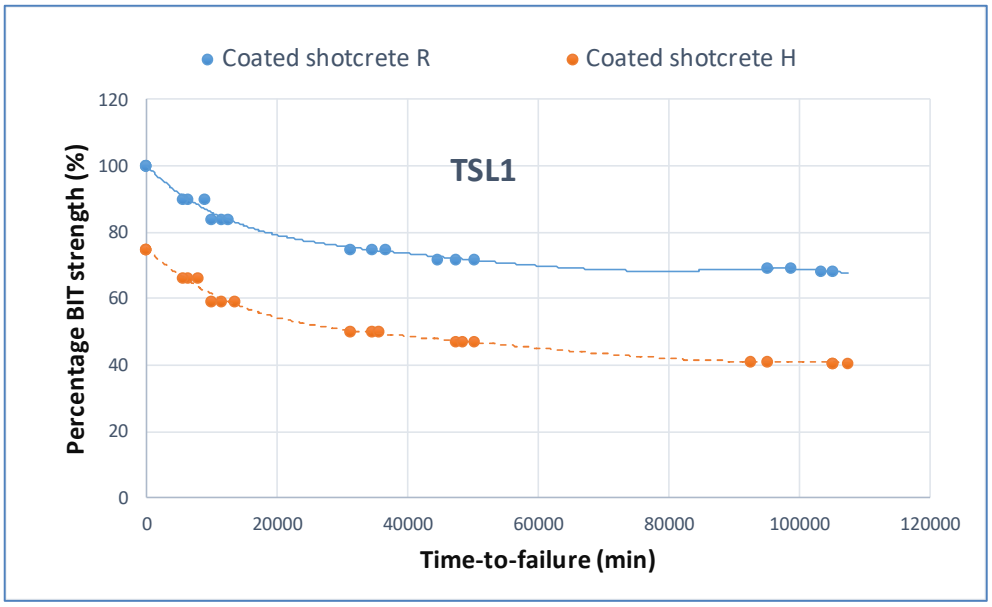


Figure 5-66 Comparison of long-term BIT strengths of coated shotcrete with TSL1 tested in room and humid conditions (R-room condition; H-humid condition)

From Figure 5-66, the long-term strengths of shotcrete coated with TSL1 and tested under R and H conditions are estimated through polynomial curves, at 67% and 40%, respectively. These values enlighten those obtained from dog-bone assessments, which were small and more theoretical, since TSL is not made to be used as a stand-alone material, but rather to be coated on a substrate. However, dog-bone assessment was crucial to determine the sole impact of TSL long-term performance before associating the substrate performance. And based on the earlier-mentioned values, it will be up to the support designer to decide on the resort to TSL1-like liners when the underground conditions are humid. By deduction based on the results from H and HT short-term tests, the recommendation for humid condition should apply to underground mines characterized by humid and high

temperature conditions. The long-term value obtained for room condition is fairly good and could lead to recommend the use of TSL as permanent support in underground mines with such conditions.

5.5 Membrane Displacement Tests

5.5.1 Introduction

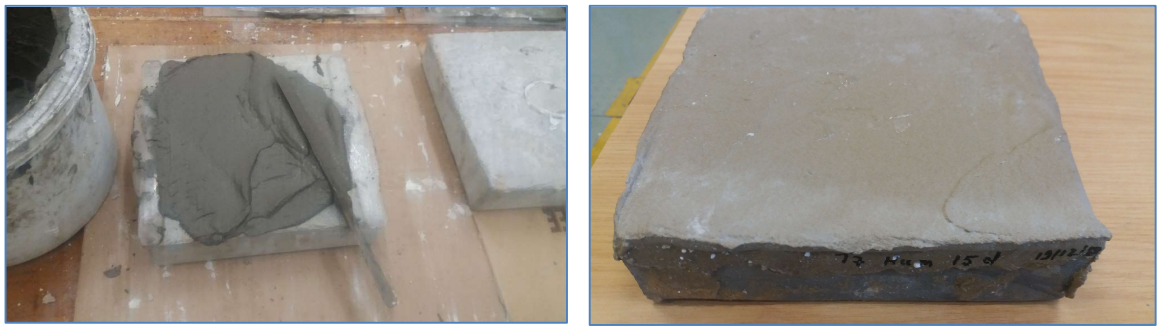
As presented earlier in the literature review, this technique of testing TSL is a representative testing method. In this thesis's case as well, numerous tests were undertaken to assess the performance of thin membranes in resisting against punch-through forces. Focus was also put on the comparison of such performances when subjected to the variation of environmental conditions throughout periods up to 112 days. Besides, an attempt will be made to standardize this representative technique for the sake of comparing the results of such tests done elsewhere, and for establishing clear concepts in the design of underground support systems that resort to thin liners. Specimen preparation techniques will be explained, and then the employed materials and methods will be presented before displaying the obtained results from short-term and creep tests that will be accompanied by a few analyses and discussions.

5.5.2 Specimen preparation

The specimen-preparation procedure was mainly inspired by the MBT procedure suggested by Spearing *et al* (2001) and the EFNARC guidelines (EFNARC, 2008). It can be summarised in the following steps:

- Collect (or reuse) shotcrete panels of about 45x45cm^2 and 55mm thick
- Drill a core-hole at the centre of the panel using a diamond drilling machine (inner diameter: 42mm, and the resulting hole diameter: 45-46mm); the obtained cylindrical shotcrete should be used as a plunger
- Grind the substrate surface-of-contact that is to be coated using either a saw cutting machine or an electric polisher (see Figure 5-69)
- Grind both sides of the plunger, making sure that both sides are flat and parallel to one another

- Place the substrate surface-of-contact facing upwards, with the plunger well-centred and levelled up with the contact surface. Whenever the plunger and the substrate are not the same height, they can be levelled up by placing a thin, stabilizing and solid piece of Perspex beneath the plunger
- Prepare pieces of Perspex of 5 mm, to control the thickness of the coating
- Mix the components of the liners, according to the specifications provided by the manufacturers
- Place a tissue paper in the space between the plunger and substrate to prevent TSL going into the gap as it can be noticed with the uncoated panel displayed in Figure 5-67 (a)
- Pour and level up the TSL mixture as displayed in Figure 5-67 (a)
- Remove the pieces of Perspex and pour more mixture to extend the coating-product to the edges of the substrate
- Wait as long as one day of setting-time before storing the prepared specimen (shown in Figure 5-67 (b)) in the appropriate environmental conditions
- After testing, the substrate (Figure 5-68 (a)) can be reused after detaching the previous coating (Figure 5-68 (b)) and then grinding the surface-of-contact again.



(a) (b)

Figure 5-67 (a) Pouring and levelling up of TSL mixture on an MBT substrate, (b) MBT specimen ready for testing



(a) (b)

Figure 5-68 (a) Aspect of MBT specimen just after testing; (b) Aspect of MBT specimen tested in preparation for reutilization

The removal of very sticky coating should be done by the means of a saw cutting machine and finalised with the grinding of the surface of contact as shown in Figure 5-69 using an electric sandpaper grinding machine.



Figure 5-69 Grinding of an MBT substrate surface for re-utilization

5.5.3 **Materials and Methods**

MBT tests were performed on TSL1, TSL2, and TSL3. The tests followed the principles by Spearing *et al* (2001), with some modifications as suggested by Kanda and Stacey (2019). The method is a punch-through test. It required the preparation and testing of about 112 specimens, gathered in two groups of 72 specimens for short-term tests and about 40 specimens for long-term tests. Each TSL was tested in room and humid conditions. For short-term tests, each of the three TSLs was tested, with at least 12 specimens being previously exposed to each of the environmental conditions for periods of 15 days, 28 days, 56 days and 112 days

before being tested on the MTS 643. These environmental conditions were elaborated in section 5.3.3. Long-term specimens were also exposed to these environmental conditions for more than 80 days before their testing. In this particular method, only TSL1 was tested. About 20 specimens were tested in each of the room and humid conditions. Similar to the previous two laboratory creep methods, in this instance as well, the HT condition was not performed due to the constraints related to the storage capacity of the oven, and the reliability of the recorded displacement data produced by the transducer which showed signs of fatigue of their strain gauges.

Short-term tests

In this testing method, only one input parameter was required to run the machine and get the load-displacement curve and the assessment parameters to be defined later in this section. The unique input parameter is the area of contact between the plunger and the thin liner. This was assumed to be the same for all specimens, since the diameters of all the plungers are assumed to be equivalent to 42mm. All the plungers were cored using the same diamond drilling tube of 42mm of the inner diameter. This assumption was also made because the actual surface of contact could not be measured as it was not visible and accessible. Therefore, the loading values were enough to characterize the liners behaviours. This is in line with the literature on MBT since in most cases, the thin membrane behaviours are represented by 'Load versus displacement' curves. The MBT strength of the liners could still be found through the following expression, particularly for the sake of comparison with other MBT trials, performed elsewhere, that could have different plunger sizes:

$$\sigma = \frac{F}{A} \text{ (MPa)} \qquad \text{(XXVII)}$$

Where: F: Punch-through load, expressed in Newtons (N)

A: Area of contact between the coating and the plunger, expressed in square millimetres (mm^2).

Figure 5-70 shows an MBT specimen placed on the MTS 643 for short-term testing.

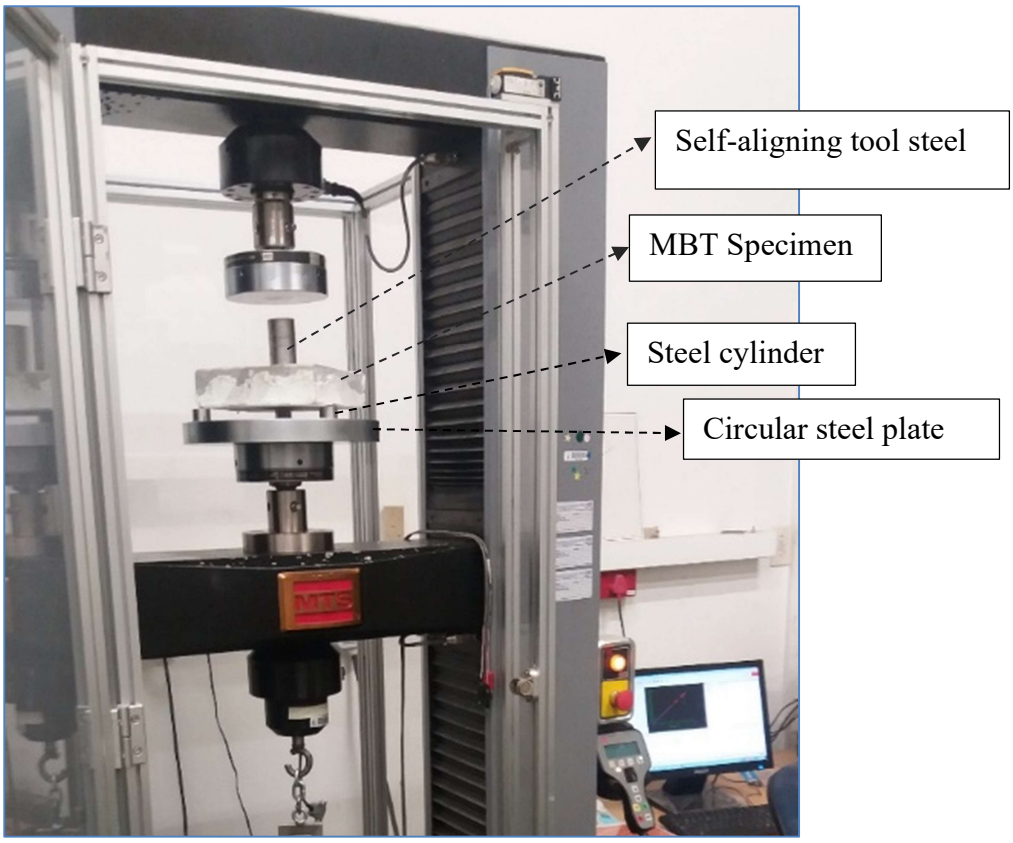


Figure 5-70 MBT specimen placed in the MTS 643 before testing

A circular steel plate of 70cm diameter and 4cm thick was placed on top of the MTS base plate to support the MBT specimen. Three steel cylinders of 20mm diameter and 25mm length were placed close to the edge of the base plate in a triangular position to give room for the downwards displacing liner and plunger. The MBT specimen was then placed on the steel supports with the coating facing downwards. A self-aligning MTS tool steel of 42mm was placed just at the top of the plunger and was the contact point with the MTS upper platen. A preload of about 15N was always applied. The MTS was set to run at a speed rate of 5N/s until the post-peak load could drop at not less than twice the preload.

Based on the observation made in section 2.11.3 concerning the standardization of MBT results, in addition to the two factors proposed by Kanda and Stacey (2019), namely the CS and the RCS, another factor is proposed in this research and will be preferred to the RCS. This is the moment of containment strength (MCS), which is

believed to better interpret a thin liner's containment ability. All these are explained based on Figure 5-71 and Table 5-14.

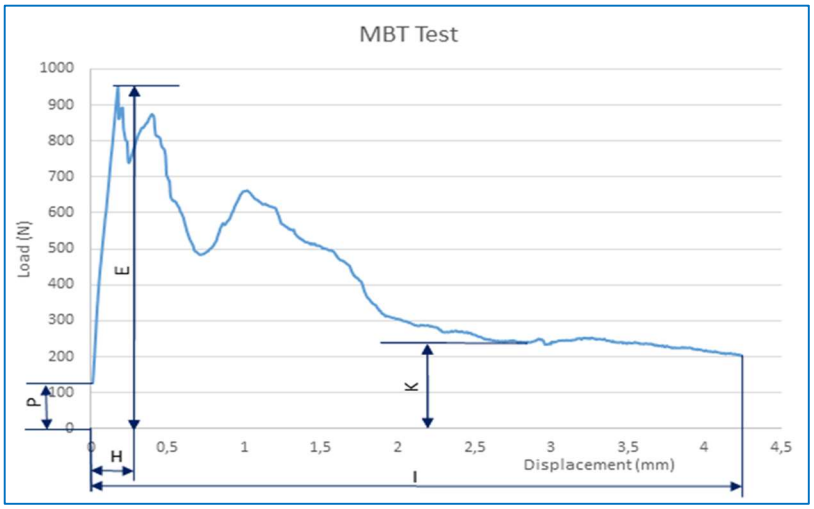


Figure 5-71 Membrane displacement test (MBT) load-displacement graph (Kanda and Stacey, 2019)

This figure is representative of MBT short-term tests. And for a better understanding of the MCS concept, a recall of the required parameters is needed and explained as follows:

- The containment load represents the TSL resisting force, illustrated by the tail of the load-displacement curve of the MBT, which shows an almost constant post-peak load before the final load decline; [K]
- The CS represents the amount of containment load applied by a plunger on a liner's surface of contact (D); [K/D]
- The RCS represents the containment strength that is capable of displacing the thin liner over a distance I; [CS/I]

And for better illustration of these parameters' determination, Table 5-14 presents the steps needed to determine CS and RCS based on data from Table 2-8. Another parameter was used by Kanda and Stacey (2019), namely the containment ratio (CR). This is also believed to characterize TSLs' behaviours, though not always easy to determine due to data availability, as compared to CS and RCS determination.

Table 5-14 MBT results from various TSLs (Modified after Kanda and Stacey, 2019)

Reference	Membrane thickness	Substrate size (m^2)	Substrate area (m^2), (A)	Piston diameter (m), (B)	Peeled distance (m), (C)	Contact point Area (m^2), ($D=pi*B^2/4$)	Initial peak load (KN), (E)	Load capacity (KN/m), ($F=E/C$)	TSL's MBT strength (Kpa), ($MBTS=G=E/D$)	LVDT displ. at max load (mm) (H)	Max LVDT displ. (mm), (I)	Relative strength (Kpa/mm), ($J=G/H$)	Containment load (KN), (K)	Containment ratio (CR), ($L=K/E$)	Containment strength (KPa), ($CS=K/D$)	Relative containment strength (Kpa/mm), ($RCS=CS/I$)	Moment of containment strength (KPa.mm), ($MCS=CS.I$)
Spearing et. al (2001)	6 mm	0.15 × 0.15	0.0225	0.102	0.175	0.00817	1.3	7.43	159.2	15.00	15	10.61	1.13	86.92 %	138.4	9.2	2076
Kuijpers (2004)	–	0.2 × 0.2	0.04	-	0.142	0.20418	–	–	–	–	185	–	0.37	–	1.8	0.01	333
Morton *et al* (2008)	5 mm	1.5 × 1.5	2.25	0.5	–	0.19625	6.2	–	31.6	7.3	14	4.33	3.25	52.42 %	16.6	1.2	232.4
Morton *et al* (2008)	6 mm	1.5 × 1.5	2.25	0.5	–	0.19625	4.1	–	20.9	7.5	15	2.79	1.2	29.27 %	6.1	0.4	91.5
Morton *et al* (2008)	7 mm	1.5 × 1.5	2.25	0.5	–	0.19625	3.4	–	17.3	6.2	17.5	2.79	0.6	17.65 %	3.1	0.2	54.25

From Table 5-14, Morton *et al* (2008) tests show no containment forces. For comparison purposes, the lowest residual force, which is considered as a permanent peeling force, will be assimilated to the containment load. And in case of a varying containment load, it was opted for the average load determined from the curve's tail. It was also observed from the same table that the initial peak peel strength, the CR, the CS and the RCS, vary considerably from one test to another. The reasons behind the gap magnitudes from one liner to the other could be the variety of TSL types, whether the liner is fibre reinforced or not (Yilmaz 2011), and probably to the liners' ductility. Through the current work, it was found that the containment strength is directly proportional to the liner's displacement. Therefore, it is preferable to use the MCS rather than the CS or the RCS, as proposed by Kanda and Stacey (2019). The MCS will be defined as the product of the CS by the maximum vertical displacement of the thin liner. The motivation to resort to this parameter is that, from two liners with the same CS, the designer should adopt that which provides a larger displacement, thus a greater MCS. This can be illustrated by comparative studies from Spearing *et al* (2001), Kuijpers (2004) and Morton *et al* (2008). Although the CS values obtained from their studies are respectively CSa=138.4, CSb=1.8 and CSc=16.6 KPa, the liner from Morton *et al* (2008), identified as liner "c", could be preferred to the liner "b" from Kuijpers (2004). The liner used by Spearing *et al* (2001) was assimilated to liner "a". However, the inclusion of the extent of TSL displacement in the assessment shows that the moment of containment strength from liner "b", MCSb, is equal to 333 KPa.mm, and greater than that of the liner c which is equivalent to 232.4 KPa.mm. Therefore, from a design point of view, liner b should be preferred to liner "c".

In light of the latter argument, the author suggests that the MBT strength (MBTS) and the MCS be considered as the main indicators of MBT performances. The MBTS is an indicator of the MBT performance based on its ability to oppose to loading forces. The MCS is an indicator that takes into consideration the ability of a liner to contain the mobilizing forces to a certain extent, and thus should be characteristic of a liner containing performance.

Both parameters should be considered in MBT performance assessments since Guner and Ozturk (2018) stated that the efficiency of a liner depends on both its strength and its elongation. However, whenever the magnitudes of these two parameters do not lead to an absolute decision on which TSL to use, such as from two liners characterized by one high indicator and another being smaller, a thorough study should be done to determine the performing liner based on either its peak strength or its containment performance. The containment strength is proposed as a decisive option. The theory of the energy absorption capacity of a thin liner by Spearing *et al* (2001) might also be applied in this instance.

The procedure for MBT assessment will be as follows:

- Plotting of MBTS trends and analysis of the environmental impacts
- Graphing of the representative MBTS curves
- Determination of the MBT indicators, the MBTS, and MCS
- Comparative analyses of the MBT indicators for each specimen when exposed to R and H conditions

For all the MBT tests, the parameters in Table 5-15 were kept constant.

Table 5-15 Some invariant parameters of the MBT

Parameters	**Values**
Membrane thickness	5 mm
Substrate size	0.4x0.4 m^2
Piston diameter	0.42 m
Contact point Area	0.138 m^2

Through the MBTS plotting, the MBT behaviours under environmental conditions will be assessed, solely based on their peak strengths. The graphing of the MBT curves will consist of plotting for each TSL, R and H graphs relative to each exposure time. The method will determine the representative test results for each TSL and periods of 28 days, 56 days and 112 days, based on the strength trends. The MBT graphs from R and H conditions will then be presented. From the

comparative charts, the MBT parameters will be identified and the MBT main indicators determined as detailed in Table 5-14. Comparative analyses will then be undertaken to determine the influence of the environmental conditions on MBT specimens coated with TSLs.

Although not directly required for this study, based on the proposed main MBT indicators, the choice of the most efficient TSL based on the MBT indicators shall be made. This process shall be done for both R and H conditions. And since the current study is focused on long-term performance, only the data from 112 days will be considered. The most performing TSLs will be determined for design purposes.

Long-term tests

Creep tests were resorted to for MBT long-term strength assessments. An MBT creep testing machine was conceived, the design of which is presented as follows:

Design

The MBT creep testing machine was built on the principle of lever to multiply the applied loads. The conceived design is presented in Figure 5-72 while the details regarding its dimensions are elaborated in APPENDIX D.

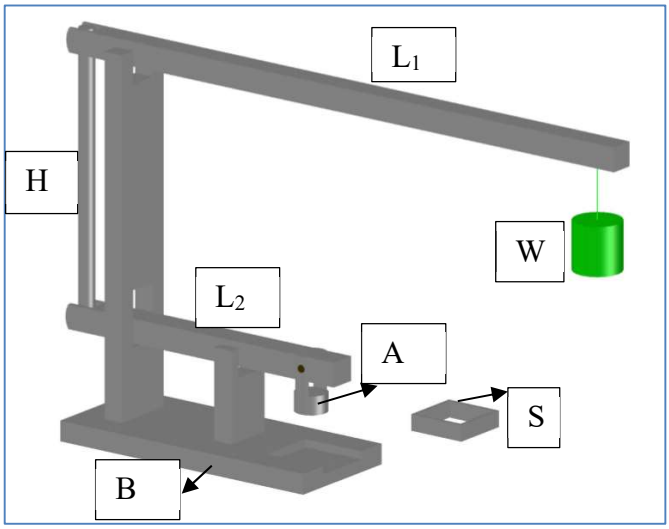


Figure 5-72 Design of MBT creep testing machine (M2) - Perspective Solid View

Where,

L1: Upper load arm

L2: Lower transmitting load arm

H: Hinge

A: Self-aligning steel

B: Base plate

S: Hollow frame

W: Weight

And practically, the MBT machine suffered few adjustments and operates as illustrated in Figure 5-73.

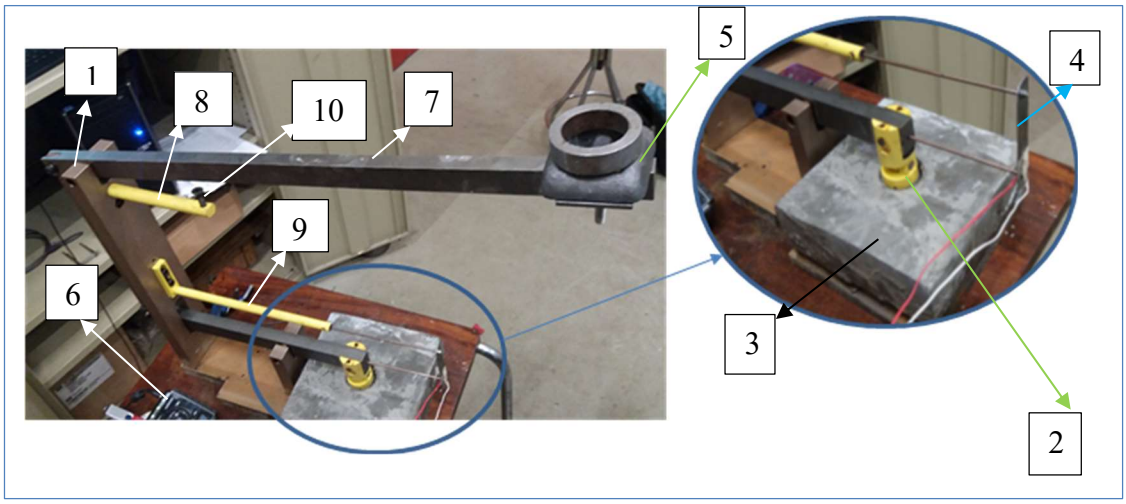


Figure 5-73 MBT specimen under creep test

Where:

1: MBT creep testing machine

2: Adapted self-aligning steel, made with 2 horizontal and perpendicular pivots

3: MBT specimen under testing

4: Displacement transducer

5: Onset weight

6: Data-logger

7: Loading arm

8: Loading arm support

9: LVDT top holding stick

10: Arm support screw

As observed in the practical testing in Figure 5-73, the MBT creep testing machine is equipped with a displacement transducer to monitor the elongation of the thin liners over the full testing period. Like the MBT creep testing machine's need for calibration, the displacement transducer also needed to be calibrated and validated for the report of accurate displacement values.

Calibration of the MBT creep testing machine

In this section, the MBT creep testing machine load factor and the dead weight are to be determined. Having earlier established the proportionality between the load cell type S readings in millivolts and kilograms, the calibration task was performed through the means of this same load cell to get the kilograms readings of various onset applied loads. A Jig was made to bear the load cell that was placed to receive load that was transmitted at the self-aligning steel. Figure 5-74 illustrates the equipment involved in the MBT creep testing machine calibration.

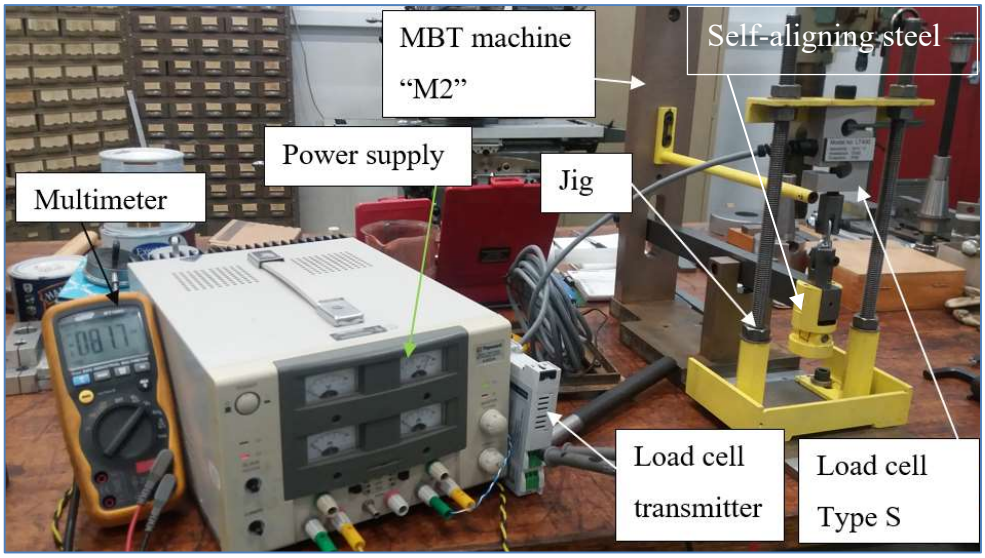


Figure 5-74 Setting up of MBT creep machine loading calibration

The outcome resulted in a linear relationship between the onset loads (kilograms) and the output load readings (millivolts) from the data-logger, which is presented in the following figure.

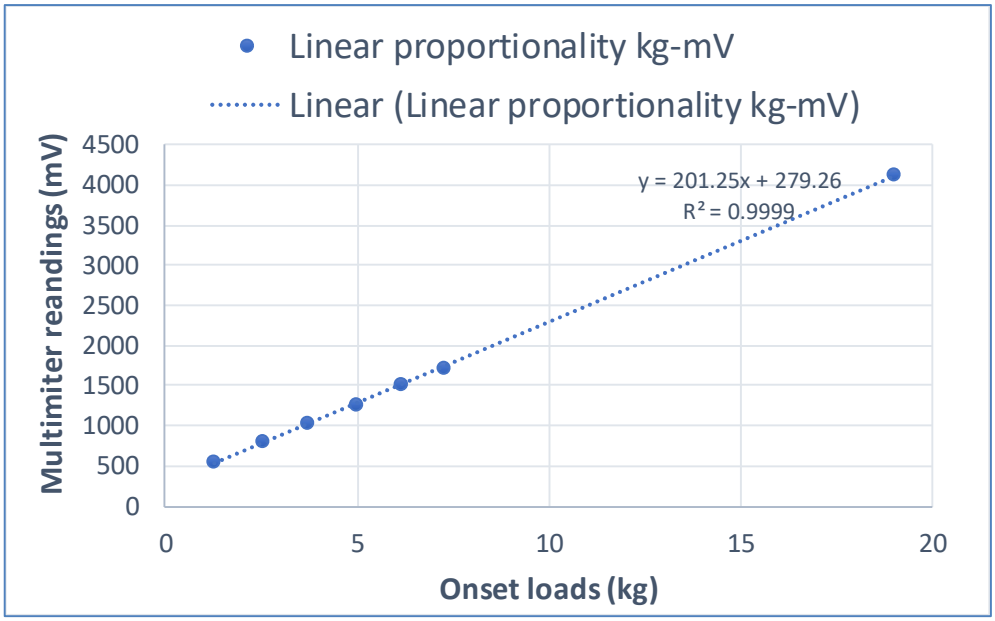


Figure 5-75 Proportionality between onset loads in kg and output mV for MBT creep testing machine

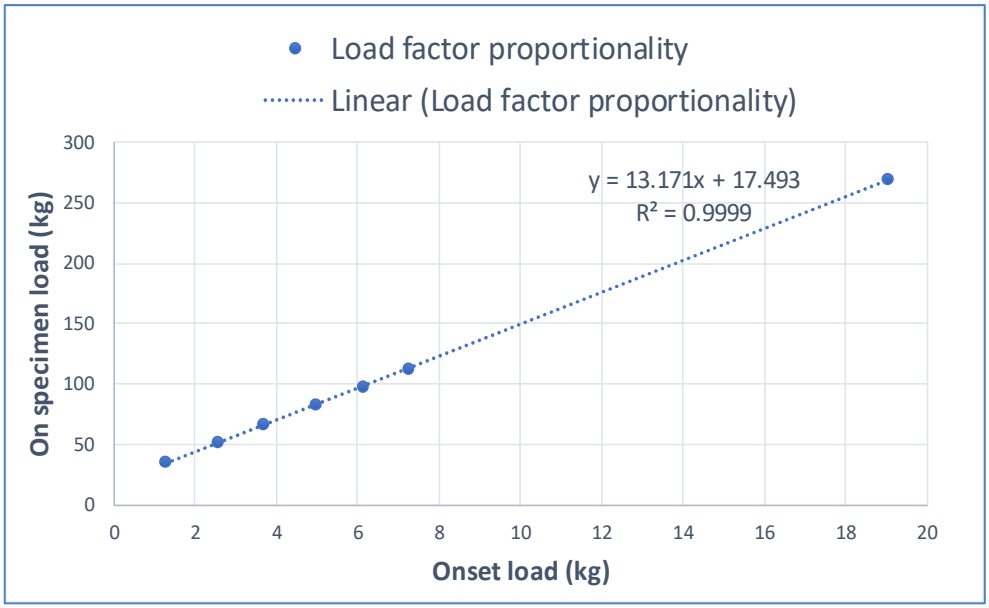


Figure 5-76 Load Factor and dead weight determination for creep testing machine M2

Table 5-16 Weighing parameters of MBT creep testing machine

Parameter	Values	Units
Load factor (F)	13.17	
Dead Weight	17.49	kg

Calibration of displacement transducers for M2 creep testing machine

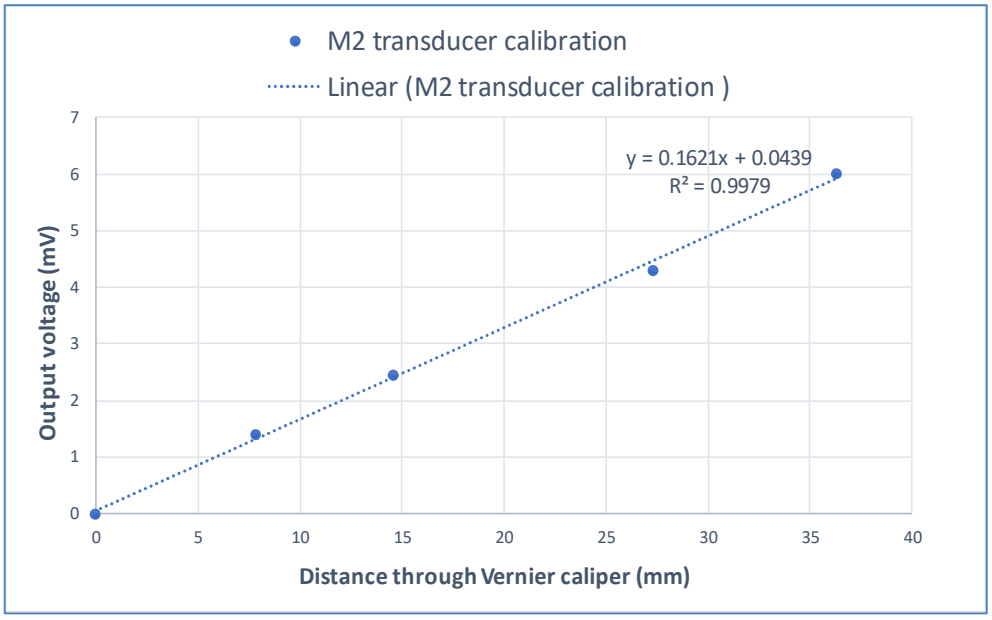


Figure 5-77 Relationship between vertical displacements of M2 transducer's arms at contact points and output voltage

The determination of specimen displacements was made through the conversion of the recorded voltages from the data loggers into metric units. The corresponding graph presenting the linear equation and the correlation coefficient is displayed in Figure F-5. The linear equation for converting the voltage readings into millimeters is:

$$x = 6.1549y - 0.2341 \quad \text{(XXVIII)}$$

Where,

x: Resulting displacement of the specimen, in millimetres
y: Data logger recorded voltage values, in millivolts

For the determination of the strain values, the initial length was assumed equal to the distance between the sticks at rest, on the displacing side. This was measured and found equal to 71.2 mm.

Mode of operation

The procedure of performing a long-term MBT test can be summarised, based on Figure 5-73, as follows:

1. Lift the loading arm "1" as high as possible to find enough room to place the MBT specimen between the self-aligning steel and the hollow frame
2. Release the arm "1" but making sure that the self-aligning steel just-touches the plunger by using the adjusting screw on the loading arm support "8"
3. Place the displacement transducer "4" in the right position as displayed, and tighten the top holding stick "9"
4. Connect the displacement transducer to the Wheatstone bridge circuit
5. Switch on the data-logger
6. Start the recording process using the data-logger
7. Carefully place the onset load on the loading arm hook or above
8. Wait until failure occurs
9. Stop the data-logger recording process
10. Lift the loading arm to allow removal of the specimen from the creep testing machine
11. Transfer the data obtained from the data-logger to a personal computer for further analyses

5.5.4 Results of short-term tests

The TSL's punch behaviours when coated on panels of shotcrete were assessed either under R or H conditions. Comparative analyses of the results were performed for each thin liner.

Influence of environmental conditions on MBT strengths

Since the contact areas between the plungers and the thin liners were assumed constant, the MBT strengths and the MBT loads should be directly proportional. Figures 5-78, 5-79 and 5-80 display the coated MBTS trends of TSL1, TSL2 and TSL3 respectively, after being exposed to room and saturated conditions and tested at the MTS 643.

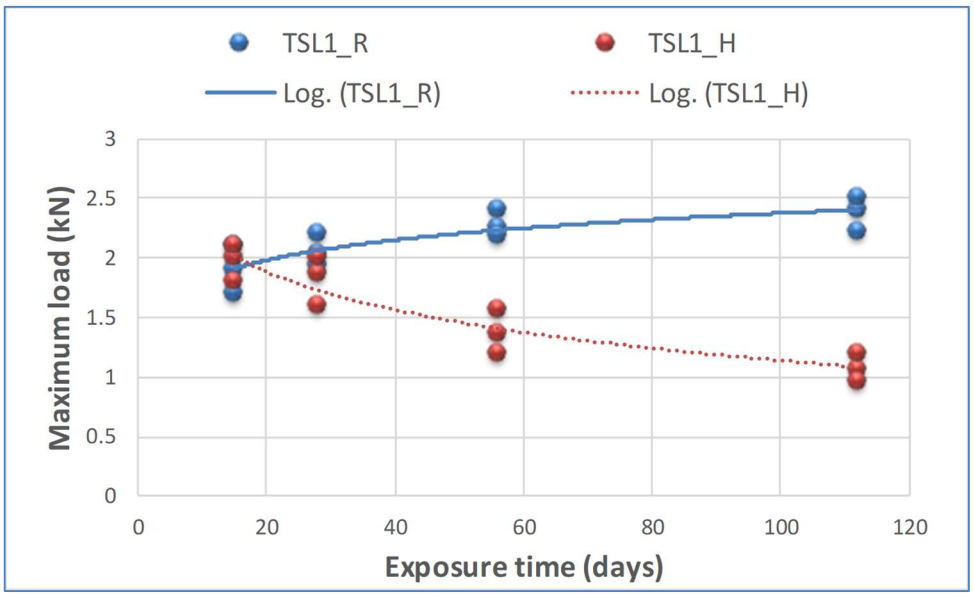


Figure 5-78 MBT strength sensitivity to environmental conditions for TSL1

The results presented in Figure 5-78 still showed an increasing strength trend for TSL1 if stored in R condition, and a decreasing MBTS trend for specimens stored under H conditions. These results follow the same trends obtained from the previous two testing methods, which are focussed on a specific property rather than being more representative properties.

The outcomes of MBT short-term tests, when using a coating of TSL2, are presented in the following Figure 5-79.

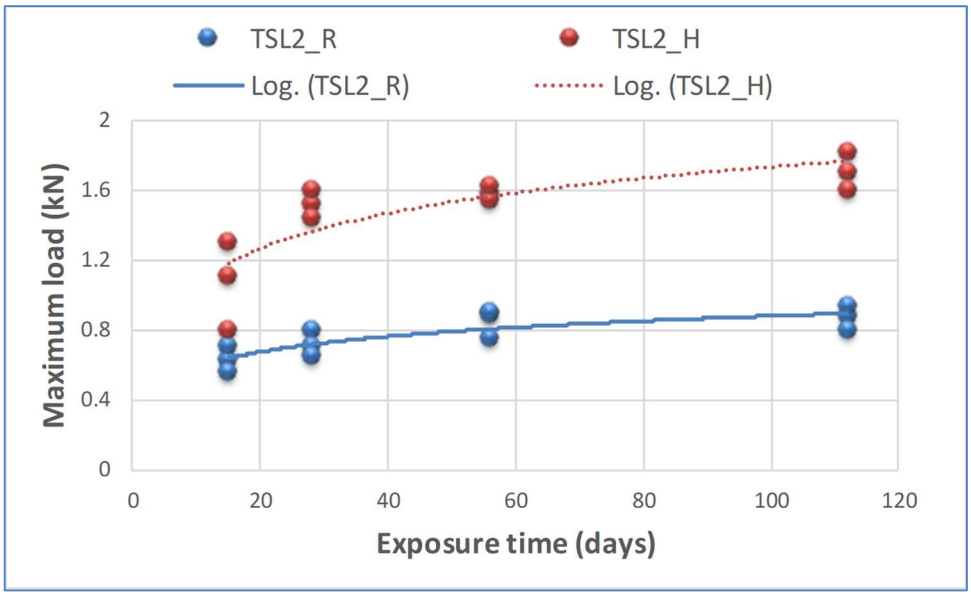


Figure 5-79 MBT strength sensitivity to environmental conditions for TSL2

If the previous UTS and BIT tests on TSL2 have shown that this thin liner is hydrophilic and can strengthen in humid condition proportionally to the exposure time, though with strengths relatively lower than in room condition, Figure 5-79 provides some interesting MBT results. It is seen that the MBTS results are this time higher for the specimens that were stored in H condition than for those exposed to room conditions. This can be supported by the observations done on the specimens. In effect, MBT coated with TSL2 and exposed to room condition showed some cracks initiations which grew bigger proportionally to the exposure duration. This phenomenon is believed to be due to the shrinkage of the liner and its increase of brittleness. However, in humid condition, the shotcrete panels coated with TSL2 did not show signs of crack development even after 112 days. Instead, it was hard to remove the coatings from a tested MBT for re-utilization, since they were always strongly bonded to the substrate, and this always needed extra work-time together with need to resort to the diamond saw cutting machine instead of a spatula.

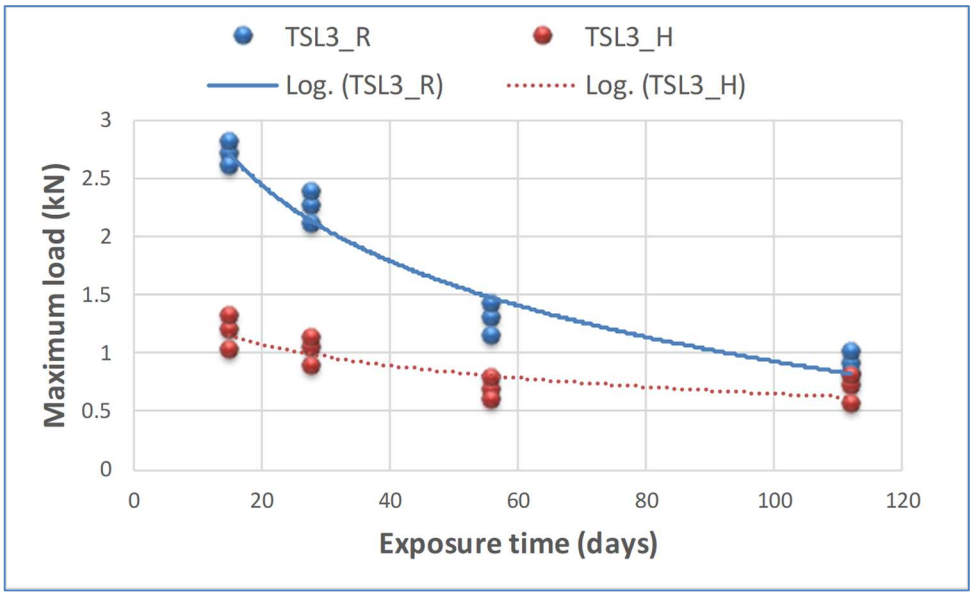


Figure 5-80 MBT strength sensitivity to environmental conditions for TSL3

The overall trend of TSL3 strength behaviour is alarming for support system usage since its behaviour is characterized by a loss proportionally to exposure time, independent of whether this exposure happened in R or H conditions. Curiously, there was no shrinkage or de-bonding sign before the testing. The MBTS magnitude of TSL3 under H condition decreases over the time of exposure similar to that of TSL1, its strength decrease rate remaining lower than that of TSL1, as it was observed for coated BIT specimen tests.

Besides, it was observed that the removal of TSL2 from an MBT panel that was earlier stored under H condition was the hardest work out of the three MBT tested under the six conditions. Therefore, TSL2 should be recommendable for H conditions. HT tests were not undertaken due to logistic constraints such as the availability of ovens big enough to store at least 60 coated panels, but it is believed that MBT specimens coated with TSL3 might produce the best HT results out of the three tested TSLs, as in the previous testing methods. However, work is recommended for assessment of the latter assumption. As suggested earlier, besides the strength capability, the effectiveness of any liner should also depend on its elongation ability.

Influence of environmental conditions on MBT strength and TSL elongation

The representative MBT curves for TSL1 are displayed in Figures 5-81, 5-82 and 5-83.

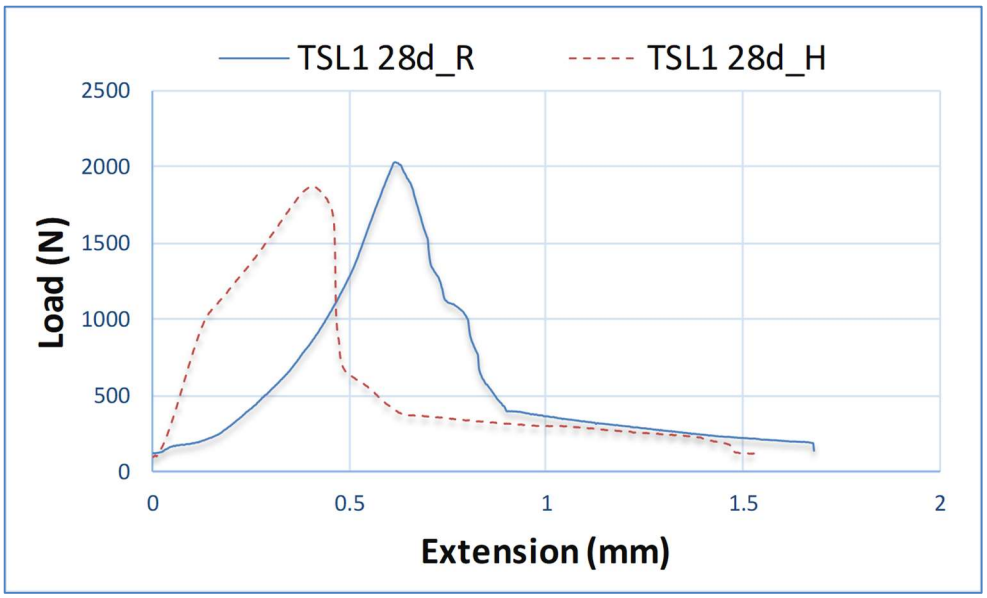


Figure 5-81 Representative curves of MBT tests for TSL1 after 28 days of exposure in R and H conditions

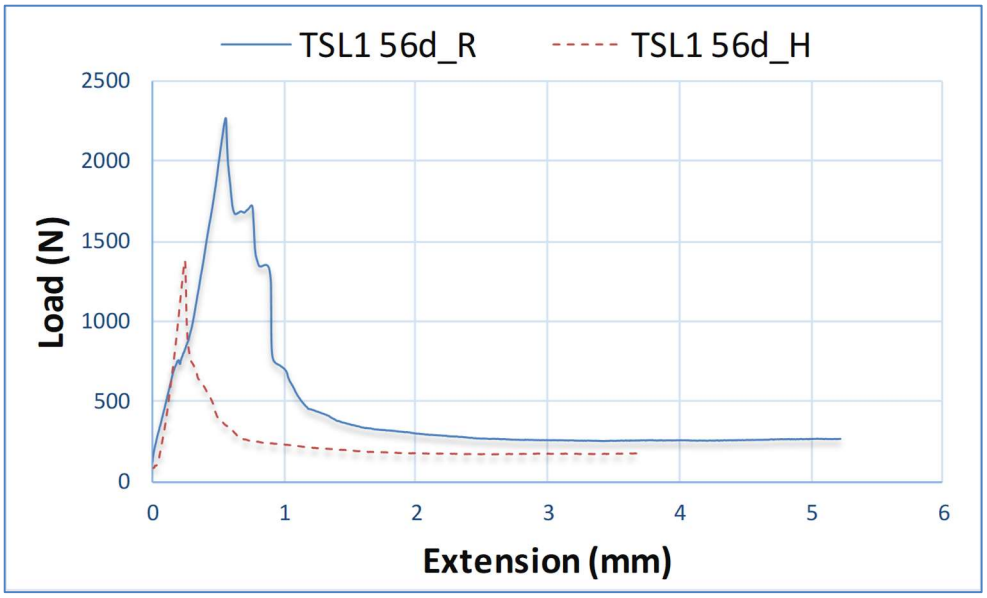


Figure 5-82 Representative curves of MBT tests for TSL1 after 56 days of exposure in R and H conditions

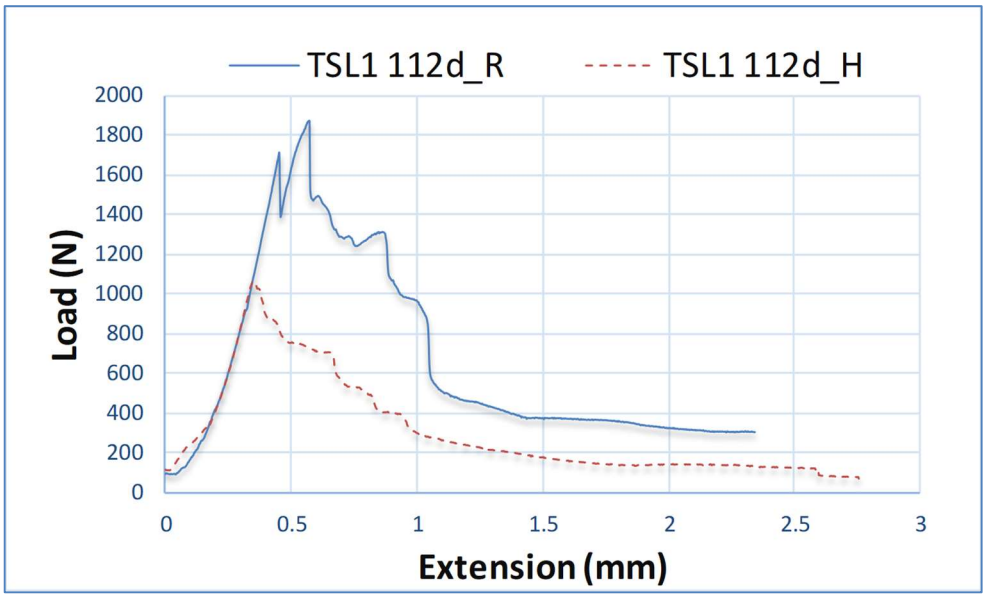


Figure 5-83 Representative curves of MBT tests for TSL1 after 112 days of exposure in R and H conditions

The parameters from all these displayed curves were measured or calculated as explained earlier, and are presented in Table 5-17:

Table 5-17 Determination of MBT indicators for TSL1 after R and H exposures

MBT-TSL1 exposure time	Environmental conditions	First peak load (KN), (E)	TSL's MBT strength (KPa), (MBTS=G=E/D)	LVDT displacement at first peak load (mm), (H)	Total LVDT displacement (mm), (I)	Relative strength (KPa/mm), (J=G/H)	Containment load (KN), (K)	Containment ratio (CR), (L=K/E)	Containment strength (KPa), (CS=K/D)	Moment of containment strength (KPa.mm), (MCS=CS.I)
28 days	**R**	2.03	14.71	0.617	1.7	23.84	0.287	14.14%	2.08	**3.54**
	H	1.87	13.55	0.407	1.5	33.29	0.291	15.56%	2.11	**3.16**
56 days	**R**	2.26	16.38	0.557	5.3	29.40	0.259	11.46%	1.88	**9.95**
	H	1.37	9.93	0.247	3.7	40.19	0.182	13.28%	1.32	**4.88**
112 days	**R**	1.87	13.55	0.571	2.3	23.73	0.371	19.84%	2.69	**6.18**
	H	1.07	7.75	0.350	2.8	22.15	0.146	13.64%	1.06	**2.96**

The comparative analysis shows that both the MBTS and MCS from TSL1 R conditions are always greater than the H respective indicators. This proves that TSL1 is more performant in R than H conditions, thus saturation condition negatively impacts MBT results of TSL1. This is not the case for TSL2, of which representative curves are displayed in Figures 5-84, 5-85 and 5-86.

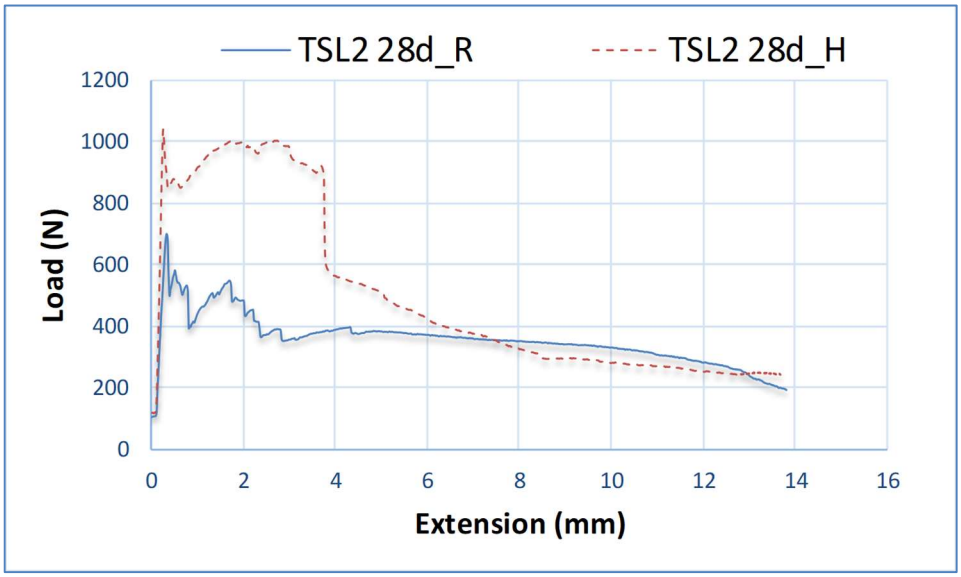


Figure 5-84 Representative curves of MBT tests for TSL2 after 28 days of exposure in R and H conditions

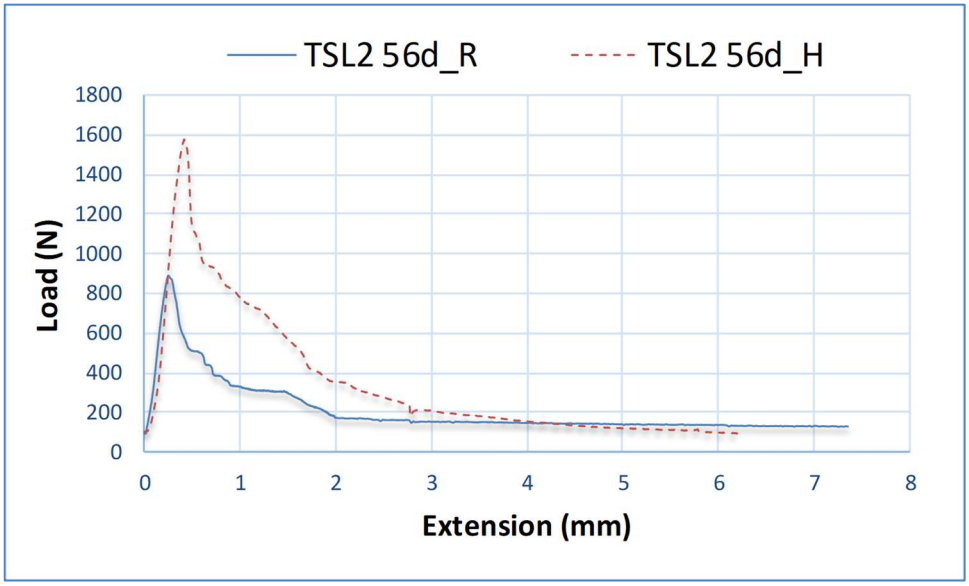


Figure 5-85 Representative curves of MBT tests for TSL2 after 56 days of exposure in R and H conditions

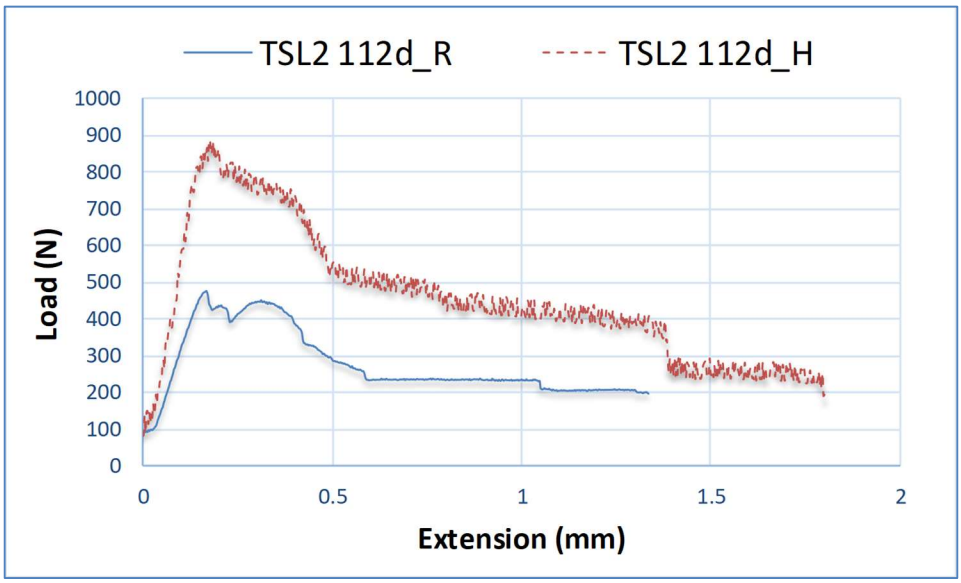


Figure 5-86 Representative curves of MBT tests for TSL2 after 112 days of exposure in R and H conditions

Likewise, the MBT parameters were measured or calculated. Their values are presented in Table 5-18:

Table 5-18 Determination of MBT indicators for TSL2 after R and H exposures

MBT-TSL2 exposure time	Environmental conditions	First peak load (KN), (E)	TSL's MBT strength (Kpa), (MBTS=G=E/D)	LVDT displ. at first peak load (mm), (H)	Total LVDT displ. (mm), (I)	Relative strength (Kpa/mm), (J=G/H)	Containment load (KN), (K)	Containment ratio (CR), (L=K/E)	Containment strength (KPa), (CS=K/D)	Moment of containment strength (KPa.mm), (MCS=CS.I)
28 days	**R**	0.703	5.09	0.340	13.83	14.98	0.358	50.92%	2.59	**35.88**
	H	1.038	7.52	0.260	13.69	28.93	0.328	31.60%	2.38	**32.54**
56 days	**R**	0.887	6.43	0.255	7.35	25.21	0.135	15.22%	0.98	**7.19**
	H	1.58	11.45	0.420	6.23	27.21	0.256	16.23%	1.86	**11.56**
112 days	**R**	0.477	3.46	0.168	1.33	20.57	0.235	49.27%	1.70	**2.26**
	H	0.884	6.41	0.177	1.80	36.19	0.426	48.19%	3.09	**5.56**

From the previous table, the MBT indicators for each exposure time show that TSL2 performs better after being exposed to H condition than when it was stored under room condition. Similar to the previous process, TSL3 MBT representative curves were selected based on the average strength. These curves are presented in Figures 5-87, 5-88 and 5-89:

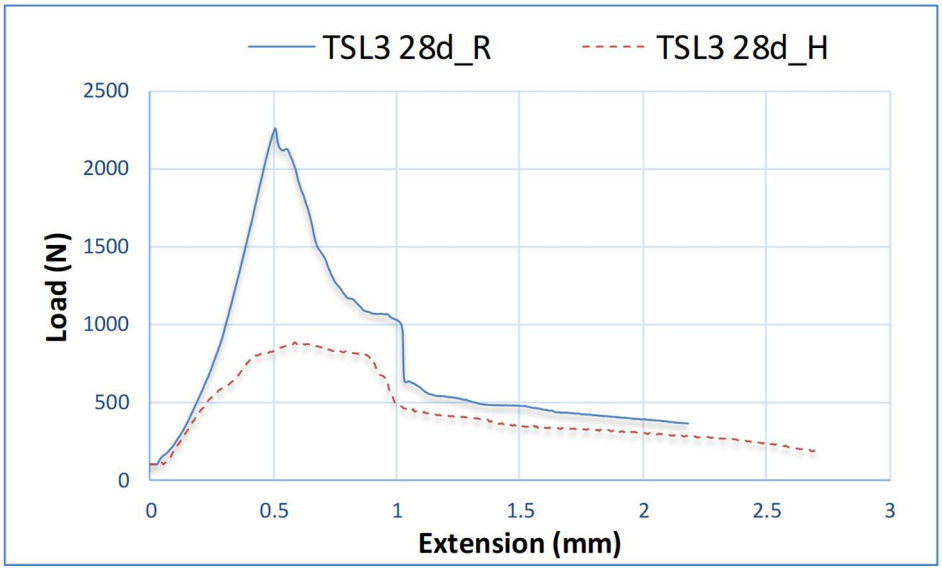


Figure 5-87 Representative curves of MBT tests for TSL3 after 28 days of exposure in R and H conditions

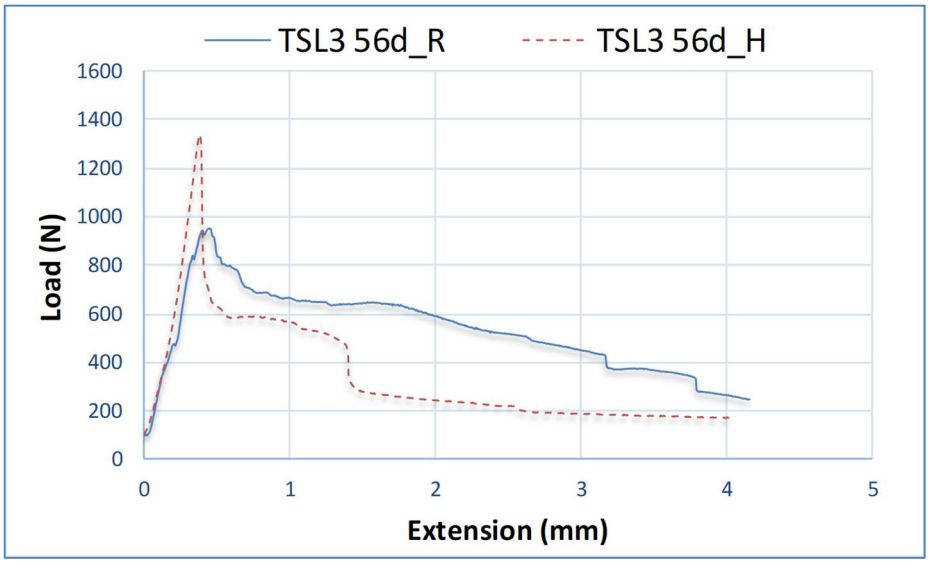


Figure 5-88 Representative curves of MBT tests for TSL3 after 56 days of exposure in R and H conditions

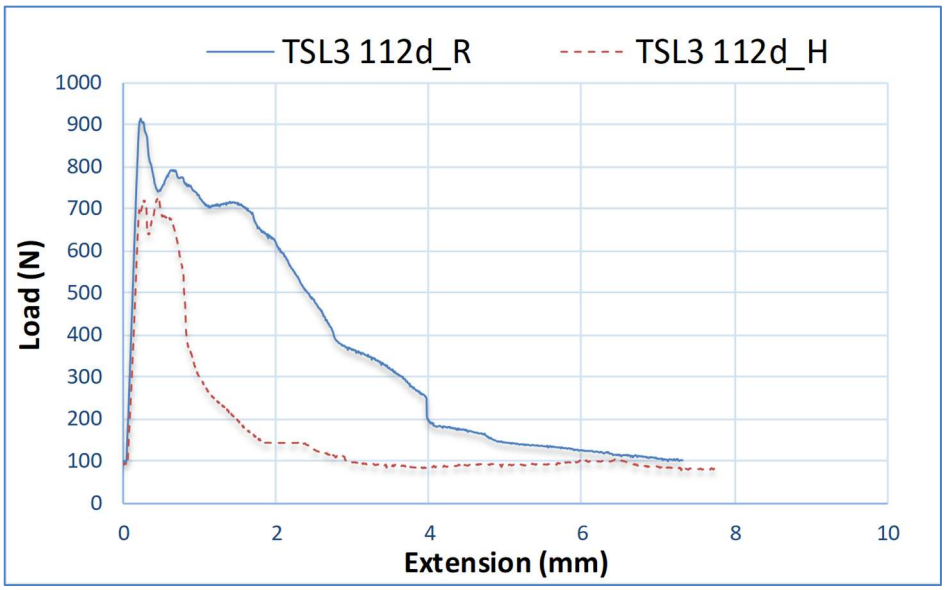


Figure 5-89 Representative curves of MBT tests for TSL3 after 112 days of exposure in R and H conditions

The analysis of TSL3 behaviour was made from the MBT indicators found in Table 5-19.

Table 5-19 Determination of MBT indicators for TSL3 after R and H exposures

MBT-TSL3 exposure time	Environmental conditions	First peak load (KN), (E)	TSL's MBT strength (KPa), (MBTS=G=E/D)	LVDT displ. at first peak load (mm), (H)	Total LVDT displ. (mm), (I)	Relative strength (KPa/mm), (J=G/H)	Containment load (KN), (K)	Containment ratio (CR), (L=K/E)	Containment strength (KPa), (CS=K/D)	Moment of containment strength (KPa.mm), (MCS=CS.I)
28 days	**R**	2.26	16.38	0.509	2.18	32.17	0.483	21.37%	3.50	**7.63**
	H	0.88	6.38	0.590	2.71	10.81	0.322	36.59%	2.33	**6.32**
56 days	**R**	0.95	6.88	0.445	4.15	15.47	0.513	54.00%	3.72	**15.43**
	H	1.34	9.71	0.385	4.04	25.22	0.236	17.61%	1.71	**6.91**
112 days	**R**	0.915	6.63	0.230	7.32	28.83	0.247	26.99%	1.79	**13.10**
	H	0.722	5.23	0.462	7.74	11.32	0.12	16.62%	0.87	**6.73**

Fluctuating MCS values were obtained as the TSL3 exposure time grew. There was also inconsistency concerning the indicators of the representative curves of 56 days. Here the MCS under R condition is greater than that under H condition, unlike the MBTS. Therefore, in this case, the resort to the CS is imperative. This value is greater in R condition than in H condition, which leads to state that MBT specimens coated with TSL3 are better performing under room conditions than under H conditions. Nevertheless, it is worth noting that in the hypothesis that two or more CS were also close values, the principle of the energy absorption capacity should be applied.

Besides assessing the impacts of the environmental conditions on panels coated with TSLs, the proposed indicators should assist in the determination of the ideal TSL under these conditions.

Choice of efficient TSL on the basis of MBT indicators

For a better assessment, the representative MBT graphs of all three TSLs tested either in R and H conditions are presented in Figures 5-90 and 5-91.

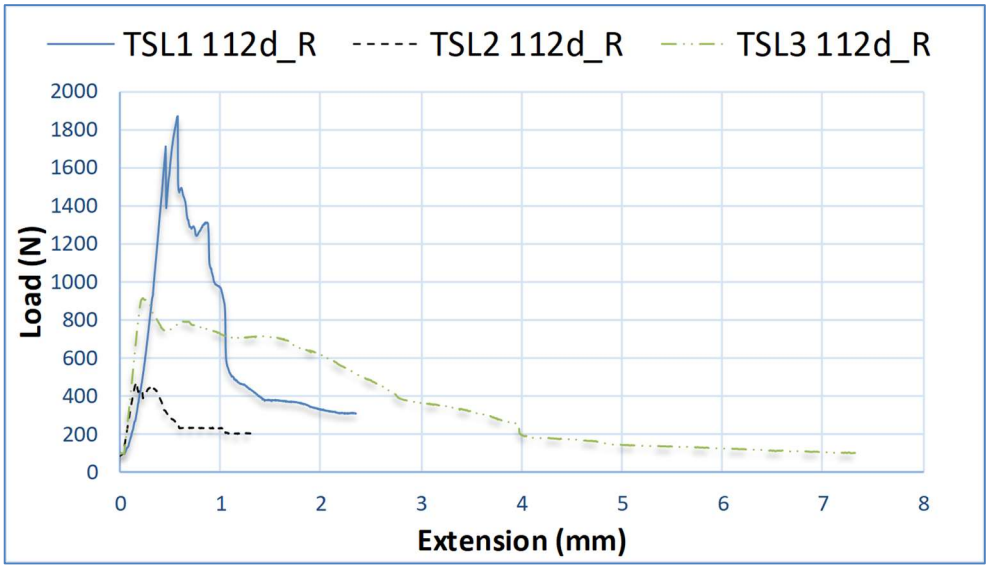


Figure 5-90 Comparison of MBT curves of TSLs exposed to R condition for 112 days

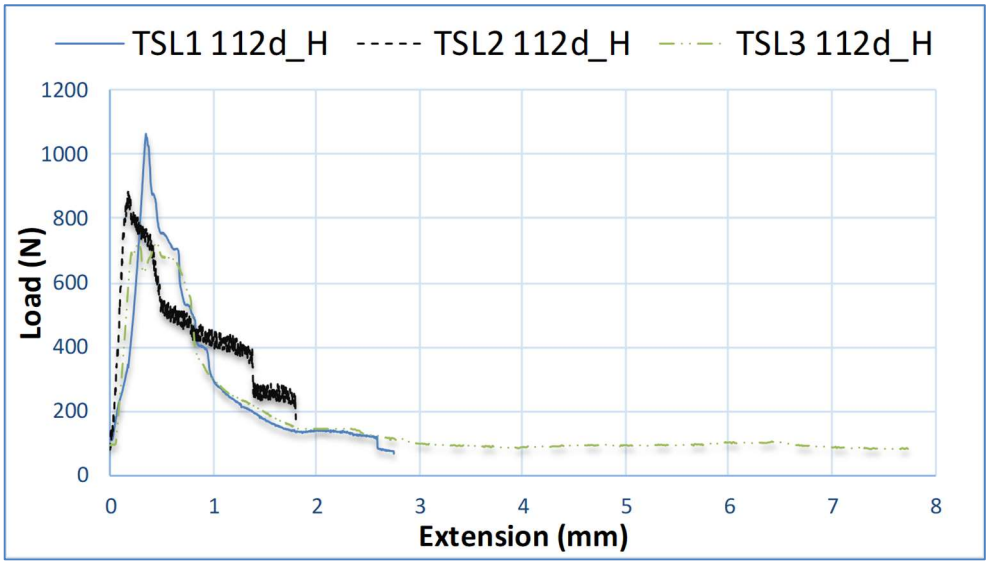


Figure 5-91 Comparison of MBT curves of TSLs exposed to H condition for 112 days

From Figures 5-90 and 5-91, TSL3 is characterised by a longer displacement than TSL1 and TSL2. No adjustment was made on the MTS to allow a longer displacement of that thin liner. But since the machine was set to stop whenever there was a sudden loss of strength in the post-peak strength zone, it is believed that TSL3 loss of strength was smoother than the other two liners.

The choice of the most efficient liner for either R or H conditions will be done from the analysis of the indicators obtained after compiling the MBT data as shown in Table 5-20.

Table 5-20 Comparison of MBT indicators for 112 days of exposure under R and H conditions

Environmental conditions	MBT-TSL1 exposure time	First peak load (KN) (E)	TSL's MBT strength (KPa) (MBTS=G=E/D)	LVDT displ. at first peak load (mm) (H)	Total LVDT displ. (mm) (I)	Relative strength (KPa/mm) (J=G/H)	Containment load (KN) (K)	Containment ratio (CR), (L=K/E)	Containment strength (KPa)(CS=K/D)	Moment of containment strength (KPa.mm) (MCS=CS.I)
R	**TSL1**	1.87	13.55	0.571	2.3	23.73	0.371	19.84%	2.69	**6.18**
	TSL2	0.477	3.46	0.168	1.33	20.57	0.235	49.27%	1.70	**2.26**
	TSL3	0.915	6.63	0.230	7.32	28.83	0.247	26.99%	1.79	**13.10**
H	**TSL1**	1.07	7.75	0.350	2.8	22.15	0.146	13.64%	1.06	**2.96**
	TSL2	0.884	6.41	0.177	1.80	36.19	0.426	48.19%	3.09	**5.56**
	TSL3	0.722	5.23	0.462	7.74	11.32	0.12	16.62%	0.87	**6.73**

From Table 5-20, the most efficient TSL for room condition is not distinctive at first sight. TSL3 presents the greatest MCS whereas TSL1 displays the greatest MBTS. TSL2 is already excluded since both of its indicators are the smallest. When comparing the CS from TSL1 and TSL3, the earlier thin liner offers greater value and should be recommended for room condition over TSL3. This outcome corroborates the recommendations made earlier in this work.

Looking at H condition, all three liners should be thoroughly examined since none of them is demarcated. If TSL3 offers the greatest MCS, TSL1 offers the best MBTS, and TSL2 has a better MCS than TSL1 and a higher MBTS than TSL3. However, the CS from TSL2 is far greater than the others, being almost thrice greater than the second-best CS. From this, out of all the tested thin coatings, TSL2 should be recommended for supporting underground infrastructures in H condition. This finding also confirms the suggestions made earlier in this thesis's research.

5.5.5 Results of long-term tests

An illustration of a failed specimen to the MBT creep test is shown in Figure 5-92.



Figure 5-92 MBT specimen failed at creep test

Similar to the previous creep tests, only TSL1 was assessed because of the time constraints. In this case as well, the adopted environmental conditions were R and H. The HT condition was not assessed because the displacement transducers failed to accurately record the data due to the high temperature environment. But for the chosen environmental conditions, there was no issue in the performance of the displacement transducer. This was connected to a data logger, a power supply and a transducer dummy to form a Wheatstone bridge configuration. The displacements were collected every 500 milliseconds and they were converted in millistrain (mstr) assuming that the initial length corresponded to that between the sticks' ends shown in Figure 5-73.

Room condition

The initial MBT trials aimed to determine the onset weights for instantaneous failure. This was done by placing incremental weights on the onset point of the loading arm until failure. The process was repeated four more times and the average failure was recorded as provided in Table 5-21.

Table 5-21 Determination of average 100% creep load for TSL1 MBT in room condition

TSL1 specimen number	Environmental Condition	Exposure time (days)	Diameter (mm)	Initial 100% Weight (kg)	Expected 100% on-specimen Load (N)	Expected 100% Strength (MPa)	Creep Strength %
1	**Room**	80	42	14.5	2044.9	1.48	100
2	**Room**	80	42	13.8	1954.5	1.41	100
3	**Room**	80	42	15.1	2122.5	1.53	100
4	**Room**	80	42	14.6	2057.9	1.49	100
5	**Room**	80	42	13.7	1941.6	1.40	100
Averages		***80***	***42***	***14.3***	***2024.3***	***1.46***	***100***

The previous table shows that an initial onset weight of about 14.3 kg is needed for an MBT specimen to fail at the instant. The equivalent on-specimen load corresponds to 2024.3 N, which is in the range on the values encountered during short-term tests of TSL1 MBT. And knowing the 100% load value, the creep tests were performed with lower loading percentages. The graphs representing the MBT creep behaviours of TSL1 tested for room condition are displayed in APPENDIX M. A superposition of these graphs was made for the sake of overall analysis and is presented through semi-logarithmic graphs in Figure 5-93.

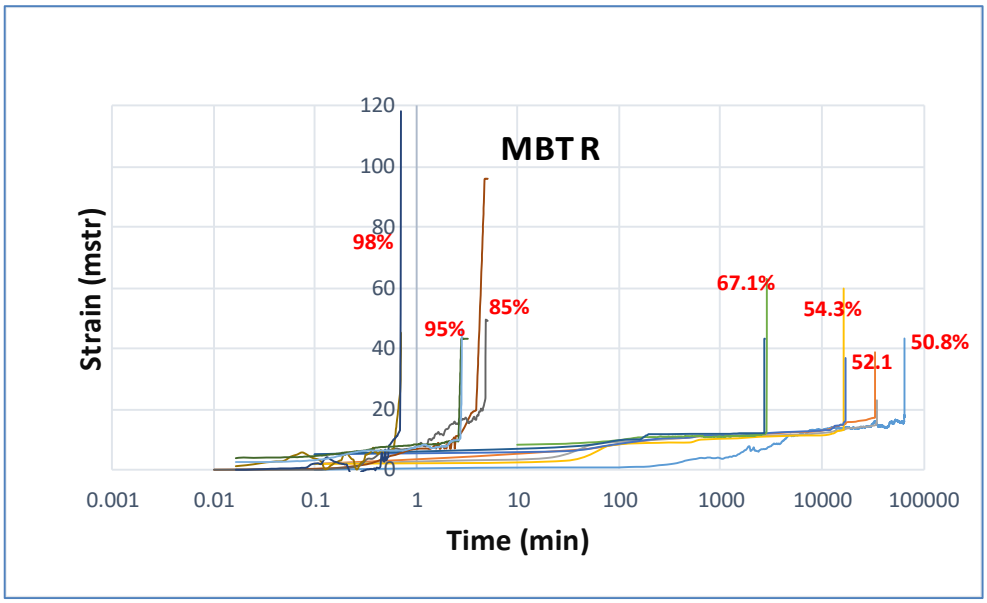


Figure 5-93 Semi-logarithmic graphs of TSL1 MBT creep behaviours tested in room condition

Similar to the observations made in the previous two laboratory creep methods, Figure 5-93 shows that the strain magnitude increases with lighter creep loads. This also shows that in room condition, TSL1 provided a higher containment capacity through creep tests than what could be suggested from laboratory short-term tests. Also, the same figure shows that the MBT long-term strength is lower but possibly closer to 50.8%. This value can be understood since rather than being a structural support and opposing higher driving forces, TSL is only capable of resisting and accommodating lower driving forces. However, understanding of the MBT creep behaviour in the humid condition is needed, since this condition is likely to approximate those of underground mines.

Humidity condition

As explained earlier, these as well initial tests were aimed at determining the load that could make the specimen fail instantaneously. Repeated tests were performed and the average value was considered. Table 5-22 presents the obtained initial 100% onset weights and the calculated strengths.

Table 5-22 Determination of average 100% creep load for TSL1 MBT in humid condition

TSL1 specimen number	Environmental Condition	Exposure time (days)	Diameter (mm)	Initial 100% Weight (kg)	Expected 100% on-specimen Load (N)	Expected 100% Strength (MPa)	Creep Strength %
1	**Humid**	80	42	8.37	1253.0	0.90	100
2	**Humid**	80	42	8.61	1284.0	0.93	100
3	**Humid**	80	42	8.01	1206.5	0.87	100
4	**Humid**	80	42	8.5	1269.8	0.92	100
5	**Humid**	80	42	8.41	1258.1	0.91	100
Averages		***80***	***42***	***8.38***	***1254.3***	***0.91***	***100***

The average onset weight for instantaneous failure was found to be 8.38kg. The transferred load directly applied to MBT specimens tested in humid condition represents a strength of 0.91MPa, equivalent to 62% of the ultimate strength in room condition. Lighter weights were also applied to complete the creep trials. The resulting behaviours are also displayed in APPENDIX M. And the superposition of these graphs is presented in Figure 5-94.

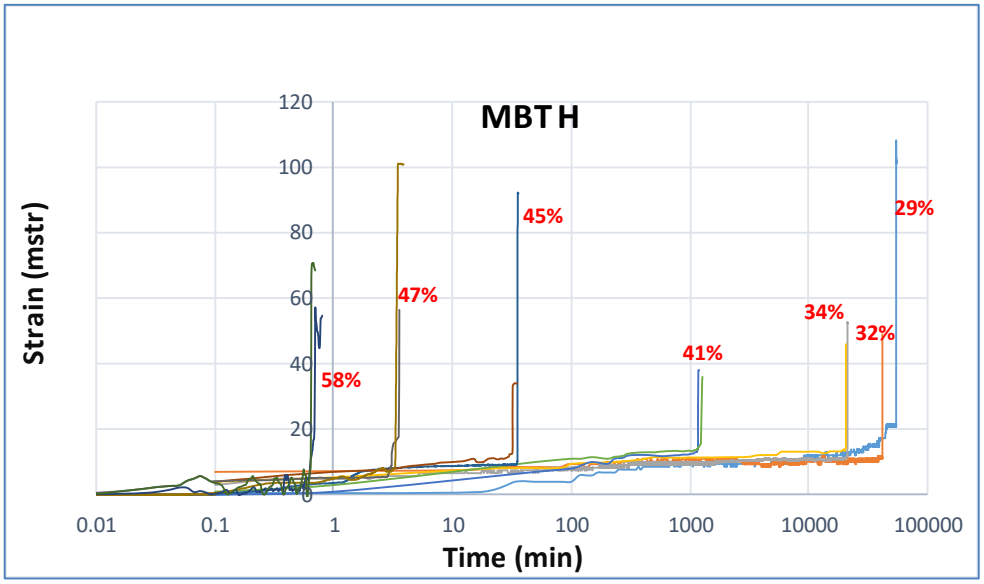


Figure 5-94 Semi-logarithmic graphs of TSL1 MBT creep behaviours tested in humid condition

Through the latter figure, TSL can show higher deformation when under longer creep mechanism in humid condition. However, it can be used as permanent support under this environmental condition, only when the applied force is less than 29% of the ultimate strength obtained in room condition. Although the clear estimation of the long-term strength of TSL1 like liners will be shown later, it is believed that this value is low and can become even lower whenever the temperature parameter is also considered. But additional tests are recommended to assess this hypothesis.

Analysis of the influence of environmental conditions on TSL for MBT long-term testing

The influence of the environmental condition on TSL for long-term testing can be assessed through a comparison of the long-term strengths obtained from room and humid conditions. These strengths can be estimated through the following Figure 5-95.

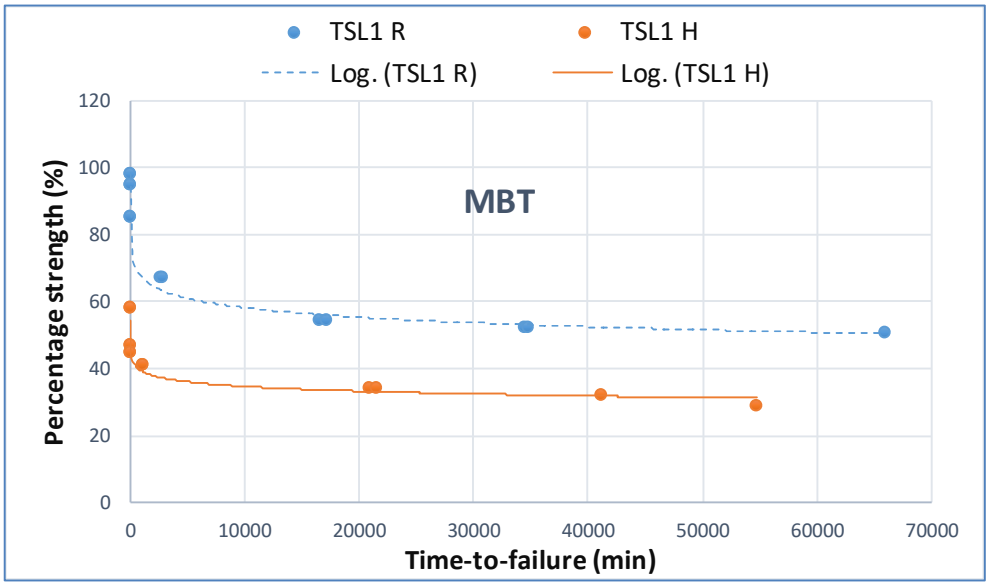


Figure 5-95 Estimation of TSL long-term membrane displacement test strengths through plotting of time-to-failure strengths from room and humid conditions

From Figure 5-95, the estimated long-term strengths in room and humid conditions are 48% and 28% of the ultimate room strength respectively. TSL shows limitations as permanent support in humid condition. This might worsen when the HT condition is investigated. Therefore, cautions should be considered when this thin

coating is designed for infrastructures with a longer life span. The disturbing stresses in humid condition should not be greater than a third of the ultimate coating strength tested in room condition, unless a combination with other supports is made.

5.6 Uniaxial Compressive Strength test

5.6.1 Introduction

The UCS tests were performed on shotcrete and TSL specimens to find additional properties of these materials for further application. Some of the material properties will later be used in numerical modelling of TSL behaviours. In this study, the environmental influence on UCS was assessed, and the exposure time factor was always included. The steps developed include the specimen preparation, materials and methodology, as well as the presentation of the results of short-term tests:

5.6.2 Specimen preparation

Two different types of specimens were prepared for UCS trials:

- Shotcrete UCS specimens
- TSL UCS specimens

All the specimens were prepared following the ISRM standards (ISRM, 2007). The logistic available in the laboratory allowed to standardize the specimens' diameter to 42mm. This lead to opt for specimen-length of 105 mm, thus abiding to length-to-diameter ratio of 2.5.

The specimens of shotcrete were obtained from coring panels of precast shotcrete presented earlier in Figure 5-30 (b). This coring process was performed through the use of a diamond drilling machine. The final length of the specimens was obtained after measuring them with a Vernier calliper, cutting them with the diamond saw cutting machine, and grinding them with the lapping machine. TSL specimens, however, were obtained from moulding thin liner mixtures in the rubber sleeves that were shown in Figure 5-33. These sleeves also have an inner diameter of 42 mm and a length of 105 mm. The final lengths were also ground by the lapping machine. Due to logistic-constraints caused by limited strain gauge availability, not

all UCS specimens had strain gauges glued onto them for moduli and Poisson's ratios assessment. This was only done on a limited number of specimens. A sample of the UCS specimens with strain gauges glued onto them is presented in Figure 5-96.



Figure 5-96 Sample of UCS specimens of shotcrete (SN'P1) and TSLs (TC'C and TC'T) with glued-on strain gauges

5.6.3 Materials and Methods

Only short-term UCS tests were performed. These were split into solely UCS tests and UCS with modulus (UCM) tests. Although the ideal situation could have been the assessment of all the specimens through UCM tests, the amount of available strain gauges (160 strain gauges) only allowed the testing of 40 UCM specimens that provided the Young moduli and Poisson's ratios in addition to the UCS values. The specimens were either shotcrete or TSL-based materials, which were previously exposed to R and HT conditions before testing on the MTS 643, earlier presented in this research. No long-term tests were needed since this was not one of the main testing methods to assess the thin liner performances, but rather a complementary method. After being proven to be the worst strengthening environmental condition, HT condition was preferred to H condition. A total of 120 specimens were tested to UCS, i.e. 12 shotcrete specimens and 36 specimens of each of the three TSLs in study. For each material, the number was split into four by two groups of specimens to be tested after 15 days, 28 days, 56 days and 112

days either in R or HT conditions. Since the compressive load cell of this equipment was of 100 kN, this machine was adequate to perform the UCS tests because shotcrete, which was the strongest material, always had a UCS less than 80 kN, in the room condition. Representative UCM stress-strain curves are displayed in Figure 5-97.

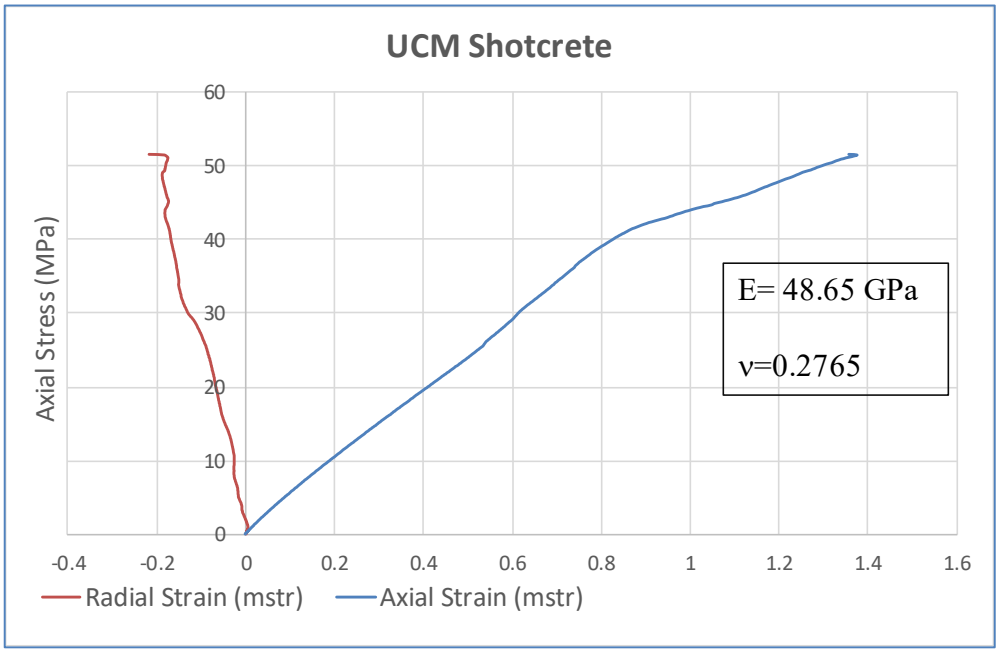


Figure 5-97 Representative UCM stress-strain curves of Shotcrete (mstr – millistrain)

Although the resulting mechanical properties of shotcrete and TSLs could be assessed regarding their UCS trends proportionally to the exposure time either in R or HT conditions, the main objective was to obtain the UCS, Young moduli and Poisson's ratios needed for numerical modelling studies. The representaive UCM curves were selected based on the values of the UCS, Young moduli and Poisson's ratios that should be equal or close to the averages. It is worth noting that shotcrete, a man-made material, showed very similar average results.

5.6.4 Results of short-term tests

Results of shotcrete's UCS

Room condition

The UCS of shotcrete specimens could not be tested for earlier stages of curing time since the panels of shotcrete were moulded and cured by the manufacturer, and were supplied about 100 days after their preparation. However, from the time of their acquisition, trials were run, and they provided almost steady values. The averages of these values are displayed in Table 5-23.

Table 5-23 Averages of UCS tests on shotcrete material for R conditioning

Exposure time (days)	**UCS Shotcrete Room (MPa)**
139	52.21
	E Shotcrete Room (GPa)
139	48.65
	Poisson's Ratio
139	0.276

A better analysis of these parameters will be done through comparison, thus after testing the same liner in HT condition:

Humid and high temperature condition

Another group of shotcrete UCS specimens was tested after being exposed to HT condition. The averages of the outcome values for 112 days of exposure are displayed in Table 5-24.

Table 5-24 Averages of UCS tests on shotcrete material for HT conditioning

Exposure time (days)	**UCS Shotcrete HT (MPa)**
112	48.95
	E Shotcrete HT (GPa)
112	31.98
	Poisson's Ratio
112	0.21

The UCS on shotcrete material is not affected by the environmental conditions but both the elastic modulus and the Poisson's ratio decrease when exposed to HT condition.

Results of TSLs' UCS

Room condition

The results from TSLs' UCS tests that were performed after room conditioning are provided in Figure 5-98.

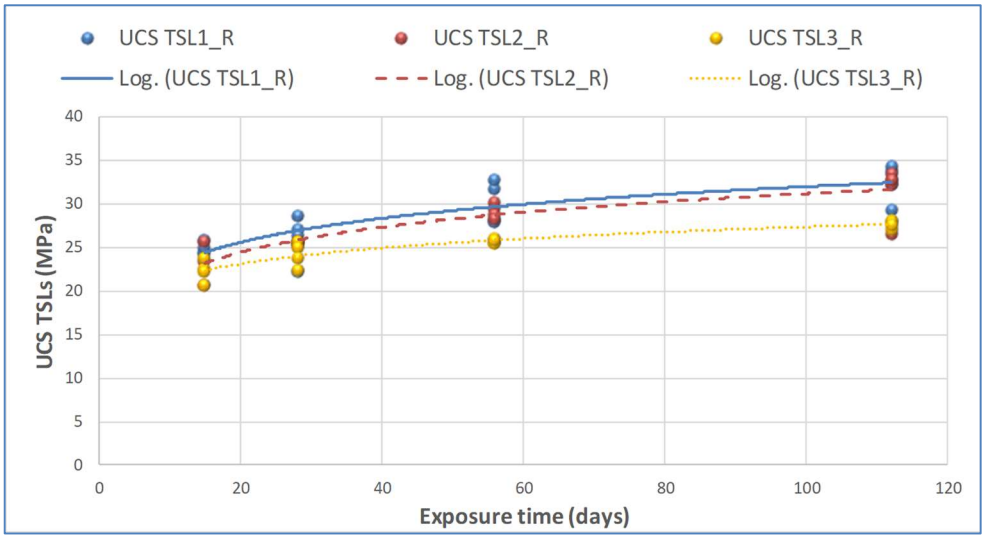


Figure 5-98 UCS behaviours of TSLs tested after various exposure times in room condition

The uniaxial compressive strengths of all three TSLs tend to improve with longer exposure to room conditions, unlike their contrasted behaviours when assessed to uniaxial tensile strengths. This specification should be taken into account when modelling TSLs behaviour. Additionally, all the three TSL's UCS are lower than the shotcrete's UCS tested in the same environmental condition.

Humidity and high temperature condition

In the same way, the impact of humidity and temperature was assessed. But since the UCS tests were not the main laboratory tests for this thesis's research, only a

few tests were performed and the average values were compiled. This study intended to solely provide an overview of the TSL's UCS behaviours in different environmental conditions. The averages UCS of all TSLs conditioned in R and HT environments were determined and then plotted as illustrated in Figures 5-99, 5-100 and 5-101.

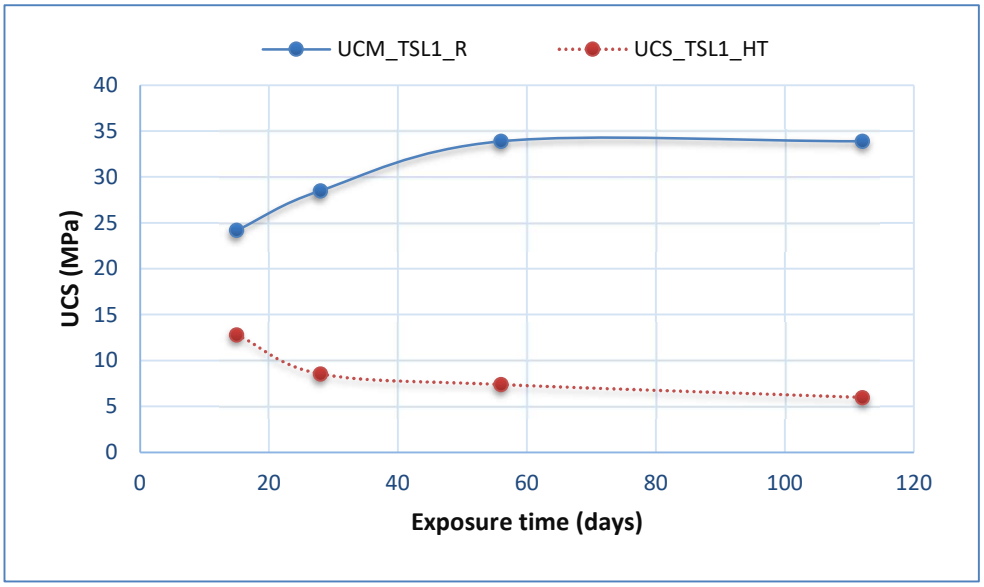


Figure 5-99 Comparison of trends of TSL1 UCS after various exposure times in R and HT conditions

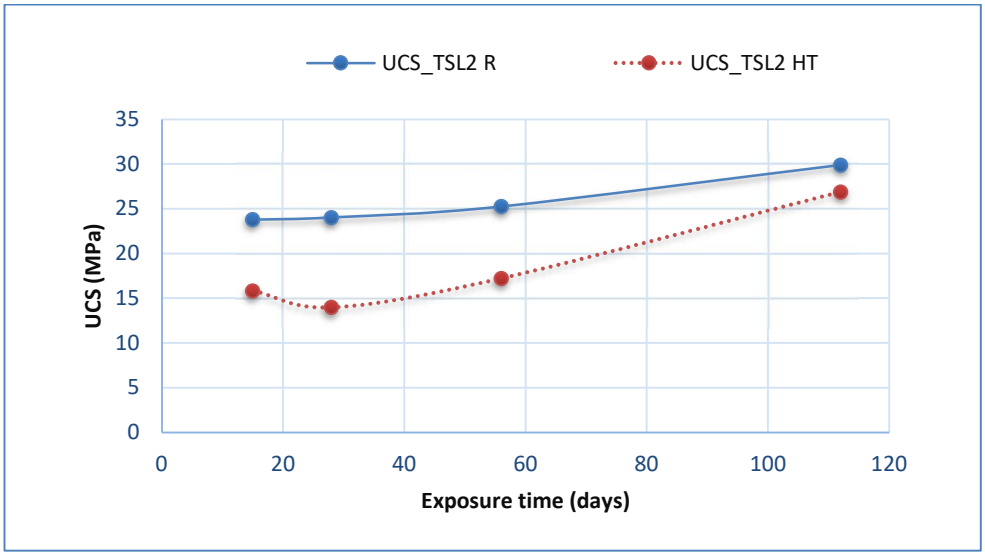


Figure 5-100 Comparison of trends of TSL2 UCS after various exposure times in R and HT conditions

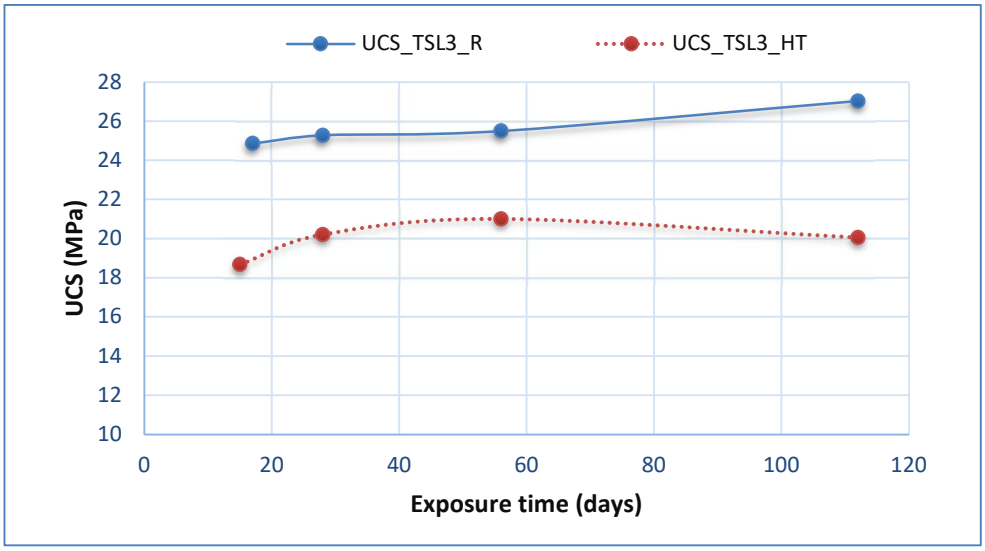


Figure 5-101 Comparison of trends of TSL3 UCS after various exposure times in R and HT conditions

In the case of all three TSLs, it was noted that HT conditions influence the decreasing of thin liners' compressive strengths. The longer the time of exposure to these conditions, the bigger is the gap between the measured UCS strengths in room conditions and in HT conditions, except for the water-based TSL (TSL2). The representative curves that define the Poisson's ratios and Young moduli of TSLs under various conditions are presented in APPENDIX K. These values are important to characterize the liners' mechanical behaviours. They are also useful information for numerical modelling simulations. Other required information on the liners' mechanical behaviours could be obtained through triaxial compressive tests.

5.7 Triaxial Compressive Strength test

5.7.1 Introduction

Similar to the aim of performing UCS trials, the Triaxial compressive strength (TCS) tests were performed to learn the mechanical behaviour of the TSL materials and to determine some intrinsic parameters, the cohesion (C) and internal friction angle (ϕ), though not needed in the numerical modelling package adopted in this thesis's research. The Mohr's strength envelopes should be established for different

TSLs and under different environmental conditions. In this study as well, the steps included the specimen preparation, materials and methodology, as well as the presentation of the results of short-term tests.

5.7.2 Specimen preparation

The specimen preparation concerned the shotcrete and TSL materials. Although the focus of this research was not on shotcrete material, but rather on TSLs, the testing of shotcrete behaviour was also justified by the need to have an overview on its performance, and possibly compare it with TSL's. The specimen preparation for TCS materials was performed in an identical way to that of UCS specimens described in paragraph 5.6.2.

5.7.3 Materials and Methods

All the TCS tests were performed as short-term tests using the Amsler compressive testing machine presented in Figure 5-2. The procedure of splitting the specimen samples into groups depending on the environmental conditions was also adopted. A total of 8 shotcretes and 36 TSL specimens were grouped for R and HT exposures before the testing process. Whereas the shotcrete specimens were tested after about 112 days due to their late supply, TSL's TCS specimens were tested after 28 and 112 days of exposure to the above-cited environmental conditions. For the testing process, the specimens were fitted in a rubber sleeve that is incorporated in a Hoek cell (see Figure 5-102) and these were placed together on the Amsler machine. This machine is hydraulic, with a load cell capacity of 500kN.

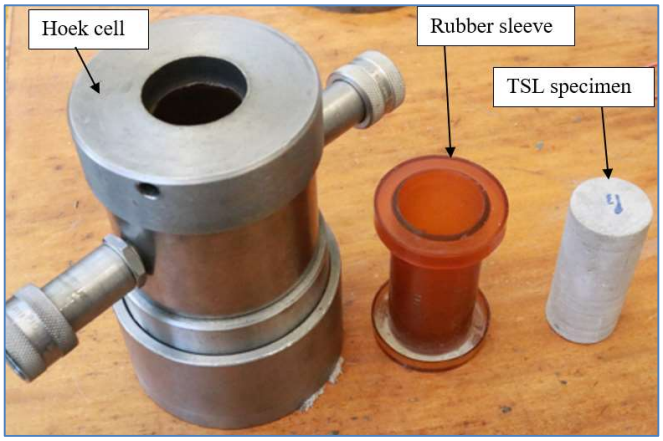


Figure 5-102 Hoek cell used for Triaxial compressive strength

The ISRM standards (ISRM, 2007) were followed to perform a multi-stage triaxial testing on a single specimen. The testing operation was manually controlled by setting a preload of about 10kN before activating the machine which ran at a constant loading rate set at the machine loading controller. The recording of the minor and major principal stresses was gradual. It started with the setting of lower confinement at the hydraulic pump following by the monitoring of the strength behaviour at the controller. The specimen testing was manually halted when the analogue reader almost stopped showing increase, indicating that the loading had almost reached specimen breakage point. The lateral pressure was then increased, and the test was continued. The process was repeated three to five times in order to provide enough data for the drawing of the Mohr's strength envelopes. The values of the angle beta were also measured for further determination of the internal friction angle. This angle can be determined by measurement, either via automatic generation from the Rocscience software program called RocData, or through the following rock-mechanics equation:

$$\emptyset = 90 - 2\beta \qquad \text{(XXIX)}$$

Where,

$\emptyset$: Internal friction angle (°)

β: Angle between the plane of failure and the principal direction of the major stress (°)

After establishing the internal friction angle, the cohesion should be determined using Mohr's circles or calculated through the following formula:

$$C = \sigma_c \left(\frac{1-sin\emptyset}{2cos\emptyset}\right) \qquad \text{(XXX)}$$

Where,

C: Cohesion (MPa)

σ_c: Uniaxial compressive strength of the rock (MPa)

$\emptyset$: Internal friction angle (°)

In this particular investigation, the RocData program was opted as the means for determining the cohesion and angle of internal friction, which were assessed solely for informative purposes.

5.7.4 **Results of short-term tests**

A sample of the tested TSL specimens to TCS is shown in Figure 5-103, and the measuring process of the angle beta is displayed in Figure 5-104.

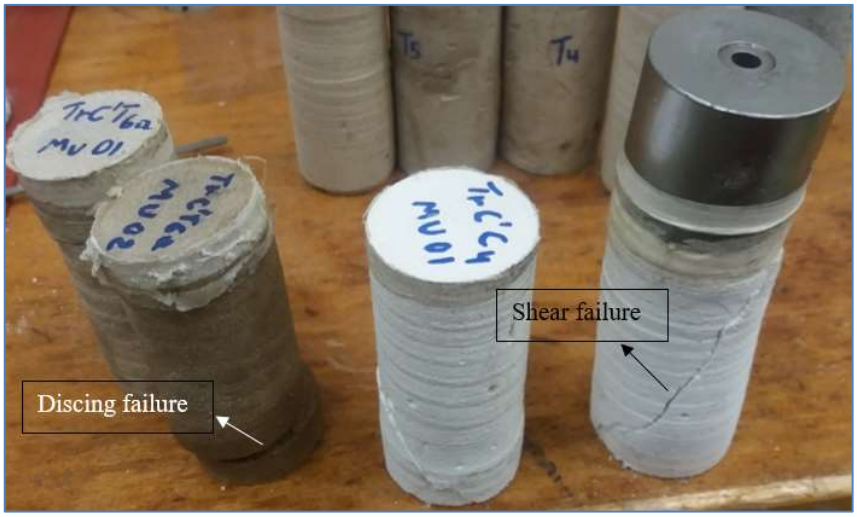


Figure 5-103 Aspect of TSL specimens tested to triaxial compressive strength



Figure 5-104 Measurement of the value of the beta angle

Based on the statistics of the TCS results, the representative data of shotcrete and TSLs were determined and are provided in APPENDIX N. Mohr envelopes could be determined, and they illustrate the strength behaviours of shotcrete and TSLs. These illustrations provide an insight into the impact of the environmental conditions on these materials' strength, which can also depend on the exposure time. Figures 5-105, 5-106 and 5-107 are illustrations of the Mohr envelopes for representative results of shotcrete and TSL1.

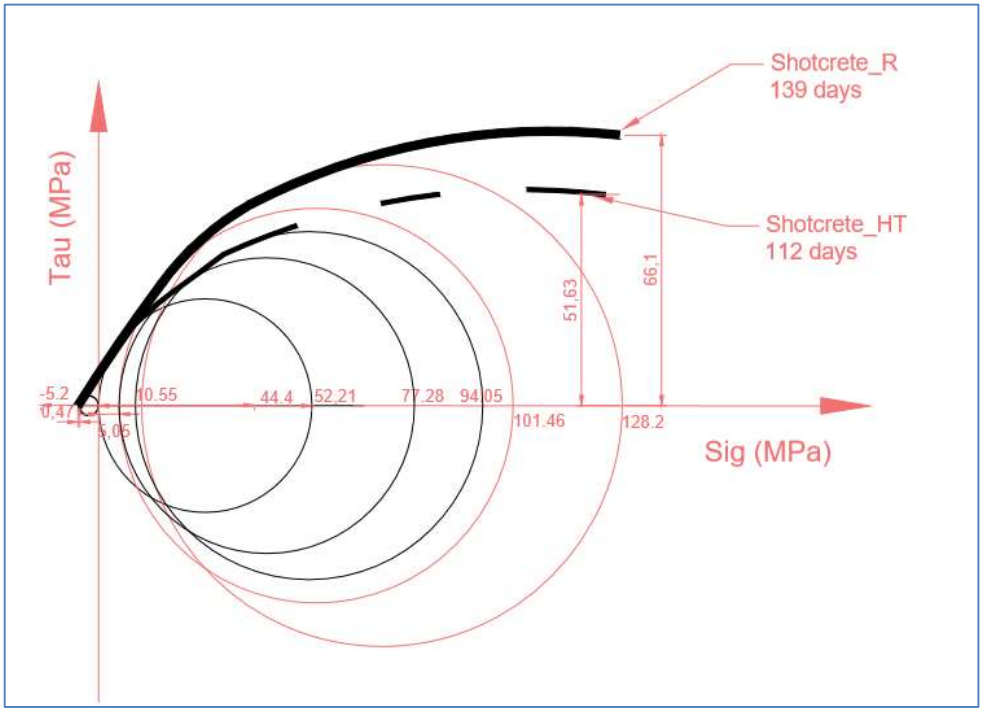


Figure 5-105 Mohr envelopes of shotcrete's Triaxial compressive strength test results from R and HT conditions

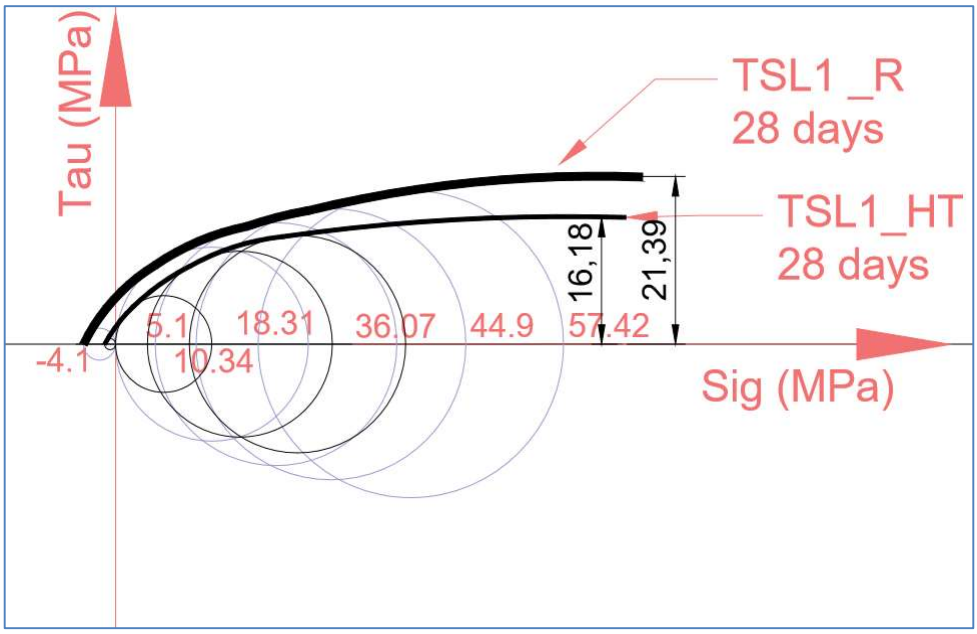


Figure 5-106 Mohr envelopes of TSL1 Triaxial compressive strength test results after 28 days of exposure in R and HT conditions

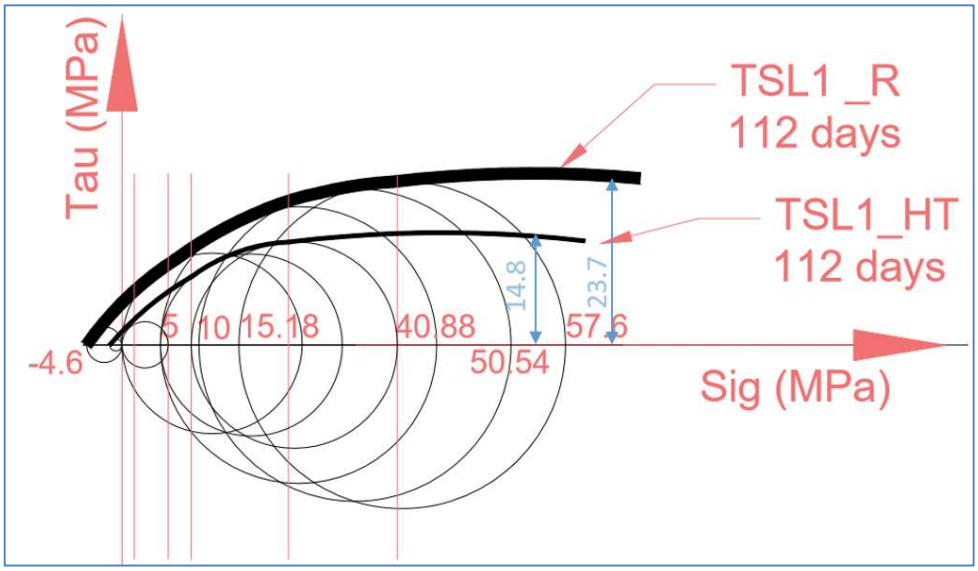


Figure 5-107 Mohr envelopes of TSL1 Triaxial compressive strength test results after 112 days of exposure in R and HT conditions

Figures 5-105, 5-106 and 5-107 show that the strength Mohr envelopes of TSL1 are always lower in HT conditions as compared to R conditions. This observation was also noted for shotcrete specimens. It should produce similar Mohr envelopes trends

based on the Triaxial and uniaxial compressive strength results presented in APPENDIX N.

The resulting values of the cohesion and the angle of internal friction of the tested materials were obtained through the RocData program and are presented in Table 5-25. More details on the RocData outcomes of which inputs were obtained from the Triaxial and uniaxial compressive tests as well as from the tensile tests are presented in APPENDIX L.

Table 5-25 Resulting cohesions and angles of internal friction of various liners tested in R and HT conditions (TCS-Triaxial compressive strength, R-room condition, HT- Humid and high temperature condition)

Liner type	**Exposure time (days)**	**Type of test**	**Internal friction angle (°)**	**Cohesion (MPa)**
Shotcrete	112	TCS_ R	42.74	4.45
		TCS HT	44.07	3.92
TSL1	28	TCS_ R	24.94	1.42
		TCS HT	33.83	0.59
	112	TCS_ R	35.59	1.86
		TCS HT	37.22	0.44
TSL2	28	TCS_ R	28.42	1.42
		TCS HT	35.62	0.95
	112	TCS_ R	28.94	1.82
		TCS HT	28.62	1.41
TSL3	28	TCS_ R	25.37	1.37
		TCS HT	30.31	1.13
	112	TCS_ R	25.03	1.43
		TCS HT	25	0.91

The information provided in the previous table should be useful as input parameters in numerical modelling analysis.

5.8 Chapter Summary

This chapter aimed to assess the mechanical behaviours of thin liners from a laboratory point of view, specifically after longer periods of exposure to various environmental conditions. Although similar tests are mentioned in the literature, particularly for short term tests, it was for the first time that TSLs were trialled to temperature and humidity conditions, with emphasis on long-term exposures. Three TSLs were made available for the testing, namely TSL1, TSL2, and TSL3.

The basic TSL properties were assessed through standardized methods, namely the UTS and the BIT. Another method of TSL assessment for representative properties was the MBT. Although presented in the literature under several variants, this testing method is yet to be standardized. The UCS and TCS tests were also performed for assessing complementary properties needed for numerical modelling analyses. The first three cited methods of assessment were performed through both short-term and long-term testing. The short-term testing resorted to the use of the Material Testing System, for various exposure times, up to 112 days, and to various environmental conditions, namely normal laboratory condition, also called room condition, humid condition, or a combination of humid and high temperature condition. The same environmental conditions were used for long-term trials, which resorted to creep machines conceived for the sake of the research. The UCS and TCS tests were only performed through short-term tests which followed the same procedure abovementioned. If the resort to the MTS did not require any validation of the loading and displacements, the use of creep testing machines needed their prior calibration and validation before proceeding with the appropriate tests.

A total of about 280 UTS specimens were prepared through moulding and subdivided into two groups, namely 225 specimens for short-term tests and 55 specimens for long-term tests. The collected and analysed results only concerned dog-bone specimens that broke at the gauge section. From the short-term UTS testing, it was found that independently of the environmental condition of exposure, TSL1 showed strength increment, even beyond 28 days of exposure time. It was found that H and HT conditions can lower the UTS of R condition by half, thus

demonstrating that it is poor practice to use TSL1 UTS results obtained from normal laboratory condition as inputs to designing supports for underground mines characterized by H and HT conditions. For this particular TSL, the humid condition is more detrimental than high temperature conditions. The scenario was almost the same for TSL2 when assessing the influence of room and humid conditions on its tensile strength. However, this water-based liner showed a better strengthening rate in H condition than the previous TSL, though still weaker than in R condition. TSL2 exposure to a combination of humidity and high temperature condition resulted in a negative strengthening rate over time, which corroborates the finding that H and HT conditions negatively impact the good performance of TSL tensile strength. This assertion was also observed in the case of TSL3, which surprisingly produced a negative strengthening rate even in room conditions. However, this liner tends to have a better strength magnitude after longer exposure time in HT condition.

The assessments of TSL's elongation and modulus behaviours revealed that in general, in room condition, the modulus and UTS strengthening trends are proportional to exposure time and inversely proportional to the elongation. This principle was also observed in H condition for only TSL2, and in HT condition for TSL3. Therefore, it was deduced that the use of a TSL depends on its ability to perform in a particular condition.

A total of about 389 BIT specimens were prepared and tested. These included the short-term tests of 100 specimens for each of the three TSLs, of which 50 were projected for coated shotcrete specimens and 50 were moulded TSL discs. A total of about 40 uncoated shotcrete discs were also projected for BIT short-term testing. The last group of trials concerned 49 BIT specimens coated with TSL1 that were assessed under creep trials. The short-term tests were performed to assess the impact of various environmental conditions on the indirect tensile strength of a thin liner coated on a shotcrete disc. Only the specimens that failed along, or close to the vertical diameter were retained. The results from all short-term BIT tests performed in room conditions demonstrated that there is a strengthening of the thin liners proportionally to the exposure time. This was, however, not the case for

shotcrete specimens, which showed almost steady strength results for longer exposures. In H condition, all the BIT test results, with the exception of TSL2 discs, showed that humidity negatively impacts on the BIT strengths of BIT TSLs, coated shotcrete, and even uncoated shotcrete. However TSL2, which is a water-based liner, showed a strengthening trend over exposure time in humid condition. This finding supported the one from UTS testing of TSL2, which was performed in the same environmental condition. The HT condition, however, unanimously provided a negative strengthening trend for shotcrete, TSL or coated shotcrete BIT specimens. This finding is in accordance with that from UTS tests. Also, studies have shown that it is only in room condition that TSL contributes to continually strengthen shotcrete substrates over time, while H and HT conditions can affect this strengthening process, resulting in uneven outcomes. And finally, assessments based on optimizing the strength and elongation parameters also confirmed the suggestion of resorting to TSL1 for R condition, TSL2 for H condition, and TSL3 for HT conditions.

The Membrane displacement test (MBT) method was also undertaken. This representative technique, essentially based on the push-through mechanism, resorted to panels of shotcrete coated with all the three adopted TSLs for this thesis's research. A total of about 112 specimens were prepared and tested. These included 72 specimens for short-term tests and 40 for creep tests. The short-term tests aimed to determine the impact of the environmental conditions on the performance of thin liners under a push-through mechanism. Additionally, an attempt was made to standardize the resulting performances. In this respect, parameters such as the membrane displacement test strength (MBTS) and the moment of containment strength (MCS) were suggested as the main indicators of MBT performances. The MBT results were obtained from short and long-term trials by resorting to the MTS 643 and a creep testing machine, respectively.

The MBT short-term testing results showed that, in room condition, TSL generally gains strength proportionally to the exposure time, except for some particular thin liners like TSL3, which produced a declined strength rate. The results from the

humid condition, however, showed that, apart from the water-based TSL2, thin liners generally lose strength. This suggestion is strengthened by the results obtained in previous tests. The higher values of TSL1 MBTS and MCS in room condition advocate resorting to this liner in similar environmental conditions. In humid condition, TSL2 possessed higher values of the proposed main indicators of the MBT performance than in room condition. Similar to TSL1, TSL3's MBTS and MCS values were almost always higher in R conditions than in H conditions. But optimization of these two indicators has leaned toward TSL1 as the performing liner in room condition. Therefore, strengthened by the consistency of the results, it can be suggested that TSL1 is more suitable for room-like conditions and TSL2 for humid conditions. And although investigations are required for HT-like conditions, it is likely that a thin liner that is similar to TSL3 will be better-suitable for these conditions.

The UTS, BIT and MBT creep trials were also undertaken at the Wits Gold Fields laboratory, through creep testing machines conceived for the current research. The testing was performed under R and H conditions after a prior exposure for periods of about 80 days. And as in short-term tests, only results from UTS specimens that broke at the gauge section, namely in the space between the transducer's grips, were considered. The BIT results were considered valid only when the failure cracks were vertical and along the diameters of discs. TSL1 was the only thin liner tested in creep trials because of time constraints. The average onset weight representing 100% of the ultimate strength in room condition was always the first parameter to be determined.

The UTS creep tests from room condition provided an average onset weight of the ultimate strength equal to 10.65 kg, equivalent to the UTS of 4.71 MPa. Subsequent lighter weights were used for creep tests. Similarly, initial tests were performed to determine the ultimate tensile strengths in humid condition. The average value of the ultimate load applied on TSL specimens was about 162.4N, equivalent to 2 MPa. However, for comparative purposes, the humid loading was expressed based on the ultimate strength obtained in room condition. And this ultimate humid

strength was about 43% of the ultimate strength obtained in room condition. It was also observed that a TSL with characteristics similar to TSL1 can accommodate higher displacements during creep tests performed in room condition as compared to relatively short-term testing. The same trend was noted in humid condition but with smaller strains than in room condition. This led to state that creep test offers a higher containment capacity of TSL than the containment ability obtained through laboratory short-term tests. And this constitutes an advantage in the practical use of TSL in underground mines. Nevertheless, it was suggested that additional creep trials be performed on various TSL types to validate the findings and to investigate on some inconsistency of the strain behaviours and the containment capacity of TSL in underground-like conditions. The values of the long-term strengths of TSL1 from uniaxial tensile tests were also assessed in R and H conditions. The outcomes showed that TSL should not be resorted to for permanent support in underground mines that are humid, or humid with high temperatures.

BIT specimens of shotcrete were coated with TSL1 and then subjected to creep test. Unlike the UTS creep displacements of TSL that could be monitored, the monitoring of BIT creep strains showed constant and unaffected strains near the centre of the discs for almost the whole testing period until a sudden increase was observed at the time of failure. Therefore, strain-failure time curves were not provided, since the analysis of the strain behaviour could not be made. The execution of the BIT creep tests required prior knowledge of the ultimate strength values to determine the subsequent onset creep loads. These strengths were found to be 6.37MPa and 4.75MPa, respectively in room and humid conditions. Therefore, the ultimate BIT strength in humid condition represented 74.5% of its equivalent in room condition. And looking to long-term strengths, it was found that BIT specimens of shotcrete coated with TSL1 in room condition can permanently support a driving load if this is lower than 67% of the ultimate load. However in humid condition, the same specimens could only permanently support a driving load if this is lower than 40% of the ultimate load tested in room condition. Finally, it will be up to the support designer to decide on the utilization of TSL1-like liners when long-term or permanent support of the mine is concerned.

The creep tests were also performed on TSL1. As in the findings from UTS creep testing, this representative method showed that TSL can accommodate longer deformations proportionally to the extent of the test, thus inversely proportional to the magnitude of the creep loading. It was also found that the ultimate strength in humid condition was 0.91MPa, representing 62% of the ultimate strength found in room testing. The long-term strengths were assessed for room and humid conditions, and were found to represent 48% and 28% of the room ultimate strength, respectively. Therefore, there is a limitation of using TSL1-like liners for permanent support in humid underground mines, unless combined with other mine supports.

The strengths of the shotcrete substrate and TSLs were assessed through short-term testing only. These assessments were done to determine additional mechanical properties that might provide more understanding of the materials' behaviours, and also might be required as inputs in the numerical modelling analysis. 120 UCS specimens were prepared and tested on the MTS 643, of which a few were performed as uniaxial compressive strength tests with modulus assessment. The total number of UCS specimens included 12 cylindrical shotcrete specimens and 36 specimens for each of the three TSLs in study. Each liner material was tested after exposure of 15, 28, 56 and 112 days to either R or HT conditions. Whereas the resulting UCS of shotcrete showed only a slight decrease of the UCS from R to HT conditions when the exposure time was considerably high, there was a clear demarcation between the higher values of Young's moduli from R condition and the small values found from the same material tested after exposure to HT condition. All these materials produced values of UCS that increased with the exposure time in R condition. In HT conditions, the UCS values of the three TSLs were always lower than those obtained in R condition, with the worst case observed for TSL1 and the best for TSL2.

The triaxial compressive strength (TCS) tests aimed to provide additional mechanical properties on the TSLs and shotcrete materials employed in this research. This information is essentially the cohesion (C) and angles of internal

friction (ϕ). As in the UCS tests, only short-term assessments were needed. In total, 8 cylindrical shotcrete and 36 TSL specimens were prepared and tested after being exposed to R and HT environmental conditions. The resulting values of the (C) and (ϕ) were automatically obtained by the means of the RocData program, after inputting the obtained values of the various minor and major stresses from triaxial tests, and the values of the tensile and uniaxial compressive tests. Besides, a sample of the Mohr envelopes showed how the environmental conditions may affect the strength of the liners.

CHAPTER 6 NUMERICAL MODELLING APPLICATIONS

6.1 Introduction

Numerical modelling (NM) has been resorted to for illustration and validation of the results obtained in laboratory. The package that was used is Rock and Soil 3-dimensional (RS3) analysis program. This program was chosen for being simple to used and available at the time. RS3 is a finite element analysis program that is generally used for modelling slopes, tunnels, and support designs in soil and rock (*Rocscience Inc.*, 2018). This 3D package was employed to model the impact of various environmental conditions on a BIT coated specimen. Rather than having the focus on the validation of the laboratory tests, the attention will be on the TSL output behaviours.

6.2 Modelling of Coated Shotcrete Disc

6.2.1 Modelling of coated rock materials with TSL revisited

Mpunzi *et al* (2015) modelled a shotcrete disc coated with TSL to assess the thin liner's rate of strength enhancement on the substrate. In their endeavour, they constrained the specimen behaviour to an amount of displacement based on laboratory experiments. They then demonstrated the positive impact of TSLs when coated on shotcrete discs. The uncoated shotcrete discs could gain strength when coated with TSL, and this gain could be in the order of 30 to 40 percent. However, their experience was limited to room conditions, leaving the underground-like conditions unsolved. This assessment is intended to be performed through this work. Besides, Guner and Ozturk (2016) have suggested considering the age of the thin liner during the modelling stage, since this affects the Young's Modulus, which is one of the input parameters. Since RS3 does not incorporate the age variation, the modelling will consider the thin membrane characteristics at only 112 days.

6.2.2 Methodology for numerical modelling assessments

The method will assist in analysing the TSL behaviour that could not be easily interpreted either from field assessment or through laboratory testing and analyses.

Data to be adopted should be well-calibrated to reflect the real behaviour under realistic stress conditions. Discs of shotcrete coated with TSL will be modelled. The TSL's properties will be borrowed from TSL1 for illustration. Two models will be assessed: Room and HT conditions. For the sake of solely investigating the coating impact on the substrate BIT strength, the material properties of the substrate in HT conditions will be assimilated to those input in room conditions. Most of the input parameters will be found from laboratory test results. Whenever not available, data from literature or RocData, a Rocscience package, will be considered. And in a few cases, data will be realistically assumed.

The study will consider a non-linear model that incorporates various geotechnical properties characterizing the field conditions of the liners and the substrate. In practice, the NM technique will be used as a tool to determine the factor of safety (FoS) under the various environmental conditions. From the deterministic analyses, probability of failure (PoF) and risk assessments will be undertaken to measure the reliability of TSL used as a coating in various environmental conditions that can be encountered in mines. It is worth noting that although the probabilistic analysis is not incorporated in RS3, it can be generated from the deterministic analysis through the resort to the Response Surface Methodology (RSM) (Chiwaye and Stacey, 2010; Kanda and Stacey, 2016). In this practice, only two variables from the thin liner were considered: UCS and tensile strength. The total number of RSM combinations was 2n+1=5. Through an Excel spreadsheet add-in simulation package, Oracle Crystal Ball, Monte Carlo simulations should be undertaken to produce the FoS response surface, leading to the determination of the PoF. The risk assessment will also be exploited to explain the impact of resorting to TSL as a relatively long-term support in humid condition. The geotechnical risk is defined by the equation:

$$\text{Risk} = \text{PoF} * \text{Consequence} \qquad \text{(XXXI)}$$

6.2.3 Model settings

A disc of 42mm diameter and 21mm thick, coated with a 5 mm TSL, was designed as illustrated in Figure 6-1. The circular section was subdivided into 40 equal parts, with the four bottom surfaces being restrained to all the displacements while the four top surfaces were loaded (Kanda and Stacey, 2019). The loading was chosen to match an FoS in the range between 1.5 and 2 in room condition.

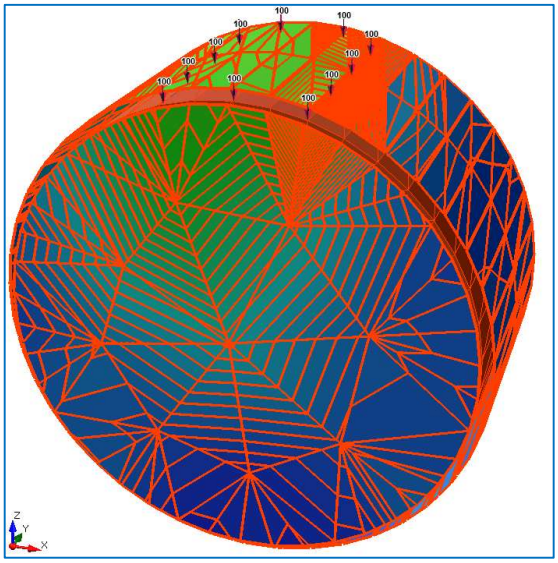


Figure 6-1 Snapshot of a coated BIT model

The input parameters of the model varied according to either representing a specimen tested in room or HT conditions

Room condition

For room condition modelling, the input parameters for shotcrete and TSL1 were adopted as described in Table 6-1. These properties were found in laboratory experiments.

Table 6-1 Input parameters of the coated BIT model for room conditions (N/A – Not available)

Material inputs	Substrate	TSL
E (MPa)	48650	13740
Compressive strength (MPa)	52	32.78
Poisson's ratio	0.276	0.186
Tensile strength (MPa)	N/A	4.6
Unit weight (MN/m^3)	0.021	N/A
Thickness (mm)	21	5
Shear strength (MPa)	N/A	4.6

The generalised Hoek Brown parameters were obtained by inputting the UCS and Young's modulus in the RocData package. For shotcrete, the GSI and mi were evaluated based on the surface conditions and the list of proposed mi. The selected values were 61 and 17, respectively. The parameters generation from the Rocscience package provided the following Hoek-Brown parameters:

- mb: 4.222
- s: 0.013
- a: 0.503

The adopted TSL material type was plastic; the shear strength was assumed equal to tensile strength.

High temperature and humidity condition

The input parameters adopted for the HT condition are presented in Table 6-2. These values were also found from laboratory experiments or the literature.

Table 6-2 Input parameters of the coated BIT model for HT conditions (N/A – Not available)

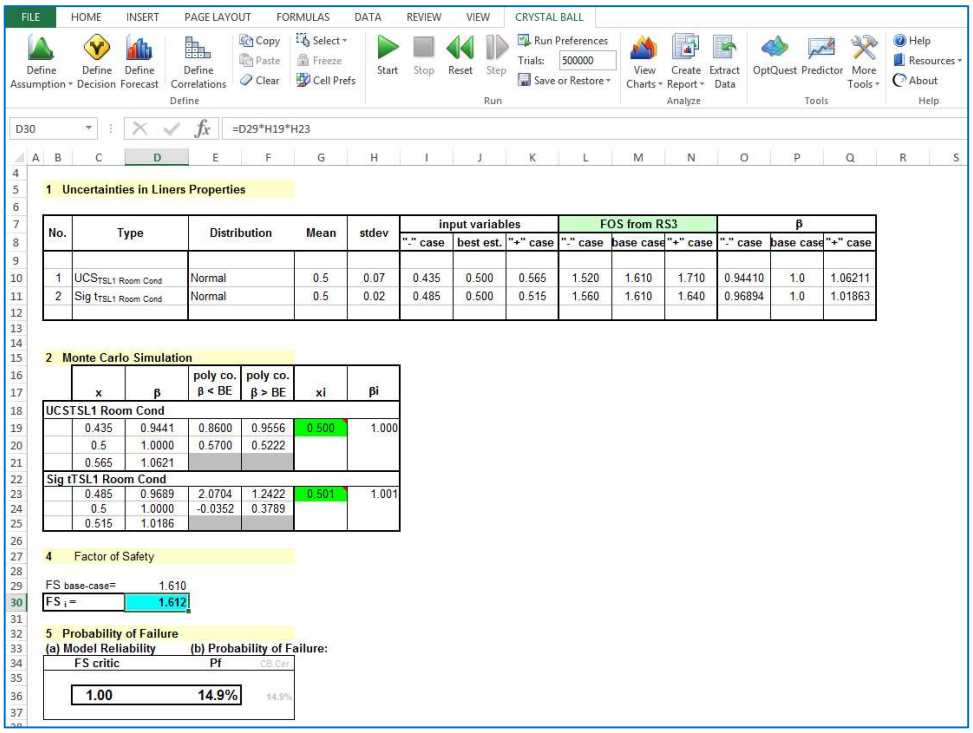
Material inputs	Substrate	TSL
E (MPa)	48650	10010
Compressive strength (MPa)	52	20.1
Poisson's ratio	0.276	0.18
Tensile strength (MPa)	N/A	1.9
Unit weight (MN/m^3)	0.021	N/A
Thickness (mm)	21	5
Shear strength (MPa)	N/A	3.8

Since no shear test was performed during the current work, and knowing that it was the first time that TSL's HT tests were performed, there was no data in the literature to indicate the range of the shear strength of a TSL stored in HT condition. Therefore, its value was assumed slightly less than that from R condition. The information was necessary for the running of the models.

6.2.4 Modelling results

Room conditions

The resulting FoS base case was 1.61. The RSM combinations of the base, negative and positive cases of the chosen TSL variables produced the FoS displayed in the snapshot presented in Figure 6-2.



1 Uncertainties in Liners Properties

No.	Type	Distribution	Mean	stdev	input variables			FOS from RS3			β		
					"-" case	best est.	"+" case	"-" case	base case	"+" case	"-" case	base case	"+" case
1	$UCS_{TSL1\ Room\ Cond}$	Normal	0.5	0.07	0.435	0.500	0.565	1.520	1.610	1.710	0.94410	1.0	1.06211
2	Sig $t_{TSL1\ Room\ Cond}$	Normal	0.5	0.02	0.485	0.500	0.515	1.560	1.610	1.640	0.96894	1.0	1.01863

2 Monte Carlo Simulation

x	β	poly co. β < BE	poly co. β > BE	xi	βi
UCSTSL1 Room Cond					
0.435	0.9441	0.8600	0.9556	0.500	1.000
0.5	1.0000	0.5700	0.5222		
0.565	1.0621				
Sig tTSL1 Room Cond					
0.485	0.9689	2.0704	1.2422	0.501	1.001
0.5	1.0000	-0.0352	0.3789		
0.515	1.0186				

4 Factor of Safety

FS base-case= 1.610

FS_i = 1.612

5 Probability of Failure

(a) Model Reliability (b) Probability of Failure:

FS critic	Pf
1.00	14.9%

Figure 6-2 Snapshot of RSM staging for PoF determination of room coated BIT disc

The reliability assessment outcome provided a PoF of 14.9% that can also be presented in a probabilistic graph as displayed in Figure 6-3.

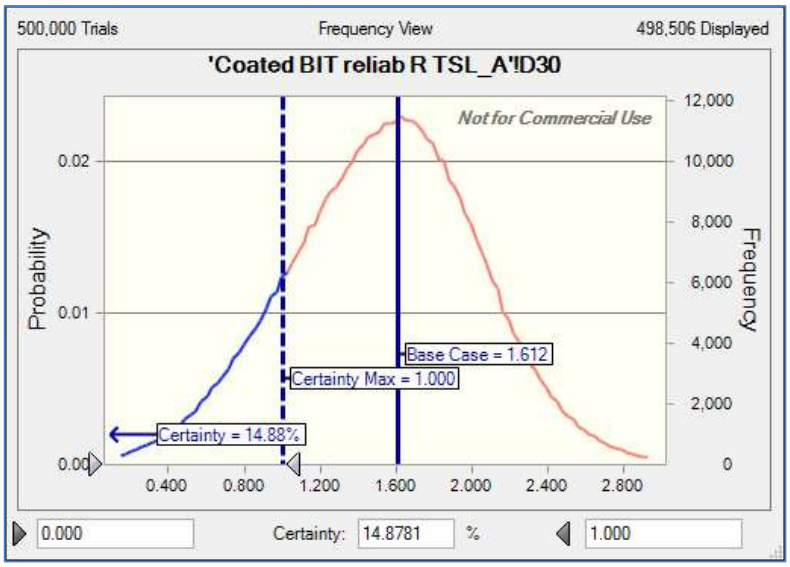


Figure 6-3 PoF chart for Room coated BIT disc created through Oracle Crystal Ball

This obtained PoF will be compared with that from HT condition, and subsequent analyses will be made.

High temperature and humidity conditions

The modelling of the coated BIT disc, with mechanical properties collected from laboratory HT conditions, provided an FoS of 1.15 for the base case. The RSM dictated the determination of a total of 2n+1 FoS, before the generation of the FoS surface through Oracle Crystal Ball that used the Monte Carlo simulation and the determination of the PoF, as shown in Figure 6-4. In this case as well, only the UCS and tensile stress from the coating were considered as variables.

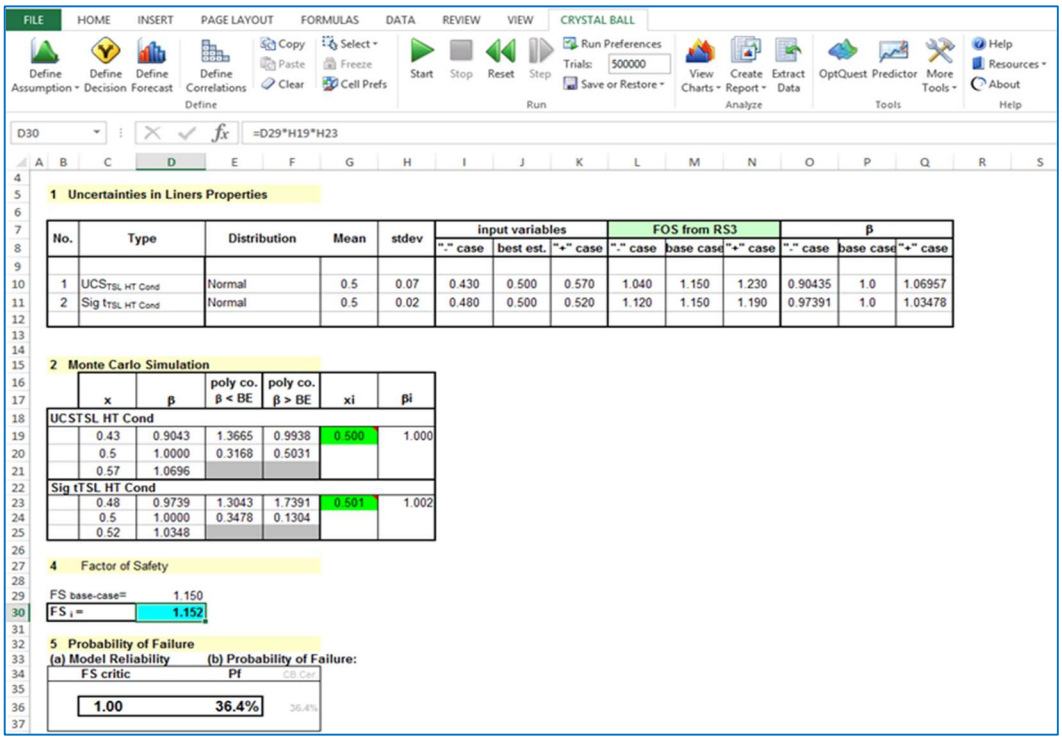


Figure 6-4 RSM staging for PoF determination of HT coated BIT disc

A few of the statistics of the FoS distribution, including the PoF, are presented through the diagram presented in Figure 6-5.

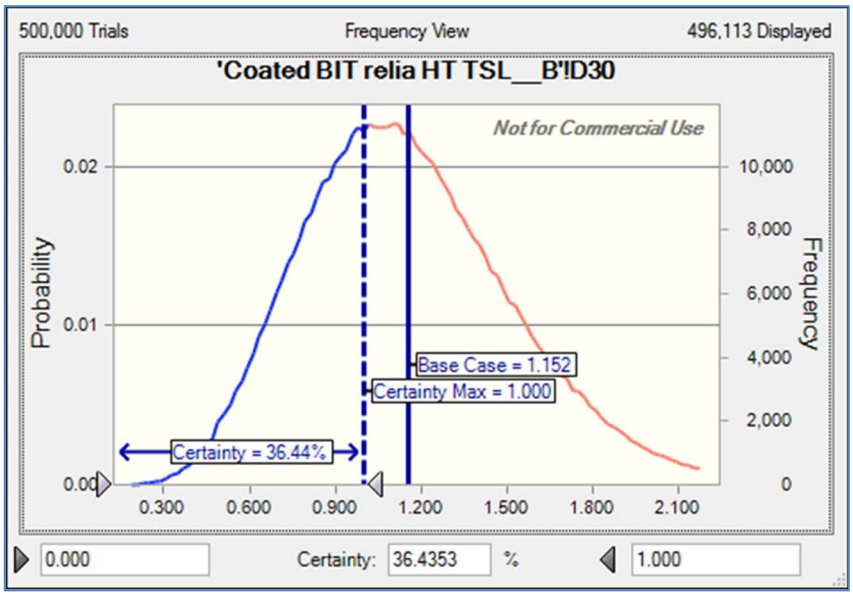


Figure 6-5 PoF chart for HT coated BIT disc created through Oracle Crystal Ball

The obtained PoF of 36.44% is greater by more than twice the value from BIT room condition modelling. The results should significantly influence the geotechnical risk depending on whether the thin liner has been applied in room or high humidity and temperature conditions. And in this instance, the consequences were assumed to be identical from both room and humid failures. Therefore, the comparative study of risk assessments of shotcrete discs coated with TSL1-like materials will only depend on the PoF outcomes. Thus, the risk of those specimens to fail in humid condition is more than twice the resulting geotechnical risk from room condition. And in light of this finding, it is poor practice to design a TSL support for deep mine openings, characterized by humidity and high temperature, based on information collected from room condition behaviours.

6.3 Chapter Summary

The Rocscience package RS3 was used to understand the impact of various environmental conditions on a BIT coated specimen. Shotcrete discs of 42mm diameter and 21mm thick, coated with a 5 mm TSL were modelled. Two types of condition models were set: Room and HT conditions. The input parameters were collected from laboratory testing and calibrated to reflect the real behaviour under realistic stress conditions. The aim was to use numerical modelling as a tool to

determine the FoS, and thus the PoF under various environmental conditions. Risk analysis was also explored to measure the reliability of TSL used as a coating in various environmental conditions that can be encountered in mines. The resulting FoS base case for room conditions was 1.61, and 1.15 for HT conditions. Through the response surface methodology, FoS surfaces were generated through the Excel spreadsheet add-in, Oracle Crystal Ball. Subsequent PoF could then be determined, and were found to be 14.88% for R conditions and 36.44% for HT conditions. With resulting consequences of failure being assumed to be identical for the two scenarios, the probabilistic risk of coated BIT failure in HT conditions was deduced to be more than twice that in room conditions. Based on this, it was found that it is poor practice to resort to TSL for deep underground mine support based on its performance in room conditions, since the supporting capability in humid HT condition is significantly lower than in R condition. TSL should always be trialled according to the environmental conditions of the sites where it is projected to be coated.

CHAPTER 7 DISCUSSIONS

The methodology opted for in this research was threefold, and three different testing methods were also adopted, involving intensive work. The testing methods were carefully chosen to cover as many scenarios as possible so that the outcomes would be as representative as possible. And the converging results supported the validation of the findings.

The fieldwork only concerned two mines. It could be better to assess TSL in more than these two mines and the assessments could be extended to the use of tools such as a dolly for TSL pull-off. However, the latter procedure was not allowed in the visited mines. Another useful parameter could be data on rock mass characterization, and data regarding the in-situ stresses. In this case, only a few data were provided such as the rock mass rating. Geological maps were not provided, which made it difficult to personally assess in-depth the reasons behind the thin coating performances. However, rather than regretting the lack of information or of using assessment tools, the visual assessment proved to be very beneficial since some failed TSLs could still be observed, and the reasons behind the failures could also be requested.

Tensile strength tests, indirect tensile tests and membrane displacement tests were performed on three TSLs under three different environmental conditions. From a study of the relevant literature, it is believed that this is the first time that TSL has been tested for long-term performance in environmental conditions that are similar to those in underground mines. These conditions included the humid (H), and humid and high temperature (HT) conditions. In both cases, Specimens were prepared and initially exposed to normal laboratory conditions for about three days to allow a proper setting before handling them and storing them in their final environmental conditions. Although the ideal exercise could have been to expose these liners to the environmental conditions chosen for assessment immediately after the liners' preparation, the undertaken approach aimed to avoid affecting the integrity of the dog-bone specimens through the processes of storage. It is also

believed that opting for such an approach could not produce weaker specimens than those immediately exposed to H and HT just after preparation. Thus the true H and HT influences on TSL's UTS strength could only be worse than the indications provided by this research. However, more studies are recommended in which specimens should be immediately exposed to these two environmental conditions after their preparation.

The limited number of 25 UTS specimens allocated to each environmental condition, in the ratio of five to six specimens tested per curing time, could have been increased. Nevertheless, the total number of dog-bone specimens was no less than 280, preparation and testing of which were very time-consuming, without accounting the large numbers of specimens prepared and tested for other testing methods adopted in this research. Furthermore, the evaluations of the test results also required much time and effort. Nevertheless, the limited number of tests carried out provided results that are believed to be very important and should constitute a warning to TSL users.

As expected, in the UTS results from TSL performance, TSL1 and TSL2 showed a strengthening trend proportionally to exposure time in room condition, even beyond 28 days. The same expectation was not observed for TSL3, which showed a surprising negative strengthening rate as the time of exposure extended. Although specimen preparation for TSL3 was repeated with thorough care and from complementary supplied bags of constituent materials, the results followed the same trend, showing that the underperformance should be attributed to the nature of the thin liner rather than to the preparation and testing processes. The use of moulding frames produced variability in the results, which could be reduced if the die-cutting technique was opted, as suggested by Guner and Ozturk (2018). However, their suggestions are suitable for ductile thin liners rather than the brittle ones used in this research.

The TSL strengthening ability with exposure time observed in room condition might not be practically observed in rock masses with limited self-supporting

capability. This is because the rock-mass could start deforming before the thin liner effectively cures. Such coating could thus be exposed to stresses at its earlier stage of application, causing it to lose strength with time instead of gaining strength as found from laboratory room testing. In such circumstances, it is recommended that the thin liner be combined with some active support such as rock bolting to oppose early disturbing forces, whilst the curing of the coating is in process.

The use of coated BIT tests in the research could be justified by the fact that this testing method is widely used in laboratory testing. Besides, there was a need to complete the findings by Mpunzi *et al* (2015) who only assessed the specimens in room condition. In the assessment of the effect of coating on shotcrete disc in H and HT conditions, the research included the strength decrease observed on uncoated shotcrete discs when stored in the same conditions. It is believed that the resulting decreases might be due to the friability of the shotcrete rather that the intrinsic loss of strength of this liner. This occurrence should, however, be minimized when the substrate is already coated with TSL, prior to its exposure in H and HT conditions. The reason is that the shotcrete faces would not be affected by the friability. The TSL real strengthening capability should, therefore, be lower than that assessed. But since the BIT applied force is exercised on the circumferential part, still exposed to friability, it was opted to consider the strength behaviour of shotcrete discs in these conditions rather than assuming that the shotcrete behaved as in room-like conditions. However, additional studies should be undertaken to assess the real strengthening capability of TSL when coated to shotcrete discs.

The choice of using shotcrete as a substrate was primarily based on the need to complete the work by Mpunzi *et al* (2015), who resorted to the same material type. And although TSL is mostly directly applied on the rock mass surface which is generally stronger than shotcrete, this latter material is also used in combination with TSL to form “superliners”. Besides, shotcrete could be a very useful soft substrate for creep testing as compared to hard rocks since it could reduce the creep failure time taken in hard rock creep testing.

The assessment of isolated shotcrete and TSL BIT specimens in addition to the coated shotcrete discs was motivated by the need to see how each of these liners behave on their own, which could shed light on the understanding of the overall behaviour of the coated specimens, and also could provide useful information on whether shotcrete could be traded off with TSL. And in this regard, shotcrete has proved to be stronger in resisting indirect tensile forces than TSL. However, this is not the case when the elongation is concerned. This parameter is crucial for the effectiveness of areal supports. And in R and H conditions, TSL has shown higher elongation values at failure than shotcrete. But a contrasting tendency was shown in HT condition, with only TSL3 matching the shotcrete elongation. This reinforces the suggestion to resort to TSL3 in HT condition.

In the MBT testing, the size of the plunger surface that was aimed to be in contact with the liner was chosen according to the provided panel dimensions. Although bigger surface areas of contact could have been chosen to ensure the non-occurrence of point loading failure, such behaviour was not observed with the adopted dimension. Although though small, the adopted dimension was closer to those proposed by Spearing *et al* (2001). In practice, the observation of the detached TSLs has shown that these failed under a combined mechanism of tensile and adhesion loss rather than being pierced through by the plunger. The obtained MBT curves also followed the standard shape indicated in the literature. Accommodating bigger panels in the MTS could make the process more difficult and hazardous if dropped.

The reuse of the shotcrete panels followed the suggestions by Yilmaz (2011) and Kuijpers *et al* (2004) concerning a new or modified testing method. Among other requirements, these authors insisted that the specimens have manageable size, the tests be repeatable, the components involved in the testing offer the possibility of re-usage, etc. However, it was crucial to ensure that the surface of contact was almost in the same conditions for all the tests. Therefore, there was a need to grind it and slightly raze the surface with the diamond saw cutting machine.

The limited number of short-term tested MBT specimens was due to the availability of the panels. At some points, there was a need to wait for scheduled tests to be performed before re-using the panels, which made the overall work very time-consuming. During the MBT specimen preparations, care needed to be taken in preparation of the surface of contact and in obtaining adequate TSL thickness. This particular parameter needed to be thoroughly measured for a fair comparative study. Doing so required at least a minute per specimen. If only one person was doing the preparation, this meant that 10 minutes later, only a maximum of 10 specimens could be prepared, since some TSL mixtures could start setting in less than 10 minutes after preparation, or at minimum, their texture might suffer some depreciation. Thankfully, time constraints could be overcome through the assistance of a second operator.

The need for standardization of the MBT method through the proposal of some indices such as the MBTS and the MCS, which take into account the containment force (K) and its extent (I), are just preliminary suggestions to what is believed to be useful studies capable of producing reliable and comparative MBT performing indices. Some difficulty was encountered in finding common and unarguable grounds for defining the containment force, since each MBT curve is identical. Therefore, the proposed tips are believed to be helpful, though subject to improvement with complementary studies.

As introduced earlier in this research, it was difficult to expose the MBT panels under HT conditions. The space offered by the oven did not allow the storage of many panels, which had to be simultaneously plunged into water. Nevertheless, small numbers of these specimens could be stored in this condition and showed results that obeyed the expectation, and were in line with the results found in other testing methods. However, these results could not be displayed in this research because they were preliminary and limited in number. Therefore, in-depth tests are recommended, and these should concern the short-term testing of MBT specimens exposed in HT condition.

Concerning creep testing, intensive work of calibration and validation of the creep machines was imperative — as it should be for any new equipment. The time-consuming work included the following aspects:

- Conception and design of the creep machines and their construction
- Validation of the loading parameters
- Wiring of the Wheatstone bridge configuration
- Making of the displacement transducers as well as their continual assessments to ensure that their gauges were still performing as initially assessed and did not suffer any fatigue. In the case of fatigue, replacement of gauges was required, needing a repeat of the whole process of calibration, validation and continual assessment
- Testing times that can extend beyond three months, such as observed during some BIT testing
- Time wasted for outlier creep results due to inconsistency of the strain at failure or of the proportionality between the percentage loading and the time at failure, resulting in discarding the whole test, etc.

The option of assessing the whole transferring load factor rather than undertaking a study based on Mechanics' principles was chosen as being more practical. The chosen study method took into account parameters that could be missed or misjudged if processed through Mechanics' principles. And above all, the very high value of the coefficients of determination validated the weighing calibration.

It was opted to determine the creep loadings that should correspond to the ultimate strength. Although these values could be borrowed from the short-term results, the exercise was not a waste of time, but rather assisted to ascertain the true loading values, and could also be used as a validation of means of the loadings assessed through short-term testing.

Although commercially available displacement transducers should be ideal for the tests, none was logistic available during the testing period. Thus, simple-to-use transducers that were able to record very small displacements needed to be

conceived. Strain gauges were glued on small rectangular steel sheets that could elastically bend following the specimen elongations. The calibration and validation of these displacement transducers was also imperative. Although the initial results of calibration showed high values of the coefficient of determination, the process was frequently repeated to assess whether the gauges did not suffer from any fatigue, which could lead to the transducers' replacement.

The limitation of creep testing to only R and H conditions without the HT condition was a concern. It would have been ideal to proceed with all the environmental conditions exploited during short-term testing. And as mentioned in the previous paragraph, the use of licensed and adequate transducers that are capable of performing in high temperature conditions without impacting on the data collection is recommended. Nevertheless, the previous short-term tests have all concluded that the HT condition is equally or more prejudicial to TSL performance than the H condition. Thus, the results obtained from the H condition could constitute a solid basis of evaluating TSL's long-term performance in deep underground mines, while appropriate HT creep tests could still be performed.

The grips used for UTS displacement transducers were adjusted to not impact on specimen failure. Any specimen that could not break in the gap between the grips was discarded. This included the specimens that broke at the contact points between the grips and the dog-bone specimens. In addition, the use of spring steel materials in the making of the displacement transducers helped to avoid the risk of these transducers affecting the liner displacement.

The observed trend of TSL capacity to accommodate larger deformations inversely proportional to the UTS creep loads was unanimous in humid condition but not in room condition. And although additional trials could be recommended, that inconsistency was dissipated in MBT creep testing, where the same trend was fully observed. This trend can also be explained in the sense that a thin liner that is under static loading can deform to its full potential before failure, unlike a liner that is subjected to dynamic loading. Nevertheless, the trials were solely performed on one

type of TSL, and there is a need to assess other types of TSL for validation of the finding.

The UTS long-term strength of 17% in humid condition was judged very low and not beneficial. In effect, to design a liner that will only be capable of offering that percentage of full TSL-designed-strength seems to be a waste, knowing that there are other areal supports such as the wire meshing or probably other TSL types that can perform better than this. However, 56% of long-term strength in room-like conditions justifies TSL1 utilization after further study on the purpose and geotechnical conditions of the support.

Out of 389 specimens prepared for all the BIT tests, only 49 specimens were used for creep tests. The relatively small number was caused consequence of the extended running time generally observed for this method of testing. This was the most time-consuming creep testing method, evidenced by the longer failure time for permanent strength. To effectively obtain enough information from this testing method, it was imperative to make a total of three creep testing machines instead of only one as observed for each of the remaining testing methods. This was, however, a delaying task but beneficial in finally getting enough conclusive data.

The long-term strengths encountered from BIT creep tests represented 67% in room condition and 40% in humid condition of the ultimate strength obtained in room condition. These values are higher than those obtained from UTS creep tests. Actually, the UTS long-term strength values only applied to TSL performance, whereas the BIT values also incorporated the substrate performance. Therefore, the obtained long-term strength values from the coated BIT should not be classified on their own, but always in conjunction with the substrate for strength gain. That is why it was imperative to undertake a more representative assessment that was completely directed on the TSL's performance.

Another limitation of the BIT creep tests concerned the inability to monitor the horizontal strains until failure. The grips were placed horizontally, each at about 5

mm from the centre, but could not help to monitor the displacements. A better option could have been the resort to strain gauges glued on specimens, but this option was not adopted for two reasons: it is believed they strengthen the BIT specimens, and the required quantity of gauges to cover all the tests was not available.

It could have been ideal to assess the long-term performance of uncoated shotcrete discs in addition to the coated ones. This could assist in determining the true impact of the coating on the substrates. But this work could require extra intensive time because of need to wait for finalization of the coated BIT tests or need to make other BIT creep machines. The timing to complete this research could not allow the performance of those tests. But the comparative study of the coated BIT specimens tested in R and H conditions helped to understand the impact of the coating, of course with some assumptions made on the substrate behaviour based on the short-term test outcomes. And as stated before, the resort to MBT tests was a great contribution to providing the missing results.

The MBT long-term strengths obtained from the room and humid trials were respectively equal to 48% and 28% of the ultimate MBT strength assessed in room condition. These results are more decisive than those obtained from UTS creep tests since they are representative of true TSL behaviour. The UTS creep tests were made on isolated dog-bone specimens rather than on TSL coated rock of shotcrete, as occurs in practice. Therefore, based on the MBT creep results, it could be said that TSL has a limited ability to perform as permanent support of a deforming rock mass in room condition. The outcome was more alarming in humid condition. And it could be worse when the trials are performed in humid and high temperature condition. Based on the findings, it was concluded that designing support that will only be able to perform at less than a third of its full capacity, should not be recommended for deep underground mines, unless combined with other mining supports. However, this suggestion is based only on TSL1 performance, and additional tests on other TSL types are needed to provide knowledge of this type of mining support.

The numerical modelling process was carried out using the Rocscience finite element method package RS3 after collecting some characteristic properties of the involved materials. When needed, some assumptions were made. The coated BIT modelling was run after assuming that the material properties of the substrate were equivalent in either R or HT conditions. Although this practice did not obey to the results obtained from laboratory testing, which showed a decrease in BIT strengths of shotcrete in HT condition, the assumption was dictated by the need to determine the extent of TSL behaviour when exposed to HT conditions for a long period, and not to study the shotcrete behaviour in such conditions.

It was opted to model only TSL1. This liner was the most used as observed during the mine visits and its resulting behaviour was balanced compared with the other two liners. However, the findings from the numerical analyses and the associated risks should only concern the TSLs with characteristics similar to TSL1. Additional studies are recommended on TSLs with characteristics and behaviours different from TSL1.

Another assumption was made in the setting of the response surface methodology through the consideration of only two variables: the TSL's uniaxial compressive and tensile strengths. These were also assumed to be normally distributed. The ideal option would have been to also assume the shear strength as a variable, but the employed modelling package did not offer the possibility to input and vary this liners parameter. This might have been automatically assumed in the program, based on other input parameters. However, an in-depth study should consider as many variables of the thin liner as possible. And this could be performed by resorting to other modelling software that offers options to include these parameters. Moreover, statistics of the liner properties should be undertaken, when possible, to resort to their real distributions. But since this study was a comparative analysis, the normal distribution assumption did not affect the outcomes since it applied to all the scenarios.

CHAPTER 8 CONCLUSIONS AND RECOMMENDATIONS

Long-term performance of TSL in underground mines was assessed through field assessments, laboratory testing, and numerical modelling analyses. It was noted that thin coatings can be encountered under various product and application categories, though essentially grouped into ductile and brittle materials. Their performance was mixed, and the causes of the underperformance could not be attributed to an isolated factor, but rather to a combination of negative triggering parameters, which are related to the TSL characteristics, the conditions of application, the environmental conditions, etc. The latter parameter was very influential on TSL performance and should be considered when designing mine supports that include the usage of multi-component polymeric materials. However, various types of TSLs characterized by a variety of the matrix and the fibres should be assessed to investigate whether they could behave differently. Nevertheless, specific in-situ conditions such as temperature, humidity, substrate conditions, in-situ stress concentrations, presence of hypersaline waters, etc. should be included in laboratory testing that aims to assess TSL behaviour prior to its application in those conditions.

From the field assessment, TSL showed mixed results. This was particularly evidenced by the discrepancy between the high rating of TSL performance provided by suppliers and manufacturers, and the moderate rating provided by mine technicians and personal observation. If the suppliers encourage the use of TSLs even in relatively critical geotechnical conditions, the personal observations showed that TSL generally behaves well in zones with less geotechnical disturbance. Thus, in mining conditions with stability issues and possible risks of fall of ground, it was noted that this liner was usually combined with other passive and active supports. And although the overall underperforming causes of TSL cannot be attributed to a single parameter, most of the visited thin liners showed alarming performances when the humid condition was characteristic of the sites. And to remediate this incapacity of supporting wet sidewalls, white-wash materials were used at some sites, but their mechanical properties need to be thoroughly investigated. The water-based thin liner was the best performing TSL in humid

condition. This type of liner should be recommended for humid environmental conditions. The approach of deep and shallow mines could not bring a clear demarcation on where TSL was best-performing. Neither could the age of the performing thin liners be used as a decisive index to characterize a TSL's good performance, since some younger TSLs showed poor performance, which was probably linked to other factors such as conditions of preparation and application rather than the performing time.

Laboratory testing of three available TSLs called TSL1, TSL2 and TSL3 were performed on the MTS 643 for short-term trials. The results of these tests, which were performed in a "standard" laboratory condition, confirmed the property of TSL strengthening proportionally to curing time. This strength gain could be observed even beyond the conventional 28 curing days. However, there were some exceptions such as those observed on the strengthening behaviour of TSL3, which could lose strength in room conditions. Besides the standard laboratory testing condition, here called room (R) condition, the thin liners were plunged in containers of tap water to simulate a humid or saturated (H) condition. These containers of water were also stored in an oven conditioned at 50°C to simulate the combined humid-and-high-temperature (HT) condition. It is recognised that submerging the specimens to achieve an HT condition is an extreme approach not representative of the real conditions. However, it was adopted because it was simple, and would easily enable tests to be carried out to provide an indication of TSL performance under HT conditions. H and HT conditions showed average to poor TSL strength performances, except for TSL2 which still exhibited good performance after being exposed to the humid condition. Three main short-term laboratory tests were undertaken after exposure of the respective specimens in the cited environmental conditions: These tests were the uniaxial tensile strength (UTS), the Brazilian indirect tensile (BIT) test and the membrane displacement test (MBT).

A total of 280 UTS specimens were tested on the MTS 643 model after being exposed to R, H and HT conditions for periods up to 112 days. The strength trends showed that TSL1 could gain strength in all three environmental conditions, but

with a higher strengthening rate in R condition and a moderated rate in H and HT conditions. Therefore, H and HT conditions were found to prevent TSL1 from performing highly, such that this performance could be reduced to half the UTS values obtained in R condition. TSL2 followed the strengthening trend of TSL1 in R condition. However, unlike TSL1, TSL2 still showed considerable strength increment in H condition before displaying a negative strengthening rate in HT condition. The strength analysis of TSL3 showed that this thin liner was the least effective out of the three. It surprisingly displayed a negative strengthening rate even in R condition. However, its negative strengthening rate produced in HT condition was less alarming. Therefore, the assessment of these three liners results in the suggestion to use TSL1 in underground conditions that are similar to R conditions and TSL2 in humid-like underground conditions. TSL3 could be used in HT underground conditions only when there is a need for a thin liner application. Above all, the use of any TSL should be based on its ability to perform in a particular condition that can encompass various factors from environmental to geotechnical. The findings from UTS long-term tests will be developed later.

The BIT testing method was performed on no less than 389 specimens that included TSL discs and coated and uncoated shotcrete discs. The conditions of testing were similar to those used for the UTS tests. The aim was to query the impact of the environmental conditions on TSLs when these are coated on a substrate and are subjected to tensile forces. The result trends obtained for UTS R condition were also found for all the BIT specimens tested in the same environmental condition. The positive behaviour of the water-based TSL2 observed in UTS H tests was also displayed in BIT humid condition testing that involved TSL2. The rest of the BIT specimens could not resist the weakening effect of the humidity condition. The confirmation of the negative impact of the HT condition on TSL performance was also recorded after assessing all the BIT specimens under this environmental condition. Practically, it was noted that the highest contributions of the three liners in strengthening the shotcrete substrates were: 21.1% of strength increase in R condition for TSL1, 23.1% in H condition for TSL2 and 18% in HT condition for TSL3. Therefore, although H and HT conditions are problematic for most of the

TSLs, since they lower their strengths relative to those produced in R condition, TSL1 could be recommended for use in R conditions, TSL 2 in H conditions, and possibly TSL3 in HT conditions.

In addition to the two described short-term testing methods, there was a need to perform a more representative short-term testing method to assess the influence of various environmental conditions on TSLs after a significant long exposure time. The MBT testing method was adopted for that purpose. Although this testing method is not yet standardized, it was a means to simulate the combination of mechanisms encountered while a thin liner is "pushed", as can happen to a thin coating in an underground excavation. A total of 112 specimens were prepared and tested following the testing conditions described for the two previous short-term testing methods. Based on the peak strengths, the results corroborated the previous findings that R condition is favourable to TSL strengthening proportionally to exposure times, while H and HT conditions prevent the thin coatings from performing as successfully as in R condition, an exception being the water-based liners. The analyses of the MBT curves were also done after suggesting new parameters that were believed to better describe the behaviour and also be capable to be determined in other similar tests. These parameters were the membrane displacement test strength (MBTS) and the moment of the containment strength (MCS). MBTS represents the ratio of the initial peak load to the contact point area between the plunger and the thin liner, while MCS is the product of the maximum vertical displacement of the plunger and the ratio of the containment load to the initial peak load. These two parameters should be optimally combined in the assessment of MBT performance. The MBTS considers the TSL's ultimate bearing strength, while the MCS considers the TSL's capacity to contain the disturbing load. The optimization of the MBTS and MCS values produced results that aligned with the findings that TSL1 should be preferred in R condition, TSL2 in H condition and TSL3-like materials could be adopted for HT condition. Although these parameters are only suggestive and should be investigated in depth, their outcomes were aligned with the previous ones.

From the UTS creep tests it was found that, when the tests are performed in room condition, TSL can accommodate larger deformations than those shown in relatively short-term testing. This finding was also observed in humid condition, but with the overall strain being smaller than in room condition. Therefore, a creep test is more likely to allow a TSL to reach its full containment ability than what can be allowed by the laboratory short-term tests. This finding works in favour of the practical use of TSL in underground mines. Nevertheless, it was suggested that additional creep trials be performed to investigate some inconsistency in the strain behaviours and the containment capacity of TSL in underground-like conditions. The long-term performance of TSL1-like liners in humid underground mines was found to be very low. Actually, the UTS long-term strength in humid condition only represents 17% of the ultimate strength found in laboratory room condition. It is believed that in humid condition, other areal supports such as the wire mesh and probably the TSL2-like liners can offer better long-term support than TSL1-like liners. But if the environmental condition of the underground sites where TSL is to be applied is similar to the room condition, the TSL1-like liner might be resorted to for long-term support since it offers about 56% of the ultimate strength in the same condition. But this choice should be made by the support designer based on the predicted mobilized rock masses.

As in the findings from UTS creep tests, MBT creep tests also displayed a TSL behaviour with more ability to accommodate large deformations proportionally to the testing time and inversely proportional to the creep load magnitudes. BIT shotcrete specimens were coated with TSL1 and showed an ultimate strength tested in room condition of 6.37MPa, while that tested in the humid condition represented 74.5% of this value. Assessing the ability of employing TSL1-like materials for permanent support, it was found that this thin liner was capable of providing permanent support only if, in room condition, the driving load was less than 67% of the ultimate strength, and in case of humid condition, this load should not be greater than 40% of the ultimate strength tested in room condition. In the case of the MBT creep testing, the ultimate strengths were 1.46MPa from room condition and 0.91MPa from humid conditions. Their corresponding long-term strengths were

estimated to be respectively equal to 48% and 28% of the room ultimate creep strength. The findings from the tests, with emphasis on the representative method, show that TSL1-like materials are underperforming in underground mine-like conditions, and they should not be recommended as standalone permanent supports in such conditions unless combined with other mine supports. Nevertheless, the results might be different for other types of TSLs. Thus, it is suggested that additional creep tests be performed on other types of TSLs, such as TSL2 in H condition, TSL3 in HT condition, or several other TSLs, including the ductile thin coatings.

The outcomes from numerical modelling through modelling of a coated shotcrete disc showed that humid condition is likely to produce a PoF that is more than twice that for room conditions. It is assumed that a similar extent of consequence would be obtained when testing an identical BIT model in room and humid conditions. The magnitudes of assessed risks were proportional to the calculated PoF. Therefore, it is suggested to avoid the use of parameters obtained in normal laboratory TSL tests for the design of thin coatings destined for use in deep underground mines.

CHAPTER 9 FRAMEWORK TO A GUIDELINE FOR TSL'S LONG-TERM PERFORMANCE

There exist a significant number of guidelines for TSL utilization in the mining environment. A few have been presented in the literature review, and among them are those proposed by Kuijpers *et al* (2004) and EFNARC (2008). However, a few more guidelines will be proposed or recalled to emphasizing the cares required for optimization of TSL benefits when coated for long-term performance in underground mines. The following list of suggestions could further be used as additional guidelines of TSL long-term utilization in underground mines:

- To expect better TSL performance, the preparation of the mixture and the obtaining of the adequate texture should be realized within the recommended timing, which varies from one TSL to another (Yilmaz, 2011).

- Since there might exist a variety of TSL products from one manufacturer, each of these having their unique performance characteristics, mines must be aware of their performances and limitations (Kanda and Stacey, 2019)

- In UTS tests, the alignment of the specimen with the pull direction by the grips should be thoroughly observed to avoid any rotary motion. Thus, only the acceptable margin of misalignment that can be compensated by the self-aligning grips should be accepted (Guner and Ozturk, 2016a)

- The UTS testing speed of TSL should be set based on the nature of each thin liner to allow the rupture to occur within 0.5 and 5 minutes of testing (Guner and Ozturk, 2016a)

- The environmental conditions in the zones where thin membranes have been applied have an impact on their performances (Guner and Ozturk, 2018). The recommendation will be to resort to only a thin liner with no altering

characteristics when applied in such conditions. Among the environmental factors that are influential to TSL good performances are humidity and temperature at the time of specimen preparation and during the testing process (Kanda and Stacey, 2019)

- Since rock temperature, air temperature, and relative humidity can hinder better performance of some TSLs, a relationship between them should be put into consideration if one aims to improve the performance of the thin liners (Espley *et al*, 2001 in Potvin *et al*, 2004b)

- When a superliner, which is a combination of shotcrete and thin coating, is opted for underground mine support, one should consider a longer curing time of the shotcrete and ensure that it is moisture-free before the thin liner application (Espley *et al*, 2001 in Potvin *et al*, 2004b)

- In underground openings characterized by a wet or humid footwall, application of TSL at lower parts of the sidewalls should be avoided. Therefore, it may be advisable to only apply TSL coatings above the sidewall's grade line or from about one metre upwards. The use of calcimine product, also called white-wash, could be recommended for application at the lower sections of the sidewalls, but the mechanical properties of these materials should be well-investigated (Kanda and Stacey, 2019)

- Care should be taken to not mix some hydrophobic TSLs with water at the time of preparation and application. The reason is that some TSLs are not water-based materials, thus are prone to quality degradation once mixed with water (Kanda and Stacey, 2019)

- A TSL substrate must be clean, rid of loose dirt and permanently dry. This is the only means for the liners to achieve a better adhesive condition and thus, to equip them with high capacity of bearing rock mass loads (Espley *et al*, 2001 in Potvin *et al*, 2004b)

- One of the challenges in testing TSL has been the inability to maintain a constant thickness. In light of this, it is suggested that a range of thicknesses be assessed during a defined laboratory testing project of TSL, and the respective ranges of outcomes be recorded, so that the worst-case might be included in further support design projects. If laboratory assessments of TSL with a specific thickness are adopted, it is advisable to undertake additional trials that follow the same settings, but at large scale and by ensuring that the coating be sprayed at irregular thickness to mimic the underground coating conditions for more representative results (Kanda and Stacey, 2019).

- With the aim of producing more representative results of TSL performances, it is recommended that not only selective TSL samples be supplied for laboratory testing. In effect, in addition to the preliminary tests done on newly introduced TSLs, laboratory assessments should also be performed, and repetitively, on TSLs sampled from the large quantities that have already been supplied to the mines and have been stored there before their application. This processing mode should provide more clarity on the true performance of TSLs. It can also assist the mines in assessing the storage conditions and the consistency of the quality of the thin liners before their utilization. This essentially comprises quality control of TSL products, which should be frequently undertaken (Kanda and Stacey, 2019)

- A TSL material that is chosen to replace mesh and bolt supports requires high values of tensile and adhesive strength, such that their values should be greater than 5 MPa or between 0.5 and 1 MPa, respectively (Espley *et al*, 2001 in Potvin *et al*, 2004b)

- Since the ability of a TSL to support the rock mass depends on the load of the rock mass, the number of mobilized blocks and the magnitude of their displacement within the rock mass, these thin membranes should not be

applied as sole structural supports in zones with excessive numbers of mobilized blocks (Kanda and Stacey, 2019)

- Thin membranes are reported to work well in slot-and-slash mining but are not recommended in vertical retreat mining (VRM) top sills since blasting repeatedly causes blowback (Espley *et al*, 2001), unless a full economical study is undertaken first (Potvin *et al*, 2004b).

REFERENCES

ACT LVDT Displacement Transducer. (n.d.). Retrieved 21 November 2019, from https://www.rdpe.com/usm/act.htm

Annual reports—Minerals Council South Africa. (2018). https://www.mineralscouncil.org.za/industry-news/publications/annual-reports

Archibald, J. F. (2001). Assessing acceptance criteria for and capabilities of liners for mitigating ground falls. *Mining Health and Safety Conference*, Sudbury, Ontario, 1–31.

Archibald, J.F. (2004). Canadian laboratory and field testing. *Surface Support in Mining Australian Centre for Geomechanics*, 135–139.

Archibald, J. F., & DeGagné, D. O. (2000). Recent Canadian Advances in the application of spray-on polymeric linings. *Mining Health and Safety Conferenc*e, Sudbury, Ontario.

Archibald, J., Mercer, R., & Lausch, P. (1992). The evaluation of thin polyurethane surface coatings as an effective means of ground control. *Rock Support in Mining and Underground Construction: Case Studies*, 105–115.

ASTM Committee D-20 on Plastics. (2010). Standard test method for tensile properties of plastics. *ASTM International.*

ASTM D-638. (2010). Standard Test Methods for Tensile Properties of Plastics. *ASTM International, West Conshohocken, PA*.

Bieniawski, Z. (1967). Mechanism of brittle fracture of rock: Part II—experimental studies. *4*, 407IN13409IN15419-408IN14418IN18423.

Biffi, M., Stanton, D., Rose, H., & Pienaar, D. (2007). Ventilation strategies to meet future needs of the South African platinum industry. *Journal of the Southern African Institute of Mining and Metallurgy*, *107*(1), 59–66.

Boeg-Jensen, P., & Swan, G. (2014). The operational and laboratory aspects of a thin spray-on liner. In *Proceedings of the Seventh International Conference on Deep and High Stress Mining.* Australian Centre for Geomechanics. 241–251.

Borejszo, R., & Bartlett, P. (2002). Tunnel guard in the mining industry. *2nd Int. Seminar on Surface Support Liners: Thin Sprayed Liners, Shotcrete, Mesh*, Sandton, South Africa.

Bowden, R. K., & Curran, J. (1984). Time-dependent behaviour of joints in Shale. *The 25th US Symposium on Rock Mechanics (USRMS).* American Rock Mechanics Association, 320-327.

Cao, P., Youdao, W., Yixian, W., Haiping, Y., & Bingxiang, Y. (2016). Study on nonlinear damage creep constitutive model for high-stress soft rock. *Environmental Earth Sciences*, *75*(10), 900.

Chiwaye, H., & Stacey, T. (2010). A comparison of limit equilibrium and numerical modelling approaches to risk analysis for open pit mining. *Journal of the South African Institute of Mining and Metallurgy*, *110*(10), 571.

Covscale. (n.d.). *DEE-A Alloy Steel S Type Load Cell 50kg—20T*. Coventry Scale Company. Retrieved 21 November 2019, from https://www.coventryscale.co.uk/s-type-load-cell/

Dirige, A., & Archibald, J. (2009). Numerical modeling simulations of spray-on liners support potential in highly stressed and rockburst prone rock conditions. *Proc. 3rd Canada-US Rock Mechanics Symposium*. Canadian Rock Mechanics Association, Toronto, 1-9

Donoghue, A. (2004). Occupational health hazards in mining: An overview. *Occupational Medicine*, *54*(5), 283–289.

Drescher, K. (2006). *An investigation into the mechanisms of time-dependent deformation of hard rocks. Doctoral dissertation, University of Pretoria.*

Drescher, K., & Handley, M. (2003). Aspects of time-dependent deformation in hard rock at great depth. *Journal of the South African Institute of Mining and Metallurgy*, *103*(5), 325–335.

EFNARC. (2008). Specification and guidelines on thin spray-on liners for mining and tunnelling. *European Federation of National Associations Representing producers and applicators of specialist building products for Concrete*.

Espley, S., Gustas, R., Heilig, J., & Moreau, L. (2001). Thin spray-on liner research and field trials at INCO. In *International Seminar on Mine Surface Support Liners.* Australian Centre for Geomechanics, Perth, Australia, *25*, 1–23.

Espley, S. J., O'Donnell, J., Thibodeau, D., & Paradis-Sokoloski, P. (1996). Investigation into the replacement of conventional support with spray-on liners. *CIM Bulletin*, *89*(1001), 135–143.

Espley, S., Tannant, D., Baiden, G., & Kaiser, P. (1999). Design criteria for thin spray-on membrane support for underground hard rock mining. *Canadian Institute of Mining and Metallurgy Annual Meeting*. Calgary.

Espley-Boudreau, S. J. (1999). Thin spray-on membrane support and implementation in the hardrock mining industry. *Master's Thesis, Laurentian University,* Sudbury, Ontario, Canada.

Finn, D. (2001). Polymer Membrane Tests. *Surface Support Liners: Membranes, Shotcrete and Mesh.* Australian Centre for Geomechanics, Australia. *Sect*, *20*.

Finn, D. (2004). Thin Spray-on Liner Tests. *Surface Support in Mining*. Australian Centre for Geomechanics, Perth, Australia, 89–95.

Finn, D., Teasdale, P., & Windsor, C. (1999). In situ trials and field testing of two polymer restraint membranes. *Rock Support and Reinforcement Practice in Mining,* Balkema, Rotterdam, 139–153.

Gay, N., & Jager, A. (1986). The influence of geological features on problems of rock mechanics in Witwatersrand mines. *Mineral Deposits of Southern Africa*, 753–772.

Golser, J. (1977). The New Austrian Tunnelling Method (NATM) Theoretical background-practical experience. *Special Publication*, *54*, 323–347.

Guner, D., & Ozturk, H. (2016a). Experimental and Numerical Analysis of the Effects of Curing Time on Tensile Mechanical Properties of Thin Spray-on Liners. *Rock Mechanics and Rock Engineering*, 1–18.

Guner, D., & Ozturk, H. (2016b). New Performance Criterion for Thin Spray-on Liners: Tensile Toughness. *50th US Rock Mechanics/Geomechanics*

Symposium, American Rock Mechanics Association, Houston, USA, 26–29

Guner, D., & Ozturk, H. (2017). Tensile-Creep Test Specimen Preparation Practices of Surface Support Liners. *IOP Conference Series: Earth and Environmental Science*, *95*, 042004. https://doi.org/10.1088/1755-1315/95/4/042004

Guner, D., & Ozturk, H. (2018). Creep behaviour investigation of a thin spray-on liner. *International Journal of Rock Mechanics and Mining Sciences*, *108*, 58–66.

Guner, D., & Ozturk, H. (2019). Finite element simulation on tensile creep behaviour of underground support liner. *Machines. Technologies. Materials*, *13*(10), 417–420.

Gyenge, M., & Coates, D. (1972). The support mechanism of sprayed thin linings. In *Proceedings Eighth Canadian Rock Mechanics Symposium,* Toronto, Canada, 101–117.

Haile, A. T. (1999). A mechanistic evaluation and design of tunnel support systems for deep level South African mines. *Doctoral Dissertation, University of Natal*.

Hawker, R. (2001). Tekflex—New areas of application. *Surface Support Liners: Membranes, Shotcrete and Mesh. Australian Centre for Geomechanics, Perth (Sect. 17)*.

Henderson, N., & Louw, D. (2001). *Underground performance of Mondi® RockHold™ a structural membrane*. *Sect. 28*.

Hepworth, N., & Lobato, D. (2002). Tekflex resin spray field trials – Neves Corvo Mine, Portugal. In *2nd Int. seminar on Surface Support Liners: Thin Sprayed Liners, Shotcrete, Mesh*. Crowne Plaza Sandton, RSA. *Sect. 19*.

Hoek, E., Kaiser, P. K., & Bawden, W. F. (2000). *Support of underground excavations in hard rock*. CRC Press.

Hoffmann, K. (1974). *Applying the Wheatstone bridge circuit*. HBM Germany.

Hudson, J. A., & Brown, E. T. (1972). Studying time-dependent effects in failed rock. In *The 14th US Symposium on Rock Mechanics (USRMS)*. American Rock Mechanics Association. 25–34.

Hudson, J. A., & Harrison, J. P. (2000). *Engineering Rock Mechanics: An Introduction to the Principles*. Elsevier.

ICTUS. (n.d.). *Mining Equipment: Lubrication Equipment*. Retrieved 19 January 2018, from http://ads.easyinfo.co.za/htm/clientproofs/ictus/tsc.html

ISRM. (2007). *The complete ISRM suggested methods for rock characterization, testing and monitoring: 1974-2006*. International Soc. for Rock Mechanics, Commission on Testing Methods.

Kanda, M.J, & Stacey, T.R. (2016). The influence of various factors on the results of stability analysis of rock slopes and on the evaluation of risk. *Journal of the Southern African Institute of Mining and Metallurgy*, *116*(11), 1075–1081.

Kanda, M.J, & Stacey, T.R. (2019). Review of the practical effectiveness of thin spray-on liners based on information from suppliers and observations from the mining industry. In *Proceedings of the First International Conference*

on Mining Geomechanical Risk. Australian Centre for Geomechanics, Perth, Australia, 443–458.

Kanda, M.J, & Stacey, T.R. (in press). Tensile strength sensitivity of thin spray-on liners to changes in environmental conditions. Accepted for publication in *Journal of the Southern African Institute of Mining and Metallurgy* on 17 February 2020.

Kanters, M. J., van Erp, T. B., van Drongelen, M., Engels, T. A., & Govaert, L. E. (2017). Loading rate dependence of failure strength as predictor for the long-term performance of thermoplastic polymeric products. *Polymer Testing*, *59*, 177–184.

Kolařík, J., & Pegoretti, A. (2008). Proposal of the Boltzmann-like superposition principle for nonlinear tensile creep of thermoplastics. *Polymer Testing*, *27*(5), 596–606.

Komurlu, E., Kesimal, A., & Colak, U. (2014). Polyurea type thin spray-on liner coating to prevent rock bolt corrosion. In *ISRM International Symposium-8th Asian Rock Mechanics Symposium*. International Society for Rock Mechanics and Rock Engineering.

Kuijpers, J. (2004). Evaluation of thin spray-on liners support behaviour. *Surface Support in Mining*, 103–112.

Kuijpers, J., Rangasamy, T., & Sellers, E. (2004). Performance and design of thin sprayed liners as rock support in mine tunnels. *1st Proceeding, SANCOT*, 1-15

Kuijpers, J., Sellers, E., Toper, A., Rangasamy, T., Ward, T., Van Rensburg, A., Yilmaz, H., & Stacey, R. (2004). Required technical specifications and

standard testing methodology for thin sprayed linings. *SIMRAC Project SIM*, *20206*.

Kyowa Electronic Instruments Co., Ltd. (n.d.). *What's a strain gage?* https://www.kyowa-ei.co.jp/english/products/gages/pdf/whats.pdf

Lacerda, L. (2004). Shotcrete and other surface support liners. *Preprint*, *04–36*, 23–25.

Lacerda, L., & Rispin, M. (2002). Current ground support membrane applications in North American underground mines. *SME Annual Meeting*, Phoenix, ASME Preprint.

Laurence, D. (2001). Membrane trials at an Australian Underground coal mine. *Surface Support Liners: Membranes, Shotcrete and Mesh.* Australian Centre for Geomechanics, Perth, Australia, *Sect*, *22*.

Laurence, D. C., Galvin, J., & Beer, L. (n.d.). Polymer Membrane Liners in Underground Coal Mines Control for the Millenium? In *Proceedings of International Conference on Ground Control in Mining*. Department of Mining Engineering, College of Mineral and Energy Resources, West Virginia University. *19*, 378.

Lewis, B. (2001). Mondi Rock-HoldTM the development of this structural membrane support. *Surface Support Liners: Membranes, Shotcrete and Mesh*. Australian Centre for Geomechanics, Perth, Australia.

Li, Z., Saydam, S., Mitra, R., & Chalmers, D. (2016). Potential use of thin spray-on liners for gas management in underground coal mines. *Journal of the Southern African Institute of Mining and Metallurgy*, *116*(12), 1091–1100.

Loadtech Load cells. (n.d.). *LT 400*. http://www.loadtech.co.za/docs/lt400-s-typeloadcell.pdf

Malan, D. (1999). Time-dependent behaviour of deep level tabular excavations in hard rock. *Rock Mechanics and Rock Engineering*, *32*(2), 123–155.

Malan, D. F., Vogler, U. W., & Drescher, K. (1997). Time-dependent behaviour of hard rock in deep level gold mines. *Journal of the Southern African Institute of Mining and Metallurgy*, *97*(3), 135–147.

Masethe, R. (2015). *Quantification of the effects of thin spray-on liner application on shotcrete tensile strength*. Dissertation, University of the Witwatersrand.

Minova Technical Data Sheet, Capcem KT White. (n.d.). [Google Search]. Retrieved 24 May 2017, from https://www.google.com/search?q=minova+technical+data+sheet,+Capcem+KT+white&ie=utf-8&oe=utf-8&client=firefox-b-ab&gfe_rd=cr&ei=z3MlWfbCBoip8web-ozgDg

Morton, E., Thompson, A., & Villaescusa, E. (2008). Static testing of shotcrete and membranes for mining applications. In *Proceedings of the 6th International Conference on Ground Support*. The Southern African Institute of Mining and Metallurgy, Cape Town, 195-212,

Moser, S., & Girmscheid, G. (1999). Fully automated Shotcrete robot. *International symposium*. IAARC/IFAC/IEEE, 385–390.

Mpunzi, P. (2012). *The properties and performance of selected thin spray on liners for rock support*. Dissertation, University of the Witwatersrand.

Mpunzi, P., Masethe, R., Rizwan, M., & Stacey, T. (2015). Enhancement of the tensile strengths of rock and shotcrete by thin spray-on liners. *Tunnelling and Underground Space Technology*, *49*, 369–375.

Myrvang, A., Stjern, G., Kompen, R., Opsahal, O. A., & Berg, K. R. (1993). Determination of in situ stress and adhesivity of sprayed concrete. *Proceedings of the International Symposium of Sprayed Concrete.* Modern Use of Wet Mix Sprayed Concrete for Underground Support, Fagernes, Norway.

Nagel, M., & Joughin, W. (2002). Thin sprayed liner trials at South Deep Mine. *Proceedings of the 2nd International Seminar on Surface Support Liners: Thin Sprayed Liners, Shotcrete and Mesh*. Sandton, RSA.

Naismith, W., & Steward, N. (2002). Comparative Performance Testing of Ultra-Thin Structural Liners. In *2nd Int. Seminar on Surface Support Liners: Thin Sprayed Liners, Shotcrete, Mesh*. The Southern African Institute of Mining and Metallurgy, Sandton, South Africa, *Sect. 18*.

Nyungu, D., & Stacey, T. (2014). Time-dependent tensile strengths of Bushveld Complex rocks and implications for rock failure around mining excavations. *Journal of the Southern African Institute of Mining and Metallurgy*, *114*(10), 765–772.

Omega. (1999). Practical strain gage measurements. *Agilent Technologies*. https://www.omega.co.uk/techref/pdf/StrainGage_Measurement.pdf

Osswald, T. A. (2015). *Understanding polymer processing: Processes and governing equations*. Carl Hanser Verlag GmbH Co KG.

Ozturk, H., & Guner, D. (2019). Laboratory and distinct element analysis of the deformability behaviour of thin spray-on liners. *International Journal of Rock Mechanics and Mining Sciences*, *123*, 104118.

Ozturk, H., & Tannant, D. (2010). Thin spray-on liner adhesive strength test method and effect of liner thickness on adhesion. *International Journal of Rock Mechanics and Mining Sciences*, *47*(5), 808–815.

Ozturk, H., & Tannant, D. (2011). Influence of rock properties and environmental conditions on thin spray-on liner adhesive bond. *International Journal of Rock Mechanics and Mining Sciences*, *48*(7), 1196–1198.

Pappas, D. M., Barton, T. M., & Weiss, E. S. (2004). The Long-Term Performance of Surface Support Liners for Ground Control in an Underground Limestone Mine. In *Y. Potvin, D. Stacey, & J. Hadjigeorgiou (eds), Surface Support in Mining.* Australian Centre for Geomechanics, Perth, Australia, 157–166.

Potvin, Y. (2002). Towards a common understanding of TSL applications in mines. *2nd International Seminar on Surface Support Liners: Thin Sprayed Liners, Shotcrete, Mesh.* The Southern African Institute of Mining and Metallurgy, Sandton, South Africa.

Potvin, Y., & Hadjigeorgiou, J. (2008). Ground support strategies to control large deformations in mining excavations. *Journal of the Southern African Institute of Mining and Metallurgy*, *108*(7), 397–404.

Potvin, Y., Stacey, D., & Hadjigeorgiou, J. (2004a). Thin Spray-on Liners (TSLs) - A Quick Reference Guide. In *Surface Support in Mining.* Australian Centre for Geomechanics, Perth, Australia.

Potvin, Y., Stacey, T. R., & Hadjigeorgiou, J. (2004b). *Surface support in mining*. Australian Centre for Geomechanics, Perth, Australia.

Riley, W. F., McConnell, K. G., Dally, J., Dally, J., & Dally, J. (1993). *Instrumentation for engineering measurements*. Wiley.

Rocscience Inc. (2018, March 8). Rocscience Inc. https://www.rocscience.com/software/rs3

Spearing, A., & Champa, J. (2000). The design, testing and application of ground support membranes for use in underground mines. *Proc. MassMin, 2000*, 199–208.

Spearing, A., Ohler, J., & Attiogbe, E. (2001). The effective testing of thin support membranes (superskins) for use in underground mines. *International seminar on mine surface support liners: Membrane, shotcrete and mesh*. Australian Centre for Geomechanics, Perth, Australia, *Section 26*.

Stacey, T. (2001a). Membrane support mechanics, loading mechanisms, desired membrane performance, and appropriate test methods. *Colloquium 2001, Shotcrete and Membrane Support.* The Southern African Institute of Mining and Metallurgy.

Stacey, T. (2001b). Review of membrane support mechanisms, loading mechanisms, desired membrane performance, and appropriate test methods. *S. Afr. Inst. Min. Metall*, *101*(7), 343–352.

Stacey, T., & Kasangula, M. (2003). Results from Testing of TSL's Using a Simple, Low Cost Laboratory Test. *3rd International Seminar on Surface*

Support Liners: Thin Spray-On Liners, Shotcrete and Mesh. Quebec City, Canada, Section 17

Stacey, T., Mason, D., & Fowkes, N. (2009). A review of mechanisms of shotcrete and thin spray-on liner support, and recent investigations. In *Proceedings of conference ''Shotcrete for Africa''*. S. Afr. Inst. Min. Metall, 237–249.

Stacey, T. R., & Yu, X. (2004). Investigations into mechanisms of rock support provided by sprayed liners. In E. Villaescusa & Y. Potvin*, eds, Ground Support in Mining and Underground Construction*. AA Balkema, Australia, *209*, 563–569.

Swan, G., & Henderson, A. (1999). Water-based Spray-on liner implementation at Falconbridge Limited. *Proceedings CIM/AGM*, Calgary.

Szwedzicki, T. (2003). Rock mass behaviour prior to failure. *International Journal of Rock Mechanics and Mining Sciences*, *40*(4), 573–584.

Tan, T.-K., & Kang, W.-F. (1980). Locked in stresses, creep and dilatancy of rocks, and constitutive equations. *Rock Mechanics and Rock Engineering*, *13*(1), 5–22.

Tannant, D. (1997). Large-scale pull tests on Mineguard Spray-on Liner. *Report to INCO Ltd.* Geomechanics Centre, Sudbury, Ontario, Canada.

Tannant, D. (2001). Thin spray-on liners for underground rock support-testing and design issues. In *International seminar and field trials on surface support liners: membrane, shotcrete and mesh.* Australian Centre for Geomechanics, Perth, Australia, *Section 27*, 1–18.

Tannant, D., Swan, G., Espley, S., & Graham, C. (1999). Laboratory test procedures for validating the use of thin spray-on liners for mesh replacement. *101st Annual General Meeting.* Canadian Institute of Mining, Metallurgy and Petroleum, Calgary, Alberta, published on CD-ROM.

Wang, Q., Zhu, W., Xu, T., Niu, L., & Wei, J. (2016). Numerical simulation of rock creep behaviour with a damage-based constitutive law. *International Journal of Geomechanics*, *17*(1), 04016044.

Wojno, L., & Kuijpers, J. (1997). Spray-on, user friendly and flexible support for mine excavations. In *Proc. Int. Symp. Rock Support—Applied Solutions for Underground Structures*, Lillehammer, Norwegian Society for Chartered Engineers, 671–683.

Xia, C., & Zhong, S. (1989). Experimental data processing method in consideration of influence of loading history on rock specimen deformation. *J. Cent. South. Univ*, *20*, 18–24.

Yang, S.-Q., Hu, B., Ranjith, P., & Xu, P. (2018). Multi-step loading creep behavior of red sandstone after thermal treatments and a creep damage model. *Energies*, *11*(1), 212.

Yang, W., Gamage, R., Huang, C., Luo, G., Guo, J., & Wang, S. (2018). Loading history effect on creep deformation of rock. *Energies*, *11*(6), 1462.

Yilmaz, H. (2007). Shear-bond strength testing of thin spray-on liners. *Journal of the South African Institute of Mining and Metallurgy*, *107*(8), 519–530.

Yilmaz, H. (2010). Tensile strength testing of thin spray-on liner products (TSLs) and shotcrete. *The Journal of the South African Institute of Mining and Metallurgy*, *110*(10), 559–569.

Yilmaz, H. (2011). *Development of testing methods for comparative assessment of thin spray–on liner (TSL) shear and tensile properties.* (Doctoral dissertation, Faculty of Engineering and the Built Environment, University of the Witwatersrand, Johannesburg).

Yilmaz, H. (2013). Comparison of tensile-bond strength of thin spray-on liners. *International Journal of Mining, Reclamation and Environment*, *27*(1), 56–71.

Yilmaz, H. (2014). Comparison of Tensile Strength of Shotcrete and Thin Spray-on Liners (TSLs). In *Proceedings of the 8th Asian Rock Mechanics Symposium*. International Society for Rock Mechanics and Rock Engineering, Lisbon, 177-182.

Yilmaz, H., Saydam, S., & Henderson, D. (2003). Torque testing of thin spray-on liner coated cores. In *3rd International Seminar on Surface Support Liners: Thin Spray-On Liners, Shotcrete and Mesh*. Quebec City, Canada. Section 15, 25–26.

Yuan, R., & Shen, B. (2017). Numerical modelling of the contact condition of a Brazilian disk test and its influence on the tensile strength of rock. *International Journal of Rock Mechanics and Mining Sciences*, *93*, 54–65.

Zhenjun, S., Porter, I., Nemcik, J., & Baafi, E. (2014). Comparing the reinforcement capacity of welded steel mesh and a thin spray-on liner

using large scale laboratory tests. *International Journal of Mining Science and Technology*, *24*(3), 373–377.

APPENDICES

APPENDIX A DIMENSIONS OF TENSILE CREEP TESTING MACHINE

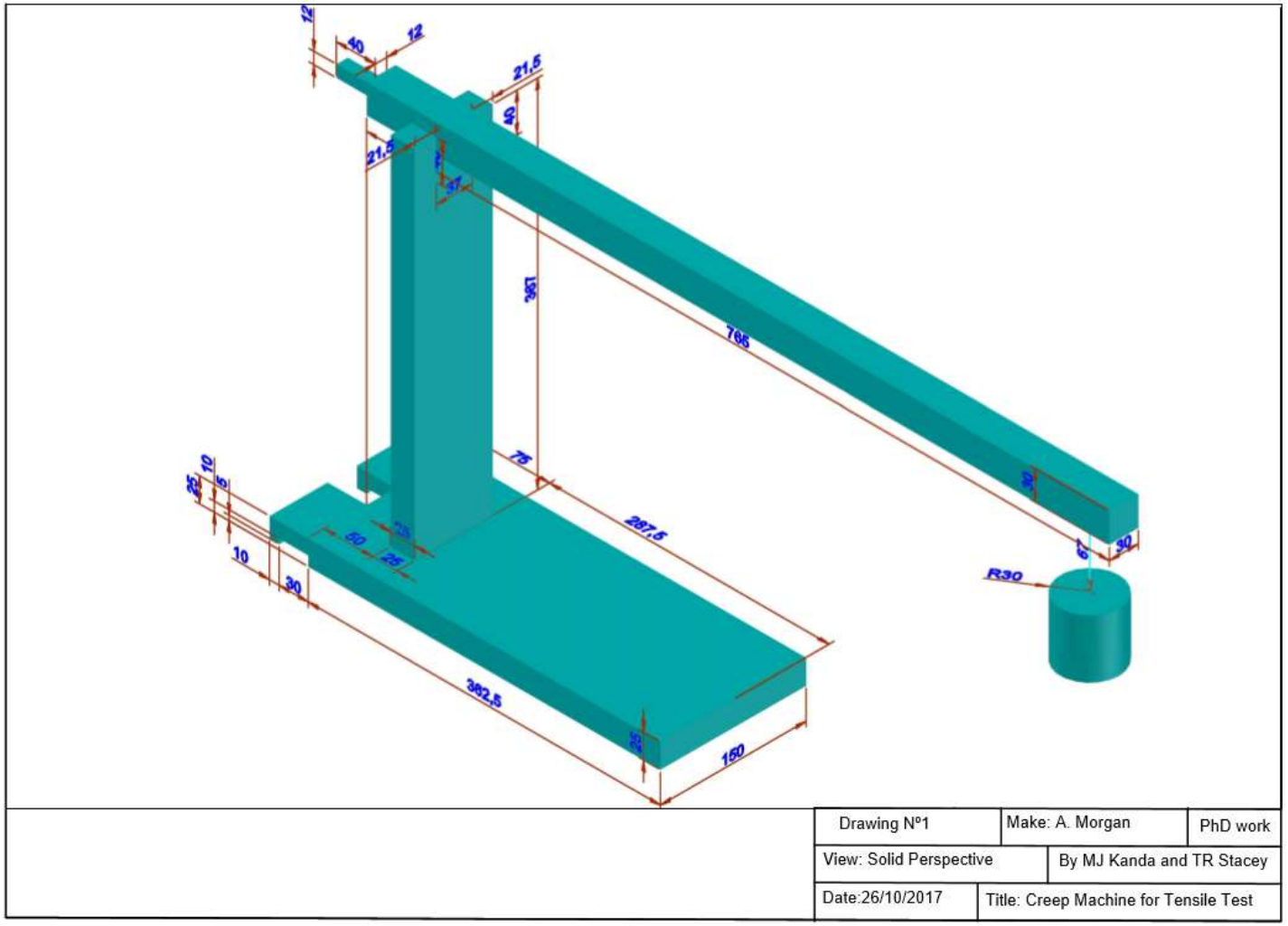


Figure A-1 tensile creep testing machine (M3) – Solid Perspective

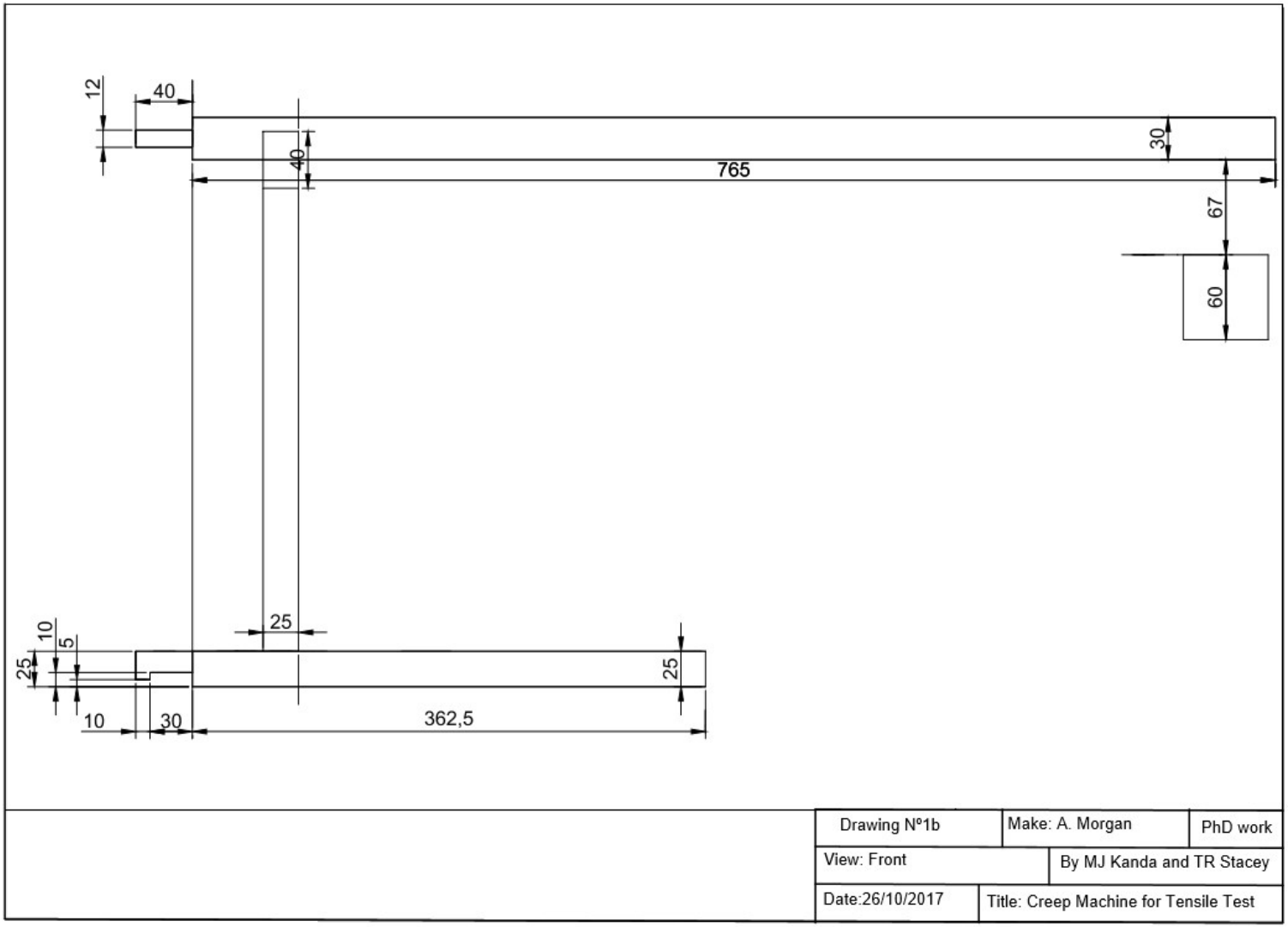


Figure A-2 Tensile creep testing machine (M3) - Front View

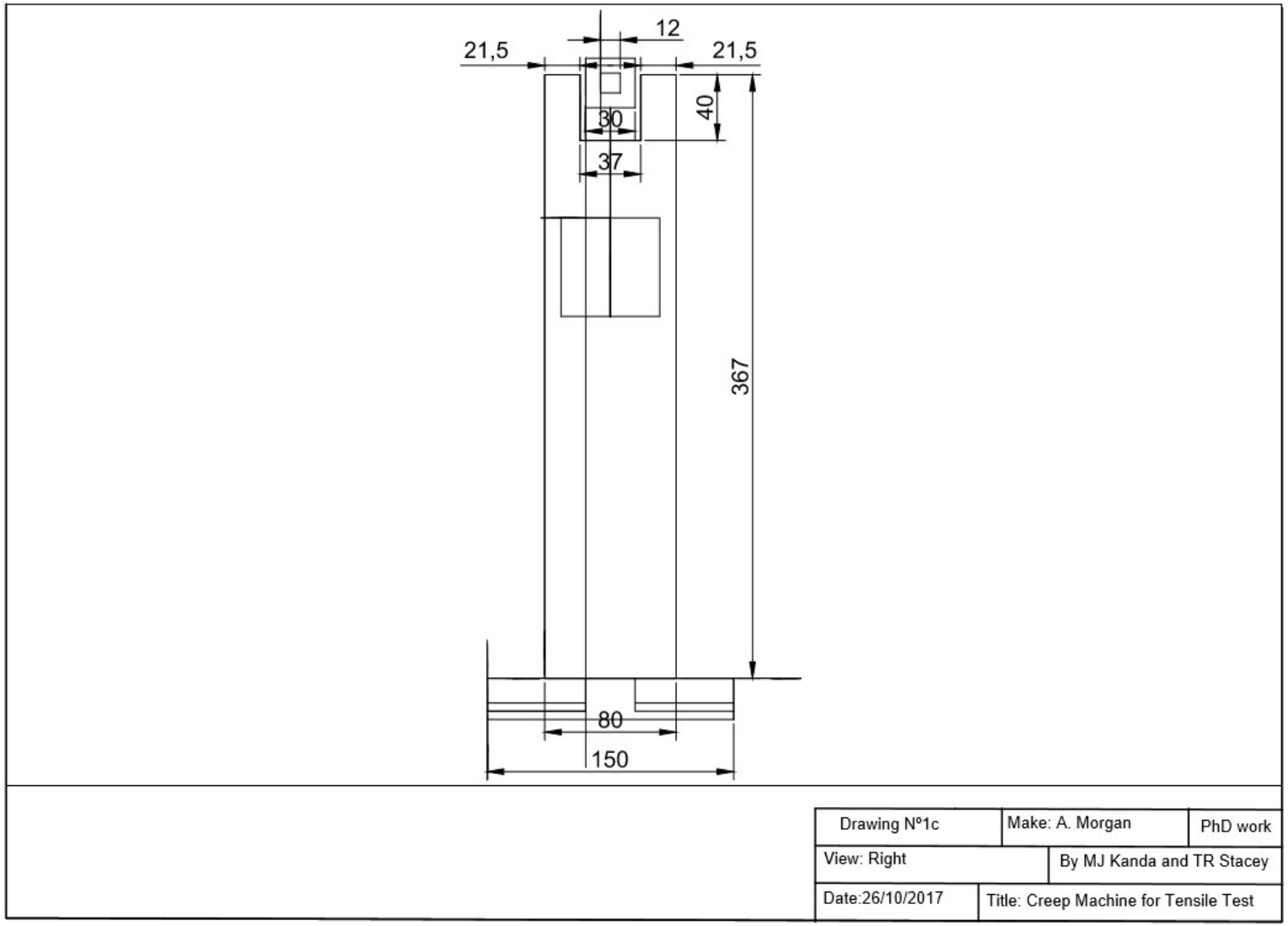


Figure A-3 Tensile creep testing machine (M3) - Right View

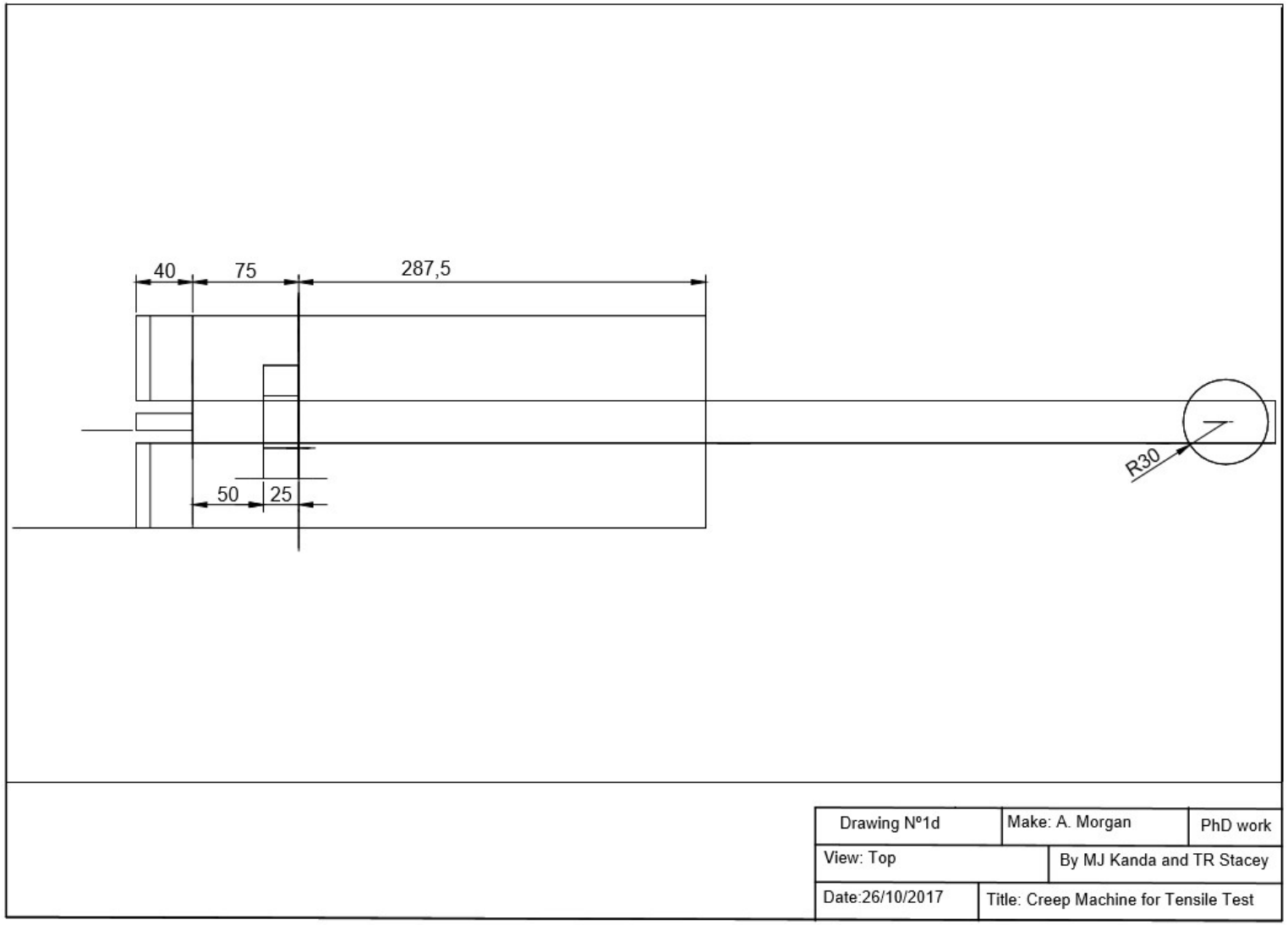


Figure A-4 Tensile creep testing machine (M3) - Top View

APPENDIX B DIMENSIONS OF BRAZILIAN INDIRECT TENSILE CREEP TESTING MACHINE "M1"

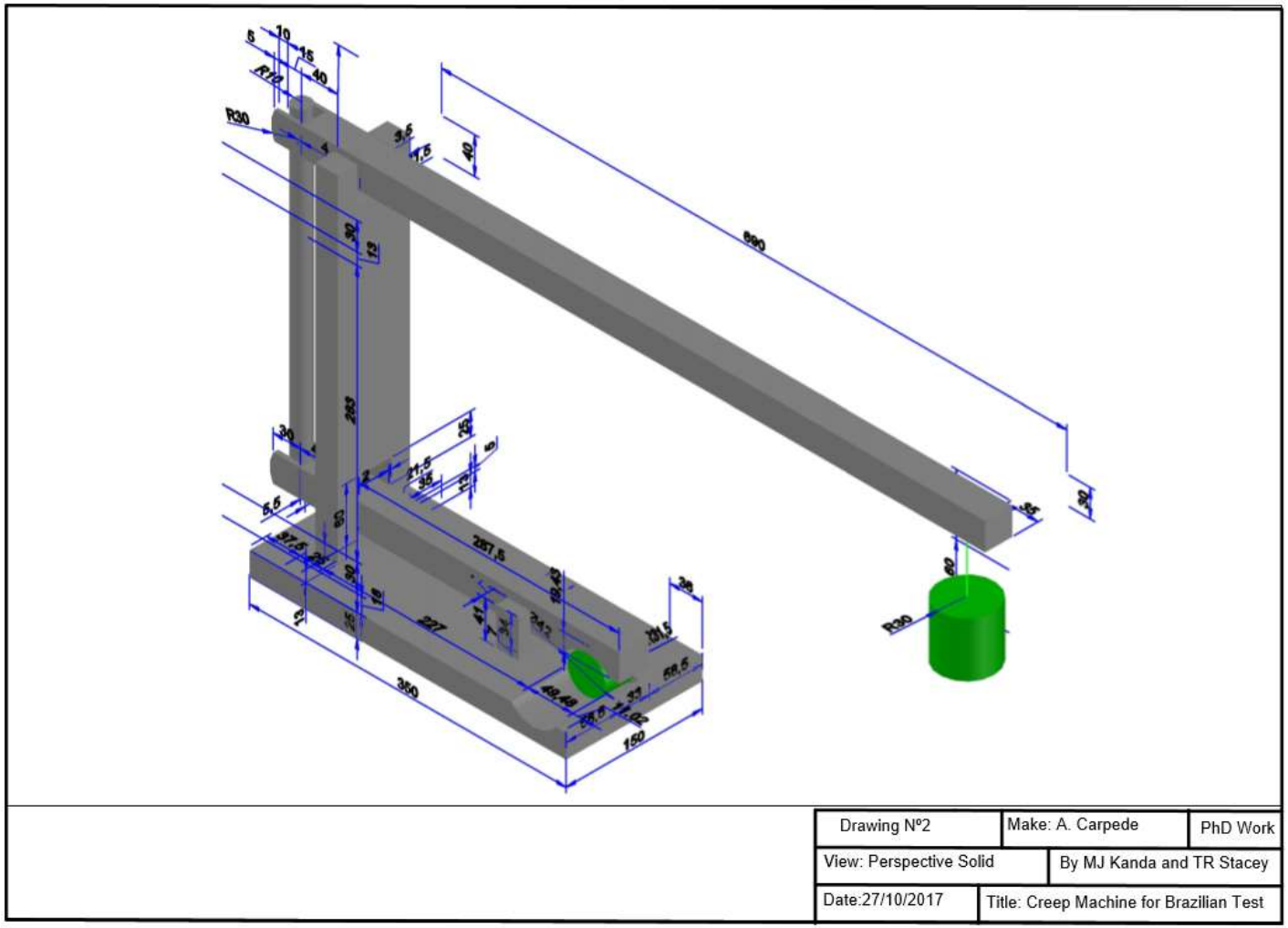


Figure B-1 Brazilian indirect tensile creep testing machine (M1)-Perspective solid view

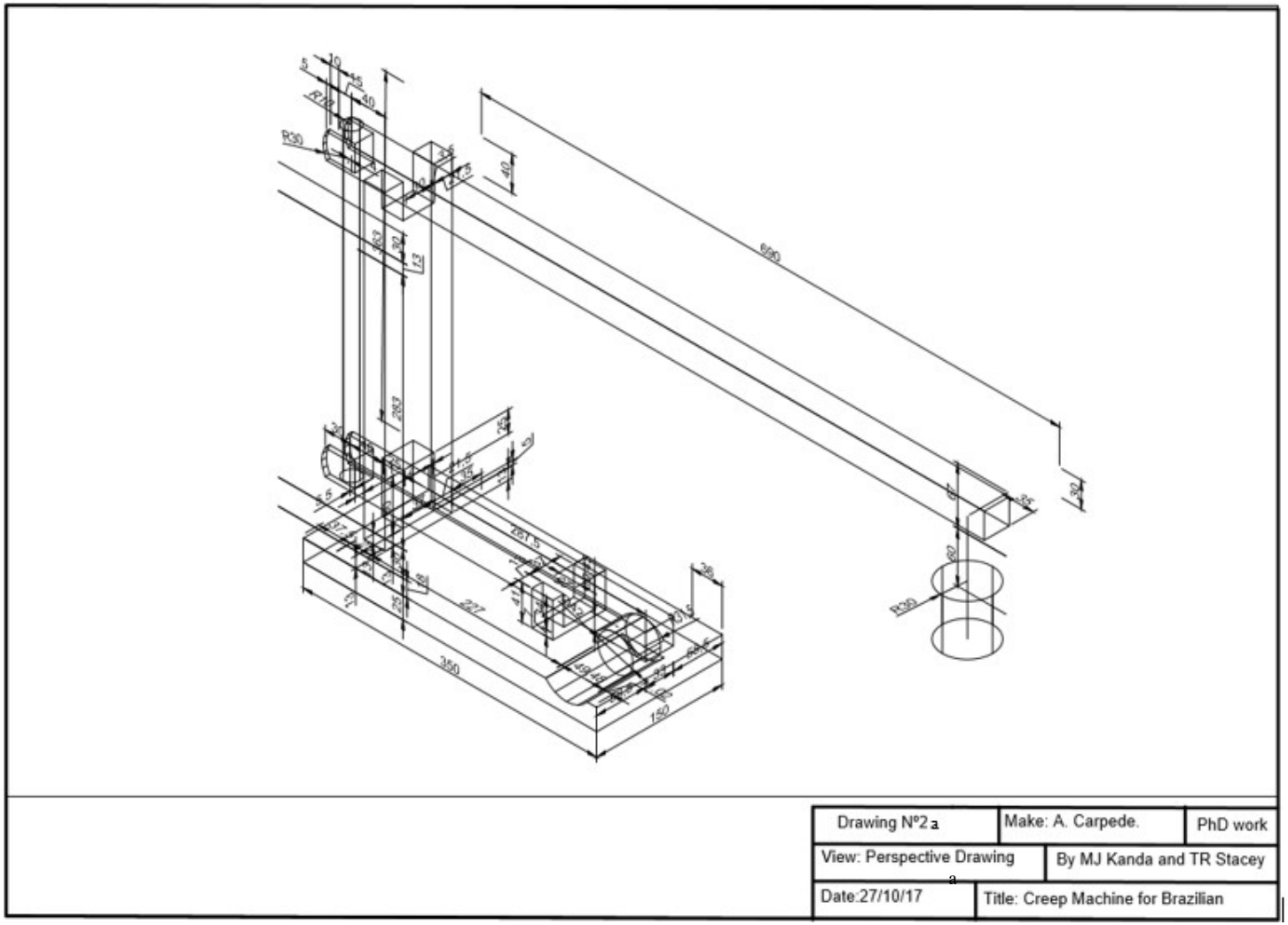


Figure B-2 Brazilian indirect tensile creep testing machine (M1)-Perspective drawing view

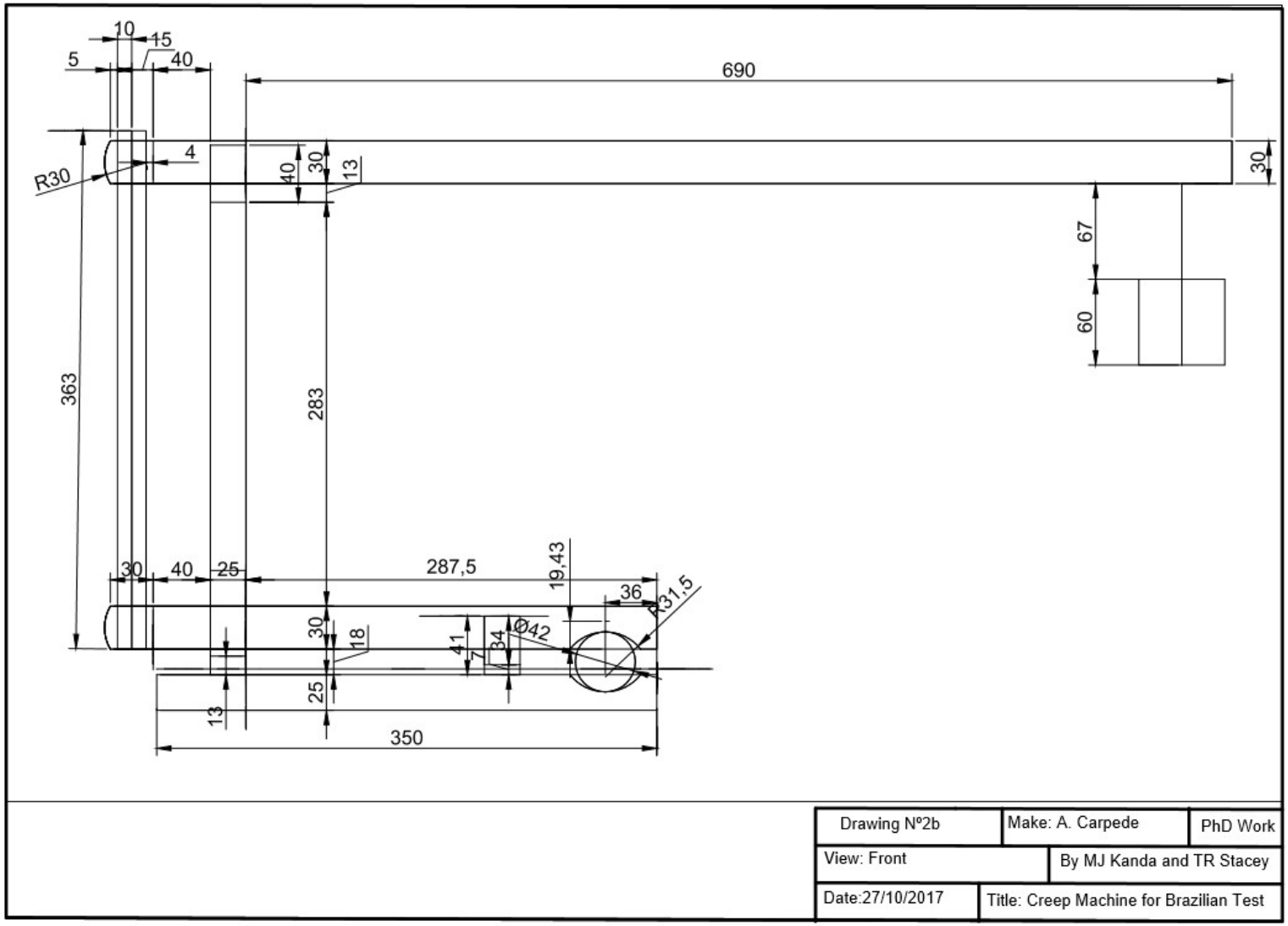


Figure B-3 Brazilian Indirect Tensile creep testing machine (M1) – Front View

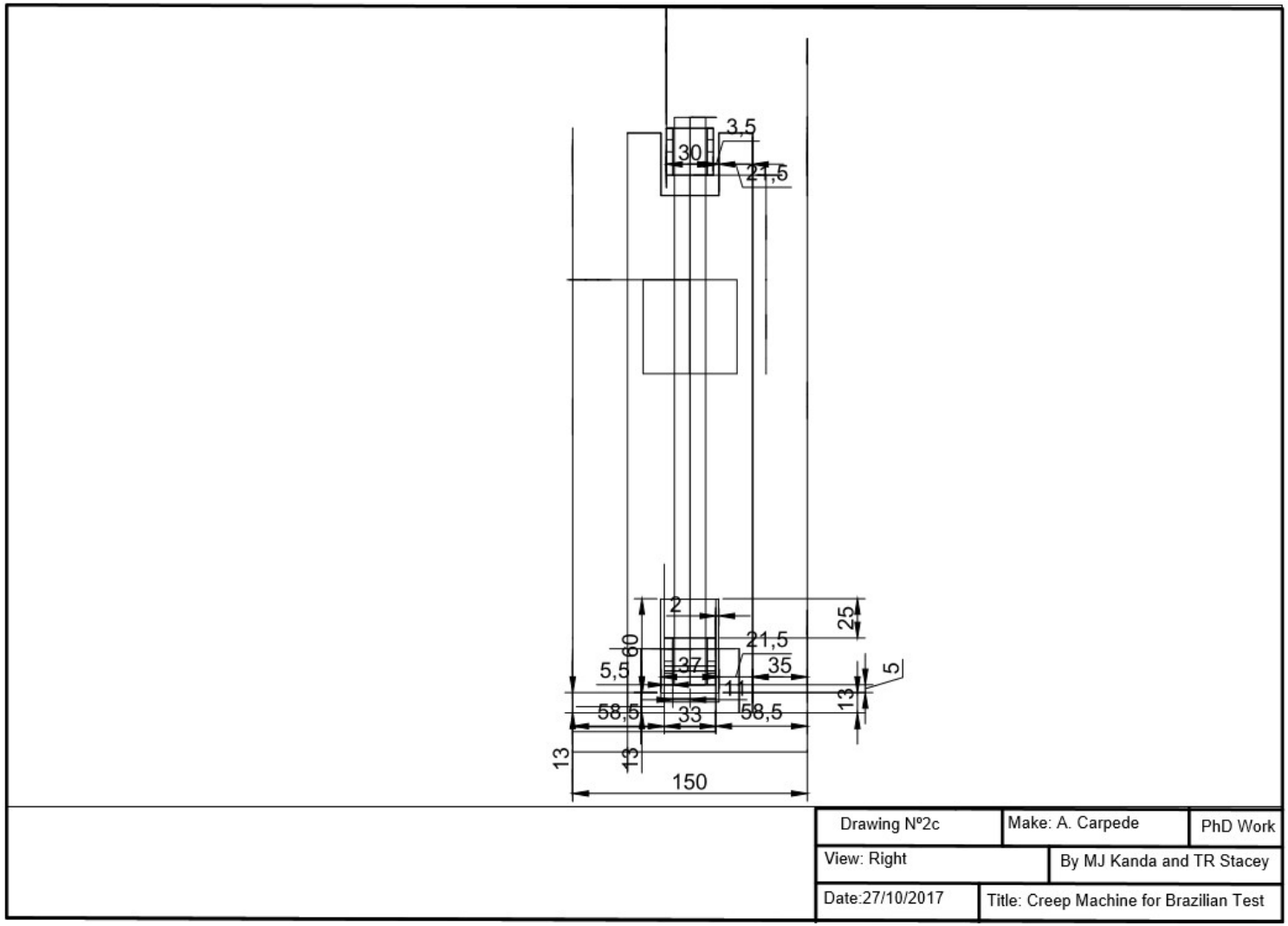


Figure B-4 Brazilian Indirect Tensile creep testing machine (M1) – Right View

APPENDIX C DIMENSIONS OF BRAZILIAN INDIRECT TENSILE CREEP TESTING MACHINE "M4"

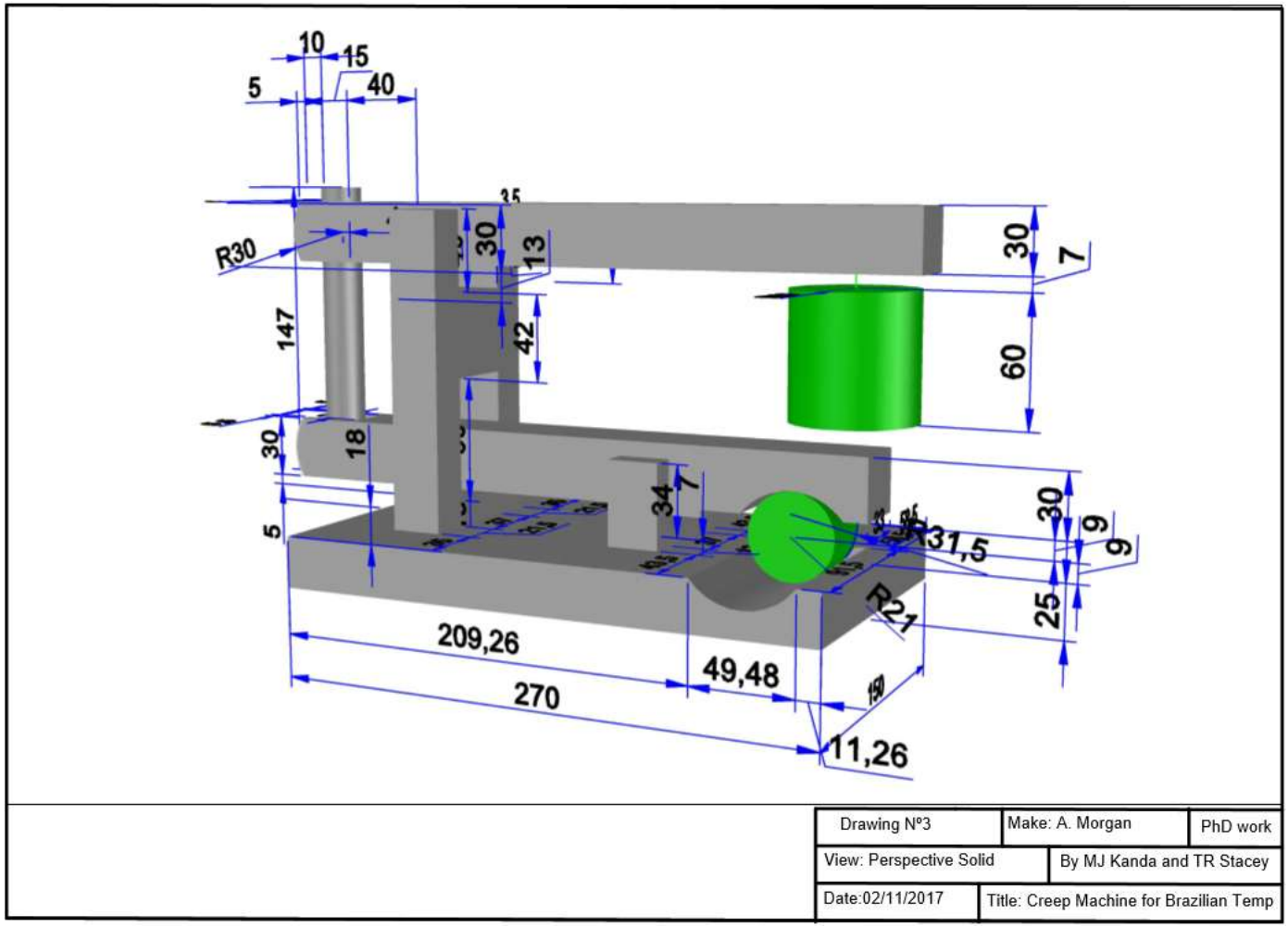


Figure C-1 Brazilian Indirect Tensile creep machine (M4) for high temperature testing – Perspective solid View

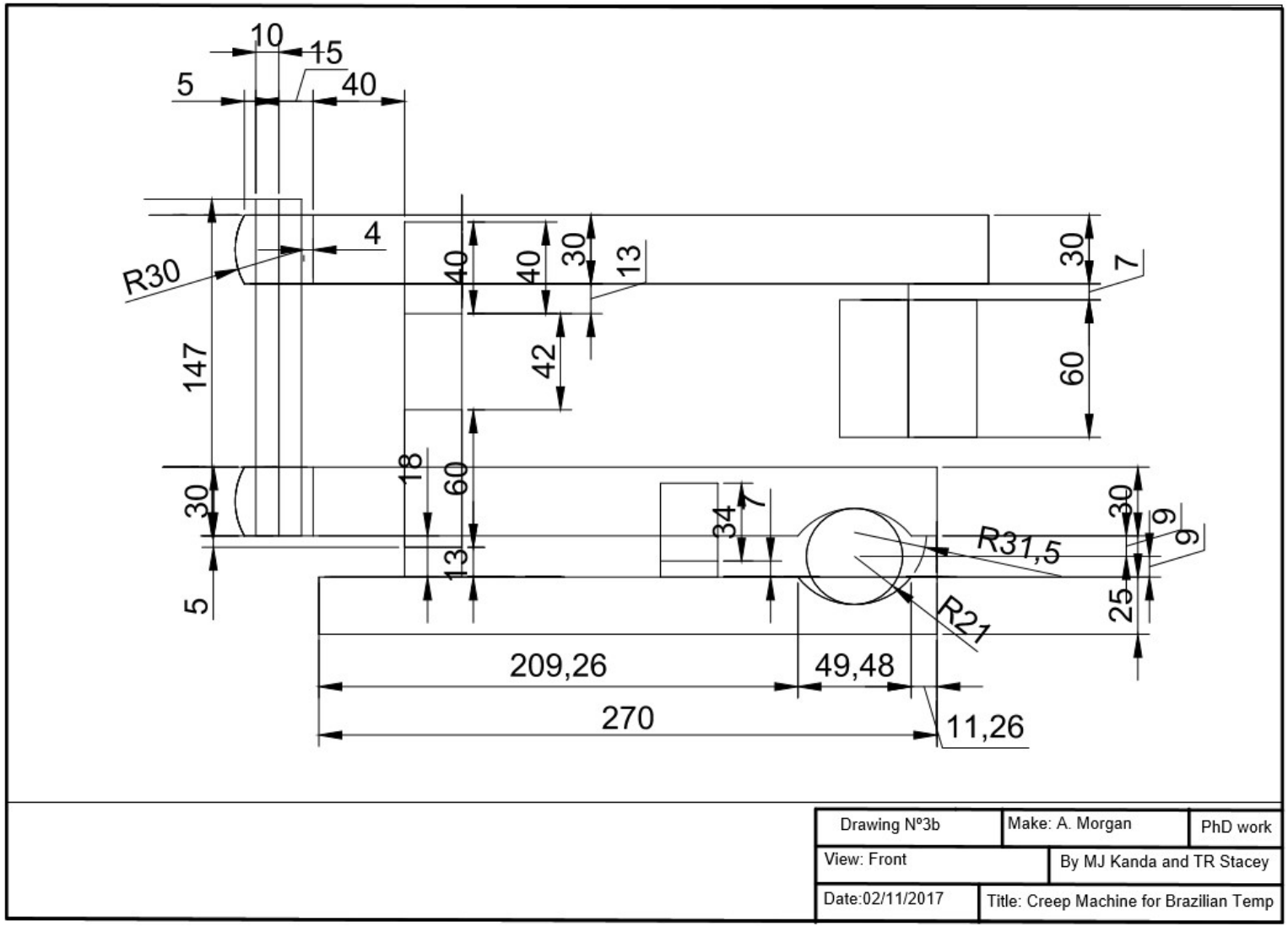


Figure C-2 Brazilian Indirect Tensile creep machine (M4) for high-temperature testing – Front View

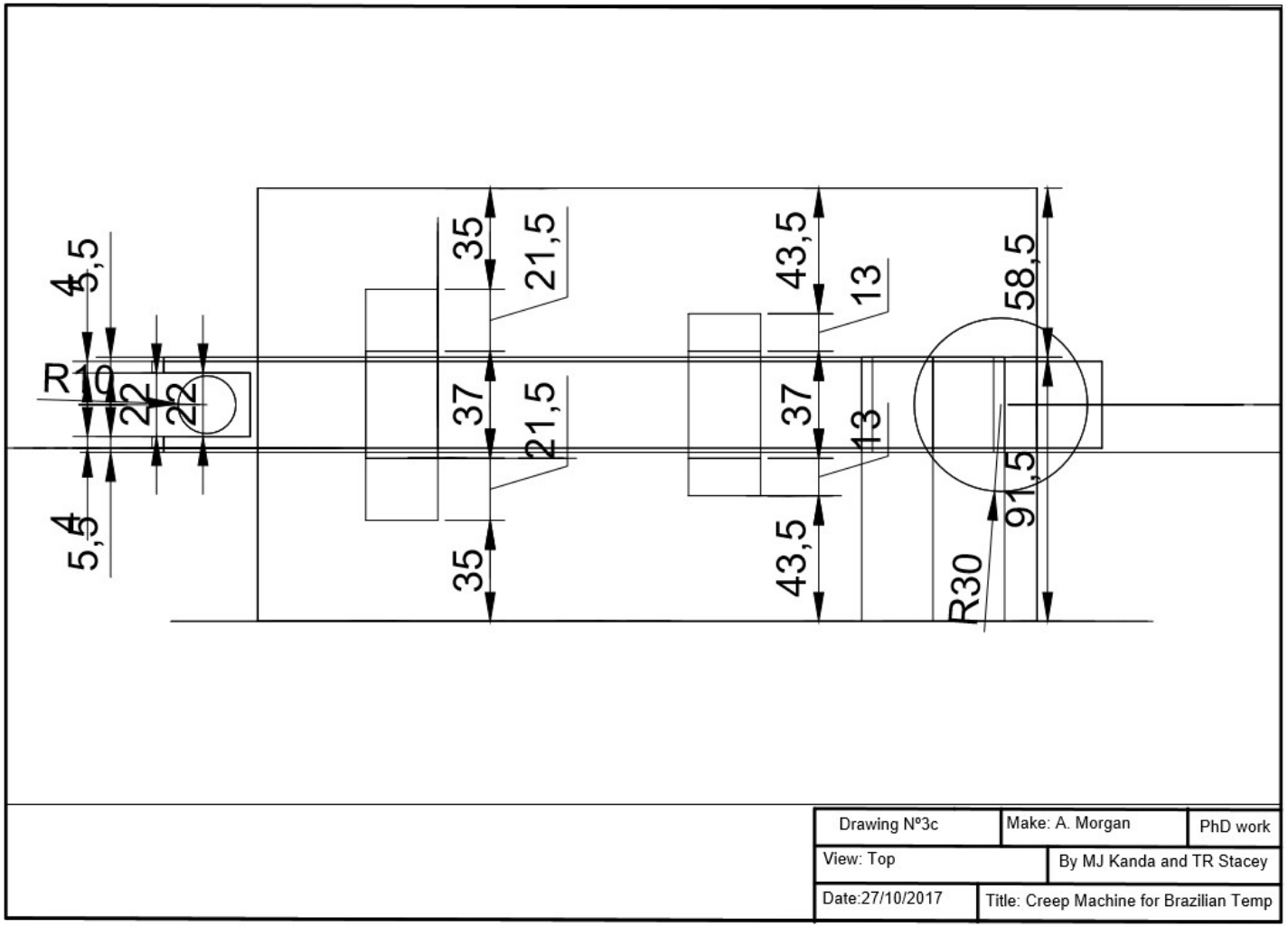


Figure C-3 Brazilian Indirect Tensile creep machine (M4) for high-temperature testing – Top View

APPENDIX D DIMENSIONS OF MEMBRANE DISPLACEMENT TESTING CREEP MACHINE “M2”

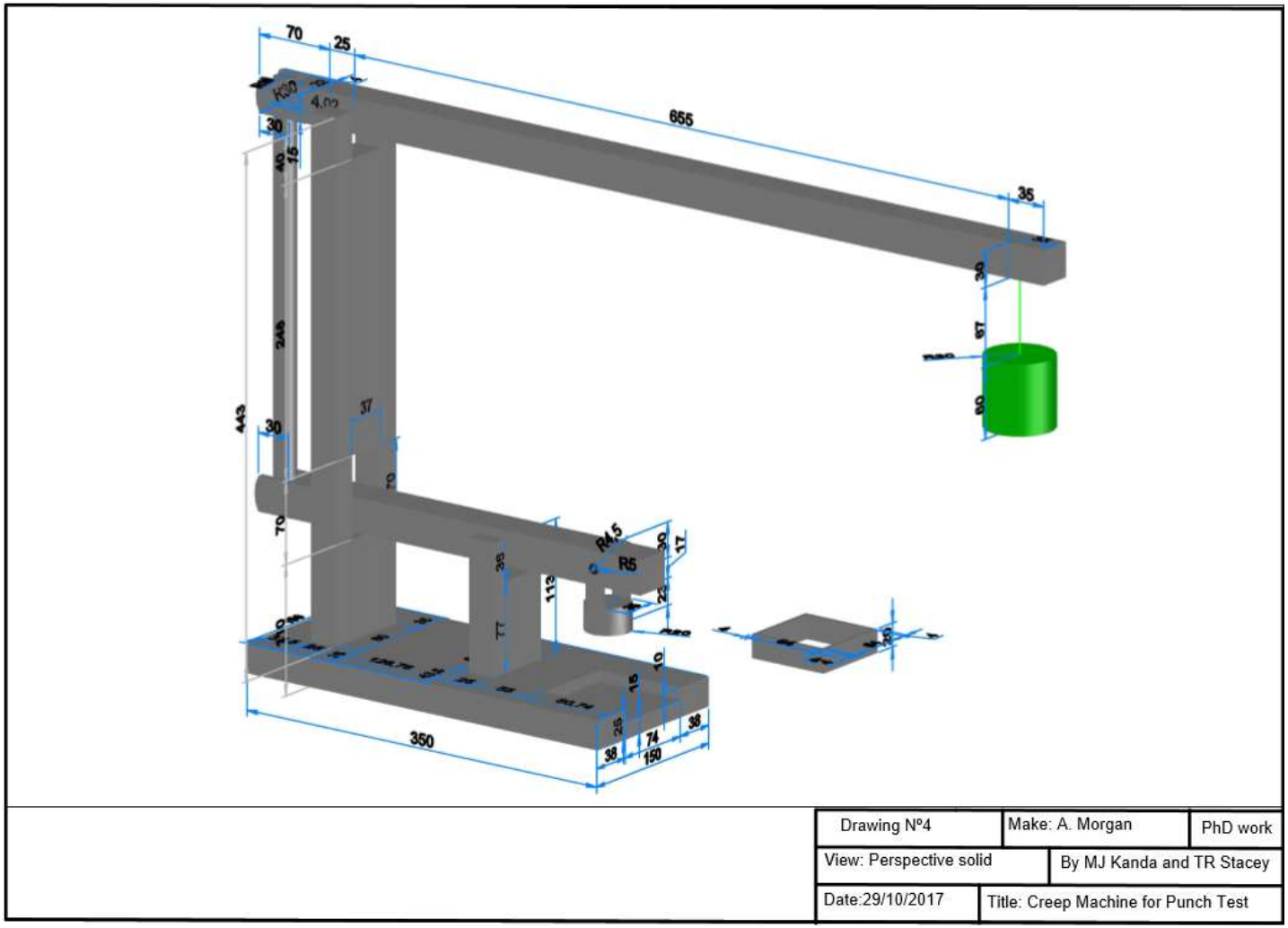


Figure D-1 Membrane displacement testing machine (M2) – Perspective solid View

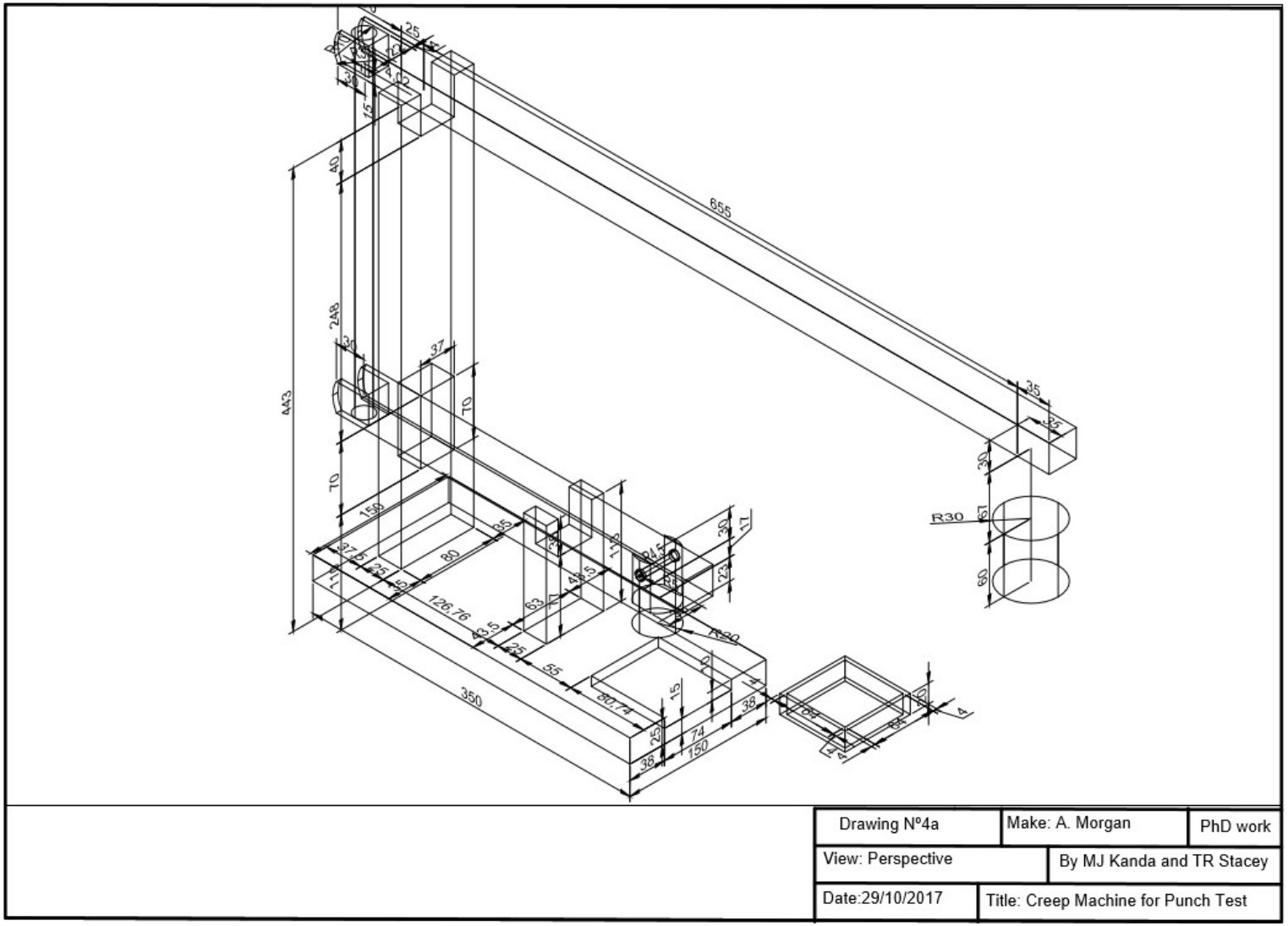


Figure D-2 Membrane displacement testing machine (M2) – Perspective drawing View

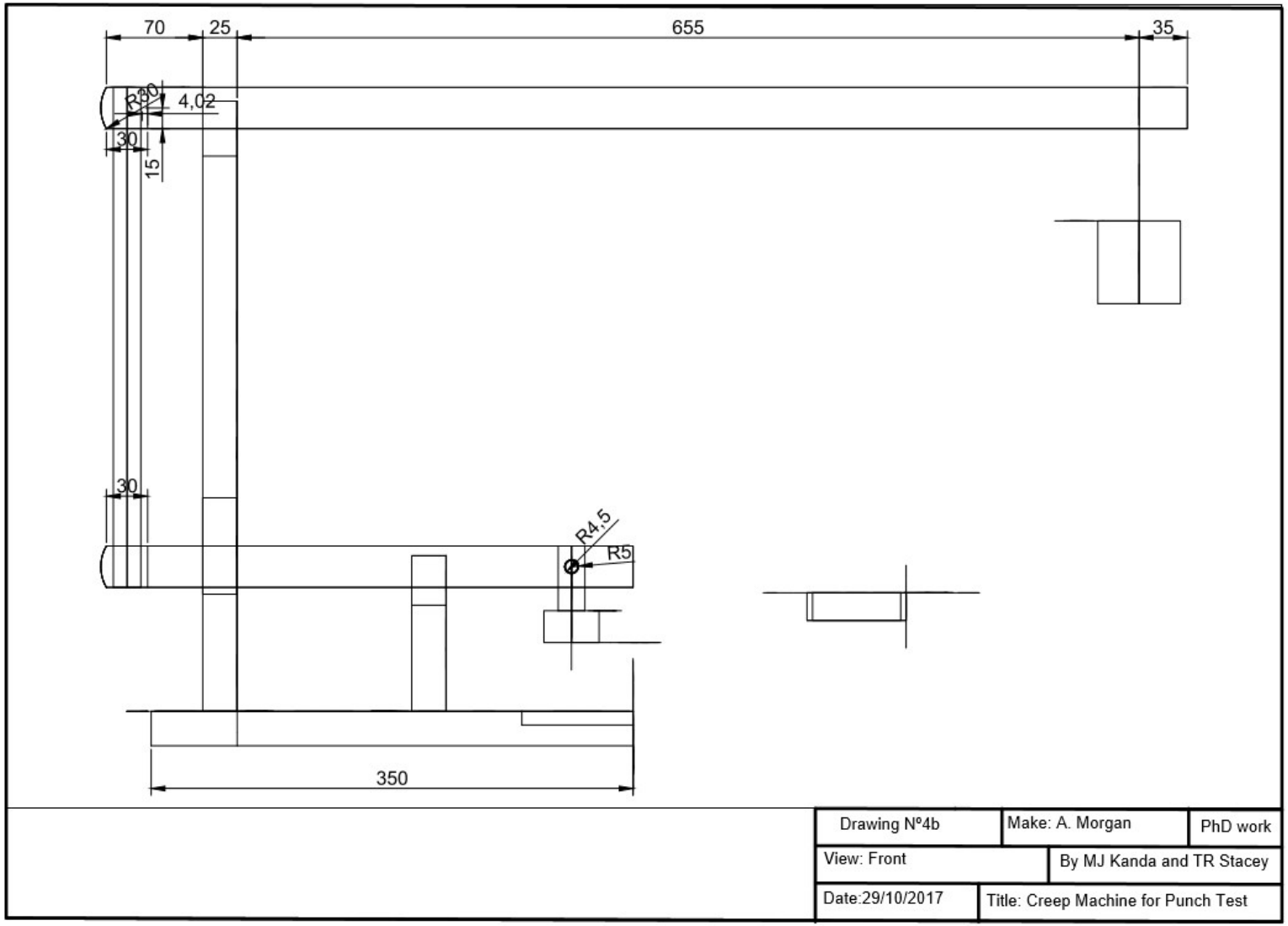


Figure D-3 Membrane displacement testing machine (M2) – Front View

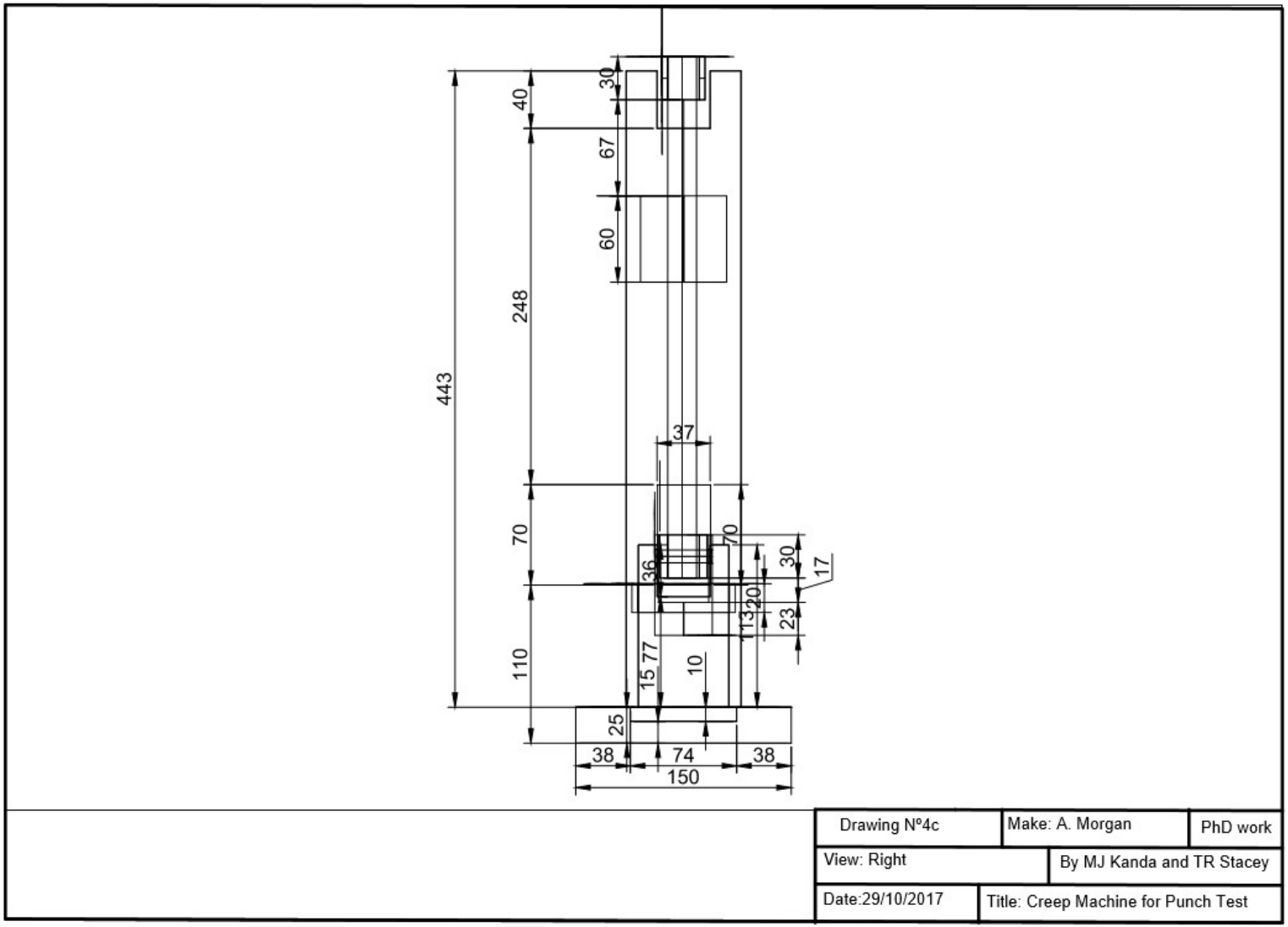


Figure D-4 Membrane displacement testing machine (M2) – Right View

APPENDIX E CREEP TESTING MACHINE CALIBRATION

Table E-1 Result of trials for calibration of load cell type S readings on the data logger

S load cell calibration	
Applied load on load cell S read from MTS (Kg)	Multimeter readings (mv)
10.14	159.8
20.39	318.3
50.97	789
81.55	1262
101.94	1575
132.52	2045
203.87	3135
254.84	3904
305.81	4676

Table E-2 Result of trials for M3 creep testing machine calibration

M3 machine calibration		**Conversion into kilograms**
load Kg	mv	load (kg)
		(1/15.28). y-0.78384
0	38.1	1.710
1.505	115.6	6.782
2.779	187.6	11.494
3.915	250.8	15.630
5.197	321.8	20.276
6.367	386.6	24.517
7.489	449	28.601
10.567	605	38.810

Table E-3 Result of trials for M1 creep testing machine calibration

M1 machine calibration		**Conversion into kilograms**
load Kg	mv	load (kg)
		(1/15.28). y-0.78384
0	1049	67.868
1.505	1975	128.470
2.779	2808	182.986
3.915	3537	230.695
5.197	4343	283.444
6.367	5078	331.546
7.489	5781	377.554
10.567	7710	503.797

Table E-4 Result of trials for M4 creep testing machine calibration

M4 machine calibration		**Conversion into kilograms**
load Kg	mv	load (kg)
		(1/15.28)y-0.78384
0	610	39.138
1.262	1186	76.834
2.536	1794	116.624
3.672	2322	151.180
4.954	2917	190.119
6.124	3459	225.591
7.246	3975	259.360
10.324	5407	353.077

Table E-5 Result of trials for M5 creep testing machine calibration

M5 machine calibration		**Conversion into kilograms**
load Kg	mv	load (kg)
		(1/15.28)y-0.78384
0	1855	120.617
1.262	2830	184.426
2.536	3837	250.329
3.672	4750	310.080
4.954	5702	372.384
6.124	6580	429.844

APPENDIX F EQUATIONS OF CONVERSION OF VOLTAGE READINGS FROM DATA LOGGER INTO CORRESPONDING SPECIMEN DISPLACEMENTS USING THE DISPLACEMENT TRANSDUCERS

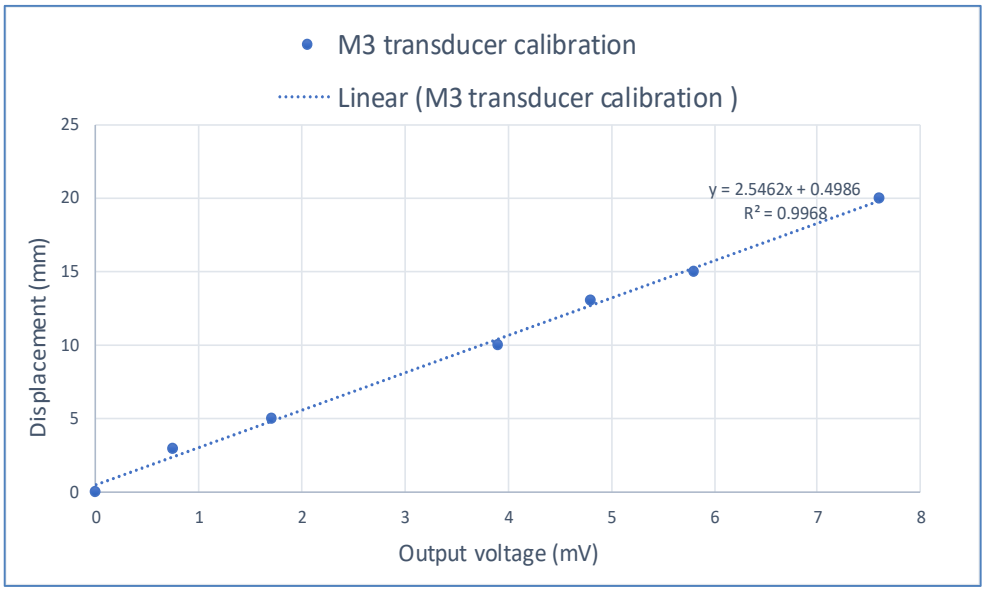


Figure F-1 Calibrating equation of M3 displacement transducer

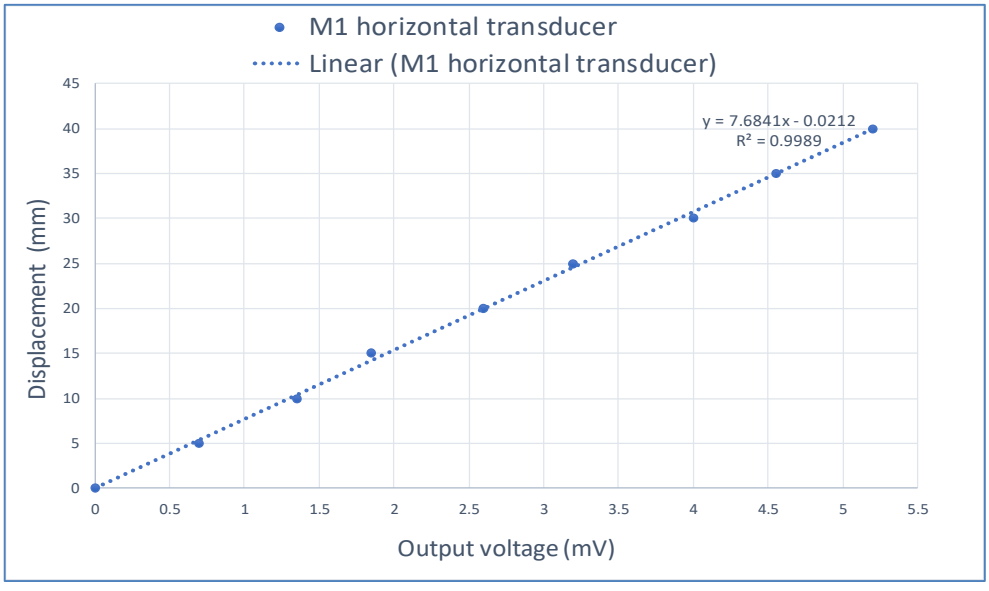


Figure F-2 Calibrating equation of M1 displacement transducer

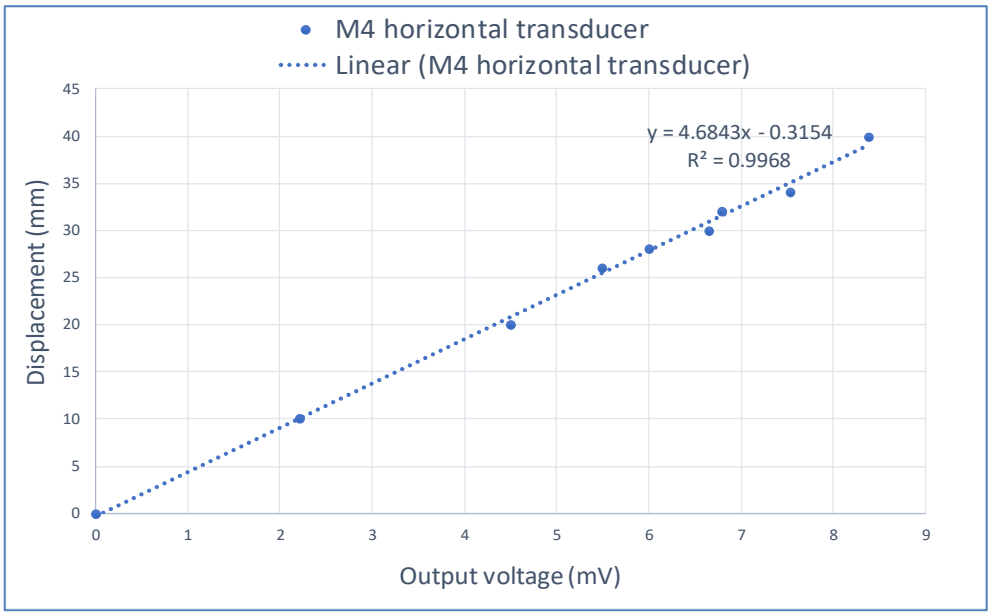


Figure F-3 Calibrating equation of M4 displacement transducer

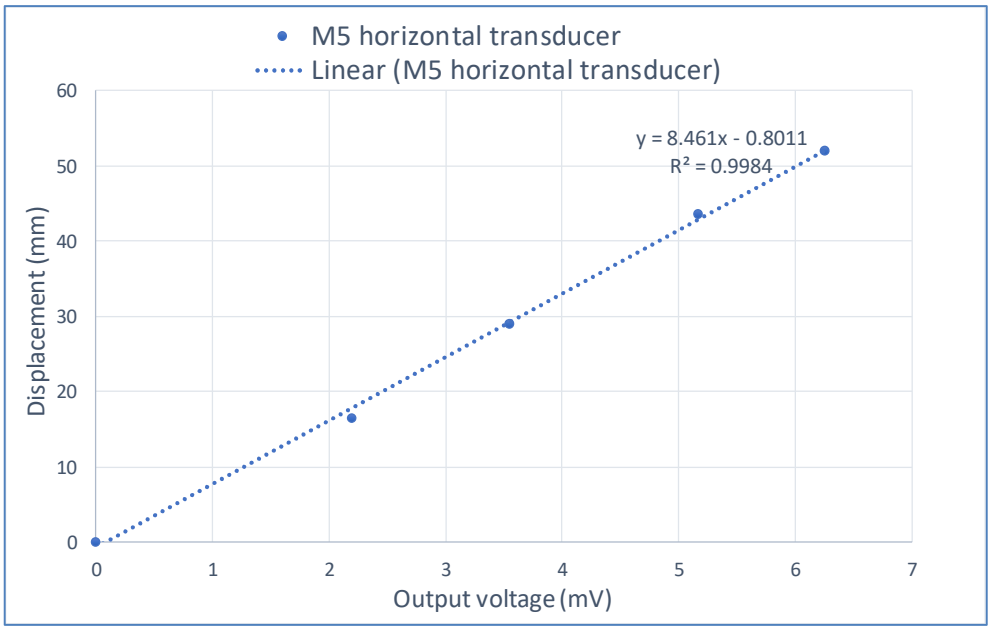


Figure F-4 Calibrating equation of M5 displacement transducer

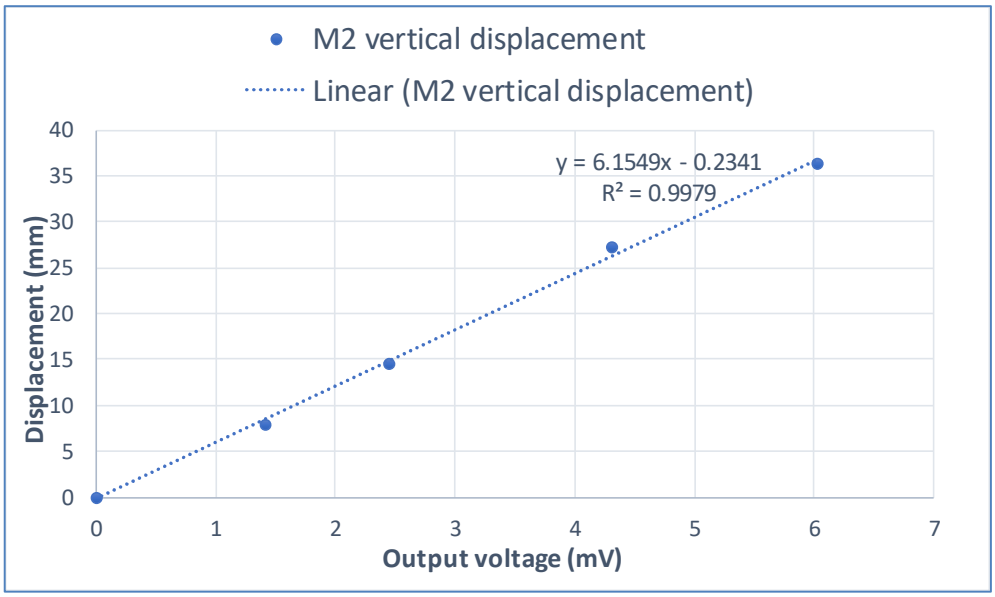


Figure F-5 Calibrating equation of M2 displacement transducer

APPENDIX G STATISTICS OF UTS SPECIMENS STRENGTH BASED ON EXPOSURE TIME

Table G-1 Statistics of TSL1 UTS under various environmental conditions

TSL Type	Statistics	15d	28d	56d	112d
TSL1 R UTS (25 specimens)	**Mean (MPa)**	3.5	4.1	4.4	4.6
	Std (MPa)	0.56	0.61	0.41	0.25
	CoV	16%	15%	9%	5%
	Stepwise strength Increase	-	17%	7%	5%
	Strength Increase from Room 28 days	-	-	7%	12%
TSL1 H UTS (25 specimens)	**Mean (MPa)**	1.3	1.4	1.5	1.6
	Std (MPa)	0.32	0.27	0.23	0.39
	CoV	24%	20%	16%	25%
	Stepwise strength Increase	-	8%	7%	7%
	Strength Increase from Room 28 days	-	-65.9%	-63.4%	-61%
TSL1 HT UTS (25 specimens)	**Mean (MPa)**	1.4	1.4	1.5	1.6
	Std (MPa)	0.24	0.25	0.28	0.24
	CoV	17%	17%	18%	15%
	Stepwise strength Increase	-	0%	7%	7%
	Strength Increase from Room 28 days	-	-65.9%	-63.4%	-61%

Table G-2 Statistics of TSL2 UTS under various environmental conditions

TSL Type	Statistics	15d	28d	56d	112d
TSL2 R UTS (25 specimens)	**Mean (MPa)**	2.8	3.2	3.4	3.7
	Std (MPa)	0.29	0.31	0.33	0.25
	CoV	10%	10%	10%	7%
	Stepwise strength Increase	-	14%	6%	9%
	Strength Increase from Room 28 days	-	-	6%	9%
TSL2 H UTS (25 specimens)	**Mean (MPa)**	2.22	2.60	2.98	3.14
	Std (MPa)	0.32	0.34	0.48	0.44
	CoV	14%	13%	16%	14%
	Stepwise strength Increase	-	17%	15%	5%
	Strength Increase from Room 28 days	-	-19%	-7%	-2%
TSL2 HT UTS (25 specimens)	**Mean (MPa)**	2.38	2.30	2.10	2.10
	Std (MPa)	0.28	0.33	0.34	0.49
	CoV	12%	15%	16%	23%
	Stepwise strength Increase	-	-3%	-9%	0%
	Strength Increase from Room 28 days	-	-28%	-34%	-34%

Table G-3 Statistics of TSL3 UTS under various environmental conditions

TSL Type	Statistics	15d	28d	56d	112d
TSL3 Room UTS (25 specimens)	**Mean (MPa)**	4.4	4.3	3.8	3.4
	Std (MPa)	0.94	0.27	0.76	0.81
	CoV	21%	6%	20%	24%
	Stepwise strength Increase	-	-2%	-12%	-11%
	Strength Increase from Room 28 days	-	-	-12%	-21%
TSL3 H UTS (25 specimens)	**Mean (MPa)**	2.57	2.10	2.09	2
	Std (MPa)	0.29	0.25	0.14	0.12
	CoV	11%	12%	7%	6%
	Stepwise strength Increase	-	-18%	0%	-4%
	Strength Increase from Room 28 days	-	-51%	-51%	-51%
TSL3 HT UTS (25 specimens)	**Mean (MPa)**	2.70	2.37	2.17	2.16
	Std (MPa)	0.24	0.32	0.21	0.40
	CoV	9%	14%	9%	18%
	Stepwise strength Increase	-	-12%	-8%	0%
	Strength Increase from Room 28 days	-	-45%	-50%	-50%

APPENDIX H IMPACTS OF THE ENVIRONMENTAL CONDITIONS ON UNIAXIAL TENSILE STRENGTH, STRAIN AT FAILURE, AND MODULUS OF TSL

Table H-1 Uniaxial tensile strengths, strains at failure and moduli of TSL1, TSL2 and TSL3 after various exposure times in room condition (R - room condition; mstr - millistrain)

TSL name	Parameter	15 days	28 days	56 days	112 days
TSL1_R	**UTS (MPa)**	3.50	4.10	4.40	4.60
	Strain (mstr)	17.50	17.44	16.83	13.36
	Modulus (GPa)	0.18	0.19	0.26	0.35
TSL2_R	**UTS (MPa)**	2.80	3.20	3.40	3.70
	Strain (mstr)	11.70	10.31	9.70	8.54
	Modulus (GPa)	0.22	0.29	0.32	0.43
TSL3_R	**UTS (MPa)**	5.11	4.59	4.13	4.33
	Strain (mstr)	18.71	16.37	15.81	21.07
	Modulus (GPa)	0.23	0.30	0.24	0.15

Table H-2 Uniaxial tensile strengths, strains at failure and moduli of TSL1, TSL2 and TSL3 after various exposure times in humid condition (H - humid condition; mstr - millistrain)

TSL name	Parameter	15 days	28 days	56 days	112 days
TSL1_H	**UTS (MPa)**	1.30	1.40	1.50	1.60
	Strain (mstr)	6.77	5.56	3.99	5.21
	Modulus (GPa)	0.25	0.17	0.20	0.18
TSL2_H	**UTS (MPa)**	2.22	2.60	2.98	3.14
	Strain (mstr)	8.34	7.41	6.96	5.03
	Modulus (GPa)	0.21	0.35	0.42	0.60
TSL3_H	**UTS (MPa)**	2.37	2.21	2.20	2.17
	Strain (mstr)	7.47	6.40	5.61	5.81
	Modulus (GPa)	0.32	0.36	0.50	0.38

Table H-3 Uniaxial tensile strengths, strains at failure and moduli of TSL1, TSL2 and TSL3 after various exposure times in humid and high temperature condition (HT – humid and high temperature condition; mstr - millistrain)

TSL name	Parameter	15 days	28 days	56 days	112 days
TSL1_HT	**UTS (MPa)**	1.40	1.40	1.50	1.60
	Strain (mstr)	5.19	5.89	7.90	5.81
	Modulus (GPa)	0.28	0.20	0.17	0.23
TSL2_HT	**UTS (MPa)**	2.38	2.30	2.10	2.10
	Strain (mstr)	6.14	5.41	7.89	11.70
	Modulus (GPa)	0.37	0.44	0.27	0.14
TSL3_HT	**UTS (MPa)**	2.59	2.50	2.14	2.05
	Strain (mstr)	11.84	12.60	10.20	5.81
	Modulus (GPa)	0.19	0.21	0.21	0.43

APPENDIX I STATISTICS FROM BIT SPECIMENS STRENGTH BASED ON EXPOSURE TIME

Table I-1 Statistics of uncoated BIT of shotcrete under Room condition

	Exposure time	**135d**	**160d**	**260d**	**340d**
Uncoated shotcrete BIT_R	**BIT strengths (MPa)**	5.10	4.30	6.30	4.60
		6.10	5.00	5.30	5.00
		4.80	5.50	5.50	5.40
		5.20	5.80	4.70	5.80
		4.40	5.00	5.10	-
		4.50	-	-	-
		5.70	-	-	-
		6.00	-	-	-
		5.10	-	-	-
		5.50	-	-	-
	BIT Average (MPa)	5.24	5.12	5.38	5.20
	Std (MPa)	0.59	0.57	0.59	0.52
	CoV	11%	11%	11%	10%
	Strength increment over time	-	-2.3%	5.1%	-3.3%

Table I-2 Statistics of uncoated BIT of shotcrete under saturated condition

	Exposure time	15d	28d	56d	112d
Uncoated shotcrete BIT_H	**BIT strengths (MPa)**	4.60	4.40	4.00	4.00
		4.20	4.50	3.90	3.90
		5.00	4.70	4.30	4.50
		4.80	4.60	4.40	4.40
		5.20	4.80	4.70	4.50
	BIT Average (MPa)	4.76	4.60	4.26	4.26
	Std (MPa)	0.38	0.16	0.32	0.29
	CoV	8%	3%	8%	7%
	Strength increment over time	-	-3.4%	-7.4%	0.0%

Table I-3 Statistics of uncoated BIT of shotcrete under combined humid and high temperature condition

	Exposure time	15d	28d	56d	112d
Uncoated shotcrete BIT_ HT	**BIT strengths (MPa)**	4.70	4.70	3.90	4.50
		5.00	4.30	4.20	4.60
		4.80	4.60	4.10	3.80
		4.30	4.20	4.40	4.10
		5.00	4.40	4.10	4.00
		4.80	4.10	4.60	4.30
	BIT Average (MPa)	4.77	4.38	4.22	4.22
	Std (MPa)	0.26	0.23	0.25	0.31
	CoV	5%	5%	6%	7%
	Strength increment over time	-	-8.0%	-3.8%	0.0%

Table I-4 Statistics of shotcrete BIT specimens coated with TSL1, exposed to room condition

	Exposure time	**15d**	**28d**	**56d**	**73d**	**112d**
TSL1 Coated BIT Room	**BIT strengths (MPa)**	5.70	5.48	5.36	5.80	6.44
		5.39	6.50	5.90	6.37	6.38
		5.00	5.20	5.54	5.90	6.49
		5.70	6.28	6.47	6.33	6.41
		5.10	5.88	6.60	6.23	6.10
		-	-	-	6.78	5.55
		-	-	-	-	6.36
		-	-	-	-	6.65
	Mean (MPa)	5.38	5.87	5.97	6.24	6.30
	Std (MPa)	0.33	0.54	0.55	0.36	0.34
	CoV	6%	9%	9%	6%	5%
	Strength increment over time	-	9.1%	1.8%	4.4%	1.0%
	Strength Increase due to coating	3.4%	12.8%	14.9%	19.9%	21.1%

Table I-5 Statistics of shotcrete BIT specimens coated with TSL1, exposed to humid condition

	Exposure time	15d	28d	56d	112d
TSL1 Coated BIT H	BIT strengths (MPa)	5.60	4.60	5.20	5.30
		5.90	4.70	4.40	5.00
		5.10	5.40	5.20	4.70
		5.20	5.10	5.10	4.70
		5.10	5.20	5.40	5.30
		-	-	5.00	-
		-	-	5.00	-
		-	-	4.60	-
	Mean (MPa)	5.38	5.00	4.99	5.00
	Std (MPa)	0.36	0.34	0.33	0.30
	CoV	7%	7%	7%	6%
	Strength increment over time	-	-7.1%	-0.3%	0.3%
	Strength Increase due to coating	13.0%	8.7%	17.1%	17.4%

Table I-6 Statistics of shotcrete BIT specimens coated with TSL1, exposed to humid and high temperature condition

	Exposure time	15d	28d	56d	112d
TSL1 Coated BIT HT	BIT strengths (MPa)	4.90	5.30	4.20	4.20
		5.60	3.90	3.80	4.70
		5.70	4.90	4.40	3.90
		5.40	4.60	5.30	4.40
		-	4.40	4.50	4.70
	Mean (MPa)	5.40	4.62	4.44	4.38
	Std (MPa)	0.44	0.53	0.55	0.34
	CoV	8%	11%	12%	8%
	Strength increment over time	-	-14.4%	-3.9%	-1.4%
	Strength Increase due to coating	13.2%	5.5%	5.2%	3.8%

Table I-7 Statistics of shotcrete BIT specimens coated with TSL2, exposed to room condition

	Exposure time	15d	28d	56d	112d
TSL2 Coated BIT Room	BIT strengths (MPa)	5.50	5.30	5.60	6.10
		4.96	4.50	4.90	4.83
		4.80	5.55	5.30	6.00
		5.80	5.57	5.60	5.70
		5.45	5.00	5.60	5.50
		5.20	5.93	5.20	5.40
		-	-	6.05	6.10
	Mean (MPa)	5.28	5.31	5.46	5.66
	Std (MPa)	0.37	0.50	0.37	0.46
	CoV	7%	9%	7%	8%
	Strength increment over time	-	0.5%	2.9%	3.6%
	Strength Increase due to coating	1.6%	2.1%	5.1%	8.9%

Table I-8 Statistics of shotcrete BIT specimens coated with TSL2, exposed to humid condition

	Exposure time	15d	28d	56d	112d
TSL2 Coated BIT H	BIT strengths (MPa)	5.39	5.97	6.17	5.01
		5.60	4.90	4.76	4.93
		5.20	5.20	5.10	5.90
		5.30	5.60	5.69	5.09
		4.90	5.80	5.84	5.30
		5.70	-	-	-
	Mean (MPa)	5.35	5.49	5.51	5.25
	Std (MPa)	0.29	0.44	0.57	0.39
	CoV	5%	8%	10%	7%
	Strength increment over time	-	2.7%	0.3%	-4.8%
	Strength Increase due to coating	12.3%	19.4%	29.4%	23.1%

Table I-9 Statistics of shotcrete BIT specimens coated with TSL2, exposed to humid and high temperature condition

	Exposure time	15d	28d	56d	112d
TSL2 Coated BIT HT	**BIT strengths (MPa)**	5.10	5.15	4.27	5.30
		5.20	4.30	4.45	4.00
		4.90	4.79	4.08	4.69
		-	4.79	4.50	4.40
		-	5.69	5.25	4.60
		-	5.25	5.16	-
		-	-	5.50	-
	Mean (MPa)	5.07	4.99	4.74	4.60
	Std (MPa)	0.15	0.48	0.55	0.47
	CoV	3%	10%	12%	10%
	Strength increment over time	-	-1.4%	-5.0%	-3.1%
	Strength Increase due to coating	6.2%	14.0%	12.4%	8.9%

Table I-10 Statistics of shotcrete BIT specimens coated with TSL3, exposed to room condition

	Exposure time	15d	28d	56d	112d
TSL3 Coated BIT Room	**BIT strengths (MPa)**	4.7	6.3	5	5.8
		5.4	6.6	5.4	6.1
		6	5.6	5.9	5.7
		5.5	5.1	5.9	6.4
		6.1	5.7	6.5	5.8
		5.7	5.9	6.8	6.6
		5.7	6.6	6.6	-
	Mean (MPa)	5.59	5.97	6.01	6.07
	Std (MPa)	0.46	0.56	0.66	0.37
	CoV	8%	9%	11%	6%
	Strength increment over time	-	6.9%	0.7%	0.9%
	Strength Increase due to coating	7.4%	14.8%	15.7%	16.7%

Table I-11 Statistics of shotcrete BIT specimens coated with TSL3, exposed to humid condition

	Exposure time	15d	28d	56d	112d
TSL3 Coated BIT H	BIT strengths (MPa)	5.5	5.3	5.5	4.5
		5.7	5.1	5.5	5.2
		5.4	5.5	5.4	4.9
		5.0	5.0	4.7	5.2
		5.8	5.7	4.8	4.8
		5.2	4.8	5.2	5.6
	Mean (MPa)	5.43	5.23	5.18	5.03
	Std (MPa)	0.30	0.33	0.35	0.38
	CoV	6%	6%	7%	8%
	Strength increment over time		-3.7%	-1.0%	-2.9%
	Strength Increase due to coating	14.1%	13.8%	21.7%	18.2%

Table I-12 Statistics of shotcrete BIT specimens coated with TSL3, exposed to humid and high temperature condition

	Exposure time	15d	28d	56d	112d
TSL3 Coated BIT HT	BIT strengths (MPa)	5.50	5.30	5.00	5.00
		5.80	5.75	4.80	5.30
		5.20	5.90	5.42	5.20
		5.10	5.00	5.30	4.50
			5.20	5.70	4.90
			4.80		
	Mean (MPa)	5.40	5.32	5.24	4.98
	Std (MPa)	0.32	0.43	0.35	0.31
	CoV	6%	8%	7%	6%
	Strength increment over time		-1.4%	-1.5%	-5.0%
	Strength Increase due to coating	13.2%	21.6%	24.3%	18.0%

APPENDIX J COMPARISONS OF COATED BIT SPECIMENS BASED ON STRENGTHS AND ELONGATION

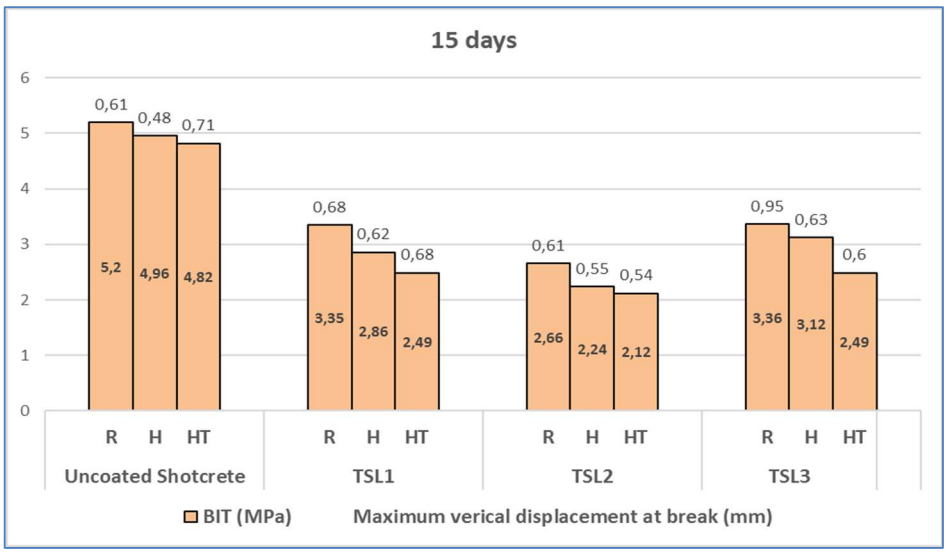


Figure J-1 Comparative charts of performances of shotcrete and TSLs combined BIT strengths and elongation after 15 days of exposure to various environmental conditions

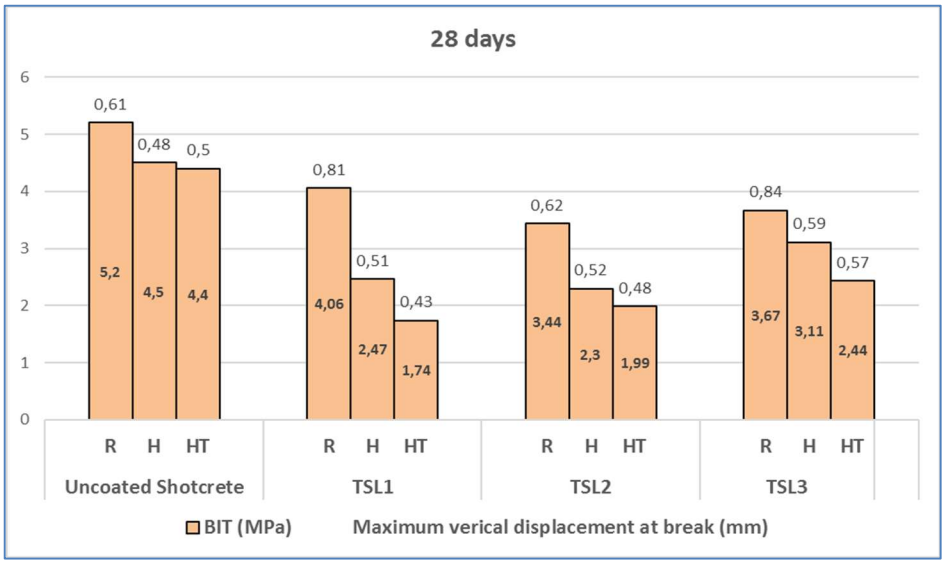


Figure J-2 Comparative charts of performances of shotcrete and TSLs combined BIT strengths and elongation after 28 days of exposure to various environmental conditions

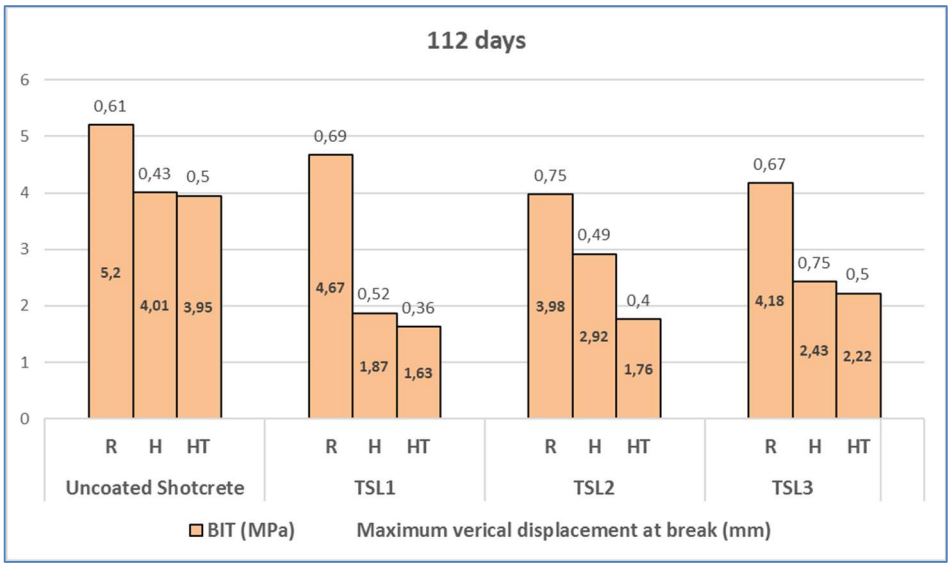


Figure J-3 Comparative charts of performances of shotcrete and TSLs combined BIT strengths and elongation after 112 days of exposure to various environmental conditions

APPENDIX K STATISTICS OF UCS TEST RESULTS

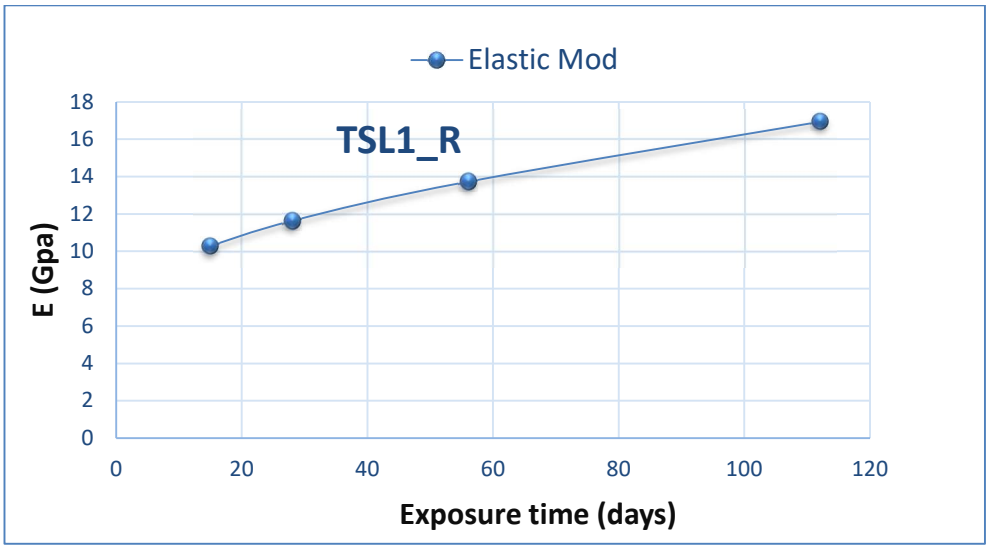


Figure K-1 Young's modulus behaviour of TSL1 after exposures in R conditions

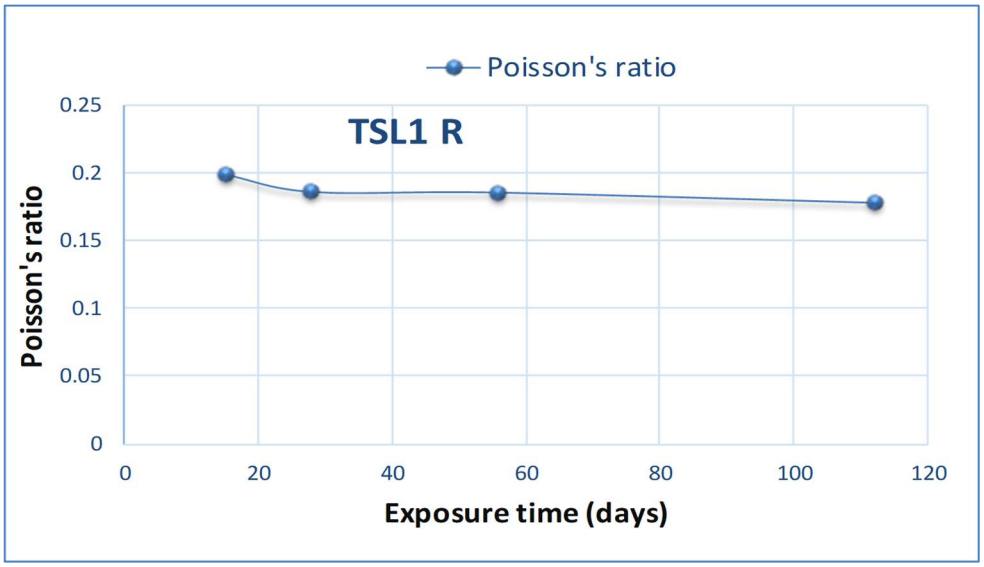


Figure K-2 Poisson's ratio behaviour of TSL1 after exposures in R conditions

And one TSL1 UCM after conditioned in the oven at 50ºC for 112days.

E=10 GPa
ν=0.18

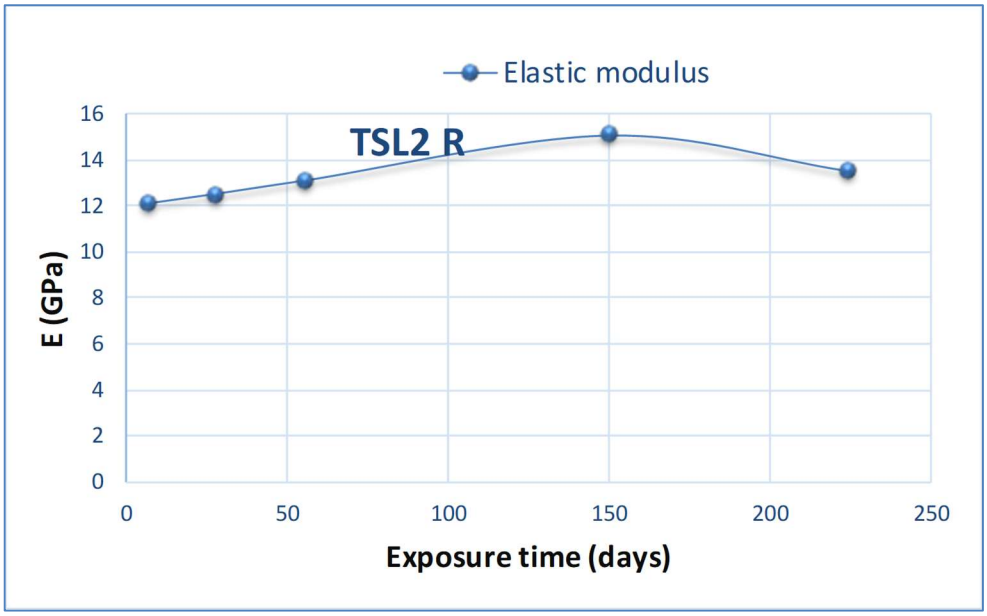


Figure K-3 Young's modulus behaviour of TSL2 after exposures in R conditions

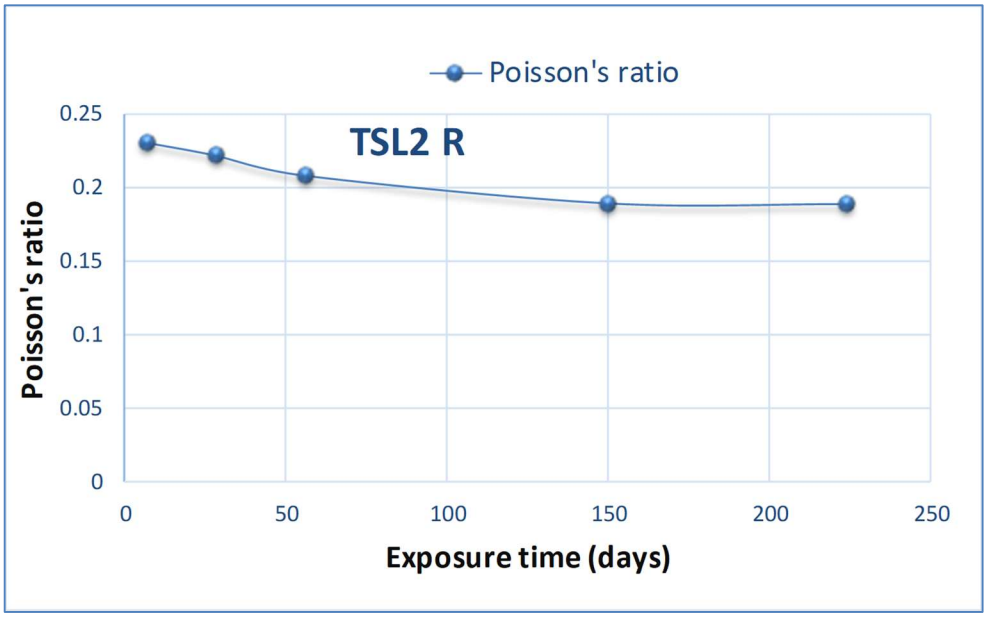


Figure K-4 Poisson's ratio behaviour of TSL2 after exposures in R conditions

And one TSL2 UCM after conditioned in the oven at 50ºC for 112days

E=11.92 GPa
ν=0.28

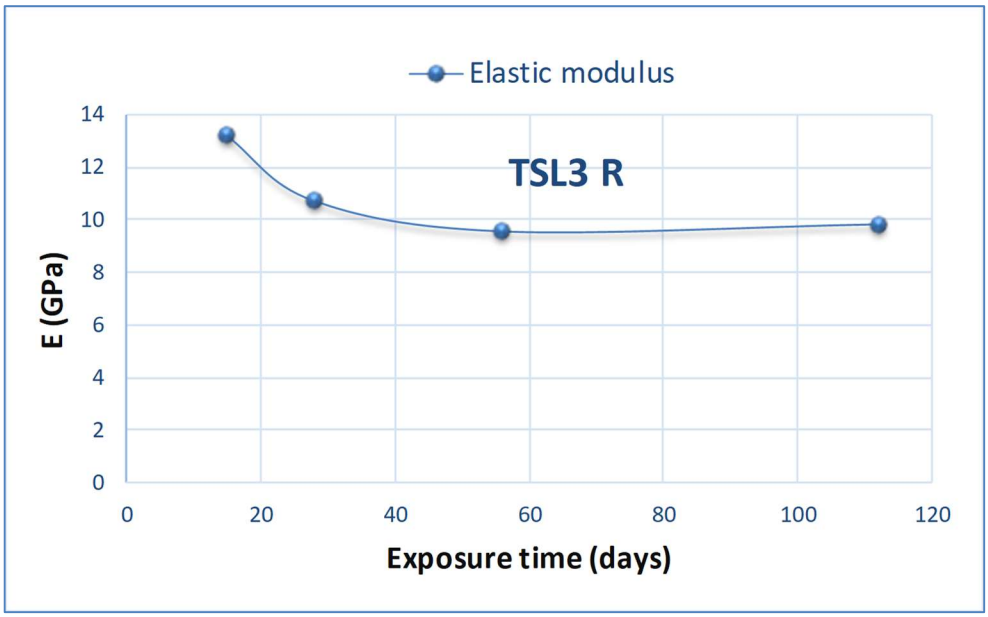


Figure K-5 Young's modulus behaviour of TSL3 after exposures in R conditions

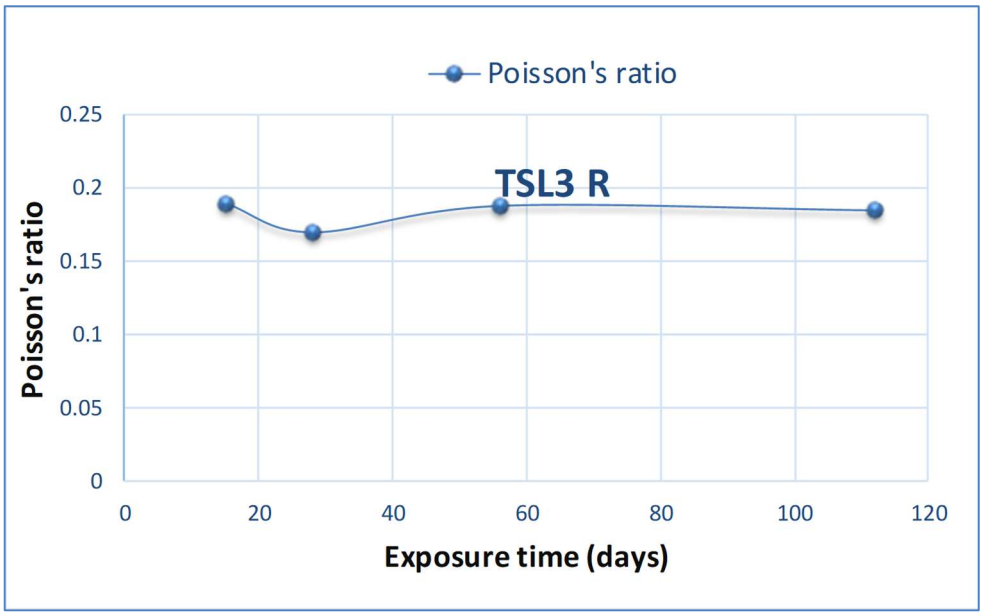


Figure K-6 Poisson's ratio behaviour of TSL3 after exposures in R conditions

And one TSL3 UCM after conditioned in oven at 50ºC for 112days

E=6.42 GPa
ν=0.23

APPENDIX L UNIAXIAL TENSILE STRENGTH CREEP TEST GRAPHS OF TSL1 TESTED IN ROOM AND HUMID CONDITIONS

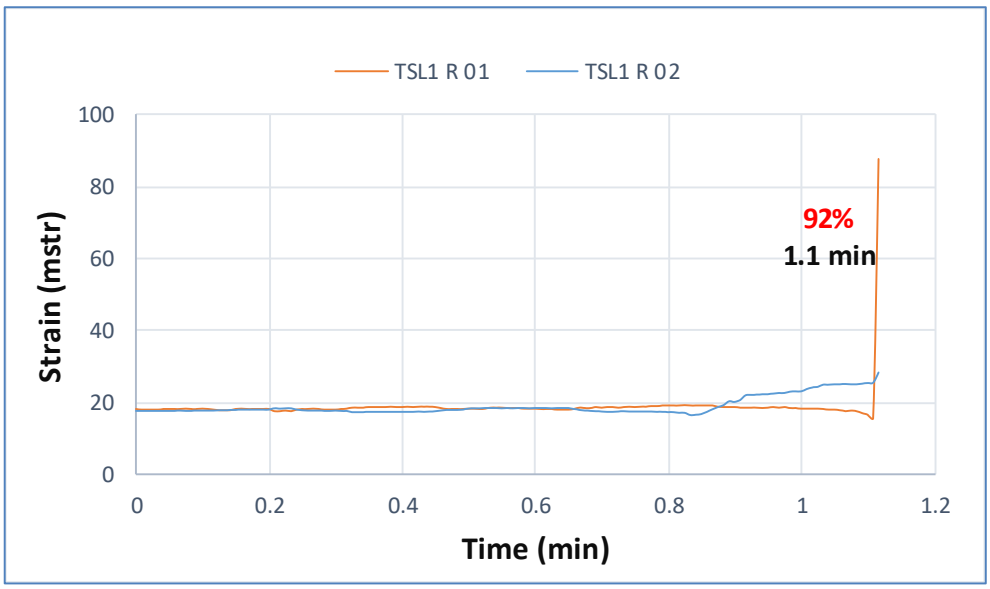


Figure L-1 UTS creep behaviour of TSL1 specimens tested in room condition at 92% of the ultimate load

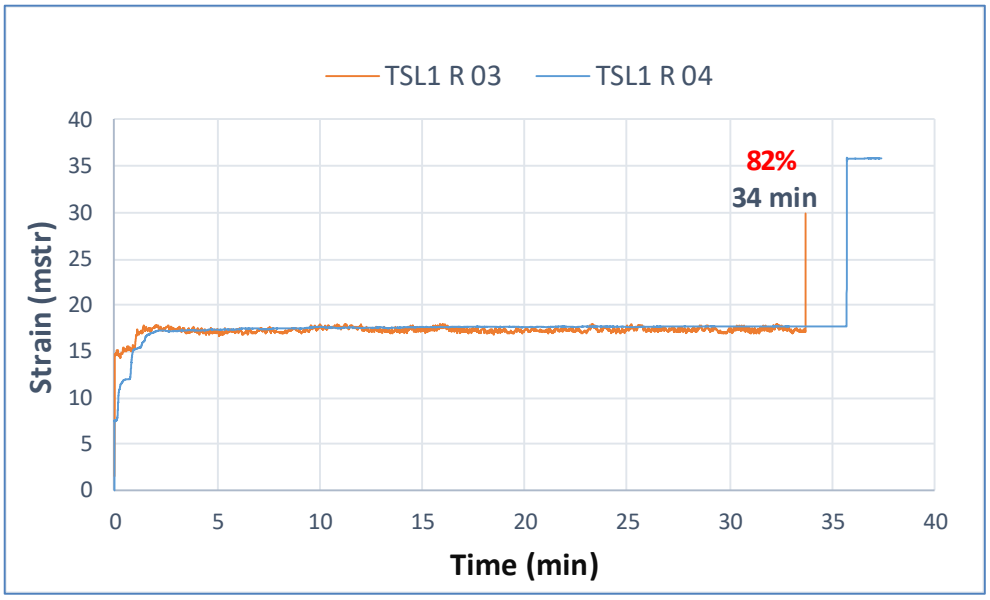


Figure L-2 UTS creep behaviour of TSL1 specimens tested in room condition at 82% of the ultimate load

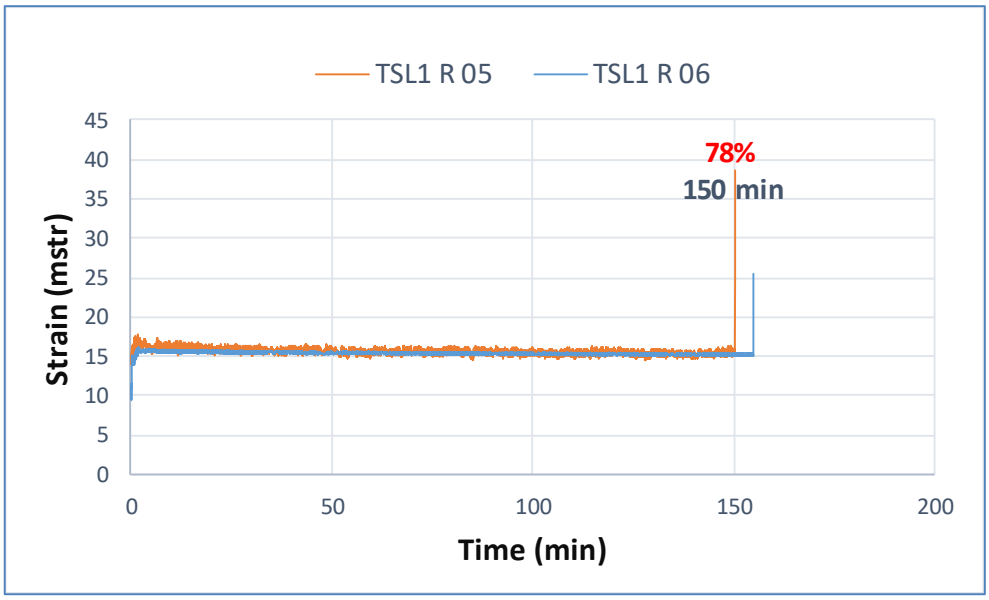


Figure L-3 UTS creep behaviour of TSL1 specimens tested in room condition at 78% of the ultimate load

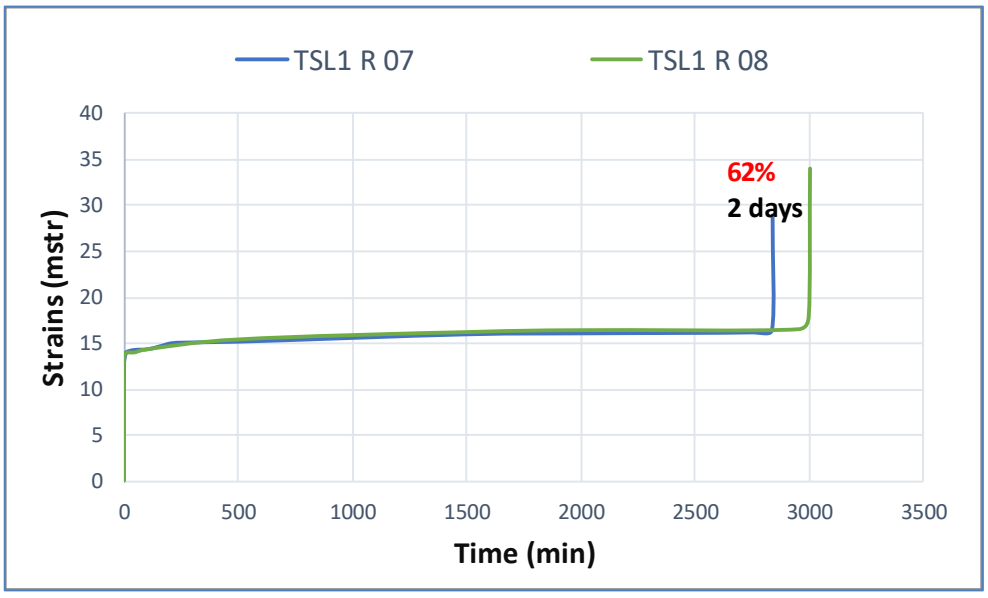


Figure L-4 UTS creep behaviour of TSL1 specimens tested in room condition at 62% of the ultimate load

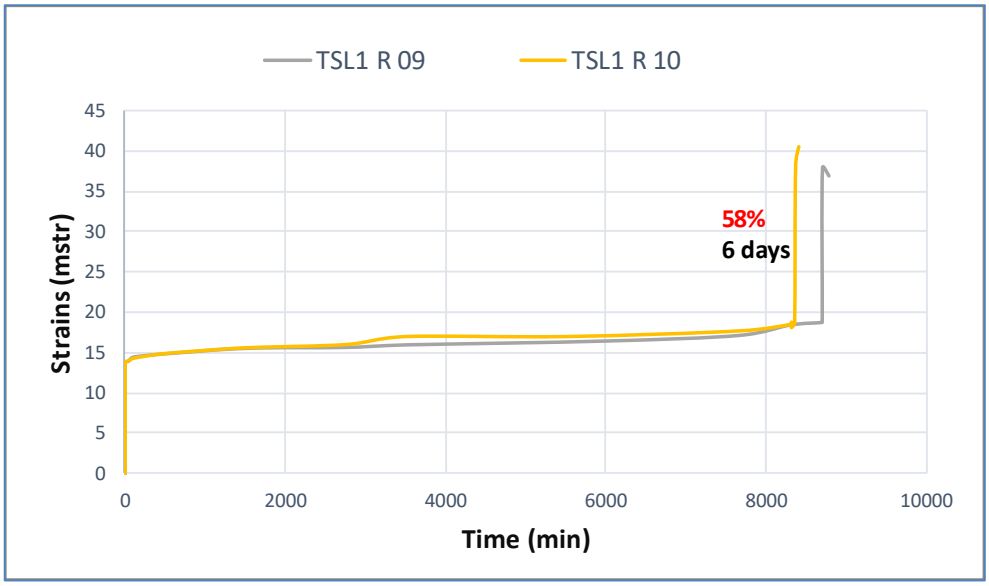


Figure L-5 UTS creep behaviour of TSL1 specimens tested in room condition at 58% of the ultimate load

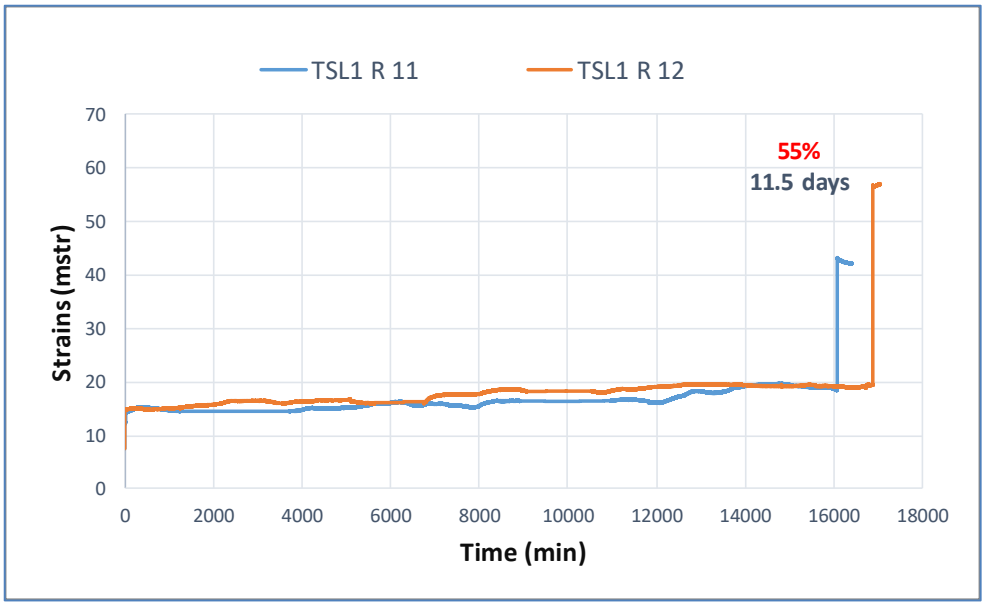


Figure L-6 UTS creep behaviour of TSL1 specimens tested in room condition at 55% of the ultimate load

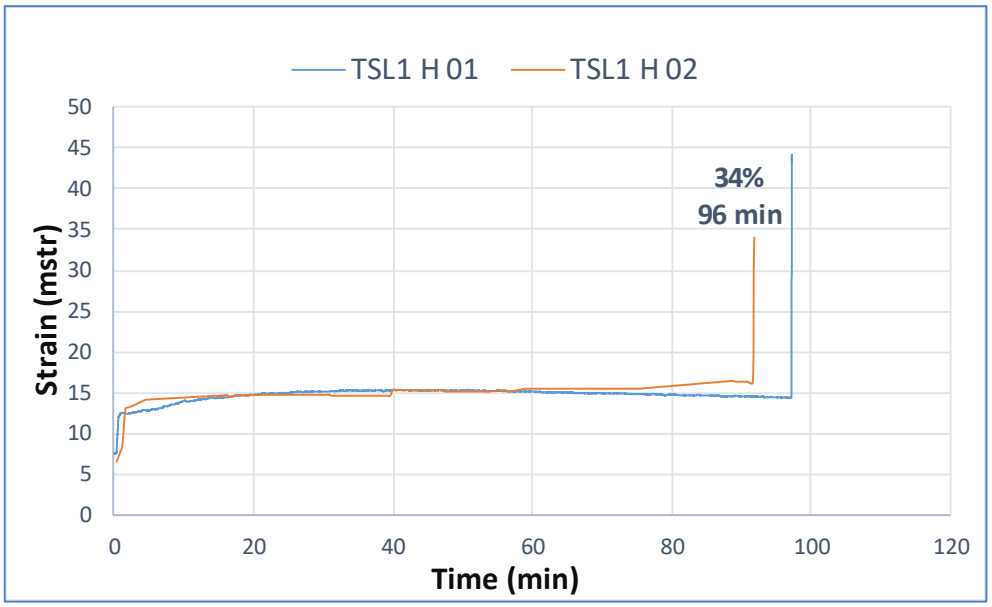


Figure L-7 UTS creep behaviour of TSL1 specimens tested in humid condition at 34% of the room ultimate load

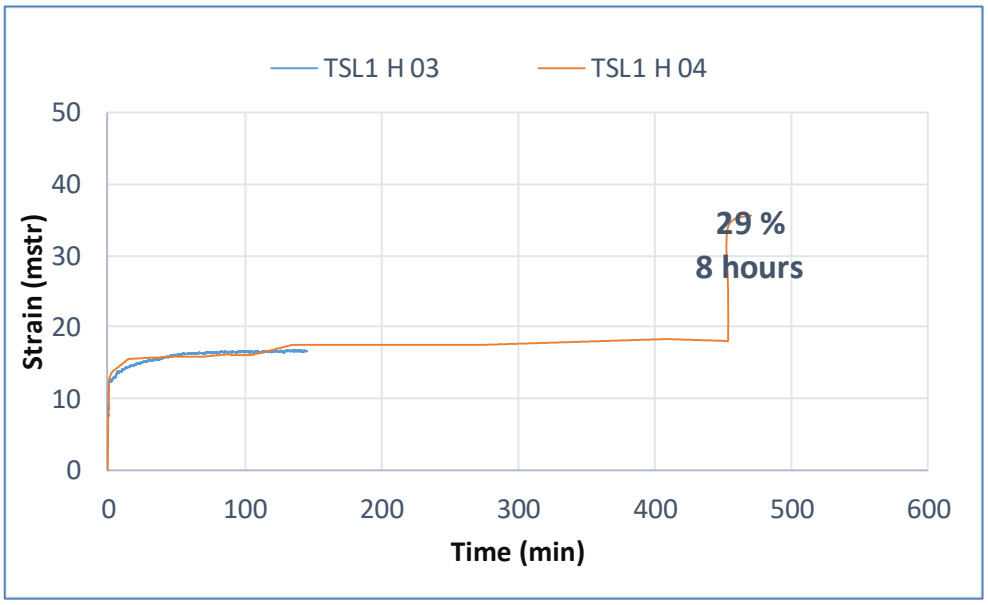


Figure L-8 UTS creep behaviour of TSL1 specimens tested in humid condition at 29% of the room ultimate load

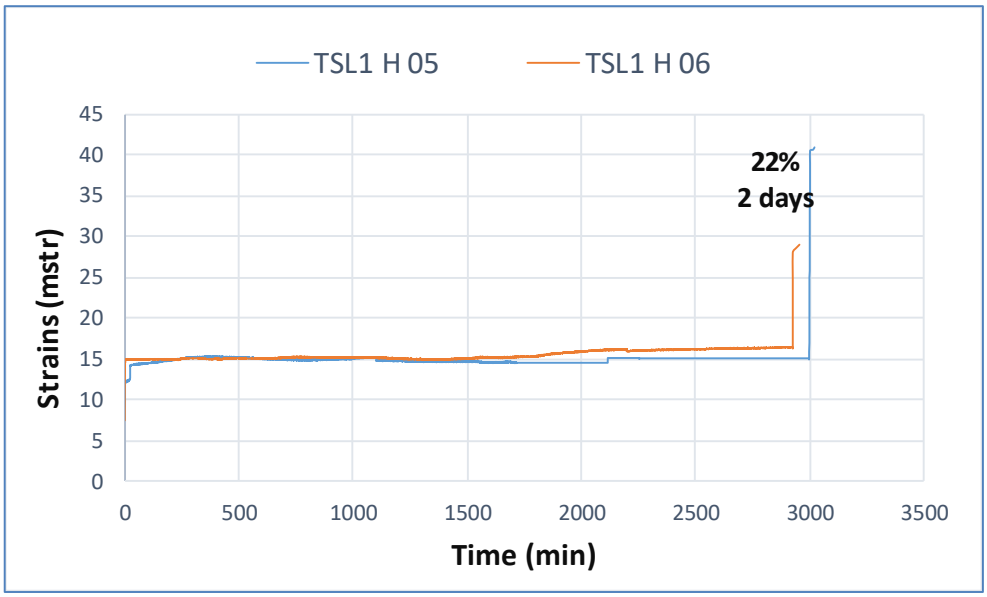


Figure L-9 UTS creep behaviour of TSL1 specimens tested in humid condition at 22% of the room ultimate load

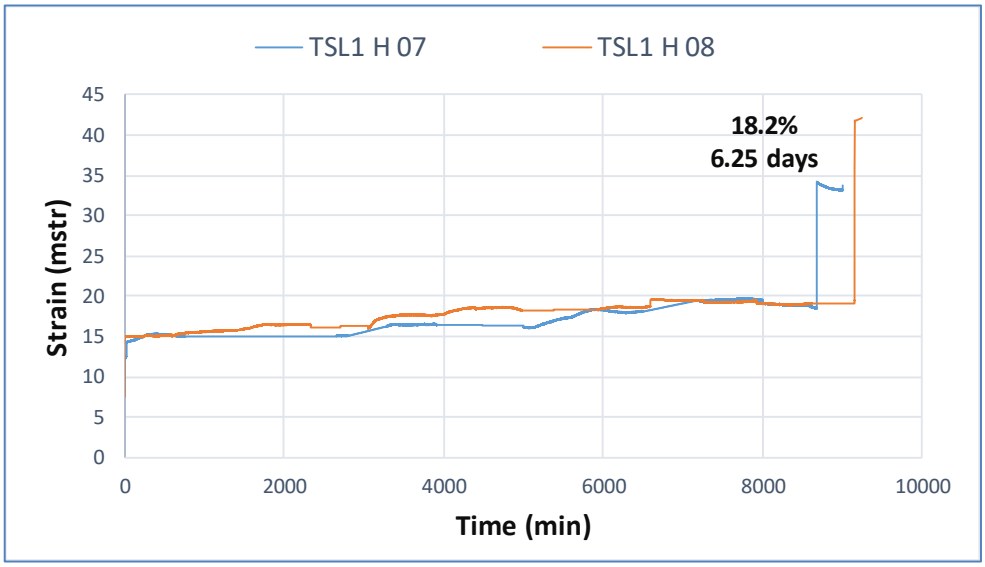


Figure L-10 UTS creep behaviour of TSL1 specimens tested in humid condition at 18.2% of the room ultimate load

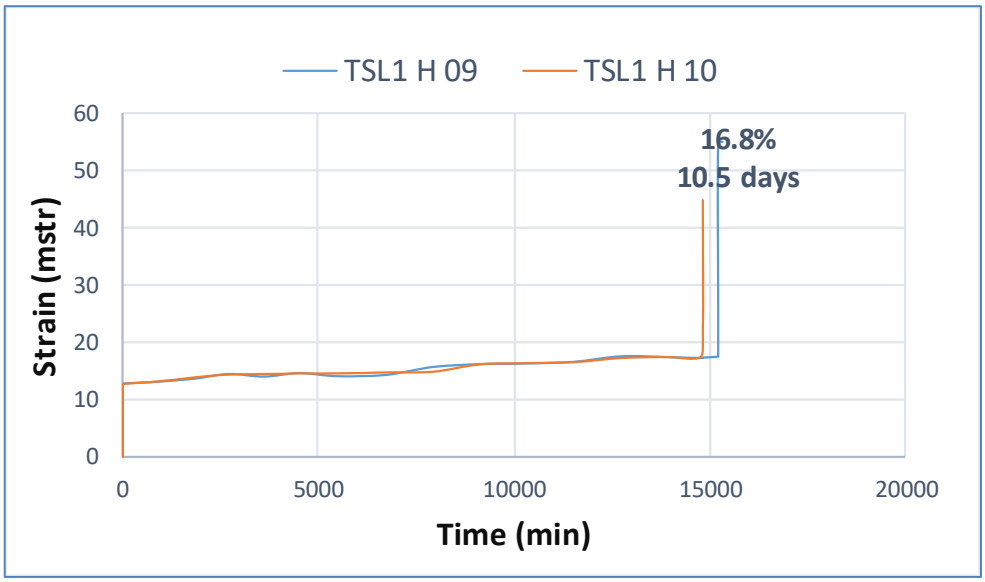


Figure L-11 UTS creep behaviour of TSL1 specimens tested in humid condition at 16.8% of the room ultimate load

APPENDIX M MEMBRANE DISPLACEMENT CREEP TEST GRAPHS OF TSL1 TESTED IN ROOM AND HUMID CONDITIONS

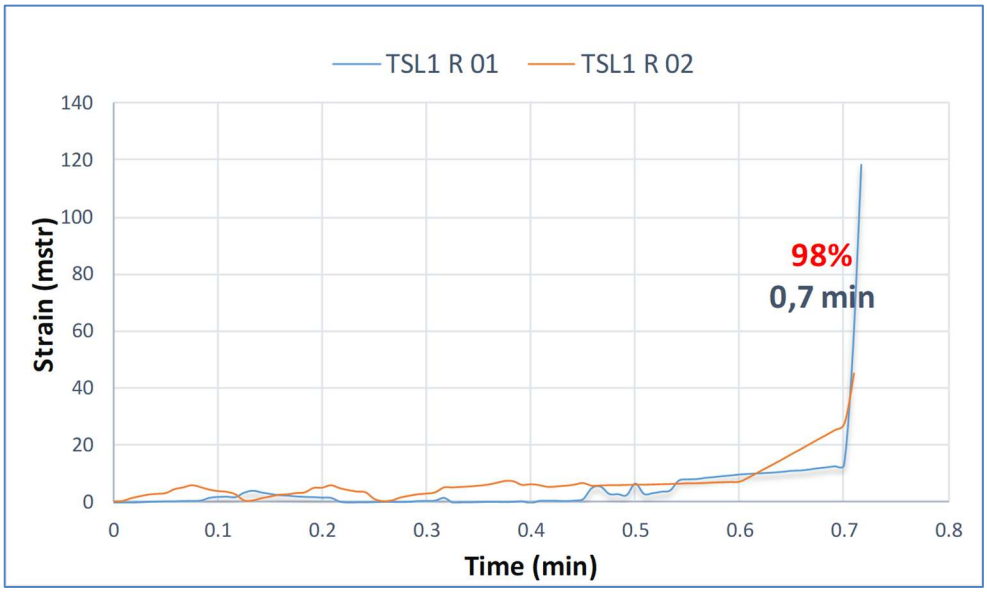


Figure M-1 MBT creep behaviour of TSL1 specimens tested in room condition at 98% of the ultimate load

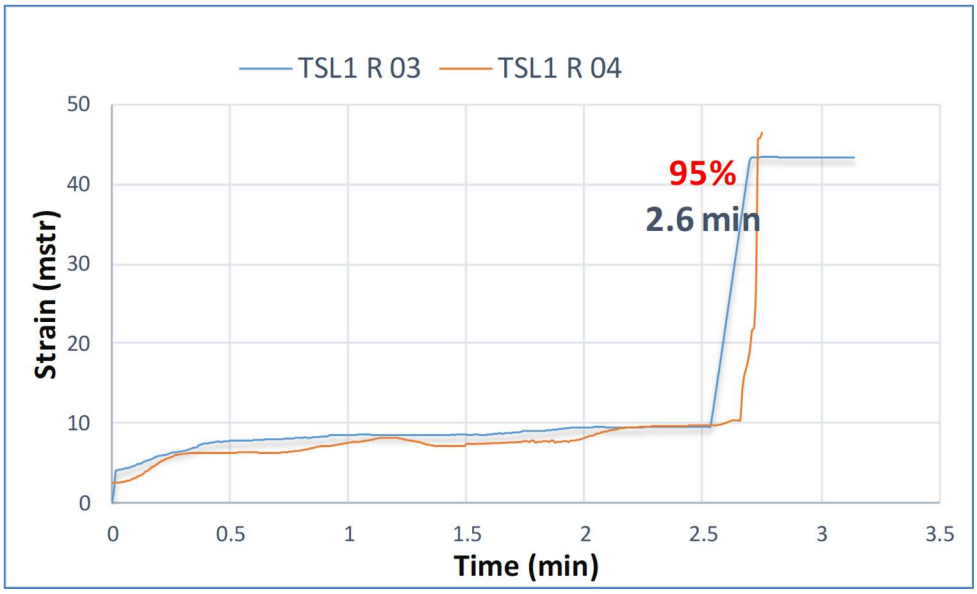


Figure M-2 MBT creep behaviour of TSL1 specimens tested in room condition at 95% of the ultimate load

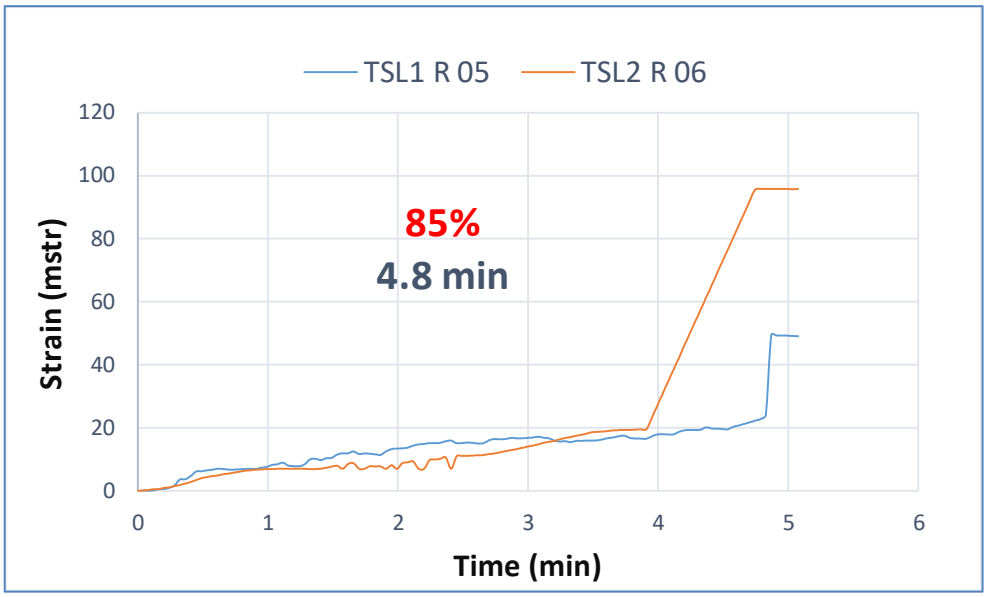


Figure M-3 MBT creep behaviour of TSL1 specimens tested in room condition at 85% of the ultimate load

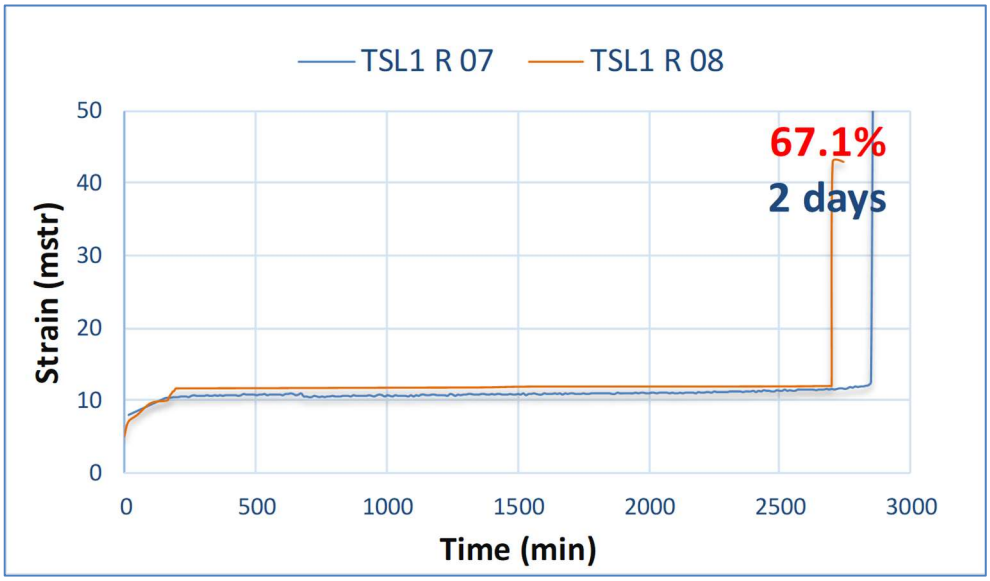


Figure M-4 MBT creep behaviour of TSL1 specimens tested in room condition at 67.1% of the ultimate load

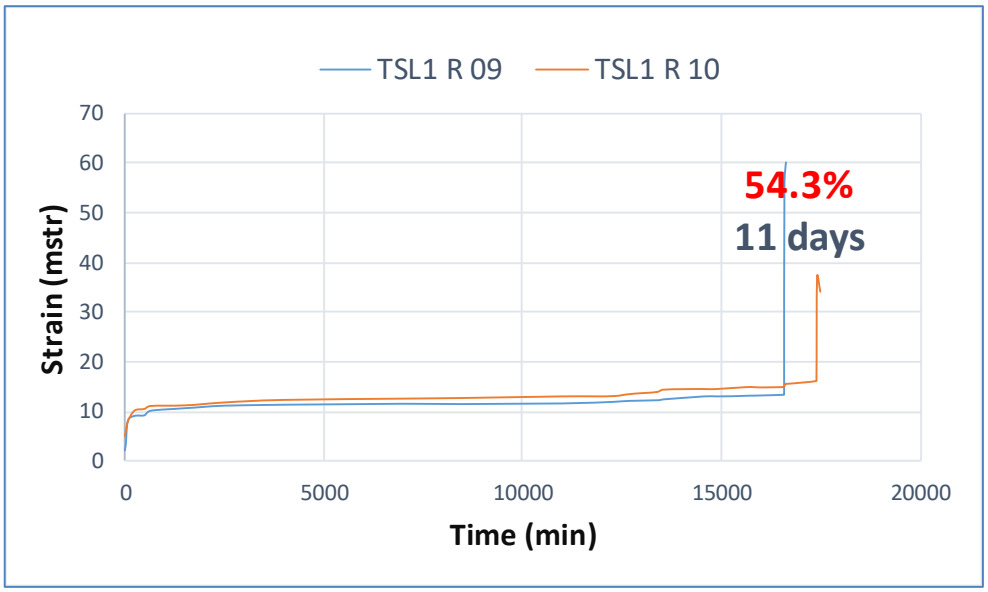


Figure M-5 MBT creep behaviour of TSL1 specimens tested in room condition at 54.3% of the ultimate load

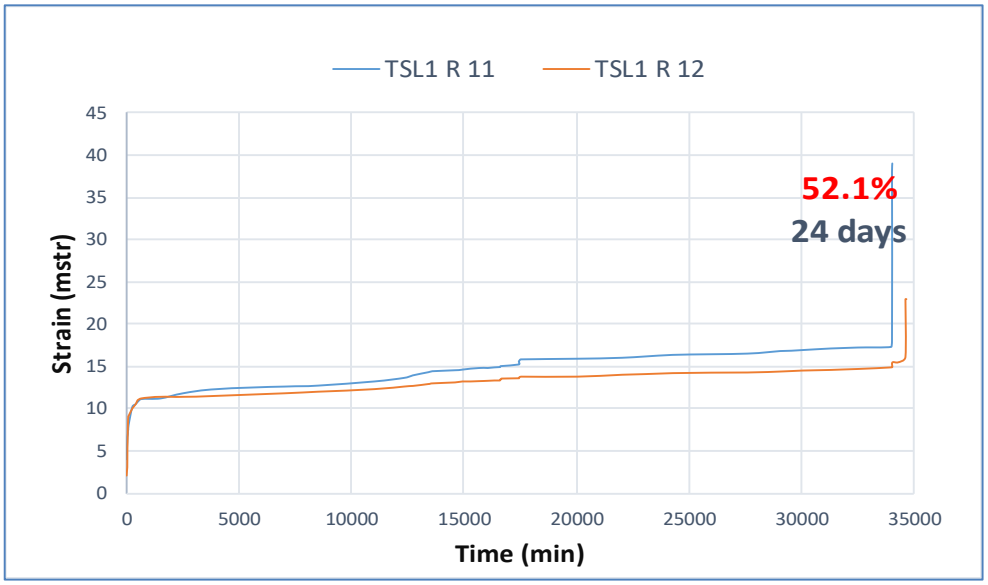


Figure M-6 MBT creep behaviour of TSL1 specimens tested in room condition at 52.1% of the ultimate load

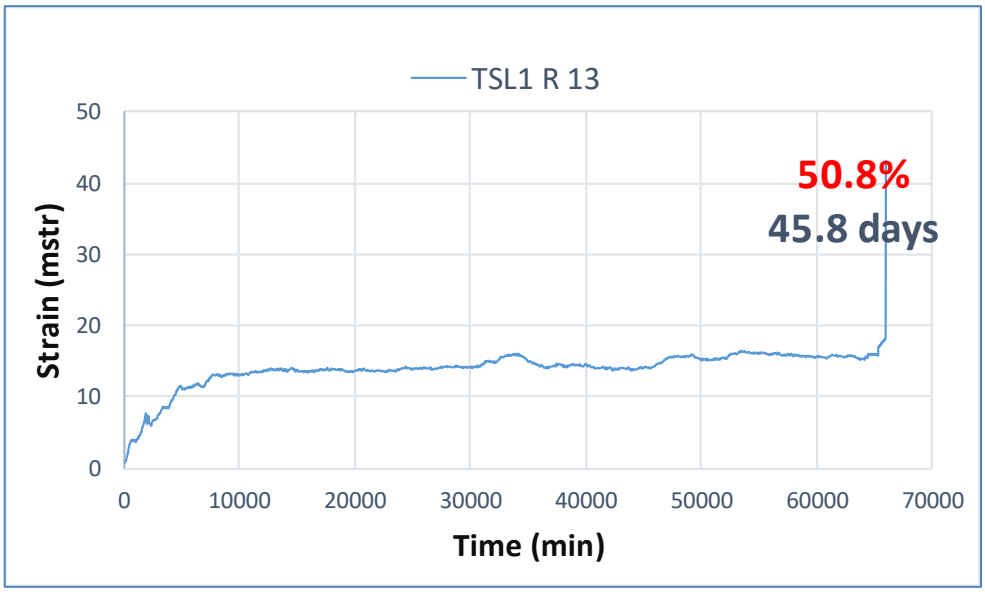


Figure M-7 MBT creep behaviour of TSL1 specimens tested in room condition at 50.8% of the ultimate load

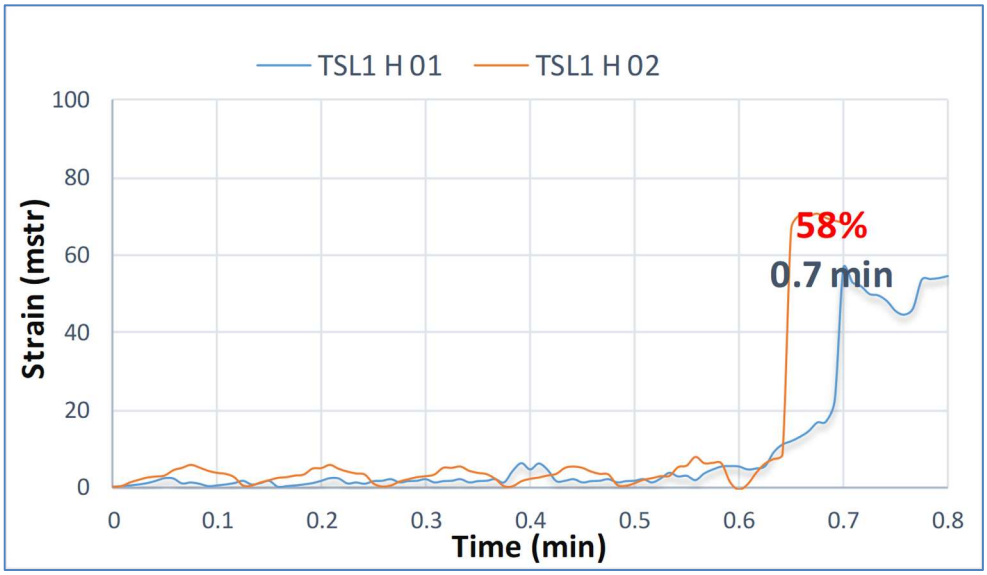


Figure M-8 MBT creep behaviour of TSL1 specimens tested in humid condition at 58% of the room ultimate load

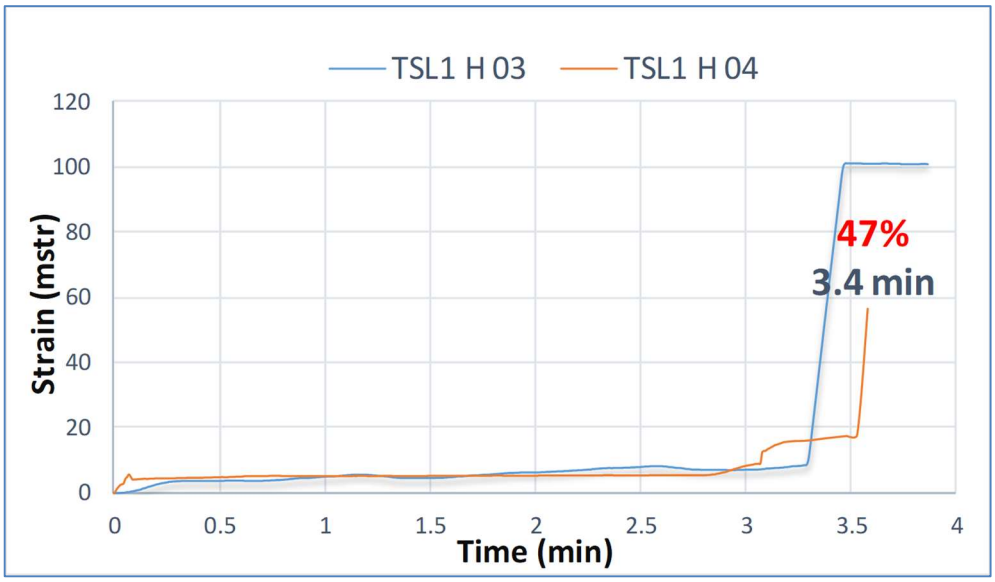


Figure M-9 MBT creep behaviour of TSL1 specimens tested in humid condition at 47% of the room ultimate load

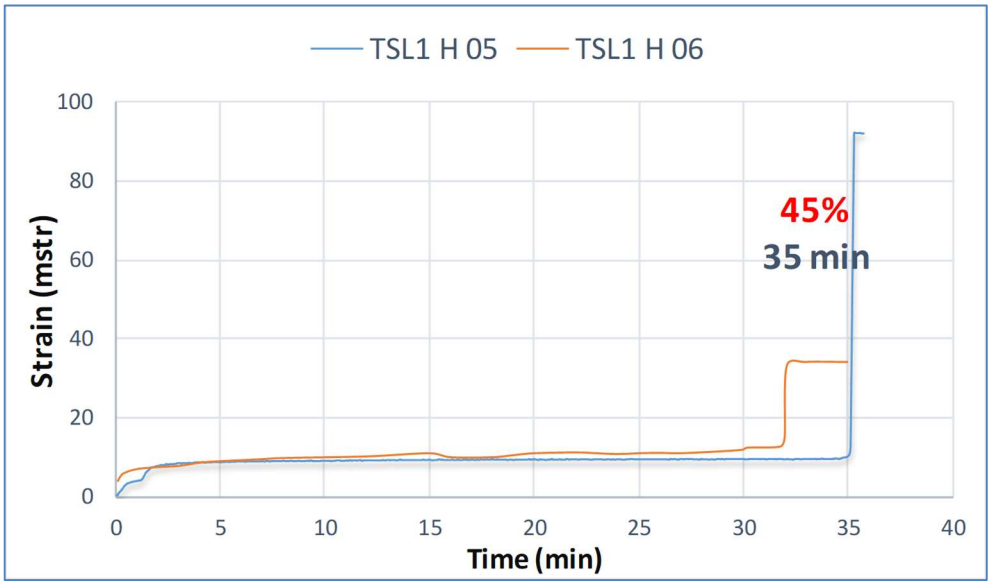


Figure M-10 MBT creep behaviour of TSL1 specimens tested in humid condition at 45% of the room ultimate load

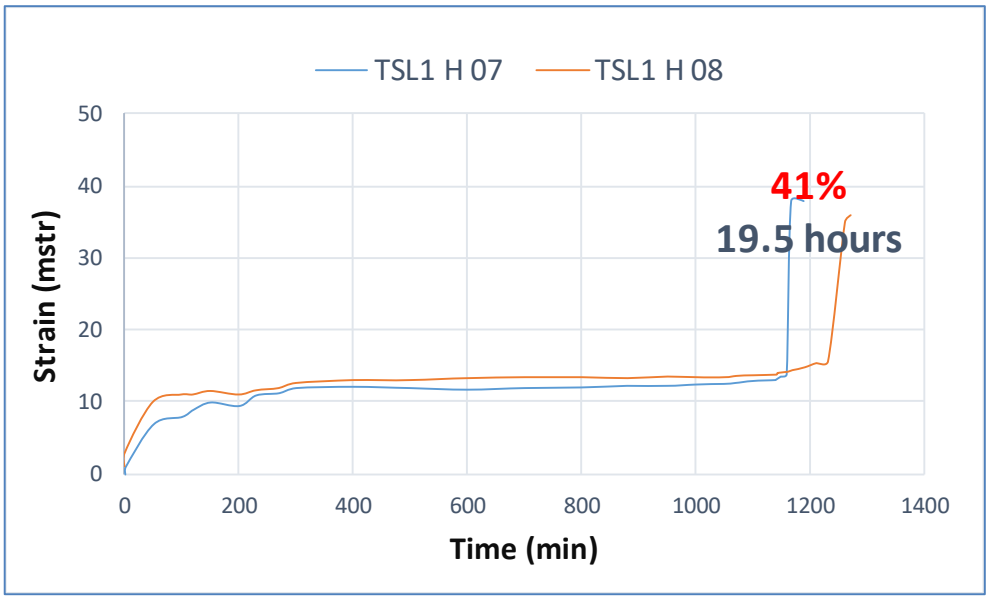


Figure M-11 MBT creep behaviour of TSL1 specimens tested in humid condition at 41% of the room ultimate load

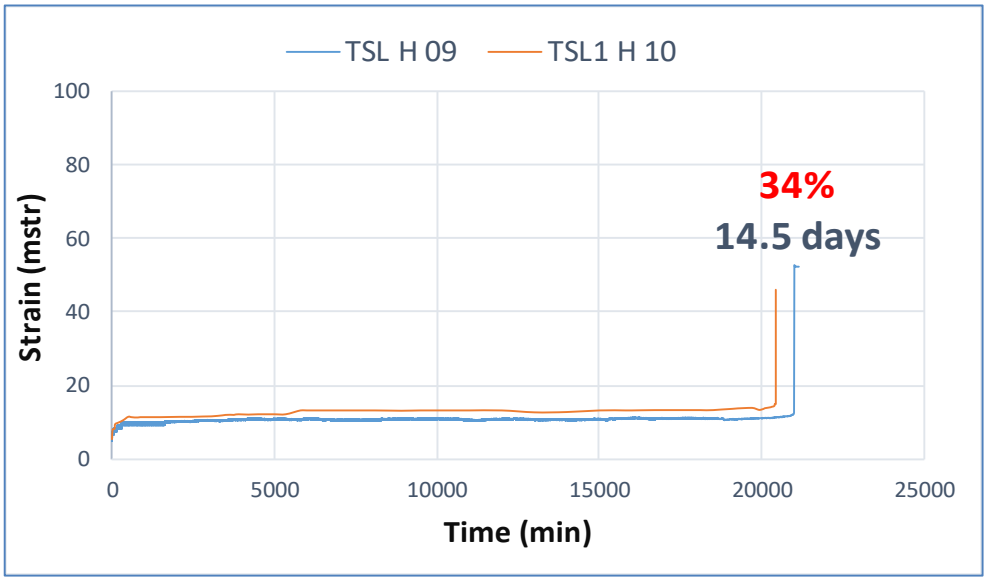


Figure M-12 MBT creep behaviour of TSL1 specimens tested in humid condition at 34% of the room ultimate load

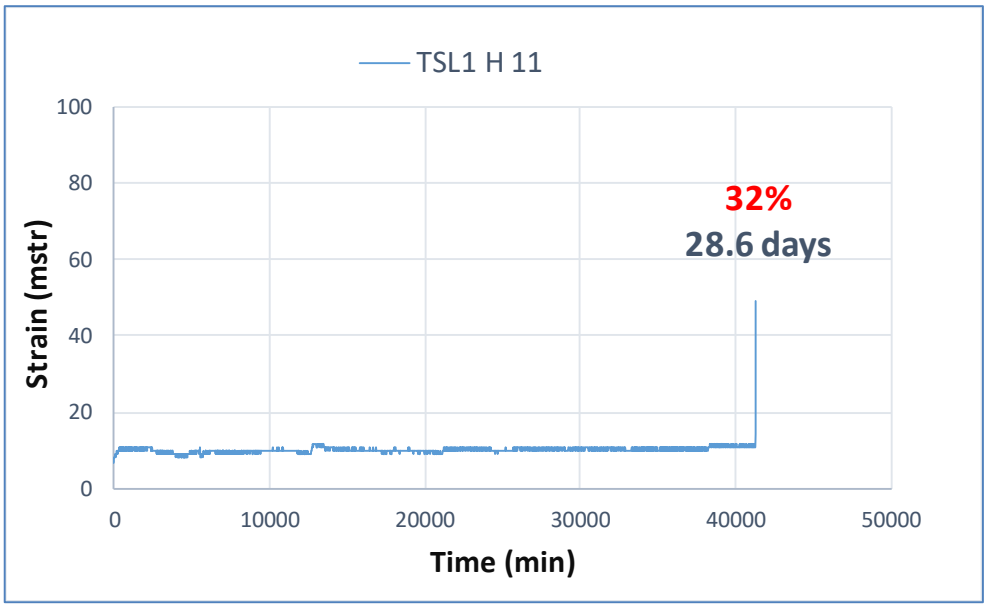


Figure M-13 MBT creep behaviour of TSL1 specimens tested in humid condition at 32% of the room ultimate load

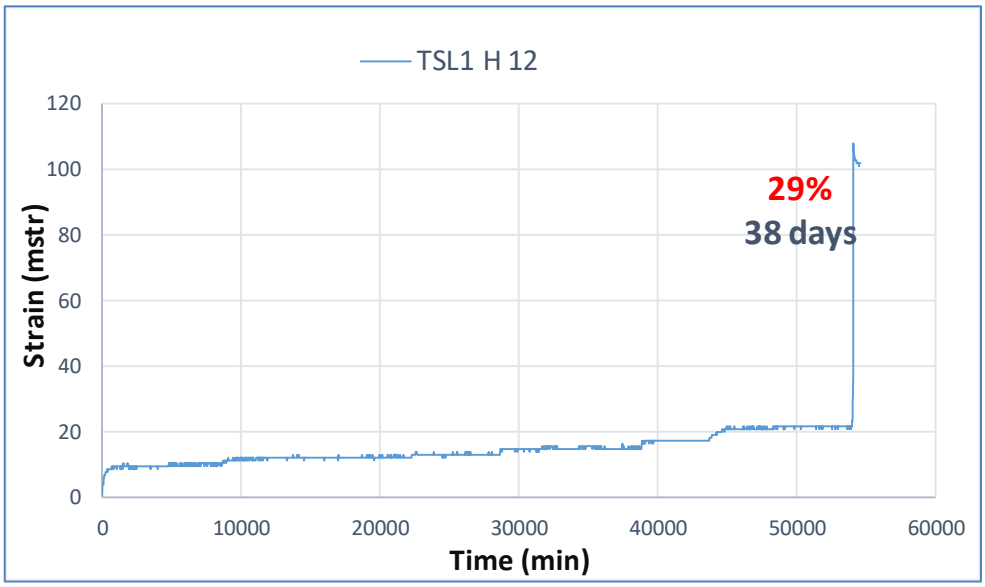


Figure M-14 MBT creep behaviour of TSL1 specimens tested in humid condition at 29% of the room ultimate load

APPENDIX N REPRESENTATIVE TRIAXIAL COMPRESSIVE RESULTS ON SHOTCRETE AND TSL

Table N-1 Results of Triaxial compressive tests of shotcrete for R and HT conditions

Tested material	Type of Test	Parameters	Input values	Sig3 (MPa)	F (kN)	Sig1 (MPa)	Additional values	
Shotcrete	**Triaxial_R**	Exposure time (days)	139	5.05	138.5	**101.46**	**UCS (MPa)**	52.21
		Diameter (mm)	41.7	10.55	175	**128.20**	**BIT (MPa)**	5.2
		Length (mm)	94.9	-	-	**-**	**Beta (°)**	24.7
	Triaxial_ HT	Exposure time (days)	112	5	106	**77.28**	**UCS (MPa)**	48.95
		Diameter (mm)	41.8	9	129	**94.05**	**BIT (MPa)**	3.6
		Length (mm)	94.5	-	-	**-**	**Beta (°)**	21

Table N-2 Results of Triaxial compressive tests of TSL1 for R and HT conditions

Tested material	Type of Test	Parameters	Input values	Sig3 (MPa)	F (kN)	Sig1 (MPa)	Additional values	
TSL1	Triaxial _R	Exposure time (days)	28	5.1	49	**36.07**	**UCS (MPa)**	28.51
		Diameter (mm)	41.6	10.34	61	**44.90**	**BIT (MPa)**	4.1
		Length (mm)	95.7	18.31	78	**57.42**	**Beta (°)**	61
		Exposure time (days)	112	5	55	**40.88**	**UCS (MPa)**	23.41
		Diameter (mm)	41.4	10	68	**50.54**	**BIT (MPa)**	4.6
		Length (mm)	95.6	15.18	77.5	**57.60**	**Beta (°)**	Disking
	Triaxial _HT	Exposure time (days)	28	4.1	38.5	27.8	**UCS (MPa)**	8.56
		Diameter (mm)	42	9.42	51.5	37.19	**BIT (MPa)**	1.40
		Length (mm)	95.8	-	-	-	**Beta (°)**	21
		Exposure time (days)	112	5	40	**28.61**	**UCS (MPa)**	6.00
		Diameter (mm)	42.2	9	50	**35.77**	**BIT (MPa)**	1.60
		Length (mm)	95.3	-	-	-	**Beta (°)**	21

Table N-3 Results of Triaxial compressive tests of TSL2 for R and HT conditions

Tested material	Type of Test	Parameters	Input values	Sig3 (MPa)	F (kN)	Sig1 (MPa)	Additional values	
TSL2	Triaxial_R	Exposure time (days)	28	5	48	**35.68**	**UCS (MPa)**	24.0
		Diameter (mm)	41.4	10	64	**47.57**	**BIT (MPa)**	3.2
		Length (mm)	95.6	-	-	**-**	**Beta (°)**	32
		Exposure time (days)	112	5.09	60.5	**45.18**	**UCS (MPa)**	29.9
		Diameter (mm)	41.3	10.32	73	**54.52**	**BIT (MPa)**	3.7
		Length (mm)	95.4	-	-	**-**	**Beta (°)**	26
	Triaxial_HT	Exposure time (days)	28	5.18	52.5	**38.65**	**UCS (MPa)**	14.0
		Diameter (mm)	41.6	8.1	62	**45.64**	**BIT (MPa)**	2.60
		Length (mm)	95.8	-	-	**-**	**Beta (°)**	23
		Exposure time (days)	112	5	54	**38.63**	**UCS (MPa)**	26.9
		Diameter (mm)	42.2	7	65	**46.50**	**BIT (MPa)**	3.14
		Length (mm)	95.7	-	-	**-**	**Beta (°)**	21

Table N-4 Results of Triaxial compressive tests of TSL3 for R and HT conditions

Tested material	Type of Test	Parameters	Input values	Sig3 (MPa)	F (kN)	Sig1 (MPa)	Additional values	
TSL3	Triaxial_R	Exposure time (days)	28	5	44	**32.23**	**UCS (MPa)**	25.28
		Diameter (mm)	41.7	10	59	**43.22**	**BIT (MPa)**	4.3
		Length (mm)	95.7	-	-	**-**	**Beta (°)**	Disking
		Exposure time (days)	112	4.82	46.5	**34.07**	**UCS (MPa)**	27.03
		Diameter (mm)	41.7	10.62	59	**43.22**	**BIT (MPa)**	3.4
		Length (mm)	95.7	-	-	**-**	**Beta (°)**	Disking
	Triaxial_HT	Exposure time (days)	28	5.12	48.6	**34.93**	**UCS (MPa)**	20.21
		Diameter (mm)	42.1	8.92	65	**46.72**	**BIT (MPa)**	2.37
		Length (mm)	95.9	-	-	**-**	**Beta (°)**	25
		Exposure time (days)	112	4.59	37.5	**27.74**	**UCS (MPa)**	20.06
		Diameter (mm)	41.5	8.08	46.5	**34.39**	**BIT (MPa)**	2.16
		Length (mm)	96	-	-	**-**	**Beta (°)**	26

APPENDIX O NUMERICAL MODELLING DATA

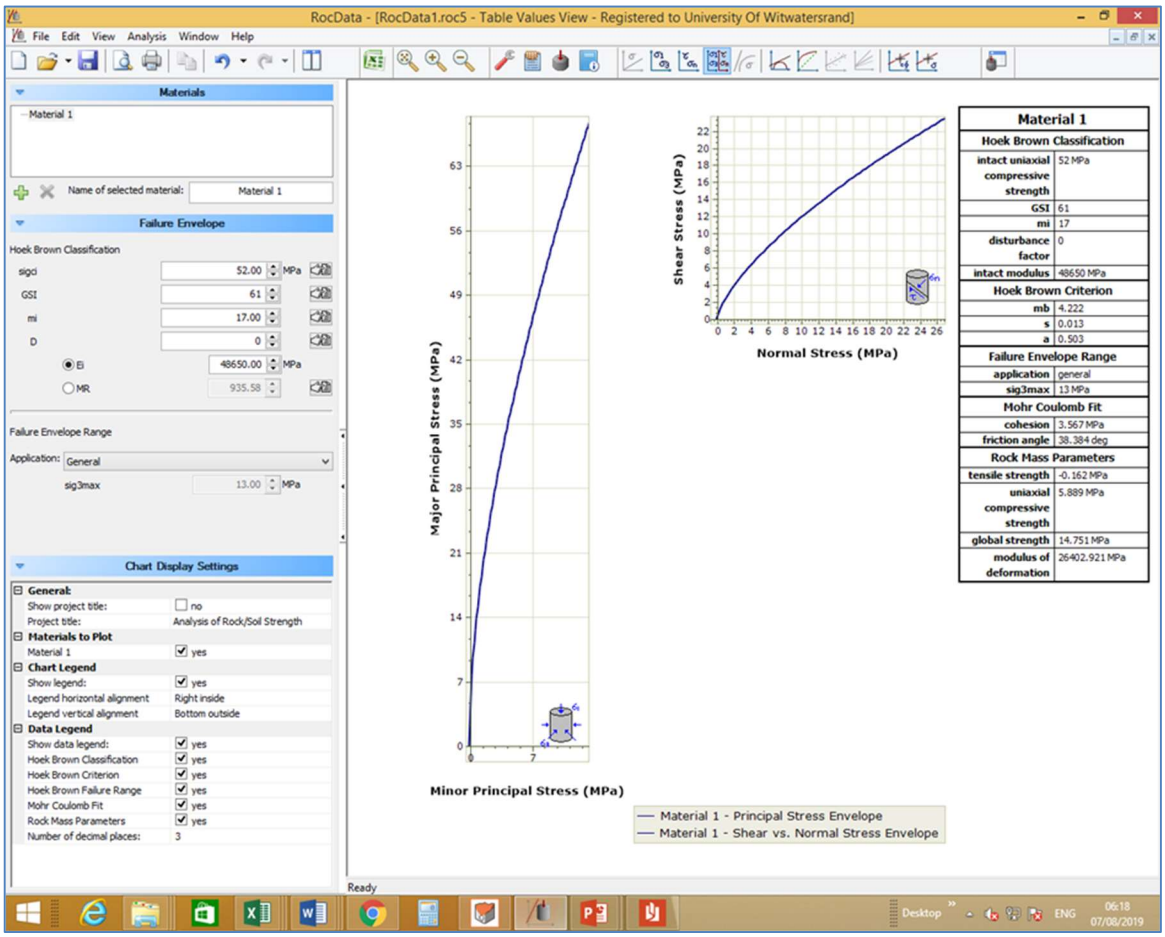


Figure O-1 Generation of rock properties through RocData package

APPENDIX P SAMPLE OF A SINGLE LONG-TERM UTS CREEP TEST

Table P-1 Sample showing the extent of data collected from a UTS creep test through channel 5 (CH5), and with failure time of 2 minutes 23 seconds

Vendor	**GRAPHTEC Corporation**						
Model	GL220						
Version	Ver1.05						
Sampling	500ms						
Total data points	287						
Start time	2018/08/29	20:26:52					
End time	2018/08/29	20:29:15					
Trigger time	2018/08/29	20:26:52					
AMP Settings							
CH	Signal name	Input	Range	Filter	Span		
CH4	" CH 4"	DC	50mV	20	25	-25	mV
CH5	" CH 5"	DC	20mV	20	10	-10	mV
Logic/Pulse	Logic						
Logic Filter	Off	Off	Off	On			
Data							
Number	Date &Time	ms	CH4	CH5	Logic	Alarm1-10	Alarm LP
NO.	Time	ms	mV	mV	1234	A1234567890	A1234
1	2018/08/29 20:26	0	6.08	0.099	HHHH	LLLLLLLLLL	LLLL
2	2018/08/29 20:26	500	6.08	0.099	HHHH	LLLLLLLLLL	LLLL
3	2018/08/29 20:26	0	6.08	0.098	HHHH	LLLLLLLLLL	LLLL
4	2018/08/29 20:26	500	6.08	0.098	HHHH	LLLLLLLLLL	LLLL
5	2018/08/29 20:26	0	6.08	0.098	HHHH	LLLLLLLLLL	LLLL
6	2018/08/29 20:26	500	6.08	0.098	HHHH	LLLLLLLLLL	LLLL
7	2018/08/29 20:26	0	6.08	0.098	HHHH	LLLLLLLLLL	LLLL
8	2018/08/29 20:26	500	6.08	0.098	HHHH	LLLLLLLLLL	LLLL
9	2018/08/29 20:26	0	6.08	0.098	HHHH	LLLLLLLLLL	LLLL
10	2018/08/29 20:26	500	6.08	0.098	HHHH	LLLLLLLLLL	LLLL

11	2018/08/29 20:26	0	6.08	0.099	HHHH	LLLLLLLLLL	LLLL
12	2018/08/29 20:26	500	6.08	0.099	HHHH	LLLLLLLLLL	LLLL
13	2018/08/29 20:26	0	6.08	0.099	HHHH	LLLLLLLLLL	LLLL
14	2018/08/29 20:26	500	6.08	0.099	HHHH	LLLLLLLLLL	LLLL
15	2018/08/29 20:26	0	6.08	0.099	HHHH	LLLLLLLLLL	LLLL
16	2018/08/29 20:26	500	6.08	0.099	HHHH	LLLLLLLLLL	LLLL
17	2018/08/29 20:27	0	6.08	0.099	HHHH	LLLLLLLLLL	LLLL
18	2018/08/29 20:27	500	6.08	0.099	HHHH	LLLLLLLLLL	LLLL
19	2018/08/29 20:27	0	6.08	0.099	HHHH	LLLLLLLLLL	LLLL
20	2018/08/29 20:27	500	6.08	0.098	HHHH	LLLLLLLLLL	LLLL
21	2018/08/29 20:27	0	6.08	0.098	HHHH	LLLLLLLLLL	LLLL
22	2018/08/29 20:27	500	6.08	0.098	HHHH	LLLLLLLLLL	LLLL
23	2018/08/29 20:27	0	6.08	0.098	HHHH	LLLLLLLLLL	LLLL
24	2018/08/29 20:27	500	6.08	0.098	HHHH	LLLLLLLLLL	LLLL
25	2018/08/29 20:27	0	6.08	0.098	HHHH	LLLLLLLLLL	LLLL
26	2018/08/29 20:27	500	6.08	0.098	HHHH	LLLLLLLLLL	LLLL
27	2018/08/29 20:27	0	6.08	0.098	HHHH	LLLLLLLLLL	LLLL
28	2018/08/29 20:27	500	6.08	0.098	HHHH	LLLLLLLLLL	LLLL
29	2018/08/29 20:27	0	6.08	0.098	HHHH	LLLLLLLLLL	LLLL
30	2018/08/29 20:27	500	6.08	0.098	HHHH	LLLLLLLLLL	LLLL
31	2018/08/29 20:27	0	6.08	0.098	HHHH	LLLLLLLLLL	LLLL
32	2018/08/29 20:27	500	6.08	0.098	HHHH	LLLLLLLLLL	LLLL
33	2018/08/29 20:27	0	6.08	0.098	HHHH	LLLLLLLLLL	LLLL
34	2018/08/29 20:27	500	6.08	0.098	HHHH	LLLLLLLLLL	LLLL
35	2018/08/29 20:27	0	6.08	0.098	HHHH	LLLLLLLLLL	LLLL
36	2018/08/29 20:27	500	6.08	0.098	HHHH	LLLLLLLLLL	LLLL

37	2018/08/29 20:27	0	6.08	0.098	HHHH	LLLLLLLLLL	LLLL
38	2018/08/29 20:27	500	6.08	0.098	HHHH	LLLLLLLLLL	LLLL
39	2018/08/29 20:27	0	6.08	0.098	HHHH	LLLLLLLLLL	LLLL
40	2018/08/29 20:27	500	6.08	0.098	HHHH	LLLLLLLLLL	LLLL
41	2018/08/29 20:27	0	6.08	0.099	HHHH	LLLLLLLLLL	LLLL
42	2018/08/29 20:27	500	6.08	0.099	HHHH	LLLLLLLLLL	LLLL
43	2018/08/29 20:27	0	6.08	0.1	HHHH	LLLLLLLLLL	LLLL
44	2018/08/29 20:27	500	6.08	0.101	HHHH	LLLLLLLLLL	LLLL
45	2018/08/29 20:27	0	6.08	0.102	HHHH	LLLLLLLLLL	LLLL
46	2018/08/29 20:27	500	6.08	0.104	HHHH	LLLLLLLLLL	LLLL
47	2018/08/29 20:27	0	6.08	0.105	HHHH	LLLLLLLLLL	LLLL
48	2018/08/29 20:27	500	6.08	0.108	HHHH	LLLLLLLLLL	LLLL
49	2018/08/29 20:27	0	6.08	0.11	HHHH	LLLLLLLLLL	LLLL
50	2018/08/29 20:27	500	6.08	0.114	HHHH	LLLLLLLLLL	LLLL
51	2018/08/29 20:27	0	6.08	0.116	HHHH	LLLLLLLLLL	LLLL
52	2018/08/29 20:27	500	6.08	0.12	HHHH	LLLLLLLLLL	LLLL
53	2018/08/29 20:27	0	6.08	0.123	HHHH	LLLLLLLLLL	LLLL
54	2018/08/29 20:27	500	6.08	0.127	HHHH	LLLLLLLLLL	LLLL
55	2018/08/29 20:27	0	6.08	0.128	HHHH	LLLLLLLLLL	LLLL
56	2018/08/29 20:27	500	6.08	0.131	HHHH	LLLLLLLLLL	LLLL
57	2018/08/29 20:27	0	6.08	0.134	HHHH	LLLLLLLLLL	LLLL
58	2018/08/29 20:27	500	6.08	0.138	HHHH	LLLLLLLLLL	LLLL
59	2018/08/29 20:27	0	6.08	0.141	HHHH	LLLLLLLLLL	LLLL
60	2018/08/29 20:27	500	6.08	0.144	HHHH	LLLLLLLLLL	LLLL
61	2018/08/29 20:27	0	6.08	0.147	HHHH	LLLLLLLLLL	LLLL
62	2018/08/29 20:27	500	6.08	0.151	HHHH	LLLLLLLLLL	LLLL

63	2018/08/29 20:27	0	6.08	0.153	HHHH	LLLLLLLLLL	LLLL
64	2018/08/29 20:27	500	6.08	0.156	HHHH	LLLLLLLLLL	LLLL
65	2018/08/29 20:27	0	6.08	0.158	HHHH	LLLLLLLLLL	LLLL
66	2018/08/29 20:27	500	6.08	0.163	HHHH	LLLLLLLLLL	LLLL
67	2018/08/29 20:27	0	6.08	0.164	HHHH	LLLLLLLLLL	LLLL
68	2018/08/29 20:27	500	6.08	0.165	HHHH	LLLLLLLLLL	LLLL
69	2018/08/29 20:27	0	6.08	0.166	HHHH	LLLLLLLLLL	LLLL
70	2018/08/29 20:27	500	6.08	0.167	HHHH	LLLLLLLLLL	LLLL
71	2018/08/29 20:27	0	6.08	0.168	HHHH	LLLLLLLLLL	LLLL
72	2018/08/29 20:27	500	6.08	0.168	HHHH	LLLLLLLLLL	LLLL
73	2018/08/29 20:27	0	6.08	0.169	HHHH	LLLLLLLLLL	LLLL
74	2018/08/29 20:27	500	6.08	0.169	HHHH	LLLLLLLLLL	LLLL
75	2018/08/29 20:27	0	6.08	0.169	HHHH	LLLLLLLLLL	LLLL
76	2018/08/29 20:27	500	6.08	0.169	HHHH	LLLLLLLLLL	LLLL
77	2018/08/29 20:27	0	6.08	0.167	HHHH	LLLLLLLLLL	LLLL
78	2018/08/29 20:27	500	6.08	0.168	HHHH	LLLLLLLLLL	LLLL
79	2018/08/29 20:27	0	6.08	0.168	HHHH	LLLLLLLLLL	LLLL
80	2018/08/29 20:27	500	6.08	0.168	HHHH	LLLLLLLLLL	LLLL
81	2018/08/29 20:27	0	6.08	0.168	HHHH	LLLLLLLLLL	LLLL
82	2018/08/29 20:27	500	6.08	0.169	HHHH	LLLLLLLLLL	LLLL
83	2018/08/29 20:27	0	6.08	0.169	HHHH	LLLLLLLLLL	LLLL
84	2018/08/29 20:27	500	6.08	0.169	HHHH	LLLLLLLLLL	LLLL
85	2018/08/29 20:27	0	6.08	0.169	HHHH	LLLLLLLLLL	LLLL
86	2018/08/29 20:27	500	6.08	0.169	HHHH	LLLLLLLLLL	LLLL
87	2018/08/29 20:27	0	6.08	0.169	HHHH	LLLLLLLLLL	LLLL
88	2018/08/29 20:27	500	6.08	0.17	HHHH	LLLLLLLLLL	LLLL

89	2018/08/29 20:27	0	6.08	0.17	HHHH	LLLLLLLLLL	LLLL
90	2018/08/29 20:27	500	6.08	0.171	HHHH	LLLLLLLLLL	LLLL
91	2018/08/29 20:27	0	6.08	0.171	HHHH	LLLLLLLLLL	LLLL
92	2018/08/29 20:27	500	6.08	0.171	HHHH	LLLLLLLLLL	LLLL
93	2018/08/29 20:27	0	6.08	0.172	HHHH	LLLLLLLLLL	LLLL
94	2018/08/29 20:27	500	6.08	0.173	HHHH	LLLLLLLLLL	LLLL
95	2018/08/29 20:27	0	6.08	0.173	HHHH	LLLLLLLLLL	LLLL
96	2018/08/29 20:27	500	6.08	0.174	HHHH	LLLLLLLLLL	LLLL
97	2018/08/29 20:27	0	6.08	0.175	HHHH	LLLLLLLLLL	LLLL
98	2018/08/29 20:27	500	6.08	0.175	HHHH	LLLLLLLLLL	LLLL
99	2018/08/29 20:27	0	6.08	0.174	HHHH	LLLLLLLLLL	LLLL
100	2018/08/29 20:27	500	6.08	0.174	HHHH	LLLLLLLLLL	LLLL
101	2018/08/29 20:27	0	6.08	0.175	HHHH	LLLLLLLLLL	LLLL
102	2018/08/29 20:27	500	6.08	0.175	HHHH	LLLLLLLLLL	LLLL
103	2018/08/29 20:27	0	6.08	0.175	HHHH	LLLLLLLLLL	LLLL
104	2018/08/29 20:27	500	6.08	0.176	HHHH	LLLLLLLLLL	LLLL
105	2018/08/29 20:27	0	6.08	0.177	HHHH	LLLLLLLLLL	LLLL
106	2018/08/29 20:27	500	6.08	0.178	HHHH	LLLLLLLLLL	LLLL
107	2018/08/29 20:27	0	6.08	0.179	HHHH	LLLLLLLLLL	LLLL
108	2018/08/29 20:27	500	6.08	0.18	HHHH	LLLLLLLLLL	LLLL
109	2018/08/29 20:27	0	6.08	0.181	HHHH	LLLLLLLLLL	LLLL
110	2018/08/29 20:27	500	6.08	0.184	HHHH	LLLLLLLLLL	LLLL
111	2018/08/29 20:27	0	6.08	0.185	HHHH	LLLLLLLLLL	LLLL
112	2018/08/29 20:27	500	6.08	0.186	HHHH	LLLLLLLLLL	LLLL
113	2018/08/29 20:27	0	6.08	0.187	HHHH	LLLLLLLLLL	LLLL
114	2018/08/29 20:27	500	6.08	0.188	HHHH	LLLLLLLLLL	LLLL

115	2018/08/29 20:27	0	6.08	0.189	HHHH	LLLLLLLLLL	LLLL
116	2018/08/29 20:27	500	6.08	0.19	HHHH	LLLLLLLLLL	LLLL
117	2018/08/29 20:27	0	6.08	0.192	HHHH	LLLLLLLLLL	LLLL
118	2018/08/29 20:27	500	6.08	0.193	HHHH	LLLLLLLLLL	LLLL
119	2018/08/29 20:27	0	6.08	0.194	HHHH	LLLLLLLLLL	LLLL
120	2018/08/29 20:27	500	6.08	0.195	HHHH	LLLLLLLLLL	LLLL
121	2018/08/29 20:27	0	6.08	0.197	HHHH	LLLLLLLLLL	LLLL
122	2018/08/29 20:27	500	6.08	0.198	HHHH	LLLLLLLLLL	LLLL
123	2018/08/29 20:27	0	6.08	0.199	HHHH	LLLLLLLLLL	LLLL
124	2018/08/29 20:27	500	6.08	0.2	HHHH	LLLLLLLLLL	LLLL
125	2018/08/29 20:27	0	6.08	0.202	HHHH	LLLLLLLLLL	LLLL
126	2018/08/29 20:27	500	6.08	0.203	HHHH	LLLLLLLLLL	LLLL
127	2018/08/29 20:27	0	6.08	0.205	HHHH	LLLLLLLLLL	LLLL
128	2018/08/29 20:27	500	6.08	0.205	HHHH	LLLLLLLLLL	LLLL
129	2018/08/29 20:27	0	6.08	0.205	HHHH	LLLLLLLLLL	LLLL
130	2018/08/29 20:27	500	6.08	0.206	HHHH	LLLLLLLLLL	LLLL
131	2018/08/29 20:27	0	6.08	0.207	HHHH	LLLLLLLLLL	LLLL
132	2018/08/29 20:27	500	6.08	0.209	HHHH	LLLLLLLLLL	LLLL
133	2018/08/29 20:27	0	6.08	0.209	HHHH	LLLLLLLLLL	LLLL
134	2018/08/29 20:27	500	6.08	0.21	HHHH	LLLLLLLLLL	LLLL
135	2018/08/29 20:27	0	6.08	0.21	HHHH	LLLLLLLLLL	LLLL
136	2018/08/29 20:27	500	6.08	0.211	HHHH	LLLLLLLLLL	LLLL
137	2018/08/29 20:28	0	6.08	0.211	HHHH	LLLLLLLLLL	LLLL
138	2018/08/29 20:28	500	6.08	0.211	HHHH	LLLLLLLLLL	LLLL
139	2018/08/29 20:28	0	6.08	0.211	HHHH	LLLLLLLLLL	LLLL
140	2018/08/29 20:28	500	6.08	0.212	HHHH	LLLLLLLLLL	LLLL

141	2018/08/29 20:28	0	6.08	0.212	HHHH	LLLLLLLLLL	LLLL
142	2018/08/29 20:28	500	6.08	0.212	HHHH	LLLLLLLLLL	LLLL
143	2018/08/29 20:28	0	6.08	0.212	HHHH	LLLLLLLLLL	LLLL
144	2018/08/29 20:28	500	6.08	0.212	HHHH	LLLLLLLLLL	LLLL
145	2018/08/29 20:28	0	6.08	0.212	HHHH	LLLLLLLLLL	LLLL
146	2018/08/29 20:28	500	6.08	0.213	HHHH	LLLLLLLLLL	LLLL
147	2018/08/29 20:28	0	6.08	0.213	HHHH	LLLLLLLLLL	LLLL
148	2018/08/29 20:28	500	6.08	0.213	HHHH	LLLLLLLLLL	LLLL
149	2018/08/29 20:28	0	6.08	0.214	HHHH	LLLLLLLLLL	LLLL
150	2018/08/29 20:28	500	6.08	0.214	HHHH	LLLLLLLLLL	LLLL
151	2018/08/29 20:28	0	6.08	0.214	HHHH	LLLLLLLLLL	LLLL
152	2018/08/29 20:28	500	6.08	0.214	HHHH	LLLLLLLLLL	LLLL
153	2018/08/29 20:28	0	6.08	0.215	HHHH	LLLLLLLLLL	LLLL
154	2018/08/29 20:28	500	6.08	0.214	HHHH	LLLLLLLLLL	LLLL
155	2018/08/29 20:28	0	6.08	0.214	HHHH	LLLLLLLLLL	LLLL
156	2018/08/29 20:28	500	6.08	0.214	HHHH	LLLLLLLLLL	LLLL
157	2018/08/29 20:28	0	6.08	0.214	HHHH	LLLLLLLLLL	LLLL
158	2018/08/29 20:28	500	6.08	0.215	HHHH	LLLLLLLLLL	LLLL
159	2018/08/29 20:28	0	6.08	0.215	HHHH	LLLLLLLLLL	LLLL
160	2018/08/29 20:28	500	6.08	0.215	HHHH	LLLLLLLLLL	LLLL
161	2018/08/29 20:28	0	6.08	0.215	HHHH	LLLLLLLLLL	LLLL
162	2018/08/29 20:28	500	6.08	0.215	HHHH	LLLLLLLLLL	LLLL
163	2018/08/29 20:28	0	6.08	0.215	HHHH	LLLLLLLLLL	LLLL
164	2018/08/29 20:28	500	6.08	0.216	HHHH	LLLLLLLLLL	LLLL
165	2018/08/29 20:28	0	6.08	0.217	HHHH	LLLLLLLLLL	LLLL
166	2018/08/29 20:28	500	6.08	0.217	HHHH	LLLLLLLLLL	LLLL

167	2018/08/29 20:28	0	6.08	0.217	HHHH	LLLLLLLLLL	LLLL
168	2018/08/29 20:28	500	6.08	0.217	HHHH	LLLLLLLLLL	LLLL
169	2018/08/29 20:28	0	6.08	0.217	HHHH	LLLLLLLLLL	LLLL
170	2018/08/29 20:28	500	6.08	0.217	HHHH	LLLLLLLLLL	LLLL
171	2018/08/29 20:28	0	6.08	0.217	HHHH	LLLLLLLLLL	LLLL
172	2018/08/29 20:28	500	6.08	0.217	HHHH	LLLLLLLLLL	LLLL
173	2018/08/29 20:28	0	6.08	0.217	HHHH	LLLLLLLLLL	LLLL
174	2018/08/29 20:28	500	6.08	0.217	HHHH	LLLLLLLLLL	LLLL
175	2018/08/29 20:28	0	6.08	0.217	HHHH	LLLLLLLLLL	LLLL
176	2018/08/29 20:28	500	6.08	0.217	HHHH	LLLLLLLLLL	LLLL
177	2018/08/29 20:28	0	6.08	0.217	HHHH	LLLLLLLLLL	LLLL
178	2018/08/29 20:28	500	6.08	0.217	HHHH	LLLLLLLLLL	LLLL
179	2018/08/29 20:28	0	6.08	0.218	HHHH	LLLLLLLLLL	LLLL
180	2018/08/29 20:28	500	6.08	0.218	HHHH	LLLLLLLLLL	LLLL
181	2018/08/29 20:28	0	6.08	0.218	HHHH	LLLLLLLLLL	LLLL
182	2018/08/29 20:28	500	6.08	0.218	HHHH	LLLLLLLLLL	LLLL
183	2018/08/29 20:28	0	6.08	0.218	HHHH	LLLLLLLLLL	LLLL
184	2018/08/29 20:28	500	6.08	0.218	HHHH	LLLLLLLLLL	LLLL
185	2018/08/29 20:28	0	6.08	0.218	HHHH	LLLLLLLLLL	LLLL
186	2018/08/29 20:28	500	6.08	0.219	HHHH	LLLLLLLLLL	LLLL
187	2018/08/29 20:28	0	6.08	0.219	HHHH	LLLLLLLLLL	LLLL
188	2018/08/29 20:28	500	6.08	0.219	HHHH	LLLLLLLLLL	LLLL
189	2018/08/29 20:28	0	6.08	0.219	HHHH	LLLLLLLLLL	LLLL
190	2018/08/29 20:28	500	6.08	0.219	HHHH	LLLLLLLLLL	LLLL
191	2018/08/29 20:28	0	6.08	0.219	HHHH	LLLLLLLLLL	LLLL
192	2018/08/29 20:28	500	6.08	0.219	HHHH	LLLLLLLLLL	LLLL

193	2018/08/29 20:28	0	6.08	0.219	HHHH	LLLLLLLLLL	LLLL
194	2018/08/29 20:28	500	6.08	0.219	HHHH	LLLLLLLLLL	LLLL
195	2018/08/29 20:28	0	6.08	0.22	HHHH	LLLLLLLLLL	LLLL
196	2018/08/29 20:28	500	6.08	0.22	HHHH	LLLLLLLLLL	LLLL
197	2018/08/29 20:28	0	6.08	0.22	HHHH	LLLLLLLLLL	LLLL
198	2018/08/29 20:28	500	6.08	0.22	HHHH	LLLLLLLLLL	LLLL
199	2018/08/29 20:28	0	6.08	0.22	HHHH	LLLLLLLLLL	LLLL
200	2018/08/29 20:28	500	6.08	0.22	HHHH	LLLLLLLLLL	LLLL
201	2018/08/29 20:28	0	6.08	0.22	HHHH	LLLLLLLLLL	LLLL
202	2018/08/29 20:28	500	6.08	0.22	HHHH	LLLLLLLLLL	LLLL
203	2018/08/29 20:28	0	6.08	0.22	HHHH	LLLLLLLLLL	LLLL
204	2018/08/29 20:28	500	6.08	0.22	HHHH	LLLLLLLLLL	LLLL
205	2018/08/29 20:28	0	6.08	0.22	HHHH	LLLLLLLLLL	LLLL
206	2018/08/29 20:28	500	6.08	0.22	HHHH	LLLLLLLLLL	LLLL
207	2018/08/29 20:28	0	6.08	0.22	HHHH	LLLLLLLLLL	LLLL
208	2018/08/29 20:28	500	6.08	0.22	HHHH	LLLLLLLLLL	LLLL
209	2018/08/29 20:28	0	6.08	0.22	HHHH	LLLLLLLLLL	LLLL
210	2018/08/29 20:28	500	6.08	0.22	HHHH	LLLLLLLLLL	LLLL
211	2018/08/29 20:28	0	6.08	0.221	HHHH	LLLLLLLLLL	LLLL
212	2018/08/29 20:28	500	6.08	0.221	HHHH	LLLLLLLLLL	LLLL
213	2018/08/29 20:28	0	6.08	0.221	HHHH	LLLLLLLLLL	LLLL
214	2018/08/29 20:28	500	6.08	0.221	HHHH	LLLLLLLLLL	LLLL
215	2018/08/29 20:28	0	6.08	0.221	HHHH	LLLLLLLLLL	LLLL
216	2018/08/29 20:28	500	6.08	0.221	HHHH	LLLLLLLLLL	LLLL
217	2018/08/29 20:28	0	6.08	0.221	HHHH	LLLLLLLLLL	LLLL
218	2018/08/29 20:28	500	6.08	0.221	HHHH	LLLLLLLLLL	LLLL

219	2018/08/29 20:28	0	6.08	0.221	HHHH	LLLLLLLLLL	LLLL
220	2018/08/29 20:28	500	6.08	0.22	HHHH	LLLLLLLLLL	LLLL
221	2018/08/29 20:28	0	6.08	0.22	HHHH	LLLLLLLLLL	LLLL
222	2018/08/29 20:28	500	6.08	0.22	HHHH	LLLLLLLLLL	LLLL
223	2018/08/29 20:28	0	6.08	0.22	HHHH	LLLLLLLLLL	LLLL
224	2018/08/29 20:28	500	6.08	0.22	HHHH	LLLLLLLLLL	LLLL
225	2018/08/29 20:28	0	6.08	0.22	HHHH	LLLLLLLLLL	LLLL
226	2018/08/29 20:28	500	6.08	0.22	HHHH	LLLLLLLLLL	LLLL
227	2018/08/29 20:28	0	6.08	0.22	HHHH	LLLLLLLLLL	LLLL
228	2018/08/29 20:28	500	6.08	0.221	HHHH	LLLLLLLLLL	LLLL
229	2018/08/29 20:28	0	6.08	0.221	HHHH	LLLLLLLLLL	LLLL
230	2018/08/29 20:28	500	6.08	0.264	HHHH	LLLLLLLLLL	LLLL
231	2018/08/29 20:28	0	6.08	0.307	HHHH	LLLLLLLLLL	LLLL
232	2018/08/29 20:28	500	6.09	0.349	HHHH	LLLLLLLLLL	LLLL
233	2018/08/29 20:28	0	6.09	0.392	HHHH	LLLLLLLLLL	LLLL
234	2018/08/29 20:28	500	6.09	0.435	HHHH	LLLLLLLLLL	LLLL
235	2018/08/29 20:28	0	6.09	0.478	HHHH	LLLLLLLLLL	LLLL
236	2018/08/29 20:28	500	6.09	0.519	HHHH	LLLLLLLLLL	LLLL
237	2018/08/29 20:28	0	6.09	0.562	HHHH	LLLLLLLLLL	LLLL
238	2018/08/29 20:28	500	6.09	0.604	HHHH	LLLLLLLLLL	LLLL
239	2018/08/29 20:28	0	6.09	0.647	HHHH	LLLLLLLLLL	LLLL
240	2018/08/29 20:28	500	6.09	0.689	HHHH	LLLLLLLLLL	LLLL
241	2018/08/29 20:28	0	6.09	0.732	HHHH	LLLLLLLLLL	LLLL
242	2018/08/29 20:28	500	6.09	0.774	HHHH	LLLLLLLLLL	LLLL
243	2018/08/29 20:28	0	6.08	0.816	HHHH	LLLLLLLLLL	LLLL
244	2018/08/29 20:28	500	6.08	0.858	HHHH	LLLLLLLLLL	LLLL

245	2018/08/29 20:28	0	6.08	0.9	HHHH	LLLLLLLLLL	LLLL
246	2018/08/29 20:28	500	6.08	0.942	HHHH	LLLLLLLLLL	LLLL
247	2018/08/29 20:28	0	6.08	0.985	HHHH	LLLLLLLLLL	LLLL
248	2018/08/29 20:28	500	6.08	1.027	HHHH	LLLLLLLLLL	LLLL
249	2018/08/29 20:28	0	6.08	1.069	HHHH	LLLLLLLLLL	LLLL
250	2018/08/29 20:28	500	6.08	1.069	HHHH	LLLLLLLLLL	LLLL
251	2018/08/29 20:28	0	6.08	1.068	HHHH	LLLLLLLLLL	LLLL
252	2018/08/29 20:28	500	6.08	1.068	HHHH	LLLLLLLLLL	LLLL
253	2018/08/29 20:28	0	6.08	1.069	HHHH	LLLLLLLLLL	LLLL
254	2018/08/29 20:28	500	6.08	1.068	HHHH	LLLLLLLLLL	LLLL
255	2018/08/29 20:28	0	6.08	1.068	HHHH	LLLLLLLLLL	LLLL
256	2018/08/29 20:28	500	6.08	1.068	HHHH	LLLLLLLLLL	LLLL
257	2018/08/29 20:29	0	6.08	1.068	HHHH	LLLLLLLLLL	LLLL
258	2018/08/29 20:29	500	6.08	1.067	HHHH	LLLLLLLLLL	LLLL
259	2018/08/29 20:29	0	6.08	1.067	HHHH	LLLLLLLLLL	LLLL
260	2018/08/29 20:29	500	6.08	1.067	HHHH	LLLLLLLLLL	LLLL
261	2018/08/29 20:29	0	6.08	1.067	HHHH	LLLLLLLLLL	LLLL
262	2018/08/29 20:29	500	6.08	1.067	HHHH	LLLLLLLLLL	LLLL
263	2018/08/29 20:29	0	6.08	1.067	HHHH	LLLLLLLLLL	LLLL
264	2018/08/29 20:29	500	6.08	1.065	HHHH	LLLLLLLLLL	LLLL
265	2018/08/29 20:29	0	6.08	1.065	HHHH	LLLLLLLLLL	LLLL
266	2018/08/29 20:29	500	6.08	1.065	HHHH	LLLLLLLLLL	LLLL
267	2018/08/29 20:29	0	6.08	1.065	HHHH	LLLLLLLLLL	LLLL
268	2018/08/29 20:29	500	6.08	1.064	HHHH	LLLLLLLLLL	LLLL
269	2018/08/29 20:29	0	6.08	1.064	HHHH	LLLLLLLLLL	LLLL
270	2018/08/29 20:29	500	6.08	1.064	HHHH	LLLLLLLLLL	LLLL

271	2018/08/29 20:29	0	6.08	1.064	HHHH	LLLLLLLLLL	LLLL
272	2018/08/29 20:29	500	6.08	1.064	HHHH	LLLLLLLLLL	LLLL
273	2018/08/29 20:29	0	6.08	1.064	HHHH	LLLLLLLLLL	LLLL
274	2018/08/29 20:29	500	6.08	1.063	HHHH	LLLLLLLLLL	LLLL
275	2018/08/29 20:29	0	6.08	1.065	HHHH	LLLLLLLLLL	LLLL
276	2018/08/29 20:29	500	6.08	1.065	HHHH	LLLLLLLLLL	LLLL
277	2018/08/29 20:29	0	6.08	1.065	HHHH	LLLLLLLLLL	LLLL
278	2018/08/29 20:29	500	6.08	1.065	HHHH	LLLLLLLLLL	LLLL
279	2018/08/29 20:29	0	6.08	1.065	HHHH	LLLLLLLLLL	LLLL
280	2018/08/29 20:29	500	6.08	1.064	HHHH	LLLLLLLLLL	LLLL
281	2018/08/29 20:29	0	6.08	1.064	HHHH	LLLLLLLLLL	LLLL
282	2018/08/29 20:29	500	6.08	1.064	HHHH	LLLLLLLLLL	LLLL
283	2018/08/29 20:29	0	6.08	1.064	HHHH	LLLLLLLLLL	LLLL
284	2018/08/29 20:29	500	6.08	1.064	HHHH	LLLLLLLLLL	LLLL
285	2018/08/29 20:29	0	6.08	1.063	HHHH	LLLLLLLLLL	LLLL
286	2018/08/29 20:29	500	6.08	1.064	HHHH	LLLLLLLLLL	LLLL
287	2018/08/29 20:29	0	6.08	1.064	HHHH	LLLLLLLLLL	LLLL